The Role of Nitric Oxide in Hindlimb Remote Ischaemic Preconditioning of the Liver

Mahmoud Abu-Amara

A thesis submitted for the degree of Doctor of Philosophy

University College London

University Department of Surgery

University College Medical School, Royal Free Campus

University College London

I, Mahmoud Abu-Amara confirm that the work presented in this thesis is my own. Help and contribution of others to this work is specified in the acknowledgement section. Where information has been derived from other sources, I confirm that this has been indicated in the thesis.

This thesis is dedicated to my wife Lubna and our children Ameen, Yousef, and Mariam, for their support and understanding. I also dedicate this thesis to my mother and late father, who have been a guiding light throughout my education and career.

Abstract

Ischaemia reperfusion (IR) injury is a major contributor to morbidity and mortality following liver resection and transplantation. Hindlimb remote ischaemic preconditioning (RIPC) reduces liver IR injury but the mechanisms underlying this protection are unknown. This thesis evaluated the effects of RIPC on the early phase of liver IR injury in a new mouse model. This model was used to assess the role of the nitric oxide (NO) pathway in mediating the protective effects of RIPC on liver IR injury.

In the initial experiments wild type C57BL/6 mice were used to establish a new model of hindlimb RIPC that protects against liver IR injury. The new experimental model hindlimb protocol consisted of 6 cycles of 4 minutes of femoral vessel clamping followed by 4 minutes of reperfusion. The IR protocol consisted of a well-described 40 minutes of lobar liver (70%) ischaemia followed by 2 hours reperfusion. This hindlimb RIPC model resulted in significant reductions in liver IR injury, as evaluated by plasma liver transaminases levels, histopathological scores, and ultrastructural assessment of cellular damage in the liver. In addition hindlimb RIPC preserved the hepatic microcirculatory blood flow (MBF) in livers subjected to IR.

In subsequent experiments administration of the selective NO scavenger C-PTIO to wild type mice abrogated the protective effects of limb RIPC on liver IR injury. In addition the RIPC-induced preservation of hepatic MBF was attenuated by C-PTIO administration. In contrast to the protective effects of limb RIPC on liver IR injury in wild type mice; mice lacking the constitutively expressed NO synthase ($eNOS^{-/-}$)

enzyme were not protected against liver IR injury by hindlimb RIPC, and MBF measurements in these mice showed no benefit of RIPC on the microcirculation. In wild type mice hepatic and limb eNOS protein expression was similar among preconditioned and non-preconditioned animals. In comparison expression of the inducible NOS (iNOS) isoform was only seen in preconditioned animals.

In order to elicit the pathway through which RIPC-derived NO protects against liver IR injury, plasma nitrite and nitrate (NOx) levels were quantified in wild type animals and shown to be significantly elevated in preconditioned compared to non-preconditioned animals. However, intravenous administration of exogenous nitrite to $eNOS^{-/-}$ mice undergoing liver IR injury failed to mimic the protective effects of RIPC-derived endogenous NOx in wild types. Administration of the soluble guanylyl cyclase (sGC) inhibitor ODQ showed a trend indicating reversal of the protective effects of RIPC on liver IR injury but this did not reach statistical significance. ODQ significantly annulled the protective effects of limb RIPC on hepatic MBF during liver reperfusion. Measurement of hepatic cyclic GMP levels in wild type animals showed a significant increase in animals subjected to limb RIPC only compared to sham. However there was no difference in the cGMP levels in the RIPC + IR compared to the IR group.

In conclusion this thesis has described a new mouse model of limb RIPC that protects against liver IR injury. It was also shown that NO and eNOS are essential in mediating the protective effects of limb RIPC on liver IR injury. Endogenous NOx metabolites of NO play a crucial role in RIPC induced protection. The hepatic sGC-cGMP pathway is at least partially involved in RIPC-induced liver protection.

Acknowledegements

I am very grateful to my supervisors, professors Brian Davidson, Barry Fuller, and Alexander Seifalian for their guidance, immense help, and enthusiasm throughout this research project.

I would like to thank Dr Shi Yu Yang in the University Department of Surgery for his endless help during this project. He taught me how to collect blood and tissue samples from experimental animals; and how to perform Western blots. I would also like to thank him for his immensely useful advice on data presentation, and manuscript organisation for publications. He is a true asset to the department.

The staff of the comparative biology unit were very supportive in preparation for and conduction of the animal experiments. A big thank you to Duncan Moore who provided great advice during application for an animal project and personal licence from the Home Office; to Mark Neal for provision of the consumables used during animal experiments; to Michelle Murphy for her expertise in setting up and propagating the $eNOS^{-/-}$ mouse colony; and to Barry Greenhalgh for help in provision of wild type mice.

I really appreciated the help I initially received from John Robertson and Niteen Tapuria in showing me how to handle small animals during anaesthesia and surgery.

I am grateful to Maxwell Owusu-Ansah for help in preparing the H & E slides; and to Dr Alberto Quaglia from the Department of liver histopathology at King's College hospital for scoring these samples. I also would like to express my gratitude to: Rosalind Sim for help and advice on the immunohistochemistry sections; Peter Rowley for preparation of the sections for transmission electron microscopy and interpretation of the images arising from these; Dr Cecil Thompson for assistance with biochemical analysis; Achela de Mel for help in performing the NOx assay; and Korsa Khan for help in performing the cGMP assay.

Table of contents

List of abbreviations

ADP	Adenosine diphosphate
Akt/PKB	Protein kinase B
ALT	Alanine aminotransferase
AMP	Adenosine monophosphate
ANP	Atrial natriuretic peptide
ANT	Adenine nucleotide transporter
AP	Activator protein
ARE	Antioxidant response element
AST	Aspartate aminotransferase
ATP	Adenosine triphosphate
cGMP	cyclic 3', 5' guanosine monophosphate
CINC	Cytokine-induced neutrophil chemoattractant
COX	Cyclo-oxygenase
CycD	Cycolphilin D
DAMP	Danger associated molecular pattern
Egr	early growth response
ENA	Epithelial neutrophil activating protein
eNOS	Endothelial nitric oxide synthase
ER	Endoplasmic reticulum
ERK	Extracellular signal-regulated kinase
aFGF	Acidic fibroblast growth factor
bFGF	Basic fibroblast growth factor
GSH	Glutathione
HGF	Hepatocyte growth factor

HCLO	Hypochlorous acid
HMGB-1	High mobility group box-1
HO-1	Haem oxygenase-1
H_2O_2	Hydrogen peroxide
HSF	Heat shock factor
ICAM	Intercellular adhesion molecule
IFN	Interferon
IKK	IκB kinase
IL	Interleukin
IMM	Inner mitochondrial membrane
iNOS	Inducible nitric oxide synthase
IP_3	Inositol triphosphate
IP-10	Inducible protein-10
IPC	Ischaemic preconditioning
IR	Ischaemia reperfusion
IRAK	IL-1 receptor-associated kinase
IRF	Interferon regulatory factor
JNK	C-Jun N-terminal kinase
LDF	Laser Doppler Flowmetry
mΔΨ	Mitochondrial transmembrane potential
MAPK	Mitogen activated protein kinase
MBF	Microcirculatory blood flow
MCP	Monocyte chemoattractant protein
MDA	Malondialdehyde
MIG	Monokine induced by interferon gamma

MIP	Macrophage inflammatory protein
MnSOD	Mitochondrial superoxide dismutase
MPT	Mitochondrial permeability transition
mP2Y	Mitochondria purinergic-like receptors
MyD88	Myeloid differentiation factor 88
Na^+ / K^+ ATPase	Sodium / potassium ATP-dependent pump
NAD^+	Nicotinamide adenine dinucleotide
$NADP^+$	Nicotinamide adenine dinucleotide phosphate
NF-κB	Nuclear factor kappa B
NHCT	Na^+ / HCO_3^- cotransporter
NHE	Na^+ / H^+ exchanger
NKT cells	Natural killer T cells
NO	Nitric oxide
NO_2	Nitrogen dioxide
N_2O_3	Dinitrogen trioxide
NOS	Nitric oxide synthase
NOx	Nitrate and nitrite
O_2	Oxygen
$O_2^{\bullet-}$	Superoxide radical
$^{\bullet}OH$	Hydroxyl radical
OMM	Outer mitochondrial membrane
$ONOO^-$	Peroxynitrite
P38	P38 mitogen activated protein kinase
PAF	Platelet activating factor
PAMP	Pathogen associated molecular pattern

PBS	Phosphate buffered saline
PG	Prostaglandin
Pi	Inorganic phosphate
PKA	Protein kinase A
PKC	Protein Kinase C
PLC	Phospholipase C
PRR	Pattern recognition receptors
RAGE	Receptor for advanced glycation end products
RIPC	Remote ischaemic preconditioning
RNS	Reactive nitrogen species
ROS	Reactive oxygen species
SEC	Sinusoidal endothelial cell
SEM	Standard error of the mean
sGC	Soluble guanylyl cyclase
SOC	Store operated Ca^{2+}
SOD	Superoxide dismutase
STAT	Signal transducer and activator of transcription
TAB	TAK1-binding protein
TAK-1	transforming growth factor β-activated kinase1
TIR	Toll – IL-1 receptor
TIRAP	TIR domain-containing adaptor protein
TLR	Toll-like receptor
TNF-α	Tumour necrosis factor-α
TRAF	TNF receptor-associated factor
TRAM	TRIF-related adaptor molecule

TRIF	TIR domain-containing adaptor inducing interferon β
TRP	Transient receptor potential
VCAM	Vascular cell adhesion molecule
VDAC	Voltage-dependent anion channels
VEGF	Vascular endothelial growth factor
XD	Xanthine dehydrogenase
XO	Xanthine oxidase

List of figures

Figure 8.6 Hepatic cGMP levels in wild type mice.

List of tables

Chapter 1

Introduction

1.1 Clinical importance of liver ischaemia reperfusion injury

Ischaemia reperfusion (IR) injury results from a prolonged ischaemic insult followed by restoration of blood perfusion. It affects all oxygen dependent cells that rely on an uninterrupted blood supply. These aerobic cells require mitochondrial oxidative phosphorylation for their energy supply. Consequently all aerobically metabolising tissues and organs (central nervous system, intra-thoracic, and intra-abdominal organs; as well as blood vessels, skeletal muscle, and adipo-cutaneous tissues) are potential targets of IR injury (1).

Significant liver IR injury during surgical resection is commonly a consequence of prolonged portal triad clamping followed by reperfusion, performed as an elective pre-planned procedure or as an emergent manoeuvre, to control excessive bleeding from the cut hepatic surface (2). Transplantation of the liver can also lead to IR injury. Here, the damage is sustained during cold preservation of the liver following explantation from the donor, and during subsequent warm reperfusion at implantation into the recipient (3). In non-heart beating transplantation there is additional warm ischaemic damage until hepatic cold perfusion is commenced. Importantly however, liver dysfunction in IR injury is not solely dependent on blood flow interruption, but is also seen with excessive handling and mobilisation of the liver during resection or procurement in transplantation, even without blood supply interruption in the former and regardless of its duration in the latter (4). This is mostly due to hepatic microcirculatory disturbances, and in some cases to hepatic artery vasospasm (4). Systemic low flow states and hypoxia such as is encountered in haemorrhage (5), sepsis, congestive cardiac failure, trauma, and respiratory failure may also lead to liver IR injury (6).

The degree of IR injury sustained is dependent on the length and method of ischaemia applied to the liver, as well as the background liver condition. Patients that undergo short intermittent periods of ischaemia sustain less liver dysfunction compared to those receiving a continuous period of ischaemia (7). This is especially the case in patients with underlying cirrhosis or steatosis (7). Animal studies also support the notion that the background liver parenchymal condition significantly determines the degree of tolerance to IR. Animal models of steatosis and cirrhosis exhibit worse liver damage when subjected to IR compared to those with normal livers (8,9). Other determinants of liver susceptibility to IR injury include: age – older livers exhibit more damage compared to young ones (10), and gender – in animal models males tolerate ischaemic insults less than females, however there is insufficient evidence for a firm clinical recommendation on the role of gender in liver IR injury (11). Systemic and localised neo-adjuvant chemotherapy is increasingly being used to down stage liver tumours prior to surgical resection. There is increasing evidence that, contrary to instinctive beliefs, neo-adjuvant chemotherapy does not increase liver susceptibility to IR injury (12-14). In fact, through suppression of inflammatory pathways, chemotherapy may attenuate the IR injury (12-14).

In the mildest form of IR injury sustained during liver resections, liver transaminase enzymes are elevated in the circulation. More severe insults lead to clinical liver dysfunction and progressive failure. Direct IR to the liver can also result in distant organ dysfunction due to remote IR injury. Lungs (15), heart (16), kidneys (17), and blood vessels (18) have all been shown to sustain remote dysfunction secondary to direct liver IR. Humoral factors such as reactive free radicals and cytokines released

from kupffer cells are the main mediators of liver – induced remote IR injury (19-22). Substantial IR injury sustained during liver transplantations increase the incidence of primary graft non-function, primary graft dysfunction, and biliary strictures (23,24). Hepatic non-function and intra-hepatic biliary strictures in transplantation, and failure of the remnant liver in resectional surgery usually necessitate transplantation, placing an even greater pressure on the limited number of donor livers.

1.2 Pathophysiology of liver IR injury

Liver IR injury is a complex process involving numerous cell types and molecular mediators in various pathways. The cellular damage occurs during both the ischaemic and reperfusion phases. The end result is cellular death via a combination of apoptosis and necrosis. Warm ischaemic damage arises when the blood supply to the liver is interrupted at normal body temperature as is the case during liver resections. Cold ischaemic damage arises during cold perfusion and storage of livers in transplantation. The following is an up to date review of the mechanisms of liver IR injury. The discussion begins by reviewing the function of each of the main cellular types within the liver, which participate in IR injury. This is followed by a description of the role of platelets, complement, cytokines, endogenous initiators of inflammation, and mitochondria in liver IR injury.

1.2.1 *Cellular contributors*

During the ischaemic phase as a result of glycogen consumption and lack of oxygen (O_2) supply, kupffer cells, sinusoidal endothelial cells (SEC), and hepatocytes suffer with lack of adenosine triphosphate (ATP) production (25,26). The lack of ATP

leads to failure of the sodium / potassium ATP-dependent plasma membrane pump (Na^+ / K^+ ATPase) and subsequent intracellular Na^+ accumulation, oedema, and swelling. Kupffer cell and SEC swelling combined with an increase in the vasoconstrictors endothelin (27) and thromboxane A2 (28) and a decrease in the vasodilator nitric oxide (29) lead to sinusoidal narrowing. In addition on reperfusion there is increased adhesion and aggregation of neutrophils and platelets in the sinusoids. The end result is significant reduction of microcirculatory blood flow on reperfusion, including some areas with complete absence of blood flow which is known as "no-reflow" (30) (figure 1.1).

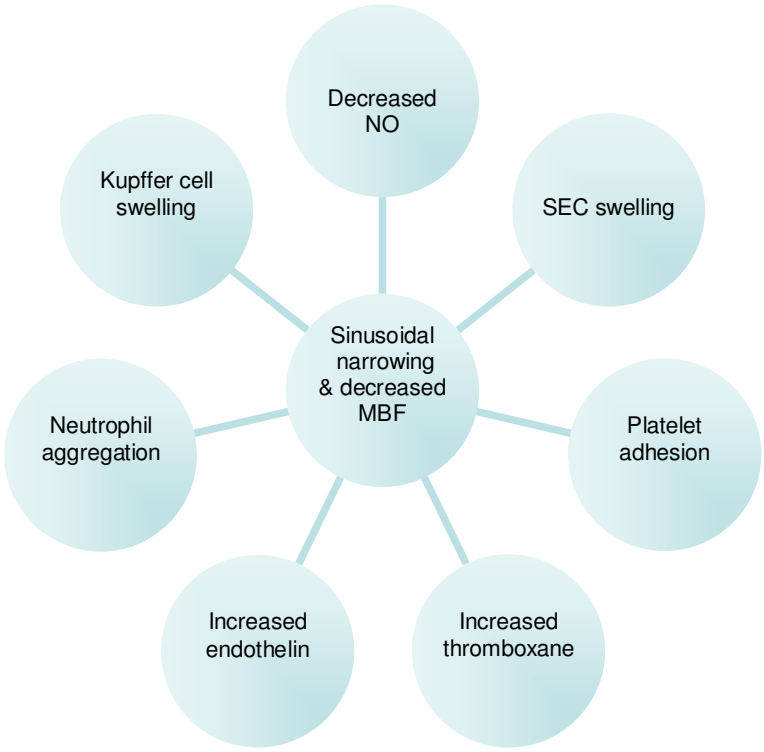

Figure 1.1. The pathophysiology of the decreased microcirculatory blood flow (MBF) seen on reperfusion of the ischaemic liver. Multiple factors contribute to sinusoidal narrowing with subsequent reduction in MBF. *NO*, nitric oxide; *SEC*, sinusoidal endothelial swelling; *MBF*, microcirculatory blood flow.

Kupffer cells are the liver resident macrophages. They play a key role in initiating and propagating cellular damage and death in IR injury (31). Kupffer cells are activated during the ischaemic phase and even more so on reperfusion. On activation they produce reactive free radicals, specifically reactive oxygen species (ROS) (32), and pro-inflammatory cytokines including tumour necrosis factor-α (TNF-α), interleukin-1β (IL-1β), and IL-1α (22,33). These ROS and cytokines have widespread effects in the initiation and propagation of IR injury. Their main role is to recruit and activate circulating neutrophils on reperfusion (34). In addition they induce remote IR injury in distant organs (22), recruit and activate CD4+ T-lymphocytes (35), activate SEC leading to expression of cell – surface adhesion molecules and contribute to their damage (35,36), stimulate hepatocytes to produce ROS and contribute to their damage (37,38), and stimulate platelet adhesion to SEC (39). Kupffer cells are mainly activated as a direct consequence of IR causing disruption of mitochondria and ATP production, they are also activated indirectly via the complement system (40,41) (figure 1.2).

Activated SEC, hepatocytes, and neutrophils express cell-surface adhesion molecules. On neutrophils L-selectin and β_2-integrins (CD11b/CD18) adhere to intercellular adhesion molecule-1 (ICAM-1) and vascular adhesion molecule-1 (VCAM-1) on the surface of SEC and hepatocytes (42,43) (figure 1.2). In liver IR injury however, early neutrophil accumulation in the sinusoids mainly results from mechanical trapping by the swollen, constricted, platelet-adhering sinusoids (44). In response to chemokines from activated and injured hepatocytes, sinusoidally-accumulated neutrophils use the surface-expressed adhesion molecules to bind their SEC's counterpart and migrate across the endothelium into the parenchyma. The

binding of CD11b/CD18 on the neutrophils to ICAM-1 and VCAM-1 on the hepatocytes triggers an enhancement of ROS production through the NADPH oxidase system as well as degranulation of cytoplasmic vesicles containing various enzymes that assist in the degradation of the extracellular matrix and dead hepatocytes, and damage viable hepatocytes (42).

The liver contains all the subtypes of lymphocytes as resident cells. These comprise B-cells, CD8+ and CD4+ T-cells (conventional T-lymphocytes), natural killer T (NKT) cells and γδ T-cells (unconventional T-lymphocytes) (45). CD4+ and to a lesser extent NKT lymphocytes play a key role in liver IR injury. CD4+ cells accumulate in the liver within one hour of reperfusion following IR, preceding any neutrophil accumulation (46,47). They are recruited to the liver and activated, by various kupffer cell-derived products (figure 1.2). These include chemokines (CXCL9, CXCL10 (IP-10), CXCL11), ROS, cytokines (TNFα, IL-6), and matrix metalloproteinase 9 (35,48,49). CD4+ cells have been shown to be important contributors in neutrophil recruitment into the post ischaemic liver which is supported by experiments demonstrating significantly reduced liver neutrophil accumulation in CD4-/- mice and in CD4+ mice administered anti-CD4+ antibodies (46,47). CD4+ lymphocytes stimulate neutrophil accumulation through production of the chemotactic agent IL-17 (46). Furthermore the CD4+ cells produce interferon-γ (IFN-γ) that activates kupffer cells to produce TNF-α and IL-1, and hepatocytes to produce chemokines (50). Thus CD4+ T-lymphocytes and kupffer cells reciprocally activate one another (35). The end result of hepatic CD4+ cell recruitment and activation post ischaemia, is hepatocyte and SEC damage with microvascular perfusion defects (47,51). NKT cells are recruited and activated into the post

ischaemic liver on a time scale similar to CD4+ cells (46). NKT cell activation is dependent on interaction with CD1d antigen presenting molecules, expressed on hepatocytes and antigen presenting cells within the liver (52,53). CD1d presents either self or foreign glycolipid antigens to NKT cells. Activated NKT cells are capable of damaging the liver directly and of producing IFN-γ with subsequent kupffer cell and hepatocyte activation (52,53).

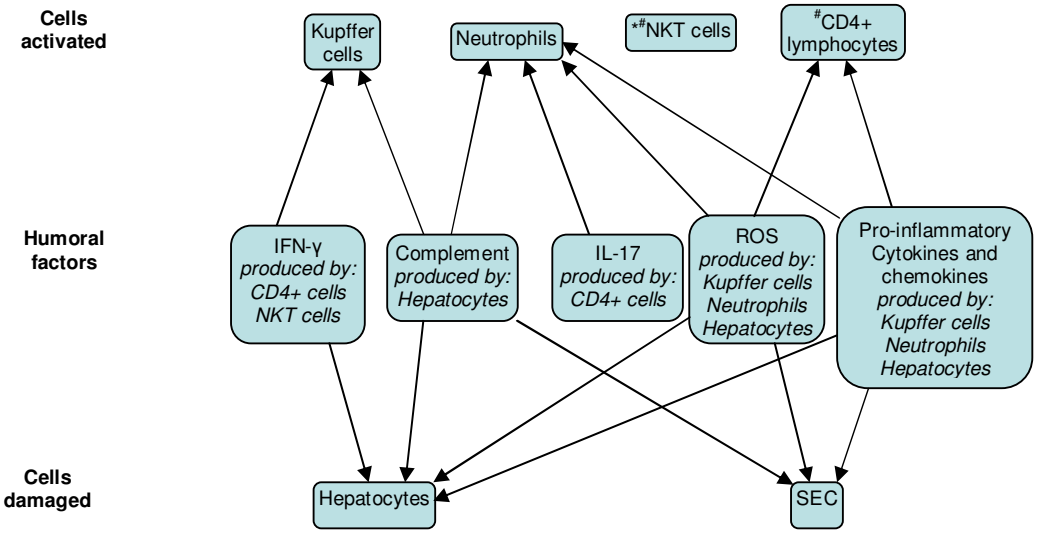

Figure 1.2. Cellular and humoral factors in liver IR injury. The figure illustrates the activation of immune cells, and damage to hepatocytes and SEC, by humoral factors. Note the humoral factors are themselves produced by the same group of cells that they activate. *NKT cells are activated by CD1d antigen presenting molecules expressed on hepatocytes and antigen presenting cells. #NKT and CD4+ T cells can directly damage hepatocytes and SECs. *IFN-γ*, interferon-γ; *IL-17*, interleukin-17; *NKT*, natural killer T; *ROS*, reactive oxygen species; *SEC*, sinusoidal endothelial cells.

1.2.2 *Platelets*

Platelet adhesion and aggregation within the sinusoids contributes to neutrophil accumulation, SEC apoptosis, and sinusoidal perfusion failure during the post ischaemic period (39,54,55). The IR-induced damaging effects of kupffer cells, neutrophils, and platelets are interdependent. Each of these acts synergistically with the other, resulting in a degree of IR damage that is greater than the damage sustained if one of these cell types is missing (56,57). In contrast, platelets may also play a beneficial role in postoperative liver regeneration. Platelet-derived serotonin has recently been shown to be an important factor in liver regeneration, and more specifically hepatocyte proliferation, as mice deficient in this effector fail to regenerate their livers (58).

1.2.3 *Complement*

The complement system comprises approximately 30 soluble and membrane-bound proteins. Hepatocytes manufacture 90% of plasma complement components (59). The majority of published studies used either a complement component-specific transgenic mouse strain or selective complement component inhibitors to elucidate the role of complement in liver IR injury. Three distinct pathways are known to activate the complement cascade, the classical, alternative, and mannose-binding lectin pathways. All three pathways are likely contributors to complement activation in liver IR (60). Once activated in IR injury, complement leads to liver damage either directly by lysing liver cells through the formation of a membrane attack complex in the plasma membrane (61), or by recruiting neutrophils and activating both neutrophils and kupffer cells (41) (figure 1.2). Therefore complement activation during liver IR injury leads to accentuation of the inflammatory cascade

and subsequent cellular death (62). Complement activation has also been implicated in the pathogenesis of remote IR injury. For example in rodents, bilateral hindlimb IR injury leads to remote liver IR injury by activation of kupffer cells via complement factor C5a (40,63). Direct liver IR injury on the other hand, results in remote endothelial damage in the lungs and small bowel in the mouse, that is significantly attenuated by mice transgenically over expressing the physiologically occurring complement inhibitor called C1 inhibitor (64). C1 inhibitor inhibits complement factor C1 and therefore the classical pathway of complement activation. These observations implicate C1 (classical pathway) as a mediator of liver IR injury-induced remote organ injury (64).

1.2.4 *Cytokines*

Cytokines are a diverse group of signalling molecules that may act in an autocrine, paracrine, or endocrine manner. They are important messengers between the cellular players in both direct and remote IR injury. Cytokines exert their effect by binding to cell surface receptors on target cells, and may play a pro- or an anti-inflammatory role. An extensive volume of literature is available on the function of a large number of cytokines in liver IR injury. In this review the action of three key (IL-12, IL-23, TNF-α) cytokines involved in liver IR injury modulation is described in detail. The actions of a further ten important (aFGF, bFGF, HGF, IFN-γ, IL-1β, IL-6, IL-10, IL-13, IL-18, VEGF) cytokines is summarised.

1.2.4a IL-12 and IL-23

IL-12 and IL-23 are heterodimeric cytokines. Each is made of a common p40 subunit, and a second cytokine-specific subunit. In the case of IL-12 this is p35, and

in the case of IL-23 it is p19 (65). Within the liver these cytokines are produced by hepatocytes and kupffer cells (65,66). IL-12 discovery preceded that of IL-23 by many years (65) and preliminary work showing that IL-12 was one of the key molecules in initiating a pro-inflammatory cytokine cascade in liver IR injury (66), was later re-examined and could have been due to either IL-12 or indeed IL-23 (67). This is because the two techniques used to illicit the role of IL-12 relied on the use of anti-p40 antibodies and $p40^{-/-}$ mice. Nevertheless, these studies indicated that IL-12 / IL-23 production occurs during the ischaemic phase and first hour of reperfusion. One or both of these cytokines is a prerequisite for the induction of TNF-α., the central component of the pro-inflammatory cytokine cascade in liver IR injury (66,67). The mechanisms through which this is achieved have not been resolved, but the transcription factors NF-κB and STAT-4 have been suggested as possible regulators of IL-12 / IL-23's effects on TNF-α expression (68).Other effects of IL-12 include leukocyte infiltration, kupffer cell activation, and cell-surface adhesion molecule expression (69); and of IL-23 include stimulation of CD4+ cells to produce IL-17 which stimulates neutrophil accumulation in the post ischaemic liver (70).

1.2.4b TNF-α

TNF-α is the central cytokine mediator of the pro-inflammatory cascade in liver IR injury. TNF-α is produced by kupffer cells and acts both locally in a paracrine fashion, and remotely as an endocrine mediator. It is a crucial effecter of remote organ damage following hepatic IR injury (71). A large number of endogenous pro- or anti-inflammatory molecules either stimulate or inhibit the expression of TNF-α respectively. These are summarised in table 1.1. TNF-α up-regulation in liver IR

injury leads to liver damage. TNF-α binds to specific TNF-receptors (TNF-R) on the surface of hepatocytes. This results in increased production of the chemokine epithelial neutrophil activating protein-78 (ENA-78) and ROS; as well as activation of NF-κB and the mitogen activated protein kinase (MAPK) C-Jun N-terminal kinase (JNK) (72-75). In addition, TNF-α up-regulates expression of the adhesion molecules ICAM-1 and P-selectin (71,76). Through various mechanisms, all these molecules are able to recruit and activate neutrophils into the post ischaemic liver. Furthermore, JNK and ROS are capable of direct cellular damage within the liver (75).

Table 1.1 Stimulators and inhibitors of TNF-α expression in hepatic IR injury.

Molecule	Reference	Effect on TNF-α expression	Transcription factor intermediate
bFGF	(77)	decreased	Not provided
IL-1	(78)	increased	Not provided
IL-4	(79)	decreased	Activates STAT-6
IL-6	(80-83)	decreased	Activates STAT-3[#]
IL-10	(84-86)	decreased	Inhibits NF-κB
IL-13	(87-90)	decreased	Activates STAT-6
ANP	(91)	decreased	Inhibits NF-κB
PGE2	(92)	decreased	Not provided
PAF	(93)	increased	Not provided
NO	(33)	decreased	Not provided
NO	(94)	decreased	Not provided
ROS	(73,75)	increased	Activates JNK[*]

[#]IL-6 has been shown to decrease TNF-α and activate STAT-3 in separate experiments.
[*]JNK is not a transcription factor, but an intracellular transduction pathway that phosphorylates transcription factors, amongst other functions.

1.2.4c Other cytokines

The role of other important cytokines in liver IR injury is summarised in table 1.2. The expression of these cytokines is under the control of a variable group of upstream regulators. Downstream, the cytokines influence the expression of various molecules that ultimately lead to either protection from, or exacerbation of liver IR injury. Each of these molecules belongs to a group that shares similar functions. There are transcription factors (AP-1, HSF, NF-κB, STAT-3, STAT-6), antioxidants (SOD, GSH), adhesion molecules (ICAM-1, E-selectin), inflammation – stimulated inducible enzymes (COX-2, iNOS, and HO-1), Intracellular signalling molecules (Akt), anti-apoptotic proteins (Bcl-2 / Bcl-x exert their effect by altering the mitochondrial membrane permeability), and chemokines (CINC, ENA-78, IP-10, MCP-1, MIG, MIP-2). The latter are chemotactic cytokines that direct and regulate the accumulation of neutrophils, monocytes / macrophages, and T-lymphocytes into the post ischaemic liver.

Table 1.2 The role of important cytokines in liver IR injury.

Cytokine	Reference (s)	Cellular source	Upstream regulator	Down stream mediator(s) of effect	Summary effect on liver
Acidic and basic fibroblast growth factors (aFGF and bFGF)	(77,95-98)	T-lymphocytes, hepatocytes, hepatic stellate cells	Not provided	*↑ expression of NO and SOD; ↓markers of oxidative stress	Reduces hepatic IR injury
Hepatocyte growth factor (HGF)	(99-101)	Non-parenchymal liver cells, mainly kupffer cells	Not provided	↑ hepatocyte DNA synthesis and hepatocyte proliferation; ↑ GSH expression, ↓ markers of oxidative stress; ↓ ICAM-1 expression on SEC; ↓ CINC, ↓ neutrophil infiltration	Reduces hepatic IR injury and pro-proliferative
Interferon-γ (IFN-γ)	(66,85,90,102-108)	T-lymphocytes, NKT cells, hepatocytes	TLR-4 activation & IL-12 stimulate IFN-γ production; A_{2A} adenosine receptor activation, IL-10, IL-13, STAT-6, & VEGF inhibit IFN-γ production	Dual action: 1. Physiological doses: ↑neutrophil recruitment & activation. 2. Pharmacological doses: ↑IP-10, ↑MIG, ↑neutrophil recruitment; ↓CINC, ↓MIP-2, ↓ENA-78, ↓neutrophil activation	Dual action: 1. Physiological doses: increase hepatic IR injury 2. Pharmacological doses: reduce hepatic IR injury
Interleukin-1β (IL-1β)	(33,109-114)	Kupffer cells	IP-10 stimulates IL-1β production; PGE1,	↑ hepatocyte NO production via Akt,	Increases hepatic IR injury

			NO, IL-10, & A_{2A} adenosine receptor activation, all inhibit IL-1β production	NF-κB, & iNOS; ↑ ROS production; ↑ leukocyte recruitment & adhesion via activation of NF-κB & MIP-2	
IL-6	(80-83,115)	Kupffer cells	NF-κB & HSF stimulate IL-6 production	Activates STAT-3; ↑ GSH expression, ↓ markers of oxidative stress	Reduces hepatic IR injury and pro-proliferative
IL-10	(84-86,104,114,116-119)	Kupffer cells, T lymphocytes	COX-2-derived prostanoids & IP-10 inhibit IL-10 production	↑HO-1; ↑Bcl-2/Bcl-x; ↓NF-κB; ↓IL-1β; ↓IL-2; ↓IFN-γ; ↓MIP-2; ↓CINC; ↓E-selectin; ↓ neutrophil accumulation	Reduces hepatic IR injury and pro-proliferative
IL-13	(87-90,120)	Kupffer cells, T lymphocytes	Not provided	Inactivates TLR-4; activates STAT-6; ↑HO-1; ↑Bcl-2/Bcl-x; ↑IL-4; ↓IL-1β; ↓IL-2; ↓IFN-γ; ↓MIP-2; ↓E-selectin; ↓neutrophil accumulation	Reduces hepatic IR injury
IL-18	(103,121)	Kupffer cells	A_{2A} adenosine receptor activation inhibits IL-18 production	Activates NF-κB & AP-1; ↓activation of STAT-6; ↑MIP-2; ↓IL-4; ↓IL-10; ↑neutrophil accumulation	Increases hepatic injury
Vascular endothelial	(108,122-125)	Kupffer cells, T	CD154-CD40 co-	Dual action:	Dual action:

growth factor (VEGF)		lymphocytes, SEC, hepatocytes	stimulation	1. Endogenous expression with hepatic IR injury: activation of VEGF receptor and cytosolic SRC tyrosine kinases, ↑ expression of TNF-α, IFN-γ, MCP-1, & E-selectin leading to hepatic accumulation of T-cells, macrophages, and neutrophils. 2. Exogenous administration: iNOS up-regulation.	1. Endogenous expression increases hepatic IR injury. 2. Exogenous administration reduces hepatic IR injury.

*Only the downstream mediators of bFGF were given. No downstream pathways were provided for aFGF.

1.2.5 *Endogenous mediators of inflammation*

1.2.5a Danger associated molecular patterns

Danger associated molecular patterns (DAMPs) are normal physiological molecular constituents of cells or the extracellular environment, that are passively released by necrotic cells or the damaged extracellular matrix; or actively secreted by stressed and injured cells. These molecules have the ability to initiate and propagate the inflammatory response in an analogous manner to the pathogen associated molecular patterns (PAMPs). PAMPs are conserved molecular motifs found in various prokaryotic pathogens but not in mammals, and are therefore recognised as foreign by the cells of the innate immune system in the host, leading to the initiation of an immune response (126). Examples of PAMPs include lipopolysaccharide from Gram negative bacteria, lipoteichoic acid from Gram positive bacteria, and double-stranded RNA from viruses (127). Examples of DAMPs released during liver IR injury include the nuclear transcription factor high mobility group box-1 (HMGB-1) (128,129), the cytoplasmic Ca^{2+} regulator S100 (130), the cell matrix component hyaluronic acid (131), urate and ATP (132). It is also important to note that DAMPs are released during both, infectious states such as severe sepsis or localised purulent infections; and during sterile inflammatory conditions other than IR injury, such as arthritis, burns, and cancer (126). Both DAMPs and PAMPs exert their effects by binding to pattern recognition receptors either on the surface of or in the cytoplasm of mammalian cells.

1.2.5b Pattern recognition receptors (PRRs)

PRRs are constitutively expressed on cells of the innate immune system and function to immediately recognise invading microorganisms by binding to their

associated PAMPs without the need to involve the adaptive immune system. PRRs have the essential function of sensing tissue damage through the recognition of DAMPs on dead and injured host cells. Different PRRs recognise specific PAMPs and DAMPs, show distinct cellular expression patterns, and activate specific signalling pathways culminating in the initiation and propagation of the inflammatory response (133). Broadly speaking, two classes of PRRs have been shown to initiate and propagate the inflammatory responses in liver IR injury; the most extensively studied of these are the toll-like receptors (TLRs) specifically TLR-4. The receptor for advanced glycation end products (RAGE) is the second family of PRRs that has been shown to mediate hepatic IR injury.

TLRs are type 1 transmembrane proteins containing an extracellular amino terminus and an intracellular carboxy terminal domain. The latter includes an IL-1 and an IL-18 receptor – like signalling motif called Toll – IL-1 receptor (TIR) homology domain (134). TLRs that detect DAMPs released during sterile inflammatory conditions of the liver provide an important link between liver parenchymal damage and the activation of the immune system. Eleven human TLRs (TLR-1 to TLR-11) have been identified. An agreed general model of TLR mechanism of action involves engagement of a TLR by its ligand(s) which triggers an intracellular signalling cascade that culminates in the up-regulation of pro-inflammatory cytokines, chemokines, and other mediators of inflammation (134). The cascade begins with the TIR domain on the cytoplasmic portion of the TLR recruiting and activating one or more TIR – containing intracellular adaptors. The type of adaptor recruited broadly defines the subsequent intracellular signalling pathway involved. The adaptor recruited maybe the myeloid differentiation factor 88 (MyD88 –

dependent) which is common to all human TLRs except TLR-3; or non-MyD88 (MyD88 – independent) adaptors. The latter includes TIR domain-containing adaptor protein (TIRAP), TIR domain-containing adaptor inducing interferon β (TRIF), and TRIF-related adaptor molecule (TRAM) (135).

In MyD88-dependent signalling and as a consequence of TLR-2 or TLR-4 activation, TIRAP is recruited to the TLR-MyD88 complex. The TLR-MyD88-TIRAP complex recruits and phosphorylates IL-1 receptor-associated kinase 4 (IRAK4), which then recruits and phosphorylates IRAK1. The activated IRAK1 then dissociates from the MyD88 receptor complex and interacts with TNF receptor-associated factor-6 (TRAF-6), which in turn activates a complex composed of the MAPK kinase kinase transforming growth factor β-activated kinase-1 (TAK-1) and TAK1-binding proteins-1, -2, and -3 (TAB-1, TAB-2, TAB-3). This TAK1-TAB1/2/3 complex leads to the activation of IκB kinase (IKK) and eventually NF-κB nuclear translocation. In addition one or more of the MAPK family members is activated leading to the eventual activation of the transcription factor activator protein 1 (AP-1). The end result is pro-inflammatory cytokine and chemokine gene transcription (133,135). TLR-3 and TLR-4 can transduce their activation through MyD88-independent signalling pathways, culminating in activation of the transcription factors interferon regulatory factors-3 or -2 (IRF-3 or IRF-2), or NF-κB. This leads to the production of type 1 IFN (133,135). Moreover, activation of TLR-7, TLR-8, and TLR-9 also leads to induction of type 1 IFN. Figure 1.3 summarises the MyD88-dependent and –independent signalling pathways downstream of TLR-4 activation. For TLRs that are capable of transducing their signal through more than one pathway such as TLR-4, the factor that determines

which pathway is recruited every time the TLR is activated is the cell type. For example MyD88 signalling exclusively transduces TLR-4 activation in the endothelium since these cells lack TRAM expression (134). However, within a defined cell type the specificity of TLR mediated signalling is determined by a combination of the TLR, the intracellular adaptor, and the intracellular signalling pathway (133).

1.2.5c DAMPs and PRRs in liver IR injury

Only endogenous DAMP signals rather than exogenous PAMP signals are involved in PRR activation in liver IR injury (129,136). The most extensively studied DAMP in liver IR injury is HMGB-1. Liver IR results in a significant increase in serum and hepatic HMGB-1 levels that contribute to hepatocellular damage (129,137). Physiologically, HMGB-1 acts as a regulator of DNA transcription, organisation, and repair. All nucleated cells posses HMGB-1 and will release it passively upon necrosis. In addition, monocytes, macrophages, and dendritic cells can secrete HMGB-1 actively (126). A further function of HMGB-1 involves mediating the increased expression of TLR-4s that is observed in liver IR injury and that leads to hepatocellular damage (138,139). This is at least partially achieved by HMGB-1 acting on liver dendritic cells (140). During the ischaemic phase of liver IR the active secretion of HMGB-1 has been shown to involve TLR4-dependent ROS production and calcium / calmodulin kinase-mediated signalling (141). In a positive feedback cycle, HMGB-1 released during liver IR, binds to and activates TLR-4 receptors (129). Downstream of this DAMP-TLR4 interaction, at least three separate signalling pathways maybe recruited (figure 1.3): 1. NF-κB (142,143); 2. p38 MAPK, JNK, and ERK (114,129,142,143); 3. the sequential activation of IRF-

3→type 1 IFN (e.g. IFN-β)→STAT-1→IP-10 (114,138,144,145). All three of the MAPK families maybe activated by HMGB-1 (129), whilst IP-10 exclusively activates ERK (114). Whatever signalling pathway is utilized, increased production of pro-inflammatory cytokines (TNF-α, IL-1β, IL-12β) and chemokines (IP-10) is the final result (114,129,142,144). TLR-4 receptors on none parenchymal liver cells that are derived from the bone marrow (kupffer and dendritic cells) are preferentially activated in liver IR injury and result in hepatocellular damage (140,143). The hepatocytes do not undergo TLR-4 activation directly by DAMPS but respond to inflammatory mediators produced from the non-parenchymal cells that are directly stimulated by DAMPs (146). The signalling pathway utilising IRF3-type 1 IFN in hepatic IR is down-regulated by HO-1. HO-1 induction blocks the expression of type 1 IFN, the subsequent activation of STAT-1, and the expression of downstream IP-10 (138,144). Furthermore, HO-1 even leads to a reduction in TLR-4 protein levels (147). The mechanisms described hitherto have all been elucidated in direct liver IR models. However in a haemorrhagic shock followed by resuscitation animal model, which is synonymous with systemic IR injury, serum and liver HMGB-1 levels are significantly elevated causing activation of TLR-4s on circulating polymorphonucleocytes. Activated TLR-4s increase ROS production through the NADPH oxidase system. This is achieved through the sequential activation of MyD88-IRAK4-p38 MAPK or MyD88-IRAK4-Akt downstream of TLR-4 (148). In addition, trauma haemorrhage followed by resuscitation results in engagement of TLR-2, TLR-4, and TLR-9 in kupffer cells with subsequent p38 and JNK activation (149). Thus, in hepatic IR injury the signalling pathway(s) mediating the activation of a PRR will at least be partly dependent on the mechanism of the IR.

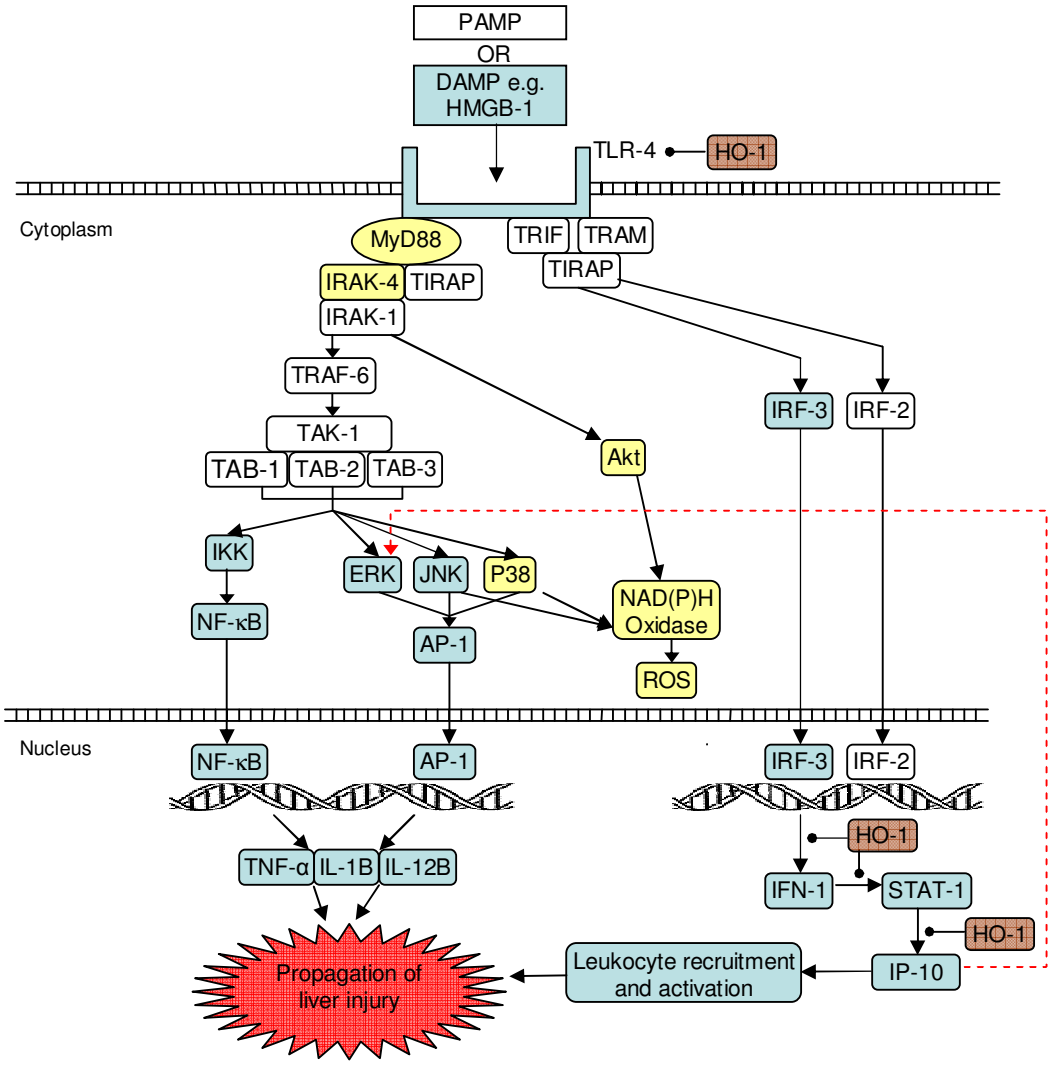

Figure 1.3. General and liver IR injury-related TLR-4 signalling. In non-liver IR injury, ligand engagement of TLR-4 leads to signal transducton through one of two pathways that are known to mediate TLR-4 signalling, a MyD88-dependent and an – independent pathway. The molecules highlighted with blue have been shown to mediate TLR-4 signalling in liver IR injury models. Those highlighted with yellow have been shown to mediate liver injury in haemorrhagic shock followed by resuscitation models, which are synonymous with systemic IR injury. The culmination of either pathway is propagation of liver injury. HO-1 down-regulates TLR-4 expression and blocks various parts of the MyD88-independent pathway. IP-10 activates ERK (dashed red line) and therefore provides a linkage between the MyD88-independent and MyD88-dependent pathways which forms a positive

feedback loop to enhance liver injury through the up-regulation of pro-inflammatory cytokines. *Akt*, protein kinase B; *AP-1*, activator protein 1; *DAMP*, danger associated molecular pattern; *ERK*, extracellular signal regulated kinase; *HMGB-1*, high mobility group box 1; *HO-1*, hemoxygenase-1; *IFN-1*, interferon-1; *IKK*, IκB kinase; *IL-1B/-12B*, interleukin-1B/12B; *IP-10*, inducible protein-10; *IRAK-1/-4*, IL-1 receptor-associated kinase; *IRF-2/-3*, interferon regulatory factor-2/-3; *JNK*, C-Jun N-terminal kinase; *MyD88*, myeloid differentiation factor 88; *NAD(P)H*, reduced nicotinamide adenine dinucleotide phosphate; *NF-κB*, nuclear factor kappa B; *PAMP*, pathogen associated molecular pattern; *P38*, P38 mitogen activated protein kinase; *ROS*, reactive oxygen species; *STAT-1*, signal transducer and activator of transcription-1; *TAB-1/-2/-3*, TAK1-binding proteins-1/-2/-3; *TAK-1*, transforming growth factor B-activated kinase-1; *TIRAP*, TIR domain-containing adaptor protein; *TLR-4*, toll-like receptor-4; *TNF-α*, tumour necrosis factor-α; *TRAF-6*, TNF receptor-associated factor-6; *TRAM*, TRIF-related adaptor molecule; *TRIF*, TIR domain-containing adaptor inducing interferon B.

The receptor for advanced glycation end products (RAGE) is the second family of PRRs that is involved in liver IR injury. Within the liver RAGE is mainly expressed on dendritic cells and to a lesser extent kupffer cells (150,151). Hepatic IR leads to increased expression of RAGE and engagement of these receptors by endogenous DAMPs such as HMGB-1 with consequent hepatocellular injury (150,151). HMGB-1 binding to RAGE in the setting of liver IR leads to a signalling cascade involving the activation of JNK / ERK, which increase the expression and activation of the inducible transcription factor early growth response-1 (Egr-1). Egr-1 acts as a coordinating up-regulator of divergent gene families affected by stress, that in the setting of hepatic IR includes MIP-2 that functions to recruit immune cells into the post ischaemic liver (151). Engagement of RAGE by other DAMPs results in the activation of other intracellular mediators of inflammation such as p38 MAPK, and

the transcription factors STAT-3 and AP-1, with a consequent increase in pro-inflammatory cytokines such as TNF-α (150) (figure 1.4).

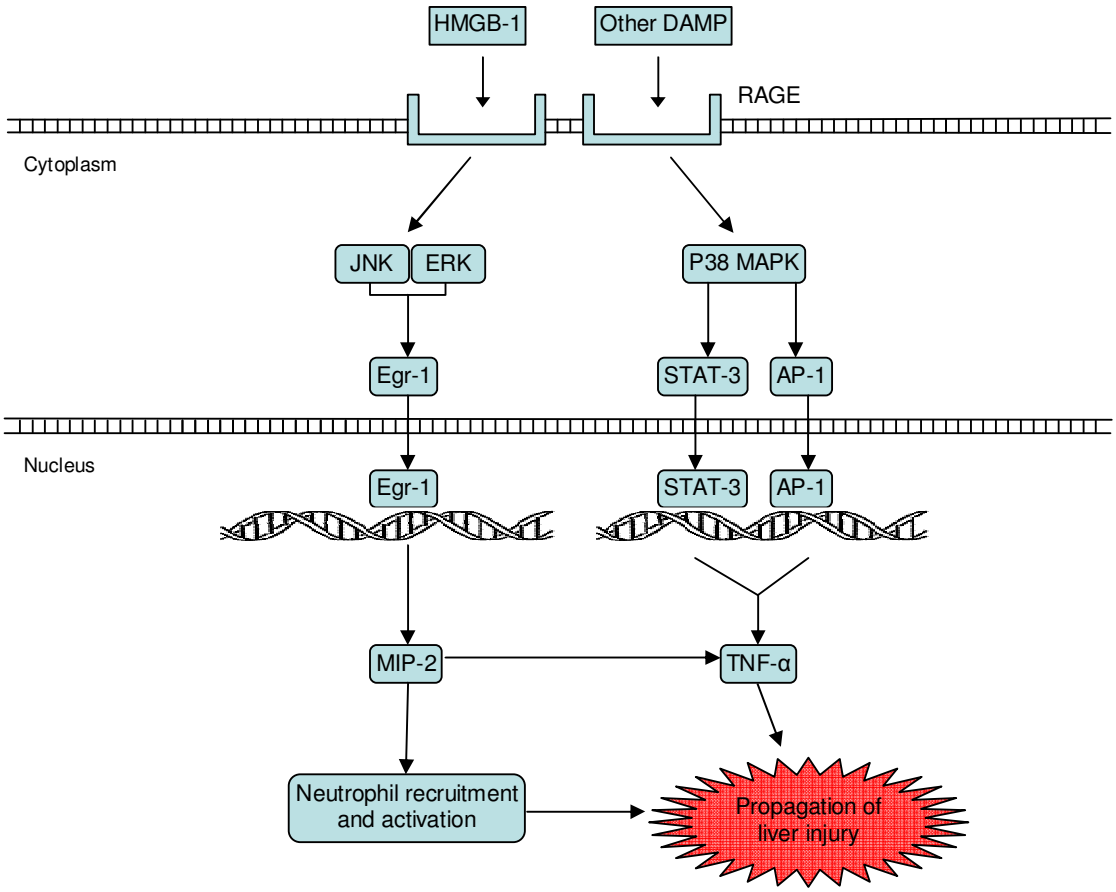

Figure 1.4. RAGE signalling in liver IR injury. Engagement of RAGE by one of its ligands leads to signal transduction through one of two pathways. The end result of both pathways is activation of transcription factors that increase expression of the chemokine MIP-2 and the cytokine TNF-α. These two mediators are pro-inflammatory and act to propagate the liver injury further. *AP-1*, activator protein-1; *DAMP*, danger associated molecular pattern; *Egr-1*, early growth response-1; *ERK*, extracellular signal regulated kinase; *HMGB-1*, high mobility group box-1; *JNK*, C-Jun N-terminal kinase; *MIP-2*, macrophage inflammatory protein-2; *P38 MAPK*, P38 mitogen activated protein kinase; *RAGE*, receptor for advanced glycation end products; *STAT-3*, signal transducer and activator of transcription-3; *TNF-α*, tumour necrosis factor-α.

1.2.6 *Mitochondria*

Physiologically, the primary function of the mitochondria is maintenance of a continuous supply of ATP to meet the cell's energy requirements. In addition, the mitochondria is involved in numerous other physiological processes, such as steroid and lipid synthesis, metabolic control of cell-cycle progression, intracellular ions regulation, cellular growth and differentiation, signalling, cytokine production, and embryonic development (152). In IR injury, the mitochondrion participates in various pathophysiological processes. There is failure of ATP production as a consequence of disruption of oxidative phosphorylation caused by the generation of and damage by ROS, RNS, and free radicals. Cytosolic ionic ($[Ca^{2+}]$ $[Na^{+}]$ $[H^{+}]$) disturbances lead to mitochondrial ionic disturbances, and vice versa, with consequent plasma and mitochondrial membrane damage, including the formation of mitochondrial permeability transition (MPT) pores.

1.2.6a ROS, RNS, and free radicals

Reactive oxygen species (ROS) are molecules or ions formed by the incomplete one-electron reduction of oxygen. Reactive nitrogen species (RNS) are nitrogenous products of nitric oxide synthase. A free radical is any atom or molecule with unpaired electrons in one or more valence shells (153). The terms ROS and RNS encompass free radicals. The physiopathologically important ROS include $O_2^{\cdot -}$ (superoxide anion), H_2O_2 (hydrogen peroxide), $^{\cdot}OH$ (hydroxyl radical), and HCLO (hypochlorous acid). The equivalent biologically important RNS include NO (nitric oxide), NO_2 (nitrogen dioxide), N_2O_3 (dinitrogen trioxide), and $ONOO^{-}$

(peroxynitrite). Out of these, $O_2^{\cdot -}$, $^{\cdot}OH$, NO, and NO_2 constitute the free radical species (153,154).

The main intracellular mechanisms for producing ROS are the xanthine oxidase, mitochondrial respiratory chain, and NADPH oxidase systems. Xanthine dehydrogenase (XD) is a dehydrogenase enzyme, meaning it uses the co-enzyme nicotinamide adenine dinucleotide (NAD^+) as an electron acceptor during its normal function of oxidising hypoxanthine and xanthine to uric acid. However, during ischaemia intracellular proteases are activated, leading to proteolytic modification of XD to yield xanthine oxidase (XO). XO does not bind NAD^+ and therefore electrons are transferred to O_2 with subsequent production of $O_2^{\cdot -}$ (155). The mitochondrial respiratory chain is involved in the production of ROS via various pathways. Physiologically, a small fraction of the electrons entering the respiratory chain are passed onto O_2 from ubisemiquinone to form $O_2^{\cdot -}$. Some of the $O_2^{\cdot -}$ is dismutated into H_2O_2 by the antioxidant superoxide dismutase present in the mitochondrial matrix (MnSOD). H_2O_2 is able to diffuse out of the mitochondria to participate in intra- and intercellular signalling. In addition H_2O_2 directly oxidises protein thiols and mediates the formation of disulfide bonds. Similarly, complexes I and III are also involved in physiological ROS production within the mitochondria. Following cytochrome C inhibition by mitochondrial NO, complexes I and III are reduced which subsequently act as reducing agents of O_2 to generate $O_2^{\cdot -}$ (154). During IR injury mitochondrial K_{ATP} channel opening increases $O_2^{\cdot -}$ generation by complex I

(156). Furthermore, 'ROS-induced ROS release' or RIRR is a recently described phenomenon involving the mitochondria. When ROS production reaches a threshold level, the MPT pore or the inner membrane anion channels, or both, are opened leading to loss of mitochondrial membrane potential with subsequent cessation of electron flow in the respiratory chain and increased ROS production by complexes I-III (157). With a disrupted mitochondrial membrane a large amount of ROS is released into the cytosol that may induce RIRR in adjacent mitochondria. Thus, this mechanism of ROS production may act as a self-perpetuating cycle leading to mitochondrial and cellular destruction (157). The NADPH oxidase system is a membrane-associated enzyme complex which normally functions to produce ROS to kill invading microbes. It is the predominant ROS – generating system in neutrophils and kupffer cells. This system generates $O_2^{\cdot -}$ from NADPH oxidase itself, H_2O_2 from SOD, and HCLO from the enzyme myeloperoxidase (155,158). All three systems (XO, mitochondrial respiratory chain, NADPH oxidase) of intracellular ROS production are utilized by the remaining cell types found in the liver, namely SEC and hepatocytes, to generate ROS (155). Other ROS species such as the $^{\cdot}OH$ radical is produced when $O_2^{\cdot -}$ or H_2O_2 interact with certain transition metals, for example iron or copper. Additionally, ROS may also interact with haem proteins, for example haemoglobin or the cytochromes to produce the porphyrin cationic radical ($^{+}$.HP-Fe^{4+}) (158).

NO is produced by the enzyme nitric oxide synthase (NOS) which has three isoforms. Endothelial NOS (eNOS) is a constitutive enzyme expressed in vascular endothelial cells. The expression of the inducible NOS (iNOS) isoform is up-

regulated in inflammatory conditions, including IR injury, and is expressed by all nucleated cells. The neuronal NOS (nNOS) is a constitutive isoform, the expression of which is mostly restricted to the nervous tissue and few other tissues. NO reacts with superoxide and molecular oxygen to produce the remaining biologically important RNS species in the following reactions (159):

$$NO + O_2^{\cdot -} \rightarrow ONOO^-$$

$$2NO + O_2 \rightarrow 2NO_2$$

$$NO_2 + NO \rightarrow N_2O_3$$

A further mechanism which increases NO and therefore RNS production involves ROS. Superoxide radicals have been shown to increase iNOS gene expression in IL-1β – treated hepatocytes. This effect is mediated by a redox-sensitive response element, termed antioxidant response element (ARE), located in the iNOS gene promoter (160). ARE has been shown to bind a redox-sensitive nuclear protein, that has not yet been characterised (160).

ROS and RNS play a dual role in liver IR injury. They may contribute to the injury of the various cell types found in the liver, leading to both apoptotic and necrotic cell death. Alternatively they may function to protect the liver from the deleterious effects of IR injury by the process of preconditioning. Their exact role is likely to be dependent on multiple factors, including the length of the ischaemic and reperfusion periods, in vitro versus in vivo experimental models, and exogenous versus endogenous sources of ROS or RNS. ROS contribute to liver IR injury by multiple mechanisms. ROS cause oxidative damage to membrane lipids (lipid peroxidation),

especially polyunsaturated fatty acids, which result in disturbances in ion homeostasis, cell swelling and death (155). The damage sustained is not limited to the plasma membrane but also extends into the intracellular compartment to encompass all membrane-bound organelles; for example the mitochondrion and the nucleus. In addition, within the mitochondria, ROS can cause oxidative damage to the enzyme complexes of the respiratory chain leading to failure of ATP production and release of cytochrome C into the cytosol triggering apoptosis (161,162), and within the nucleus the DNA can be oxidatively damaged resulting in failure of protein transcription and translation (163). Antiproteases can also sustain ROS damage leading to their inactivation which allows inappropriate activation of proteases to inflict cellular damage. Kupffer cells and neutrophils generate ROS into the extracellular space through the antimicrobial NADPH oxidase system. Some of these ROS species such as hydrogen peroxide and hypochlorous acid are capable of diffusing through the plasma membrane of hepatocytes and SEC to inflict intracellular oxidative damage. ROS can also activate the redox-sensitive transcription factors, namely NF-κB and AP-1 (75,164). Amongst their functions NF-κB up-regulates pro-inflammatory cytokines like TNF-α (165), and AP-1 promotes hepatocyte apoptosis through cytochrome C release and caspase-3 activation (75). RNS inflict their damage by any of the mechanisms described for ROS, and in addition they cause post translational protein modifications that may result in the inactivation or introduction of a new function to a protein (166,167). A detailed discussion of the molecular biology of RNS and their redox reactions is beyond the scope of this review but can be found elsewhere (168,169).

1.2.6b Ionic disturbances

Intracellular Ca^{2+} plays an important physiological role in regulating the hepatocyte's function in response to extracellular signals such as hormones and growth factors. Ca^{2+} is mainly found in three cellular compartments, the cytosol, the mitochondria, and the endoplasmic reticulum (ER). The interplay of Ca^{2+} movement across the membranes of these structures determines the temporal and spatial distribution of $[Ca^{2+}]$ in the three compartments. Within each of these compartments Ca^{2+} has various functions. That of the cytosol is by far the most diverse ranging from cellular contraction to proliferation to modulation of numerous intracellular signalling pathways (170). The ER Ca^{2+} stores represent a mechanism to regulate $[Ca^{2+}]_{cytosol}$. Mitochondrial Ca^{2+} has three main functions: regulation of metabolism (ATP production), stimulation of apoptosis, and regulation of $[Ca^{2+}]_{cytosol}$ (171). In order to understand the pathological disturbances of Ca^{2+} homeostasis in liver IR injury, it is important to have a good comprehension of the various mechanisms that control Ca^{2+} movement across the membranes of the three Ca^{2+}-regulating cellular compartments (summarised in table 1.3).

Table 1.3 Physiological Ca^{2+} pathways in the plasma, mitochondrial, and ER membranes of hepatocytes.

Ca^{2+} pathway	Membrane location	Main regulating signal(s) of Ca^{2+} movement	Direction of Ca^{2+} movement	Ref.	Role in IR
Ligand gated Ca^{2+} channels	Plasma	Extracellular signalling molecule (e.g. hormone, growth factor) binds to receptor on extracellular domain of Ca^{2+} channel	From extracellular space to cytosol	(172,173)	√
Store operated Ca^{2+} (SOC) channels	Plasma	Activated by a decrease in $[Ca^{2+}]$ in ER	From extracellular space to cytosol	(172)	√
Receptor activated Ca^{2+} channels	Plasma	Extracellular signalling molecule (e.g. hormone, growth factor) binds to G-protein or tyrosine kinase coupled receptor, leading to generation of second messengers that bind to the cytoplasmic domain of the Ca^{2+} channel that is separate from the receptor	From extracellular space to cytosol	(172,173)	√
Stretch activated Ca^{2+} channels	Plasma	Mechanical force applied to hepatocytes leads directly to Ca^{2+} channel opening	From extracellular space to cytosol	(172)	√
Ca^{2+} ATPase	Plasma	Inhibited by low $[Ca^{2+}]_{cytosol}$ and by hormones (vasopressin, epinephrine, angiotensin II, PTH, calcitonin, endothelin B) through a mechanism that involves activation of G-proteins	From cytosol to extracellular space	(174)	√
Na^+ / Ca^{2+} exchanger	Plasma	The Na^+ and Ca^+ gradients across the plasma membrane. In the heart, the Na^+ / Ca^+ exchanger is regulated by phosphorylation by protein kinase A (PKA) and C (PKC), which in turn are activated by numerous extracellular signals (e.g. hormones)	Normally extrudes Ca^+ into extracellular space but may act in reverse if Na^+ / Ca^+ gradient is altered, e.g. if $[Na^+]_{extracellular}$ is decreased massively	(175,176)	
Ca^{2+} ATPase	ER	SOC stimulation and raised $[Ca^{2+}]_{cytosol}$	From cytosol into lumen of ER	(174)	√

Inositol triphosphate (IP_3) and Ryanodine receptors	ER	Extracellular signalling molecule (e.g. vassopressin, ADP, angiotensin II, noradrenalin) binds to plasma membrane G-protein coupled receptor leading to production of phospholipase C (PLC). PLC produces IP_3 and diacylglycerol (DAG) which stimulate IP_3 and ryanodine receptors, resulting in Ca^{2+}release into the cytosol	From ER to cytosol	(174,177)	√
Na^+ / Ca^{2+} exchanger	Inner mitochondrial	Mitochondrial transmembrane potential across the inner membrane ($m\Delta\Psi$), and cytosolic [Na] and [Ca^{2+}]. Other cations either stimulate (K^+) or inhibit (Mg^{2+}, Ba^{2+}, Ni^{2+}) the activity of the exchanger	Extrudes Ca^{2+} into the cytosol from mitochondrial matrix in exchange for cytosolic Na^+. Can act in reverse if mitochondrial membrane potential is depolarised	(178,179)	
H^+ / Ca^{2+} exchanger	Inner mitochondrial	Mitochondrial transmembrane chemical (pH) gradient, and $[Ca^{2+}]_{cytosol}$	Extrudes Ca^{2+} into the cytosol from mitochondrial matrix	(179)	
Ca^{2+} uniporter channel	Inner mitochondrial	Cytosolic [Ca^{2+}] and $m\Delta\Psi$. Mitochondrial purinergic – like (mP2Y) receptors regulate Ca^{2+} flow through the uniporter. Specifically $mP2Y_1$ are activated by ADP and AMP and lead to increased mCa^{2+} uptake; $mP2Y_2$ are activated by ATP and leads to inhibition of mCa^{2+} uptake. Both P2Y receptors use PLC to regulate mCa^{2+} uptake through the uniporter	From cytosol to mitochondrial matrix	(180-182)3	√

Liver IR injury leads to disturbances in the Ca^{2+} regulating mechanisms in the plasma, ER, and inner mitochondrial membranes (figure 3). The consequence is Ca^{2+} overload in the cytosol and mitochondrial matrix (183-185). The rise in cytosolic [Ca^{2+}] results from a combination of increased Ca^{2+} entry across the plasma membrane as well as Ca^{2+} release from ER stores. This is brought about by the activation of SOC channels in the plasma membrane and ryanodine receptors in the ER membrane (186,187). How these channels and receptors are activated is not clear. However, there is evidence that ROS and RNS can activate some Ca^{2+}-permeable non-selective cation channels – the so called transient receptor potential (TRP) channels (188). TRP channels include some ligand gated, receptor activated, and stretch activated Ca^{2+} channels (see table 1.3) (172). Specifically the TRPM7 channel subtype is found in liver cells, and ROS and RNS can activate these channels leading to Ca^{2+} influx from the extracellular space into the cytosol (188,189). In addition, cold ischaemic injury inhibits both the plasma membrane and ER Ca^{2+} ATPases, which normally function to extrude cytosolic Ca^{2+} into the extracellular space and ER lumen respectively, thereby compounding the rise in $[Ca^{2+}]_{cytosol}$ (185).

The rise in cytosolic Ca^{2+} during liver IR injury leads to a secondary rise in mitochondrial Ca^{2+} (mCa^{2+}) (183). This is a consequence of stimulation of the mitochondrial Ca^{2+} uniporter (190,191). How these Ca^{2+}-selective channels are activated in IR injury hasn't been fully elucidated but probably involves the PLC – dependent mP2Y – like receptors that regulate Ca^{2+} flow through the mCa^{2+} uniporter (192,193). $mP2Y_1$ are activated by ADP and AMP and lead to stimulation of Ca^{2+} uptake by the uniporter. $mP2Y_2$ are activated by ATP, ADP, and AMP and

lead to the inhibition of the uniporter. During the ischaemic phase of IR injury, there is a relative decrease in $[ATP]_{cytosol}$ and an increase in $[AMP \text{ and } ADP]_{cytosol}$ resulting in an overall increase in the activity of the Ca^{2+} uniporter and therefore in mitochondrial $[Ca^{2+}]$ (181). This increase in mitochondrial $[Ca^{2+}]$ results in a reduction of the mitochondrial transmembrane potential ($m\Delta\Psi$). In response, and in order to maintain $m\Delta\Psi$, ATP-synthase reverses its activity and hydrolyses ATP to provide energy for the various ionic pumps in the mitochondrial membrane that maintain the mitochondrial potential. This results in partial restoration of $m\Delta\Psi$, which in turn leads to a further increase of Ca^{2+} inflow through the mCa^{2+} uniporter. Therefore a cycle of increasing mCa^{2+} overload and ATP depletion (as the mitochondria become a net consumer of ATP during ischaemia as a consequence of the reversed activity of ATP synthase) is established (183). The mCa^{2+} overload leads to Bax translocation from the cytosol to the mitochondria and subsequent MPT pore formation, cytochrome C release, and cellular death (190,194).

Sodium (Na^+) and hydrogen (H^+) ions also have important functions in determining the liver's response to IR insults. Hepatic ischaemia results in intracellular acidosis through anaerobic respiration (195,196). To restore intracellular pH towards normal, the liver cells activate the Na^+ / H^+ exchanger (NHE) and the Na^+ / HCO_3^- cotransporter (NHCT) (197) (figure 1.5). The NHE extrudes H^+ into the extracellular space in exchange for Na^+ inflow into the cell. The NHCT transports Na^+ and HCO_3^- intracellularly. Both these mechanisms of correcting the ischaemically-induced intracellular acidotic pH result in intracellular Na^+ accumulation. It is the increase in intracellular $[Na^+]$ ($[Na^+]_i$) secondary to intracellular acidosis that contributes to cellular death. Intracellular acidosis per se is actually cytoprotective (198,199).

Support for this finding comes from five experimental observations. Firstly, blocking the function of the NHE and the NHCT protects against hepatic IR injury (195,200). Secondly, in vitro experiments using Na^+-free incubation buffers results in hepatocyte and SEC protection by inhibiting the rise in $[Na^+]_i$ (198,199). Thirdly, IPC protects hepatocytes by the activation of vacuolar (H^+)-ATPase (V-ATPase) which lead to H^+ extrusion from the cells, with a subsequent decrease in intracellular $[Na^+]$ (201). Fourthly, maintenance of an acidotic pH at reperfusion, results in a decrease in $[Na^+]_i$ and cellular protection, a phenomenon known as the 'pH paradox' (199,200,202). Fifthly, ischaemia – induced hepatocyte death is a result of ATP depletion with subsequent inhibition of the Na^+ / K^+ ATPase and an increase in $[Na^+]_i$ (197,200). The question as to how increased $[Na^+]_i$ promotes, and decreased $[H^+]_i$ inhibit cellular death in liver IR injury is not fully resolved. Two experimental observations have been reported that shed light on this. The first is that $[Na^+]_i$ accumulation does not lead to hepatocyte death by promoting cellular swelling (198); and the second is that maintenance of an acidotic pH at reperfusion prevents the formation of MPT pores (196,199). Further research is needed to fully explain how $[Na^+]_i$ and $[H^+]_i$ mediate their respective action in hepatic IR injury.

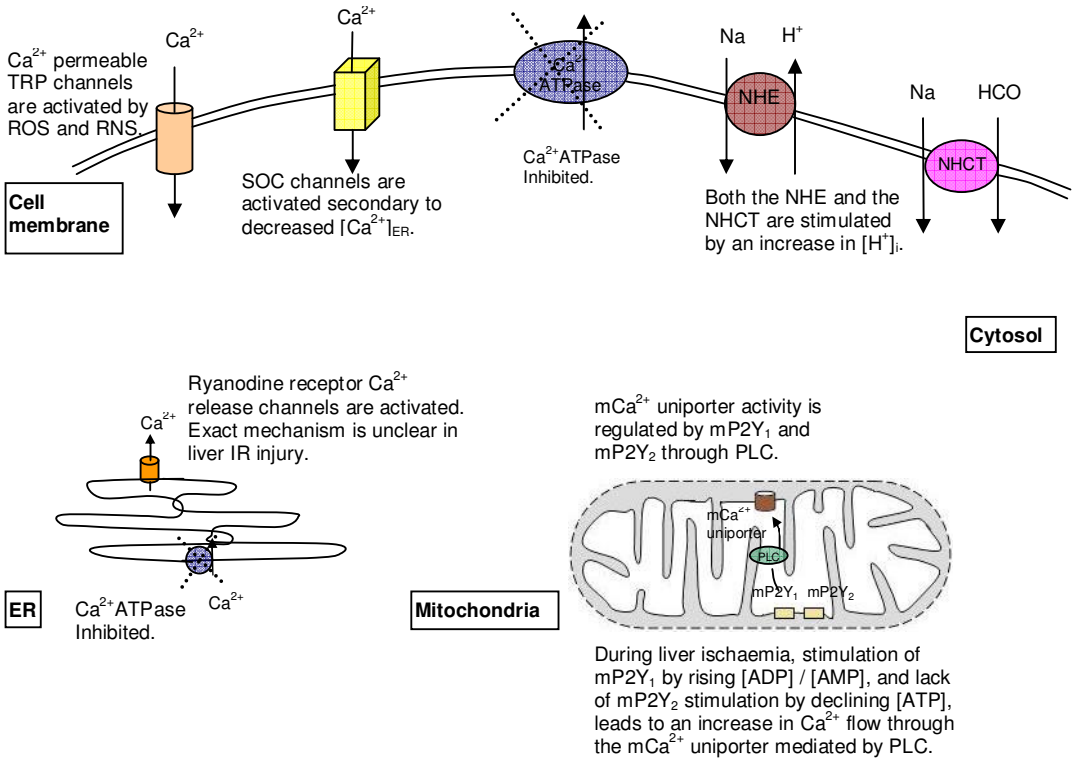

Figure 1.5. Ionic disturbances in liver IR injury. The perturbations of membrane-associated ion channels, pumps, and carriers results in an increase in cytosolic [Ca2+] and [Na+], and mitochondrial [Ca2+] that have important consequences in promoting cellular injury – see main text. *AMP / ADP / ATP*, adenosine mono / di / tri-phosphate; *Ca2+*, calcium ions; *ER*, endoplasmic reticulum; *H+*, hydrogen ions; *HCO3-*, bicarbonate; *mP2Y*, mitochondrial purinergic-like receptors; *Na+*, sodium ions; *NHCT*, Na+/HCO3- cotransporter; *NHE*, Na+/H+ exchanger; *PLC*, phospholipase C; *RNS*, reactive nitrogen species; *ROS*, reactive oxygen species; *SOC*, store operated Ca2+; *TRP*, transient receptor potential.

1.2.6c Mitochondrial permeability transition

The mitochondria is surrounded by a double membrane. The outer mitochondrial membrane (OMM) is significantly more permeable than the inner mitochondrial membrane (IMM). This is due to the presence of voltage-dependent anion channels (VDAC) in the OMM that non-selectively permit the passage of solutes up to 5 kDa. Under normal physiological conditions the IMM is permeable to solutes only through specific exchangers, channels, and transporters. However, under certain circumstances such as IR injury, the IMM becomes non-selectively permeable to molecules up to 1500 Da, resulting in mitochondrial depolarization and collapse of the $m\Delta\Psi$, uncoupling of oxidative phosporylation, and mitochondrial swelling due to colloid osmotic forces that lead to the release of pro-apoptotic factors such as cytochrome C. These changes are known as the MPT (196). The MPT is due to the formation and opening of pores, with an average diameter of 3 nm when fully opened, through the IMM. It used to be thought that these pores are formed from VDAC in the OMM, adenine nucleotide transporter (ANT – responsible for exchanging ADP/ATP across the IMM) in the IMM, and cycolphilin D (CycD – a mitochondrial matrix protein) in the matrix. However this model did not explain experimental observations such as why ANT knockout mice still undergo MPT (203). The current prevailing hypothesis is that the MPT is formed from integral mitochondrial membrane proteins, that as a consequence of modifications by ROS and by reactive chemicals, lead to exposure of hydrophilic residues in the protein to the hydrophobic membrane environment, and as a result the proteins aggregate at these hydrophilic residues to form channels that conduct aqueous solutes (204,205) (figure 1.6). The identity of proteins in the MPT pores is not known for certain but is thought to include misfolded ANT and anion transporters such as aspartate-

glutamate and phosphate carriers (206). The MPT pore protein composition is not consistent but depends on the relative abundance of the misfolded proteins. Therefore even in ANT deficient mitochondria, MPT pore formation can still occur (206). Moreover, two conductance modes of MPT pores are thought to be operational depending on the number of misfolded proteins and therefore on the number of pores formed. In the regulated conductance mode the MPT pores associate with chaperone-like proteins, including CycD on the inner surface of the IMM (figure 1.6). These proteins serve to inhibit conductance through the MPT pores. When the number of newly formed MPT pores exceeds the number of chaperones available then unregulated pore opening occurs (207). CycD confers Ca^{2+}, ROS, and cyclosporine A sensitivity on pore conductance (208). A rise in matrix [Ca^{2+}] increases, and cyclosporine A inhibits pore opening. Many other factors influence opening of and therefore conductance through the pores (209). Aside from Ca^{2+}, other divalent cations such as Mg^{2+}, Sr^{2+}, and Mn^{2+} inhibit pore opening. H^{+} (and therefore acidotic pH) inhibit pore opening by the reversible protonation of histidyl residues, thereby explaining why maintenance of acidosis at reperfusion of ischaemic hepatocytes significantly decreases cellular death (199). ROS induce pore opening. Inorganic phosphate (Pi) plays a dual role in regulating MPT pore opening. In the mitochondrial matrix Pi binds H^{+} and Mg^{2+} blocking their pore – inhibitory effect, and resulting in pore opening. On the other hand Pi can bind to MPT pores directly leading to inhibition of pore opening only when CycD has been ablated or in the presence of cyclosporine A which inhibits CycD activity. This is because it is thought that active CycD normally binds to the Pi – binding sites on the MPT pores thereby preventing Pi binding. In the absence or inactivation of CycD, Pi binds to and inhibits the opening of MPT pores (209).

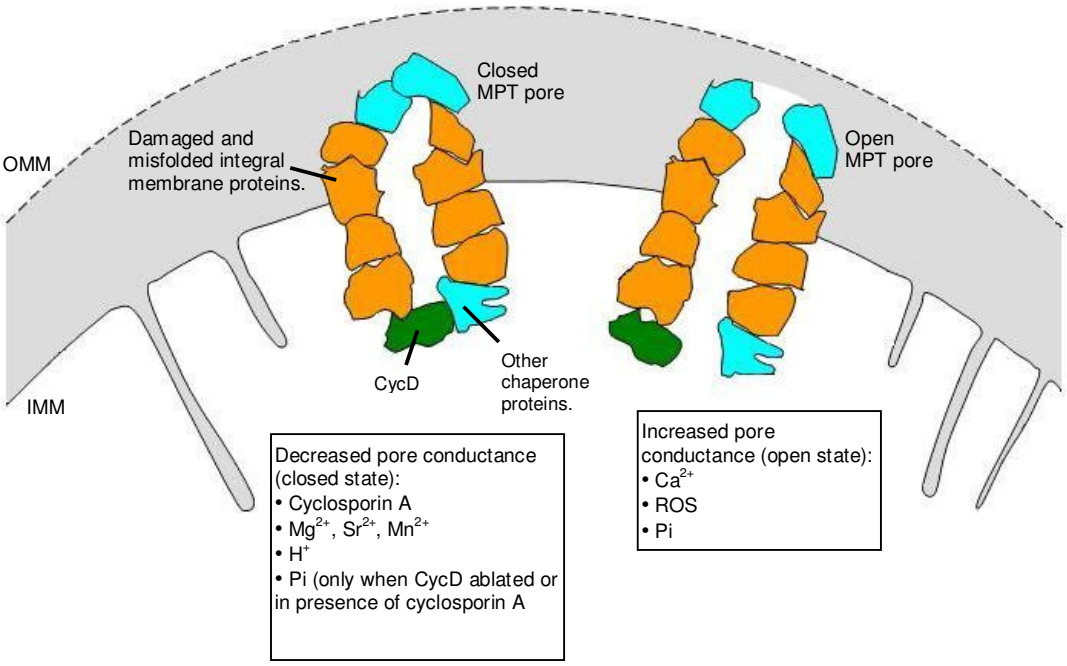

Figure 1.6. Current model of MPT pore structure and function. A cross section of the mitochondrial double membrane illustrating damaged integral mitochondrial membrane proteins that misfold and aggregate at their hydrophilic residues to form aqueous pores through the IMM. The conductance through the pores is inhibited by CycD and other chaperone proteins. These are in turn regulated by other ions and molecules as described in the figure. The fenestrations in the OMM denotes the high physiological conductivity of this membrane. *Ca2+*, calcium ions; *CycD*, cyclophilin D; *H+*, hydrogen ions; *IMM*, inner mitochondrial membrane; *Mg2+*, magnesium ions; *Mn2+*, manganese ions; *MPT*, mitochondrial permeability transition; *OMM*, outer mitochondrial protein; *Pi*, inorganic phosphate; *ROS*, reactive oxygen species; *Sr2+,* strontium ions.

The end result of MPT depends on the number of mitochondria affected and therefore cellular ATP levels. When mitochondria within a hepatocyte are afflicted by MPT then these mitochondria are depolarised and are permanently damaged. When the number of these dysfunctional mitochondria is small then the hepatocyte removes these by the process of mitophagy (210). Mitophagy is the process of sequestration of mitochondria into autophagosomes and their delivery to lysosomes for degradation. This is an important process for cells, as damaged mitochondria are a source of accelerated ROS production and ATP consumption (211,212). As the number of mitochondria undergoing MPT rises, with relative preservation of cellular ATP levels, apoptotic cell death occurs due to cytochrome C release and subsequent formation of the ATP – dependent apoptosome (213). As the majority of the hepatocyte's mitochondria undergo MPT, the ATP levels plummet, causing cell death by necrosis (196,214,215). In summary, with an increasing number of mitochondria undergoing MPT the hepatocyte's graded response is:

$$\text{Mitophagy} \rightarrow \text{Apoptosis} \rightarrow \text{Necrosis}$$

Whilst in the preceding discussion, the majority of the experimental data supports the observation that IR resulting in MPT leads to mitophagy, there has also been recent work showing that on the contrary, anoxia / reoxgenation of cultured hepatocytes which results in MPT does not cause mitophagy but leads to accumulation of dysfunctional mitochondria (216) that are the source of increased ROS production and subsequent mitochondrial damage, including mitochondrial DNA damage (212). The discrepancy in whether IR with subsequent MPT formation results in mitophagy maybe due to differences in the models used such as in vitro versus in vivo settings. This discrepancy along with the fact that the molecular constituents of the MPT pores have not been discovered, seek to highlight the need

for much more research in this field to better characterise the main players and their interrelationships in MPT pore formation and control of conductance.

1.2.7 *Conclusions and future directions*

Despite two decades of research into the pathophysiological basis of liver IR, many questions remain unanswered. The complex interactions woven by each of the cellular contributors is only just beginning to be mapped. The function of different TLRs and their respective DAMPs is a relatively new field of research about which little is known. The detrimental means by which disturbances of the homeostatic concentrations of Ca^{2+}, Na^{+}, and H^{+} arise, and the pathways mediating the consequences of these disturbances are incompletely understood. The structure and regulation of conductance of MPT pores in liver IR injury is poorly characterised and warrants further research. Only by understanding the action of these factors and how they interact with each other will it be possible to design therapeutic strategies to ameliorate liver IR injury.

1.3 Strategies to reduce liver IR injury

Over the past two decades extensive research has gone into attempting to better understand the molecular pathophysiology that underlies both the ischaemic and reperfusion phases of liver IR injury and that culminate in cellular death. Understanding these processes will pave the way for the development of new therapeutic strategies to ameliorate the effects of IR. The current strategies, albeit mostly limited to experimental settings, revolve around three methods: in situ cooling, pharmacological interventions, and ischaemic preconditioning (IPC). The first two of these strategies, in situ cooling and pharmacological preconditioning, are

beyond the scope of this thesis and will not be discussed here in detail. Suffice to say that in situ cooling, which is performed when total vascular exclusion (TVE) of the liver is required during surgical resection, has been shown clinically and experimentally, to significantly reduce liver IR injury compared to resections performed under TVE without in situ cooling (217-220). A large number of pharmacological agents have been investigated and shown to ameliorate liver IR injury in experimental settings, summarised by Iniguez *et al* (221). However, systematic reviews and meta-analysis of human randomised clinical trials of pharmacological interventions in liver resections performed under vascular occlusion have failed to show clear benefits for any pharmacological agent in reducing clinical liver IR injury (222,223).

IPC involves subjecting an organ to brief ischaemic stimuli that afford the same organ, protection against subsequent prolonged ischaemic insults. IPC has been shown to be beneficial in many organs including the liver, heart, brain, kidneys, intestine, and skeletal muscle (224,225). IPC is the only strategy that has reached clinical practice in some centres. A variation on IPC is remote IPC (RIPC) which involves a brief ischaemic stimulus to one organ that affords protection against a subsequent sustained ischaemic insult to a second organ that is at a distance from the first organ. RIPC is known to exist across multiple organ combinations. The following two subsections will summarise our current understanding of preconditioning non-liver organs that subsequently protect the liver against IR injury (subsection 1.3.1), and the evidence that nitric oxide plays a role in mediating the beneficial effects of RIPC of one organ against IR injury of a second distant organ (subsection 1.3.2).

1.3.1 *Mechanisms of remote ischaemic preconditioning protection against liver IR injury*

Four publications have evaluated the mechanisms underlying the protective effects of RIPC on liver IR injury. The findings of each of these studies will now be discussed in turn.

Wang *et al* (226) applied an elastic band around the thigh for 10 minutes to induce hindlimb ischaemia followed by 10 minutes reperfusion in a mouse model. The liver IR protocol consisted of 1 hour partial hepatic ischaemia and up to 4 hours of reperfusion. Their results demonstrated significant reductions in liver IR injury in the RIPC + IR compared to the IR alone group. The mechanisms underlying the protection afforded by RIPC were further explored in this study, and through the use of transgenic mice expressing mutant TLR-4 receptors, they were able to demonstrate that hindlimb RIPC require functional TLR-4 receptors to exert its protective effect. Moreover, HMGB-1 levels increase following RIPC; injection of HMGB-1 into mice with functional but not into mice with mutant TLR-4 receptors protected against liver IR; and injection of anti-HMGB-1 antibodies prior to RIPC reversed its protective effects (226). The conclusion of this study was RIPC reduces liver IR injury through the release of HMGB-1 that act on TLR-4 receptors.

The work described by Kanoria *et al* (227) consisted of a rabbit model with hindlimb RIPC achieved through the use of a tourniquet to induce 3 cycles of 10 minutes ischaemia followed by 10 minutes reperfusion. Liver IR consisted of total hepatic inflow occlusion for 25 minutes followed by 2 hours reperfusion. The RIPC + IR group had significant improvements in liver IR injury compared to the IR alone

group. This study evaluated the effect of RIPC on the haemodynamics and showed RIPC + IR preserves total hepatic blood flow at the end of the 2 hour reperfusion period compared to IR. Similarly the RIPC + IR group had significantly higher mean arterial pressure and peripheral oxygen saturation at the end of 2 hours liver reperfusion compared to IR alone (227). The conclusion from this work is that RIPC offers liver protection, at least partially, through preservation of haemodynamic parameters.

The experiments by Lai *et al* (228) described hindlimb RIPC consisting of 4 cycles of 10 minutes femoral artery clamping followed by 10 minutes reperfusion. The liver IR protocol consisted of partial liver ischaemia for 45 minutes followed by 4 hours reperfusion. RIPC + IR group had significantly less liver IR injury compared to the IR alone group. Hindlimb RIPC also resulted in a significant increase in the expression and activity of hepatic HO-1 with no increase in circulating lymphocyte HO-1 expression. Zinc protoporphyrin IX (a specific inhibitor of HO enzymatic activity) reversed the effects of RIPC on liver IR injury and enzymatic activity (228). The conclusion being that the protective signal from the RIPC site acts through the HO-1 pathway within the liver.

The final study by Tapuria *et al* (229) used a specially designed tourniquet to induce 4 cycles of 5 minutes ischaemia followed by 5 minutes reperfusion in the rat hindlimb. Liver IR consisted of 45 minutes of partial hepatic ischaemia and 3 hours reperfusion. This RIPC protocol resulted in a significant reduction of liver IR injury in the RIPC + IR compared to the IR alone group. Whilst this study did not investigate the signal that transmits the protective effects from the RIPC site to the

liver, it did evaluate the intrahepatic consequences of hindlimb RIPC. The study demonstrated RIPC + IR had significantly higher hepatic sinusoidal RBC velocity, sinusoidal blood flow, and sinusoidal perfusion compared to the IR group. Moreover, sinusoidal neutrophil adhesion and hepatocellular death were significantly less in the RIPC + IR compared to the IR group (229). The conclusion from these results was that hindlimb RIPC modulates the hepatic microcirculation to reduce the effects of hepatic IR injury.

1.3.2 *Nitric oxide as a mediator of the beneficial effects of remote ischaemic preconditioning on IR injury*

A summary of the published studies that have evaluated the capacity of NO to act as an important facilitator of the protective effects of RIPC is provided in table 1.4. All these studies with the exception of one (230) have indicated NO could be an important molecule in the beneficial effects of RIPC. The results of four of these studies (227,230-232) need further corroboration as each of these only used a single technique to evaluate the role of NO (table 1.4). The study by Kanoria *et al* (227) is the only one to allude to the effects of NO in ameliorating liver IR injury by RIPC; however, the only pertinent endpoint measured by the investigators was the plasma NOx levels, and therefore more research is needed not only to substantiate these results, but also to assess how NO generated by RIPC attenuates liver IR injury.

Table 1.4 A summary of the actions of NO in RIPC.

Ref.	species	RIPC site and protocol	IR site and protocol	Effect of RIPC on endpoints of IR injury	Assessment of nitric oxide's involvement in mediating effects of RIPC	Conclusions
(233)	Rats	Bilateral femoral arteries ischaemia (I.) for 15 min followed by 2 hrs reperfusion (R.)	Left anterior descending (LAD) coronary artery I. for 30 min followed by 2 hrs R.	↓myocardial infarct size; ↑maximal rate of rise of LV pressure; ↓Left ventricular end diastolic pressure (LVEDP); ↓serum CK-MB and LDH levels	Administration of L-NAME prior to RIPC + IR abolished protective effects of RIPC on all endpoints of IR injury. Administration of L-arginine before IR protected against IR injury	NO is a mediator of protective effects of RIPC
(232)	Rats	Contralateral hindlimb I. for 10 min followed by 30 min R.	Abdominal adipocutaneous flaps raised on superficial epigastric artery I. for 3 hrs followed by up to 5 days R.	↑flap survival; ↑p38 MAP kinase phosphorylation in flaps (30 min after RIPC but not following 3 hrs of ischaemia)	Administration of L-NAME prior to RIPC + IR abolished flap survival advantage conferred by RIPC, and diminished phosphorylation of p38 MAP kinase	NO mediates increased tissue survival following IR through phosphorylation of p38 MAP kinase
(230)	Rabbits	Two cycles of left renal artery I. for 5 min followed by 15 min R.	Spinal cord (through aortic) I. for 40 min followed by 48 hrs R.	↑(improved) neurological score; ↑viability index; ↓inflammatory response; ↓neuron-specific enolase measured at 2 hrs post reperfusion (marker of ischaemic neuronal injury)	Measurement of serum NOx levels at 2 and 48 hrs post reperfusion showed no significant differences between RIPC + IR and IR alone group	NO does not mediate effects of RIPC
(231)	Rats	Four cycles of bilateral hindlimbs I. for 5 min followed by 5 min R.	LAD coronary artery I. for 30 min followed by 2 hrs R.	↓myocardial infarct size	Administration of L-NAME prior to RIPC + IR abolished protective effects of RIPC on myocardial infarct size	NO is a mediator of protective effects of RIPC

(234)	Mice	Six cycles of bilateral hindlimb I. for 5 min followed by 5. min R.	24 hrs following RIPC, hearts were langendorff-perfused, and subjected to 40 min of global I. followed by 60 min R.	↓myocardial infarct size; ↑Left ventricular developed pressure (LVDP); ↓LVEDP	↑cardiac iNOS levels post RIPC. $iNOS^{-/-}$ mice lost protective effects of RIPC on infarct size, LVDP, and LVEDP	iNOS-derived NO is a mediator of protective effects of RIPC
(235,236)	Rats	Right hindlimb or right fem. artery and vein I. for 10 minutes followed by 30 min R.	Epigastric adipocutaneous flaps raised on left superficial epigastric artery I. for 3 hrs followed by 5 days R.	↓mean flap necrosis area	Administration of L-NAME prior to RIPC + IR abolished protective effects of RIPC on mean flap necrosis area. I.V. administration of NO donor Sper/NO prior to IR simulated the effects of RIPC	NO is a mediator of protective effects of RIPC
(237,238)	Rats	Hindlimb I. for 10 min followed by 30 min R.	Cremaster muscle flap I. for 2 hrs followed by 1 hr R.	↑RBV in arterioles and capillaries; ↑capillary flow; ↓number of leukocytes adherent to endothelium of venules.	Administration of L-NAME prior to RIPC + IR abolished protective effects of RIPC on RBV, capillary flow, and number of adherent leukocytes. I.V. administration of NO donor Sper/NO prior to IR simulated the effects of RIPC	NO is a mediator of protective effects of RIPC
(227)	Rabbits	Three cycles of hindlimb I. for 10 min followed by 10 min R.	Total liver I. for 25 min followed by 2 hrs R.	↓serum ALT, AST, and LDH; ↑total hepatic blood flow	Measurement of plasma NOx showed higher levels in the RIPC+IR compared to IR	NO is a mediator of protective effects of RIPC

1.4 Thesis hypothesis

The foregoing review on the mechanisms of liver IR injury, and our knowledge base of the therapeutic strategies to ameliorate liver IR injury specifically through the actions of NO (chapter 2), resulted in the following hypothesis (summarised in figure 1.7):

Liver IR injury in the mouse is ameliorated by hindlimb preconditioning through the production of NO from eNOS (and iNOS). This NO is transported in the circulation as nitrite and nitrate to reach the liver where it provides hepatic protection against IR injury through the sGC-cGMP pathway which acts to preserve the hepatic microcirculation.

1.5 Objectives of the thesis

1. To investigate if hindlimb RIPC affords protection against liver IR injury in the mouse.
2. To investigate the putative beneficial role of NO in mediating the protection afforded by hindlimb RIPC on liver IR injury.

The next chapter reviews the literature with regards to the beneficial effects of NO in IR injury and in mediating organ protection afforded by IPC.

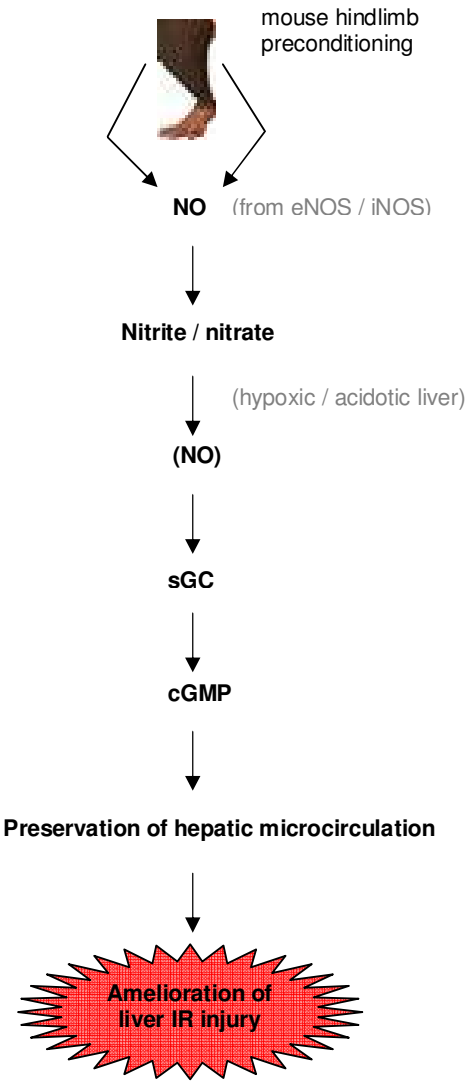

Figure 1.7. Thesis hypothesis. Mouse hindlimb preconditioning leads to the release of NO from both eNOS and iNOS. NO is then oxidised to nitrite and nitrate that travel in the circulation and reach the post-ischaemic hypoxic and acidotic liver. Under these conditions the nitrite and nitrate are reduced to NO which acts locally through the sGC-cGMP pathway to preserve the hepatic microcirculation and ultimately attenuate live IR injury. *cGMP*, cyclic 3', 5' guanosine monophosphate; *eNOS* and *iNOS*, endothelial and inducible nitric oxide synthase respectively; *NO*, nitric oxide; *sGC*, soluble guanylyl cyclase.

Chapter 2

The mechanisms of nitric oxide protection in liver IR injury

2.1 Introduction

Nitric oxide (NO) is a gas with a molecular mass of 30.0 daltons. It is a free radical due to the presence of an unpaired electron in its valence shell. This structural configuration results in NO being highly reactive, with a consequent half life in the order of 5-10 seconds. In vivo synthesis of NO is catalysed by the enzyme nitric oxide synthase, which has three isoforms (section 2.2). The effects of NO production in liver IR may be harmful or beneficial, or a combination of both. The determining factors are the length of the ischaemic insult and the NOS source of NO. This concise review focuses on the hepato-protective mechanisms of action of NO in liver IR injury. Specifically, three core areas are discussed: nitric oxide synthase, arginine, and the soluble guanylyl cyclase-cyclic GMP-protein kinase G pathway.

2.2 Nitric oxide synthase

The synthesis of NO is catalysed by nitric oxide synthase, an enzyme with three isoforms of distinct tissue distribution. Neuronal NOS (nNOS) is found in neural tissue and will not be discussed further. Endothelial NOS (eNOS) is Ca^{2+} / calmodulin dependent and catalyses the electron transfer reactions during the synthesis of NO from L-arginine. This electron transfer requires eNOS binds calmodulin, a process that is in turn dependent on the cellular concentrations of Ca^{2+} (239). eNOS is constitutively expressed in many cell types, including sinusoidal endothelial cells and hepatocytes (240-243). Inducible NOS (iNOS) is Ca^{2+} independent as it is tightly bound to calmodulin at all cellular concentrations of Ca^{2+} (244). iNOS is not expressed under normal circumstances, but is up-regulated in various nucleated cell types in inflammatory conditions, including hepatocytes,

neutrophils, T-lymphocytes, endothelial, biliary, and kupffer cells in liver ischaemia reperfusion (IR) injury (245-249). NOS catalyses NO formation in a two-step oxidation of L-arginine to L-citrulline and NO (250,251):

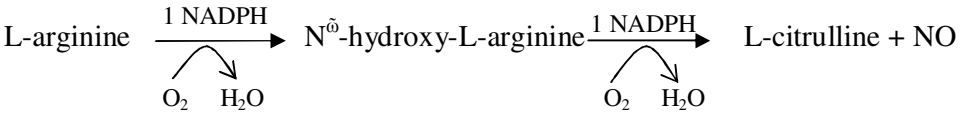

The reaction also requires the co-factors tetrahydrobiopterin, flavin adenine dinucleotide (FAD) and flavin mononucleotide (FMN) (250,251).

Experimental evidence indicates that eNOS-derived NO is hepato-protective against liver IR injury. This has been demonstrated using various animal models and experimental techniques. eNOS knockout ($eNOS^{-/-}$) mice exhibit significantly greater liver injury following warm IR compared to wild type (WT) counterparts (94,252-254). Similarly, $eNOS^{-/-}$ mice demonstrate more severe liver injury following cold preservation (cold ischaemic injury) and warm reperfusion in a mouse orthotopic liver transplantation (OLT) model (255). It is not just the baseline constitutive eNOS-derived NO that is protective, but mice with transgenic overexpression of eNOS show greatly reduced liver IR injury compared to WT animals (256). The protective effects of eNOS overexpression would raise the possibility that IR injury may act by down-regulating the expression of eNOS. This has indeed been shown in mouse and rat liver IR models (240,257).

The role of iNOS-derived NO in liver IR injury is much less clear than that of eNOS. However, there is some evidence that the effects of iNOS expression on liver IR injury maybe be dependent on the length of ischaemia the liver is subjected to.

Animal experiments with relatively short ischaemic insults of less than 60 minutes show either exacerbation of (254), or no effect (253,258) of iNOS expression on the degree of liver injury. These seemingly incongruent results could be a consequence of the specific methods used to ascertain the functions of iNOS in liver IR injury. For example, Hines et al (258) described a significant increase in liver IR injury in $iNOS^{-/-}$ mice with 45 minutes ischaemia followed by 3 hours of reperfusion compared to WT animals. However, using exactly the same ischaemic protocol, whilst varying the reperfusion period length, they could not illicit a difference between $iNOS^{-/-}$ and WT animals with either 1 or 6 hours of reperfusion (258). The investigators also showed a time-dependent increase of liver IR injury in WT mice, but without an increase in iNOS expression. Moreover, administration of the relative iNOS inhibitor L-NIL to WT animals did not worsen the IR injury or alter serum nitrate and nitrite (NOx) levels, indicating that iNOS-derived NO does not influence liver IR injury with 45 minutes of ischaemia. However, $iNOS^{-/-}$ mice exhibit worse liver injury at 3 hours reperfusion due to a mechanism that is independent of iNOS-derived NO, which the authors hypothesised could be for example due to altered expression of a different gene(s) that is influenced by the iNOS deletion in $iNOS^{-/-}$ (258).

In contrast to the confusing situation with short ischaemic periods, iNOS-derived NO has consistently been shown to contribute to liver IR injury with prolonged (> 60 minutes) cold (247,259,260) and warm (249,259,261) liver ischaemic insults. The mechanisms underlying the deleterious effects of iNOS-derived NO with prolonged ischaemic insults are beyond the scope of this review, suffice to say that excessive iNOS-derived NO generation in kupffer cells and neutrophils (247),

promote pro-inflammatory cytokine and chemokine release, and leukocyte activation and trafficking into the liver (260). In addition, exorbitant NO production reacts with superoxide resulting in the formation of peroxynitrite (261,262), a molecule that is extremely toxic to cells (262).

Some experimental evidence points to the protective effects of iNOS-derived NO during the late phase of liver IR injury, starting at 6 hours and continuing to 48 hours post reperfusion. In one study of rat OLT (263), donor livers were transduced with an adenovirus encoding iNOS four days prior to harvest. The livers were then explanted from donors, cold preserved for 18 to 24 hours and transplanted into recipients. The adenovirally-transduced livers showed significant expression of iNOS and elevated serum NOx levels compared to control livers that had been transduced with a control gene. In addition livers that were transduced with iNOS showed significant reductions in IR injury and administration of a relative iNOS inhibitor to these livers abrogated the protection afforded by iNOS transduction (263). As good a study as this was, clearly the precise role of iNOS in protecting against or exacerbating liver IR injury, has not been fully elucidated and requires more research to establish the exact conditions under which iNOS-derived NO will prove beneficial or harmful.

The actions of eNOS-derived NO and iNOS-derived NO in direct and remote ischaemic preconditioning are discussed in section 6.1.

2.3 L-arginine

Arginine is an amino acid that is physiologically active in the L-form. It is metabolised either by NOS as outlined in the previous section, or by arginase. The latter catalyses the reaction:

$$\text{L-arginine} + H_2O \xrightarrow{\text{arginase}} \text{L-ornithine} + \text{urea}$$

L-arginine protects the liver from IR injury. However, a review of published experimental studies indicate that the mechanisms of this protection are not necessarily through L-arginine's metabolism to NO by NOS enzymes in every experimental model, but rather depends on the type of ischaemic insult the liver is subjected to. Table 2.1 lists the studies which measured hepatic, plasma, or serum NOx levels as a marker of NO production following reperfusion in hepatic IR models. In all these studies, with the exception of two (264,265), L-arginine was administered to the animals and resulted in significant amelioration of liver IR injury. The two studies that did not administer L-arginine, instead administered the selective arginase inhibitor nor-NOHA which resulted in a significant increase in endogenous L-arginine levels associated with protection against liver IR injury (264,265). Table 2.1 indicates that L-arginine protects against liver IR through an NO-dependent pathway during short warm ischaemic injury and through an NO-independent mechanism during prolonged cold ischaemic insults. The in vivo experimental evidence summarised in table 2.1 does not shed light if it is the ischaemic length, type of ischaemia (cold vs warm), or a combination of both, which determines if an NO-dependent or -independent pathway is responsible for L-arginine's fate when protecting against hepatic IR injury. However, an in vitro study

(266,267) that subjected rat livers to 60 minutes of cold ischaemia followed by warm reperfusion with oxygenated Krebs-Henseleit solution in an organ bath, showed the livers are protected with L-arginine administration from the effects of cold ischaemia in association with a rise in NOx levels, albeit statistical significance was only achieved during the first 10 minutes of reperfusion, indicating that short ischaemic lengths result in L-arginine protecting against liver IR through an NO-dependent mechanism regardless of the type of ischaemia (266,267). Nonetheless these results need to be corroborated by in vivo short-length cold ischaemic models. The question remains how could L-arginine protect against prolonged ischaemic insults through an NO-independent pathway? Two explanations are possible. The first of these is supported by experimental results showing NOx levels are non-significantly elevated following prolonged cold ischaemic injury to livers either supplemented with L-arginine (268-270) or the arginase-selective inhibitor nor-NOHA (265) and resulting in significant elevation of plasma L-arginine levels. With this explanation L-arginine indeed is metabolised by NOS to form NO which then acts to protect the liver, but there is simply insufficient L-arginine to result in significant elevation of NOx Levels (265,271) due to the release of arginase from livers subjected to prolonged ischaemia (265,268,270,272) that divert L-arginine metabolism from NOS to metabolism by arginase. In support of this, prolonged cold ischaemia in the setting of OLT results in increased plasma levels of ornithine due to metabolism by arginase (265,268,270,272), without an increase in citrulline levels from metabolism by NOS (268,270). Moreover, it has also been shown that L-arginine administration in OLT results in elevated plasma levels of both ornithine and citrulline indicating that both pathways, including NOS, catabolise L-arginine (268). Therefore it is likely that L-arginine protects against prolonged ischaemic

insults through an NO-dependent pathway, but at the same time there is release of arginase from these livers subjected to prolonged ischaemia that results in the partial diversion of L-arginine away from NOS metabolism to be consumed by arginase. The second explanation is that apart from NO and ornithine, L-arginine can be catabolised to various other products (273), some of which may yet prove to offer a degree of protection against IR injury. However, these products are likely to be of minor importance especially with short ischaemic insults, and are therefore not discussed in this review.

Table 2.1 The effects of L-arginine administration on NOx levels in vivo in liver IR injury. In all these studies L-arginine administration significantly ameliorated liver IR injury.

Experimental evidence showing L-arginine significantly increases NOx levels				Experimental evidence showing L-arginine does not increase NOx levels			
Ref.	Species	Type of ischaemia	Length of ischaemia	Ref.	Species	Type of ischaemia	Length of ischaemia
(274)	Rats / pigs	Warm	60 min.	(268)	Pigs	Cold	20 hours
(275)	Rats	Warm	45 min.	(269)	Rats	Cold	18 hours
(276)	Pigs	Warm	120 min.	(270)	Rats	Cold	18 hours
(277)	Rats	Warm	30 min.	*(265)	Rats	Cold	18 hours
(278,279)	Rats	Warm	45 min.				
(240)	Rats	Warm	45 min.				
(280,281)	Rats	Warm	60 min.				
*(264)	Mice	Warm	60 min.				
#(266,267)	Rats	Cold	60 min.				

*L-arginine was not administered in these studies but the arginase inhibitor nor-NOHA was, leading to a rise in endogenous L-arginine levels.
#This study was performed in vitro in an organ bath. Warm reperfusion was performed using oxygenated Krebs-Henseleit solution at 37 ℃.

The protective mechanisms of L-arginine in liver IR injury are a reflection of the widespread protective effects of NO in this condition. Specifically, L-arginine protects hepatocytes and liver endothelial cells from the deleterious effects of IR

injury (275,282). The mechanisms of L-arginine's protection in liver IR are detailed in figure 2.1. These may conceptually be divided into L-arginine's effects on hepatic circulation (283-289), energy stores (276,279,287,290-292), oxidative status (276,281,287,290,293), leukocyte activation (283-287,291,294,295), mitochondria (280,282,294), and other effects on the liver (279,284,286,287,291,294) (figure 2.1).

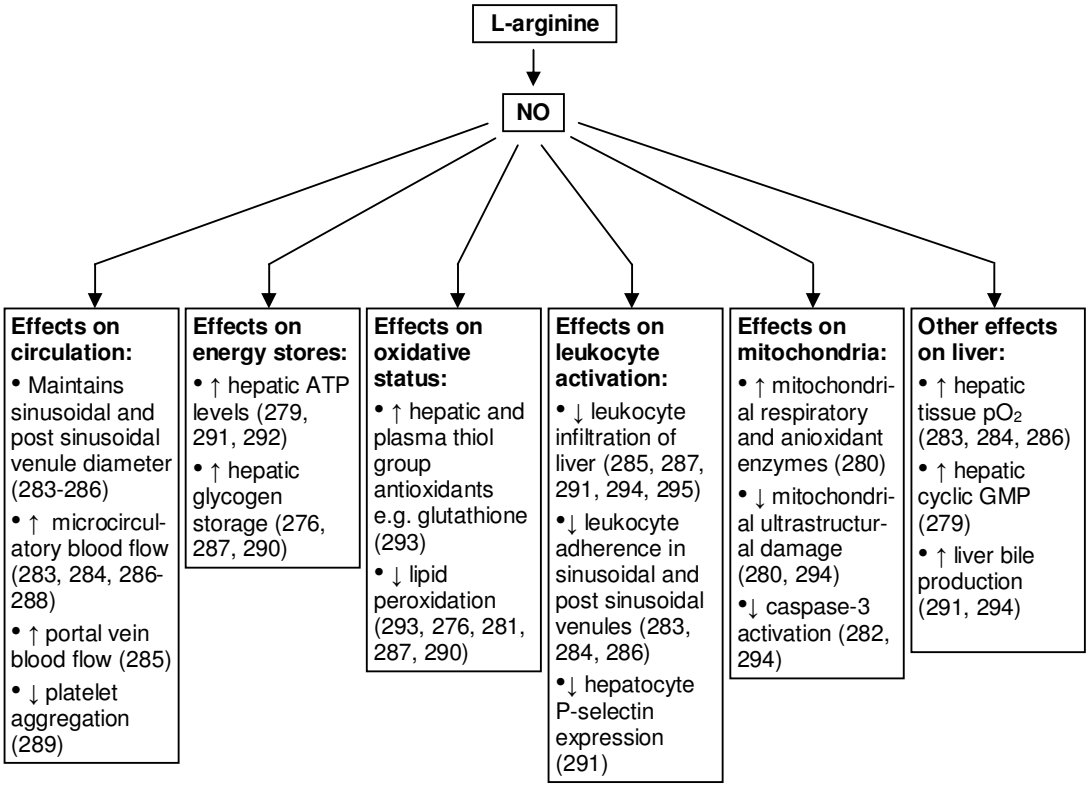

Figure 2.1. Mechanisms of protection of L-arginine in liver IR injury, references are in brackets. *ATP*, adenosine triphosphate; *NO*, nitric oxide; *pO2*, partial pressure of oxygen.

2.4 sGC-cGMP-PKG

The soluble guanylyl cyclase (sGC)-cyclic 3', 5' guanosine monophosphate (cGMP)-protein kinase G (PKG) pathway is one of the commonest utilized by NO in mammalian biology. A detailed discussion of the function of sGC and cGMP in liver IR is given in section 8.1.

cGMP-dependent protein kinase or PKG is a serine and threonine specific protein kinase that is activated by cGMP. PKG plays an important role in the downstream pathway of cell protection elicited by NO. It has been shown that isolated hepatocytes pre-incubated with a NO donor are resistant to hypoxia-induced cellular death through a PKG-dependent pathway, as the protection of the NO donor was inhibited by the PKG-selective blocker KT5823 (296). Moreover the protection offered by PKG resulted in the phosphorylation, and therefore activation, of p38 MAPK leading to a significant reduction in intracellular $[Na^+]$ ($[Na^+]_i$) in hypoxic hepatocytes (296). Preconditioning-induced phosphorylation of p38 MAPK in hepatocytes results in activation of vacuolar H^+-ATPase (V-ATPase) (297). V-ATPases are proton pumps spanning the membranes of various intracellular compartments as well as the plasma membranes of hepatocytes. They are responsible for acidification of organelles such as lysosomes and endosomes; and play an important role in maintaining intracellular pH homeostatsis (298). Hepatic ischaemia results in intracellular acidosis through anaerobic respiration. To restore intracellular pH towards normal, the liver cells activate the Na^+ / H^+ exchanger (NHE) and the Na^+ / HCO_3^- cotransporter (NHCT). The NHE extrudes H^+ into the extracellular space in exchange for Na^+ inflow into the cell. The NHCT transports Na^+ and HCO_3^- intracellularly (299). Both these mechanisms of correcting the

ischaemically-induced intracellular acidotic pH result in intracellular Na^+ accumulation (299). It is the increase in $[Na^+]_i$ secondary to intracellular acidosis that contributes to hepatocytes death. Preconditioning- and NO-induced phosphorylation of p38 MAPK activates V-ATPases leading to extrusion of H^+ from the cytosol of hepatocytes into the extracellular environment (297), thereby resulting in inhibition of the NHE and NHCT with a consequent reduction in $[Na^+]_i$ and protection from hypoxic cellular death. The NO-PKG pathway does not only lead to the activation of V-ATPases but may also, through the activation of PI3K in hepatocytes, result in the exocytosis of lysosomes and consequent insertion of lysosomal V-ATPases into the plasma membrane (300). Therefore through activation of two separate molecules (p38 MAPK and PI3K), the NO-PKG cascade results in not only the activation of but also in the increase in number of plasma membrane V-ATPases. Activated PKG has one other consequence and that pertains to the prevention of onset of the mitochondrial permeability transition (MPT) in hepatocytes (301); an effect that averts hepatocytes death. It is postulated this effect on the MPT could be due to phosphorylation of serine / threonine residues of mitochondrial proteins that participate in MPT formation (301) but this has not been corroborated by experimental evidence.

A summary of the mechanisms through which the NO-PKG pathway exerts its protective actions in liver IR injury is provided in figure 2.2.

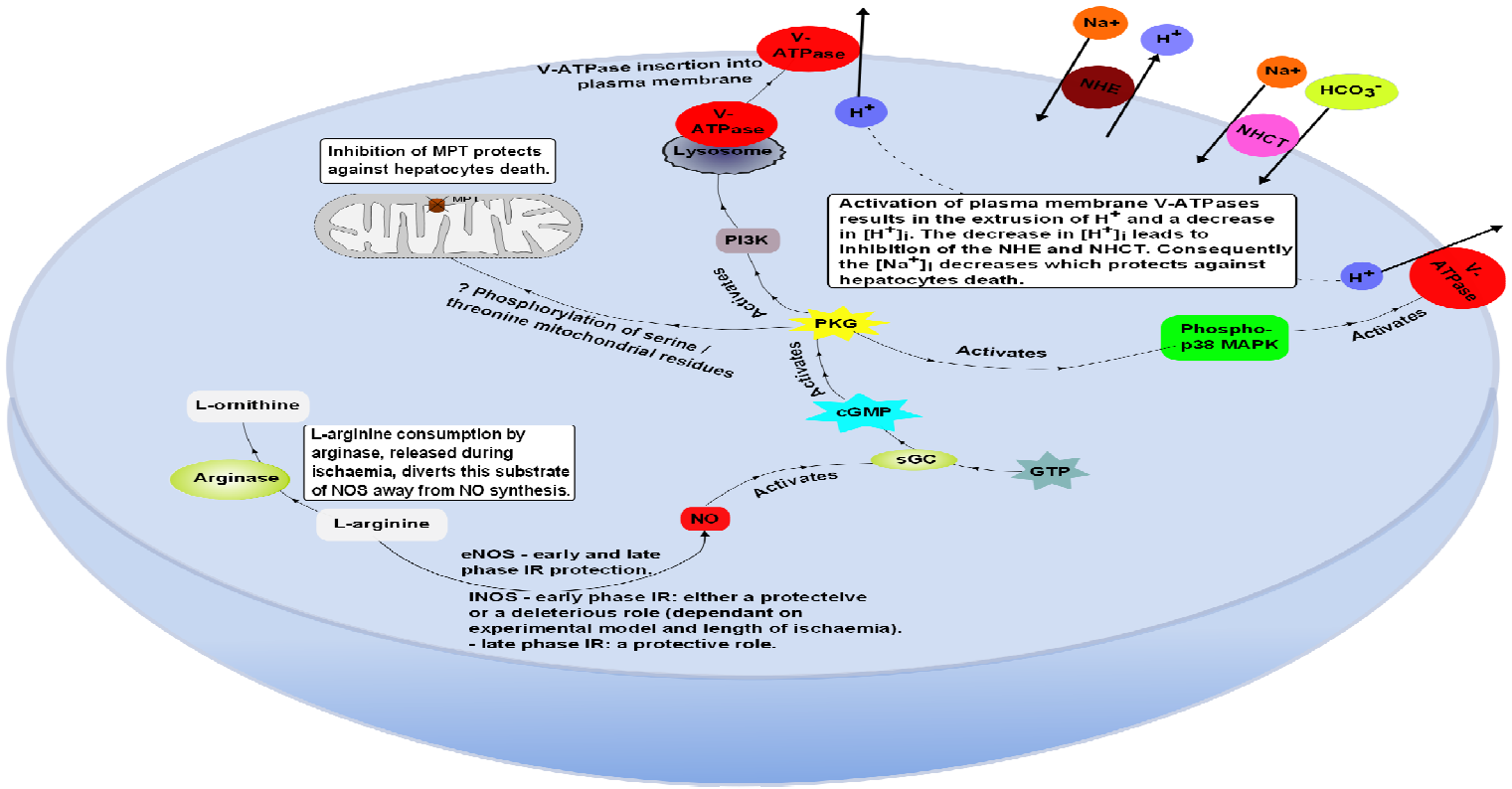

Figure 2.2. A summary of the main mechanisms involved in NO-mediated protection against liver IR injury. A schematic representation of a liver cell with NO-mediated protective pathways shown. *cGMP*, cyclic 3', 5' guanosine monophosphate; *eNOS*, endothelial nitric oxide synthase; *GTP*, guanosine triphosphate; H^+, hydrogen ions; HCO_3^-, bicarbonate; *iNOS*, inducible nitric oxide synthase; *MPT*, mitochondrial permeability transition; Na^+, sodium ions; *NHCT*, Na^+/HCO_3^- cotransporter; *NHE*, Na^+/H^+ exchanger; *NO*, nitric oxide; *PI3K*, phosphoinositide 3-kinase; *PKG*, protein kinase G (cGMP-dependent protein kinase); *sGC*, soluble guanylyl cyclase; *V-ATPase*, vacuolar H^+-ATPase.

2.5 Conclusions and future directions

NO is a ubiquitous free radical. Liver IR increases NO synthesis. The ramifications of this may be one of protection against or one of contribution towards liver IR injury. Whilst eNOS-derived NO is hepato-protective in liver IR injury, the role of iNOS-derived NO is much less clear and needs further research to shed light on the specific circumstances that determines the benefits, or otherwise, of NO generated from iNOS. Furthermore, there is very limited published literature on the effects of direct and remote ischaemic preconditioning on eNOS and iNOS expression and function. L-arginine supplementation attenuates hepatic IR injury through increased NO synthesis. At the same time, IR injury results in the release of arginase with the repercussion of diversion of L-arginine away from NO synthesis and towards urea and ornithine synthesis. The full significance of arginase release during IR is incompletely understood; indeed the implications of preconditioning (direct or remote) on arginase release are unknown and require further research. Most of the work investigating the actions of PKG in IR was performed in vitro using hepatocyte cultures. In vivo work is desperately needed to confirm the applicability of these results to liver IR injury. Only by understanding the detailed protective actions of NO, including the factors that influence its synthesis, will it be possible to design therapeutic strategies against liver IR injury that exploit the full potential of this molecule.

Chapter 3

Materials and Methods

3.1 Introduction

In this thesis an experimental animal model was used to investigate the role of nitric oxide (NO) in mediating the protective effects of hindlimb remote ischaemic preconditioning (RIPC) on liver ischaemia reperfusion (IR) injury. A mouse hindlimb RIPC protocol was developed and validated. Wild type (C57BL/6) and $eNOS^{-/-}$ mice were used. Throughout the thesis, quantification of liver injury was assessed by plasma liver enzymes and H & E stained liver histopathological sections. Transmission electron microscopy was used to provide an insight into the cellular structures and organelles that are affected by NO in RIPC. Hepatic microcirculatory blood flow measurements were used to understand the effects of RIPC and NO on blood flow in the hepatic microcirculation in the context of IR injury. eNOS and iNOS protein expression were assessed by Western blots. Plasma nitrite and nitrate act as circulating reservoirs of NO and were assessed by a colorimetric assay. NO can act through various pathways to exert its effects, including the guanylyl cyclase – cGMP route. Therefore, hepatic cGMP levels were quantified using an enzyme immunoassay kit.

3.2 Chemicals and reagents

C-PTIO (2-(4-carboxyphenyl)-4,4,5,5-tetramethylimidazoline-1-oxyl-3-oxide.potassium salt; Alexis Biochemicals) is a direct intravascular NO scavenger. It was dissolved in Dulbecco's – phosphate buffered saline (D-PBS) and was administered intravenously at a dose of 1 mg/kg in a volume of 50 µl, based on a previous study by Duranski *et al* (302). C-PTIO reacts with NO stoichiometrically (303) and was used to inhibit the effects of NO produced during RIPC. ODQ (1H-[1,2,4]oxadiazole[4,3-a]quinoxalin-1-one; Alexis Biochemicals) is a highly selective

inhibitor of soluble guanylyl cyclase (sGC). It binds to the haem site on sGC in an irreversible NO-competitive manner (304,305). It was dissolved in DMSO and was administered topically to the liver prior to hindlimb preconditioning and liver IR (302) in a volume of 100 µl containing 600 µg of ODQ (256). Sodium nitrite ($NaNO_2$, Sigma-Aldrich) was dissolved in D-PBS and was administered into the peritoneal cavity in a volume of 50 µl containing 48 nmol (3.31 µg) sodium nitrite (167,302). In hypoxic and acidotic environments, typically encountered in ischaemic tissues, sodium nitrite is reduced to NO (306), and therefore we administered it to $eNOS^{-/-}$ mice undergoing liver IR to replace the deficient NO production.

3.3 Animals

Male inbred C57BL/6 wild type mice (Charles River laboratories, UK); and mice lacking the constitutively expressed enzyme, endothelial nitric oxide synthase ($eNOS^{-/-}$, bred in-house) (307), were utilized in the present study. All mice used were aged 8-12 weeks, were kept in a temperature-controlled environment, had a 12 hour light-dark cycle, and were freely allowed standard mouse chow pellets and drinking water.

3.4 Mouse model of hindlimb remote ischaemic preconditioning of the liver

The study was conducted under a license (PPL 70/6626; PIL 70/20759) granted by the Home Office in accordance with the Animals (Scientific Procedures) Act 1986. In addition the experimental protocols were also approved by the institutional animal ethics and welfare committee. Randomly selected mice were anaesthetised in

an induction chamber using 2% isoflurane. Maintenance of anaesthesia was achieved by the use of 1.5-2.0 % isoflurane via a concentric oronasal mask connected to an anaesthetic circuit. Core body temperature was maintained at 37.0 ± 0.5 ℃ using a heating pad and a rectal temperature probe.

3.4.1 *Hepatic IR protocol*

Laparotomy was performed through a midline incision. The falciform ligament and the ligament connecting the caudate to the left lobe were divided. A bolus of 400 µl of 2.5 U/ml warmed heparinised saline was administered into the peritoneal cavity to maintain rehydration and prevent blood clotting. A microvascular clamp was then applied to the portal triad supplying the left and median lobes, rendering approximately 70% of the liver ischaemic. This well established partial hepatic ischaemia model prevents mesenteric venous congestion, intestinal mucosal damage caused by venous ischaemia, and subsequent bacterial translocation across the intestinal wall by permitting portal decompression through the caudate and right lobes of the liver (308-310). Successful occlusion of the portal triad in question was confirmed by a change in colour and a reduction in the microvascular blood flow as measured by Laser Doppler Flowmetry (LDF). The abdominal wall was sutured shut during hepatic ischaemia which lasted 40 minutes. Upon reperfusion of the ischaemic lobes, 400 µl of warmed normal saline was administered into the peritoneal cavity to prevent dehydration during the subsequent two hours of reperfusion in which the abdominal cavity was kept open to permit hepatic microcirculatory blood flow (MBF) measurements using LDF.

At the end of the reperfusion period blood was collected by cardiac puncture and immediately centrifuged at 3500 rpm (1150 g) for 10 minutes. The plasma supernatant was stored at -70 ℃ until assayed for liver transaminases and NOx.

The liver lobes subjected to IR were harvested at the end of each procedure. The median and part of the left lobe were snap frozen in liquid nitrogen and subsequently stored in the same for eNOS, iNOS, and cGMP concentrations. The majority of the reminder of the left lobe was stored in 10% formal saline for histopathology and immunohistochemistry processing. Samples for transmission electron microscopy were also obtained from the left liver lobe at the end of the experiment and were stored in 1.5% glutaraldehyde and 2% paraformaldehyde.

Preconditioned hindlimbs were de-skinned and de-skeletonised at the end of the experiment. The skeletal muscle remaining was processed in two ways. The majority of each sample was snap frozen in liquid nitrogen and subsequently stored in the same for eNOS and iNOS protein quantification, the remainder was placed in 10% formal saline for immunohistochemistry processing.

3.4.2 *Technique of hindlimb preconditioning*

Two techniques of RIPC were used. In the preliminary experiments non-invasive preconditioning was achieved by alternate inflation and deflation of a pneumatic tourniquet placed around the proximal right hindlimb. Based on the neuromuscular damage (see results section in chapter 4) observed on recovery of these mice, a second method of preconditioning was developed that utilized an open technique. A longitudinal skin incision was made over the right antero-medial thigh that extended

from the inferior end of the midline laparotomy down to the right knee. The femoral vascular bundle (femoral artery and vein) was isolated from the surrounding muscles and was clamped using an operating microscope just proximal to its confluence with the femoral nerve (figure 3.1). In both techniques of RIPC a protocol of four minutes of limb ischaemia followed by four minutes reperfusion for a total of six cycles was used. This was based on a study that utilized a similar protocol of hindlimb preconditioning prior to myocardial IR, applied via non-invasive finger pressure to the femoral vessels (311). Cessation of blood flow to the hindlimb was confirmed by the change in foot colour and by the reduction in foot MBF measured by LDF. Furthermore, in the tourniquet technique, the LDF was used to determine the inflation pressures at which blood flow to the hindlimb ceased in order to prevent over inflation of the tourniquet and subsequent soft tissue damage of the hindlimb.

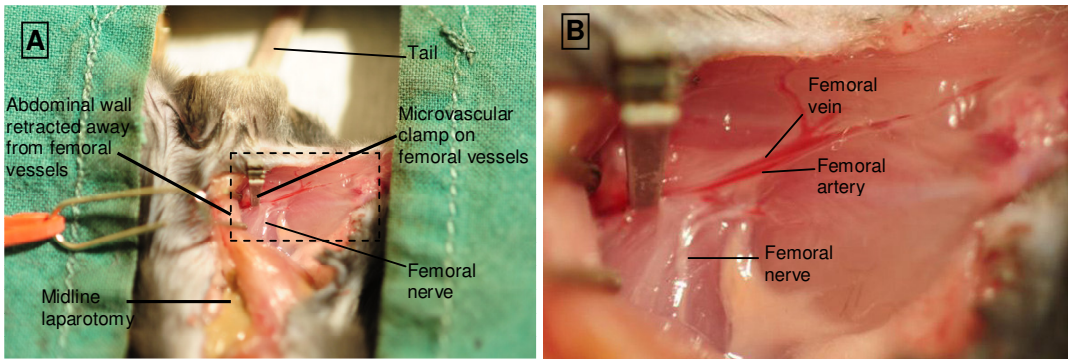

Figure 3.1. (A) Mouse photograph showing the dissected right femoral vessels and nerve with a microvascular clamp on the former. **(B)** Close up magnification of outlined area in (A) with the microvascular clamp applied to the femoral artery and vein before the vessels are joined by the femoral nerve thereby protecting the latter from any damage.

In these preliminary studies, mice that were preconditioned with a tourniquet (n = 2), and mice from the open clamp technique of RIPC (n = 4) were allowed to recover from anaesthesia during the two hour liver reperfusion period in order to assess general mobility and hindlimb function following RIPC. From these it became clear that the tourniquet technique resulted in limb paralysis probably secondary to hindlimb neuromuscular damage as evidenced by gross neuromuscular bruising in the preconditioned hindlimb soft tissues. Therefore the tourniquet technique was abandoned and all remaining experiments were performed using the open method of preconditioning.

3.4.3 *Experimental groups*

The experimental groups in the wild type and eNOS$^{-/-}$ mice are summarised in figures 3.2 and 3.3 respectively. Each group had a minimum of six animals. The total anaesthetic time was equal in all the groups. All animals underwent laparotomy, mobilization of the liver, and mobilization of the right femoral vascular bundle. In addition some of the groups were each subjected to a specific procedure as follows:

Wild type groups:

Sham: Only underwent the laparotomy, mobilization of the liver, and mobilization of the right femoral vascular bundle described above.

RIPC: The right hindlimb was preconditioned with 6 cycles of 4 minutes ischaemia followed by 4 minutes reperfusion, using a microvascular clamp to occlude the femoral vessels under an operating microscope.

IR: The median and left hepatic lobes were rendered ischaemic for 40 minutes followed by 2 hours reperfusion, using a microvascular clamp to occlude the portal triad branch to these lobes.

RIPC + IR: Animals were subjected to the RIPC followed by the IR procedures.

C-PTIO + RIPC + IR: The NO scavenger C-PTIO was administered intravenously at a dose of 1 mg/kg in 50 µl of D-PBS, followed by the RIPC + IR procedure.

ODQ + RIPC + IR: The sGC inhibitor ODQ was administered topically to the liver, in a volume of 100 µl of DMSO containing 600 µg of ODQ, followed by the RIPC + IR procedure.

eNOS$^{-/-}$ groups:

Sham: Only underwent laparotomy, mobilization of the liver, and mobilization of the right femoral vascular bundle.

RIPC: The right hindlimb was preconditioned with 6 cycles of 4 minutes ischaemia followed by 4 minutes reperfusion, using a microvascular clamp to occlude the femoral vessels under an operating microscope.

IR: The median and left hepatic lobes were rendered ischaemic for 40 minutes followed by 2 hours reperfusion, using a microvascular clamp to occlude the portal triad branch to these lobes.

RIPC + IR: Animals were subjected to the RIPC followed by the IR procedures.

Nitrite + IR: Underwent the IR procedure with administration of sodium nitrite, at a dose of 48 nmol in 50 µl of D-PBS, topically into the peritoneal cavity 20 minutes into liver ischaemia. To elicit the optimal time of sodium nitrite administration, plasma transaminases levels and liver MBF were measured in two additional eNOS$^{-/-}$ groups (n = 2 each) that received the sodium nitrite either immediately preceding liver ischaemia or just before liver reperfusion at the end of liver ischaemia.

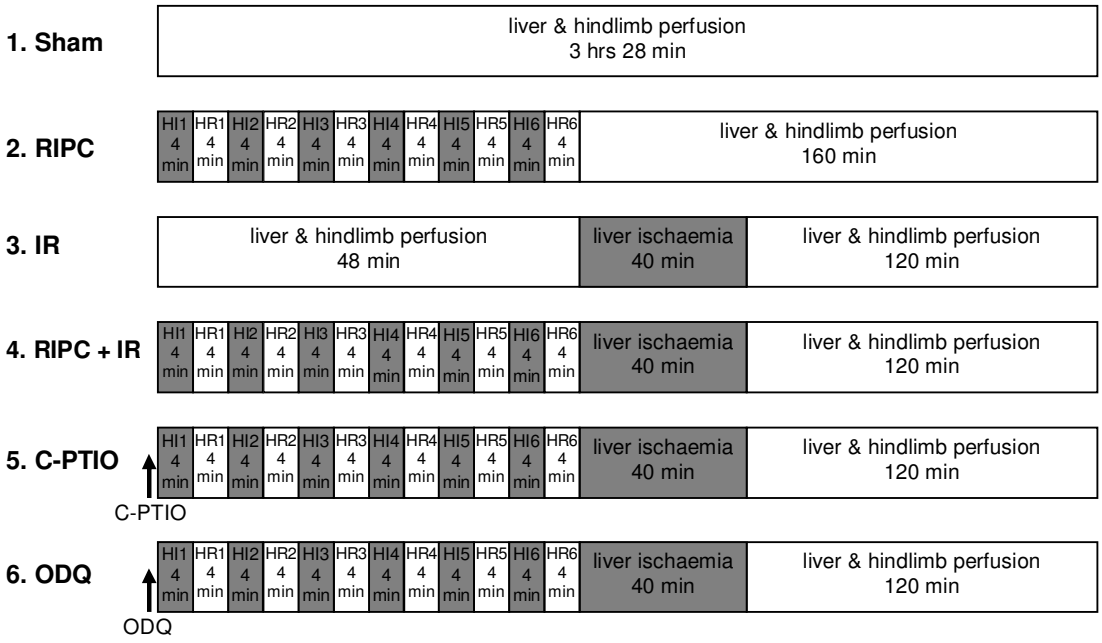

Figure 3.2. Wild type animal groups. Group 1 (sham) underwent laparotomy, mobilization of the liver, and mobilization of the right femoral vascular bundle. RIPC (group 2) had the right hindlimb preconditioned with 6 cycles of 4 min ischaemia (using direct femoral vessels clamping) followed by 4 min reperfusion. IR (group 3) had 40 min of ischaemia to the median and left liver lobes followed by 2 hrs reperfusion. RIPC + IR (group 4) underwent the RIPC followed by the IR procedures. C-PTIO + RIPC + IR and ODQ + RIPC + IR (groups 5 and 6) were administered C-PTIO and ODQ respectively, followed by the RIPC + IR procedure. Note the total anaesthetic time was equal in all the groups. *HI*, hindlimb ischaemia; *HR*, hindlimb reperfusion.

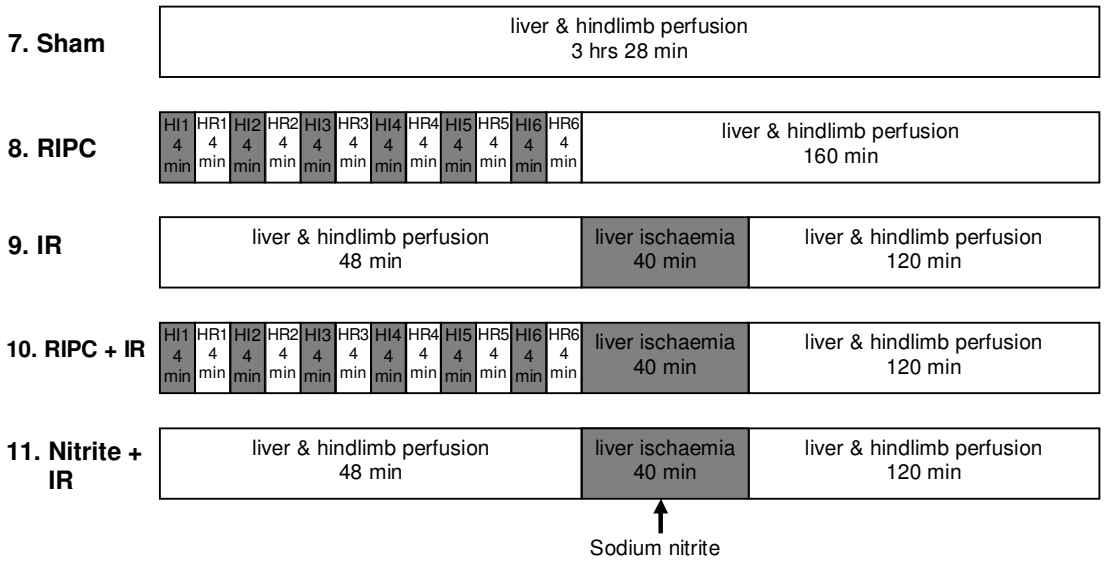

Figure 3.3. eNOS-/- animal groups. Group 7 (sham) underwent laparotomy, mobilization of the liver, and mobilization of the right femoral vascular bundle. RIPC (group 8) had the right hindlimb preconditioned with 6 cycles of 4 min ischaemia (using direct femoral vessels clamping) followed by 4 min reperfusion. IR (group 9) had 40 min of ischaemia to the median and left liver lobes followed by 2 hrs reperfusion. RIPC + IR (group 10) underwent the RIPC followed by the IR procedures. Nitrite + IR (group 11) underwent the IR procedure with administration of sodium nitrite 20 min into liver ischaemia. Note the total anaesthetic time was equal in all the groups. *HI*, hindlimb ischaemia; *HR*, hindlimb reperfusion.

3.5 Measurement of liver enzymes

Plasma concentrations of alanine aminotransferase (ALT) and aspartate aminotransferase (AST) were measured by a standard spectrophotometric method using an automated clinical analyzer (Modular Analytics P, Roche Diagnostic Ltd, West Sussex UK). These enzymes are sensitive markers of liver injury which are released from injured hepatocytes into the circulation.

3.6 Histopathology

A liver biopsy was taken from the left lobe at the end of the experiment for each of the animals and was immediately fixed in 10% formal saline. The fixed tissues were then embedded in paraffin, cut into 3 μm sections and stained with haematoxylin and eosin (H&E). Sections were examined under a light microscope using 50x or 100x magnification for assessment of the degree of liver injury by a liver pathologist blinded to the grouping of the animals. Each H&E sample was scored using two different methods. In the first of these an overall histopathological injury grade was assigned to each sample based on the extent of the injury seen on examining each section. This overall grading system was a modification of the ordinal grading scale reported by Camargo *et al* (81) and was as follows:

grade 0 – minimal or no evidence of injury;
grade 1 – **mild injury characterised by cytoplasmic vacuolization and focal nuclear pyknosis**;
grade 2 – moderate injury exhibiting cytoplasmic vacuolization, confluent areas of hepatocyte ballooning but no frank necrosis, sinusoidal dilatation and congestion, and blurring of intercellular borders;
grade 3 – moderate to severe injury with areas of coagulative necrosis, cytoplasmic hypereosinophilia, extensive sinusoidal dilatation and congestion;
grade 4 – severe injury consisting of severe confluent coagulative necrosis, and disintegration of and haemorrhage into hepatic cords leading to loss of tissue architecture.

A photomicrograph example of each of these grades is given in figure 3.4.

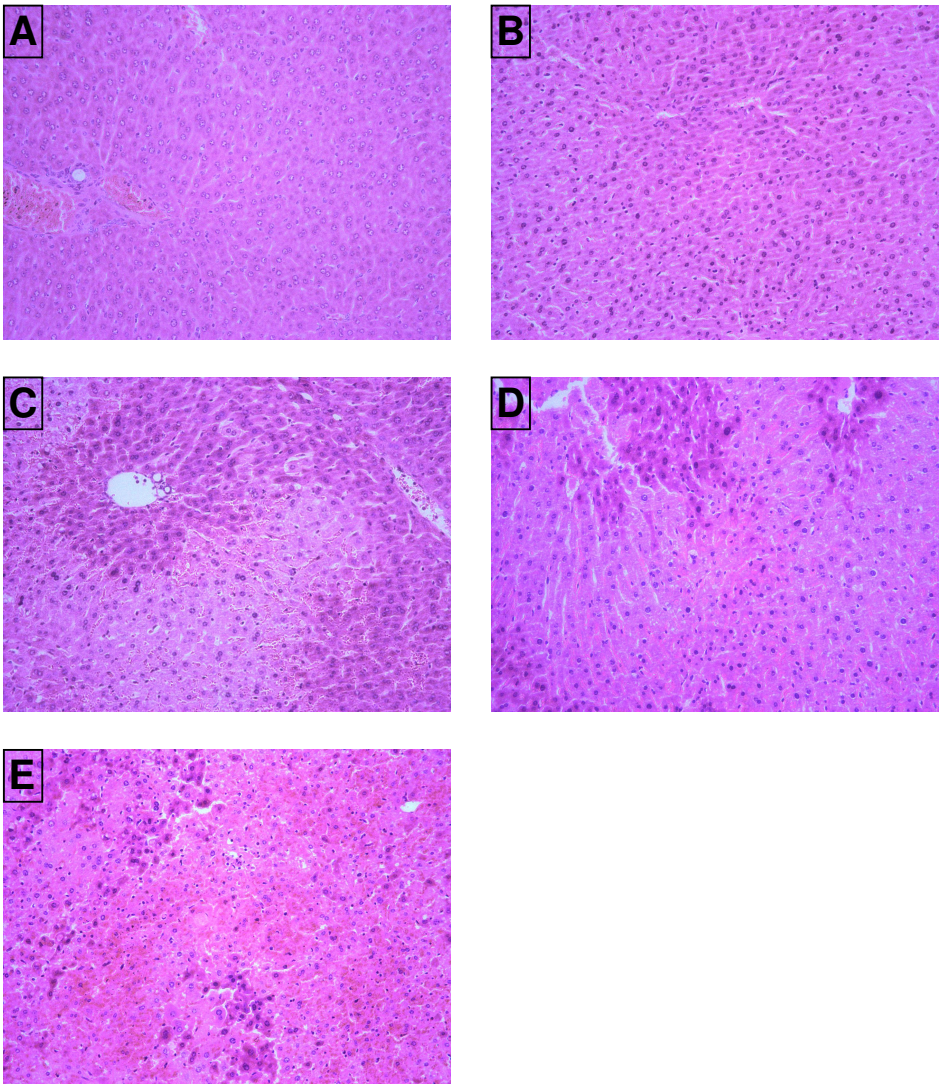

Figure 3.4. Representative photomicrographs of liver sections demonstrating the overall histopathological injury grades: **(A)** Grade 0; **(B)** Grade 1; **(C)** Grade 2; **(D)** Grade 3; **(E)** Grade 4. See main text for a description of each of these grades.

The second method of analysing the samples consisted of a semi-quantitative evaluation of individual histological features of liver IR injury in each sample (Table 3.1). The individual features are those reported previously (294,302,312,313) but with additions and modifications to the scoring criteria of each feature as shown in table 3.1. Each of these features was scored in affected areas identified by the histopathologist in each of the sections.

Table 3.1. Scoring system for individual histopathological features of liver IR injury.

Histopathological features of liver injury	Score (S)	Interpretation of scores
Neutrophil infiltration	0 1 2 3 4 5	None Rarely seen Scattered in some lobules Scattered in most lobules On the verge of confluence or with some confluence Dense clusters
Cell necrosis	0 1 2 3 4 5 6 7 8	None 1-2 apoptotic bodies > 3 apoptotic bodies Focal necrosis with 1-2 foci seen Focal necrosis with 3 or more foci seen One confluent area of necrosis Multiple bridging confluent areas of cellular death Areas of necrosis exceed areas of viable parenchyma No or very focal viable parenchyma identified
Eosinophilic changes of hepatocytes	0 1 2 3 4	None Rarely seen Scattered in some lobules Scattered in most lobules Widespread
Discohesive hepatocytes	1 2 3	Mild Moderate Severe
Liver cell ballooning	0 1 2 3 4	None Focal, spotted after extensive search Some lobules affected Most lobules affected Widespread
Cytoplasmic vacuolization	0 1 2 3 4	None Rarely seen Scattered in some lobules Scattered in most lobules Widespread
Nuclear pyknosis	0 1 2 3 4	None Rarely seen Scattered in some lobules Scattered in most lobules Widespread
Blurring or loss of intercellular borders	0 1 2 3 4	None Rarely seen Scattered in some lobules Scattered in most lobules Widespread

Red blood cell extravasation / haemorrhage	0 1 2 3 4	None Rarely seen Frequent perivenular Frequent perivenular midzonal Frequent panlobular
Sinusoidal dilatation	0 1 2 3 4	None Rarely seen Frequent perivenular Frequent perivenular midzonal Frequent panlobular

3.7 Transmission electron microscopy

Transmission electron microscopy (TEM) was performed to identify the cellular structures and organelles that are protected by hindlimb preconditioning prior to liver IR (RIPC + IR group) compared to IR alone, thereby providing an insight into the cellular organelles that are receptive to the effects of the remote preconditioning process. Furthermore, TEM assessment in $eNOS^{-/-}$ animals, and animals administered C-PTIO, ODQ, or sodium nitrite undergoing RIPC allows an assessment of cellular ultrastructures that are utilized by nitric oxide in mediating the protective effects of RIPC on liver IR injury.

Liver biopsies of approximately 1 mm^3 dimensions were cut from the left lobe and fixed in a solution containing 1.5% glutaraldehyde and 2% paraformaldehyde in PBS overnight. An automated tissue processor (Leica EM TP) was utilized to process the samples in the following sequence: repeated washings with PBS; post-fixation in 1% osmium tetroxide; dehydration through 30, 50, 70, 90, and 100 % alcohol; and embedding in Lemix epoxy resin. Semi-thin (1 μm) sections were cut and stained with 1% Toluidine Blue – 1% Borax and examined under light microscopy to determine the areas to be cut and processed for TEM. Ultrathin (70

nm) sections were stained with 2% aqueous uranyl acetate followed by Reynold's lead citrate, and viewed using a Philips 201 TEM. Representative areas were photographed and the images were interpreted by a TEM scientist who was blinded to the groups. Multiple parameters of ultrastructural injury were evaluated based on modifications to those previously reported in liver IR injury studies (314-316). Within hepatocytes these were: mitochondrial damage evident by outer membrane disruption and cristae shortening and disruption; endoplasmic reticulum dilatation and vesiculation; formation of cytosolic vacuoles; formation of phagolysosomes; and abundance of lipid droplets and glycogen granules. In addition, injury of the bile canaliculi was determined by dilatation and loss of the microvilli; and damage to the sinusoids was determined by disruption of the sinusoidal endothelial cells' cytoplasm, presence of sinusoidal luminal debris, extravasation of red blood cells, and obliteration of the space of Disse microvilli.

3.8 Assessment of microcirculatory blood flow

3.8.1 *Principle of laser Doppler flowmetry*

Laser Doppler flowmetry (LDF) is an optical technique for assessing tissue microcirculation that provides continuous measurements of blood flow in the capillaries, arterioles, and venules. Measurements utilising LDF necessitate probe placement on the tissue surface. Therefore there is no disruption of tissue architecture or interruption to blood flow (317).

The basic principle that underlies LDF is the Doppler shift which describes the frequency change that a wave undergoes when emitted from a moving object relative to a static detector (318). LDF emits a monochromatic laser light that is

carried by the transmitting optical fibre to the tissue. Some of the light photons will be scattered by moving red blood cells and therefore undergo Doppler shift. Photons that encounter static tissue will not have any frequency change of the light wavelength (no Doppler shift). Both Doppler shifted and non-Doppler shifted back-scattered light from the tissue is conducted through the receiving optical fibre (separate from the transmitting optical fibre) to a photo detector that produces an electrical signal containing all of the Doppler frequency shift information (318,319). Further processing of the signal is performed by the photo detector, and the final output signal is displayed as blood flow perfusion units or blood cell 'Flux' units. The blood flow displayed represents the product of the number of moving red cells and their mean velocity (319).

The relationship between total tissue blood flow, such as in the liver or hindlimb, and the signal measured by LDF on the surface of the tissue has been shown to be linear and reproducible (320). Furthermore, LDF is sensitive to rapid blood flow changes within tissues (320). However it is important to note that LDF is only accurate in assessing relative changes in tissue perfusion but should not be used to quantify tissue MBF in absolute units as there is no conversion factor to achieve this (321,322). Hepatic and hindlimb MBF assessments in the mouse using LDF are well described (323,324). Hindlimb MBF is assessed by LDF measurements made in the foot (323,325).

3.8.2 *Measuring liver and hindlimb microcirculatory blood flow*

A dual channel laser Doppler flowmeter (DRT4, Moor Instruments Ltd., UK) was used to measure blood flow in the microvasculature of the liver and hindlimb. For

each experiment one probe was placed on the left liver lobe, whilst the second was placed on the sole of the right foot. In both cases the probe was positioned so that it was just in contact with the tissue surface. The hepatic probe was mounted in a tubular probe holder in order to prevent the probe from pressing on the hepatic surface and causing microvascular occlusion. For a similar reason, the hindlimb probe was fixed to the operating table using adhesive tape, with the tip positioned on the sole of the right foot (figure 3.5). LDF data was collected as the means of four readings recorded over a one minute period. Figure 3.6 shows the time points of LDF recordings during the study protocol. The hindlimb LDF measurements were made but not recorded, as these were performed only to ensure adequate blood flow interruption to the hindlimb during ischaemia, with recovery of blood flow during hindlimb reperfusion.

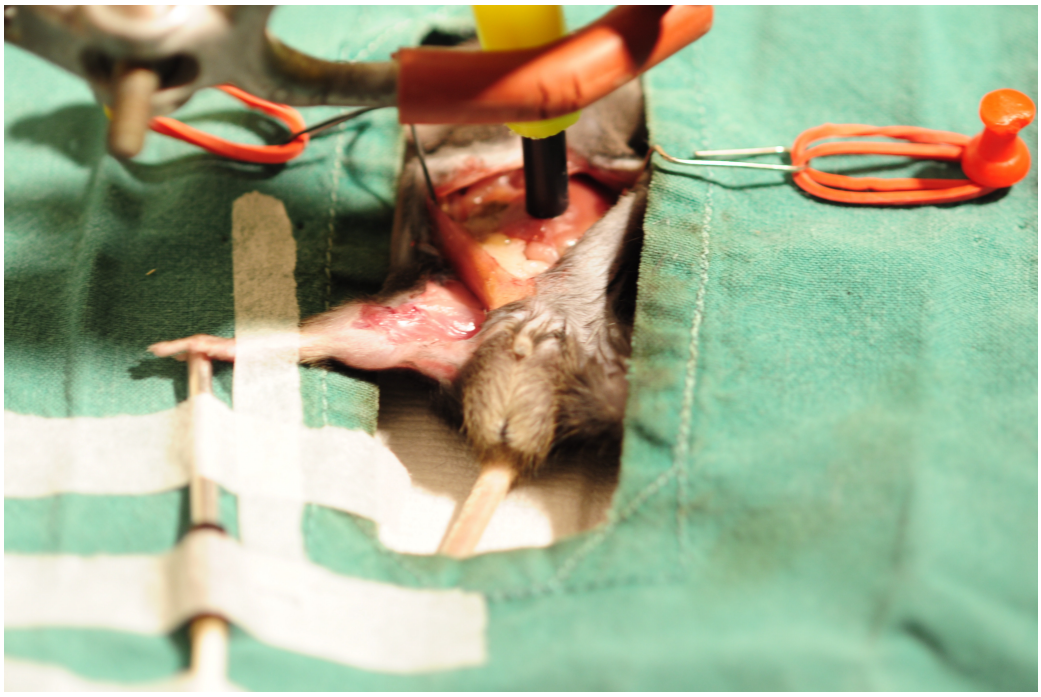

Figure 3.5. Photograph of a mouse illustrating LDF probes positioned on the left hepatic lobe and sole of the right foot.

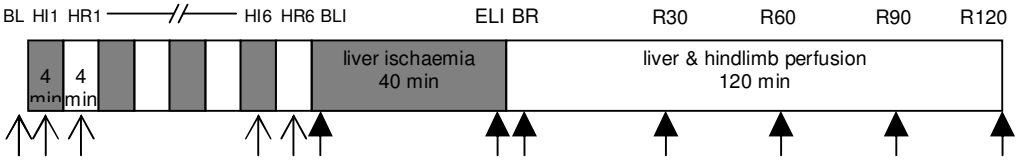

Figure 3.6. Time points of Laser Doppler Flowmetry (LDF) measurements. ↑ indicates time points of foot and liver LDF measurements; ↑ indicates time points of liver only LDF recordings. The mean of four LDF readings over a one minute period was recorded at each time point indicated. Note during cycles 1 to 6 of HI and HR the hindlimb LDF measurements were made but not recorded, as these were performed only to ensure adequate blood flow interruption to the hindlimb during HI, with recovery of blood flow during HR. *BL*, baseline; *HI*, hindlimb ischaemia; *HR*, hindlimb reperfusion; *BLI*, beginning of liver ischaemia; *ELI*, end of liver ischaemia; *BR*, beginning of liver reperfusion; *R30* to *R120* - liver reperfusion at 30, 60, 90, and 120 min post ischaemia.

3.9 eNOS and iNOS Western blot analysis

3.9.1 *Protein extraction and quantification*

Individual samples of liver and skeletal muscle tissues (100 mg) were homogenised in liquid nitrogen. Cell lysis was achieved by the addition of RIPA buffer (Sigma) containing a protease inhibitor (Roche), and repeat vortexing. The samples were then centrifuged at 12,700 rpm (15150 g) for 15 min at 4 ℃. Protein concentrations in the supernatants were measured by the modified Lowry protein assay kit (Pierce Biotechnology, USA).

3.9.2 *SDS gel electrophoresis and Western blotting*

Protein denaturation was achieved by the addition of Laemmli sample buffer (2X, Sigma, UK) to each protein sample (made up with RIPA buffer to a concentration of 8 μg / μl) in a volumetric ratio of 1:1, followed by heating to 95 ℃. Nu-

polyacrylamide gel electrophoresis (NuPAGE 4-12% Bis-Tris Gel, Invitrogen, USA) in NuPAGE running buffer was used to separate the proteins, which were then electro-blotted onto polyvinylidene difluoride (PVDF) membrane (Bio-Rad, USA) soaked in NuPAGE transfer buffer. The membranes were blocked with 5 % semi-skimmed milk powder (Marvel) dissolved in PBS, followed by incubation over night with either polyclonal rabbit anti-eNOS or anti-iNOS (Santa Cruz Biotechnology, USA) in a 1:200 dilution. The membranes were then washed with PBS, incubated with secondary goat anti-rabbit IgG antibody conjugated with HRP in a 1:1000 dilution for 45 min, washed with PBS, illuminated with Super Signal West Dura Extended Duration Substrate (Pierce, USA), and exposed to x-ray films (Fuji medical x-ray films) for variable duration to visualise the proteins bound to antibody. The x-rays were scanned and the density of the eNOS protein bands were analysed with Bio-Rad densitometry software (Molecular Analyst, Windows software for Bio-Rad's image analysis system version 1.5, USA).

3.10 eNOS immunohistochemistry

The left liver lobe and the thigh of the right hindlimb were biopsied at the end of the experiment in each of the animals and were immediately fixed in 10% formal saline. The fixed tissues were then embedded in paraffin, cut into 3 μm sections, dewaxed in xylene, and taken through alcohol. Endogenous peroxidase was blocked with hydrogen peroxide in methanol followed by washing with water. The sections were then pressure cooked for three and a half minutes in citrate buffer (pH 6.0), washed with water, soaked in Tris Buffered Saline with Tween (TBS-T), and treated with a protein solution (Casein- Leica Microsystems) to block background staining. Incubation with rabbit polyclonal eNOS primary antibody (Santa Cruz

Biotechnology, CA, USA) was done overnight at 4 ℃ in a 1:100 dilution. The sections were then washed with buffer, incubated with secondary antibody conjugated with HRP for 30 min, washed with buffer, developed with 3,3'-Diaminobenzidine, washed with water, counterstained with Mayer's Haematoxylin, and mounted for microscopic examination. Placental tissue was used as positive control. For negative controls, liver sections were processed without primary antibody.

3.11 Nitrite and nitrate measurements

The plasma nitrite and nitrate (NOx) levels were measured in wild type mice using a commercially available colorimetric assay kit (Cayman Chemical, catalogue No. 780001). The plasma was first deproteinated using 30 kDa centrifugal filters and diluted 1 in 8 using assay buffer. Total nitrite and nitrate concentrations were determined by the reduction of nitrate to nitrite using nitrate reductase (Cayman Chemical, catalogue No. 780010) in the presence of enzyme cofactor (Cayman Chemical, catalogue No. 780012). Greiss reagent was then added to the solution containing nitrite and the resultant colour development was quantified by reading the absorbance at 550 nm. The total NOx (μM) were calculated using the nitrate standard curve.

3.12 Measurement of hepatic cGMP

cGMP (cyclic 3', 5' guanosine monophosphate) accumulation in liver tissue was determined in wild type mice. To extract cGMP from liver tissue 250 μL of 0.1M HCL was added to each liver tissue followed by homogenisation at 50 Hz for 2 minutes using a TissueLyser (Qiagen). The samples were then centrifuged at 13000

rpm for 5 minutes at 4 C and the supernatant was filtered through 30 kDa centrifugal filters. The filtrates were dried under vacuum for 4 hrs. Quantification of cGMP in the samples was performed using a commercial enzyme immunoassay (EIA) kit (Cayman Chemical, catalogue No. 581021). Briefly, the dry pellets were resuspended in EIA buffer. Samples (50 µL) or standard solutions of cGMP (50 µL of 30 pmol/ml to 0.23 pmol/ml) were incubated together with cGMP EIA antiserum (50 µL) and acetylcholinesterase linked to cGMP tracer (50 µL) in a plate pre-coated with mouse monoclonal anti-rabbit IgG at room temperature for 18 hours. After the plates were washed, colour development was achieved by the addition of Ellman's Reagent (200 µL) and incubation for 60 minutes. Absorbance was measured at 410 nm. cGMP concentrations were calculated using the standard curve generated.

3.13 Statistical analysis

Values are expressed as mean ± standard error of the mean (SEM). One way analysis of variance (ANOVA) with Post Hoc Bonferroni correction for multiple comparisons was used. Independent-samples t-test was used to compare means when there were only two groups. Paired-samples t-test was used to compare the means within a single group at different points in time. $P < 0.05$ was considered statistically significant in all analyses.

Chapter 4

Development of a new mouse model to study the effect of hindlimb ischaemic preconditioning on liver IR injury

4.1 Introduction

Hepatic IR injury is seen either in clinical settings causing direct liver ischaemia such as liver surgery and transplantation, or in the setting of systemic hypoxemia (e.g. respiratory failure) or shock states followed by resuscitation (e.g. haemorrhage, sepsis). The consequences of liver IR injury depend not only on the length of the ischaemic insult, but also on the background condition of the liver (7). For example cirrhotic and steatotic livers are more susceptible to IR compared to normal livers (8,9). One of the therapeutic strategies to lessen liver IR injury is remote ischaemic preconditioning (RIPC). This concept involves brief ischaemia to one organ protecting a remote organ against prolonged ischaemic insults. RIPC was first described by Przyklenk et al (326) in 1993 who showed that brief occlusion of the circumflex artery in the heart protected against a subsequent prolonged ischaemic insult of the myocardial territory supplied by the left anterior descending artery. RIPC is a systemic phenomenon, meaning preconditioning of one body region will protect all other organs to varying degrees. This observation has led to the search for both humoral and neuronal mediators of RIPC, reviewed by Tapuria *et al* in 2008 (327). The hepato-protective effects of direct liver preconditioning (IPC) are seen over two time windows (328). The early phase of preconditioning commences immediately following a brief ischaemic stimulus and lasts under four hours. The late phase begins 12-24 hours after preconditioning and lasts 72-96 hours. Similarly, RIPC has also been shown to exert its beneficial effects over the same timeframe (327).

The main advantage of RIPC over direct IPC is the applicability of the former to the upper or lower limb in a non-invasive manner through the use of external pressure

on the limb, to achieve vessel occlusion and blood flow cessation. Simple devices such as tourniquets and blood pressure cuffs are ideal. The clinical attractiveness and safety of this non-invasive approach to preconditioning is obvious. Human studies, including randomised clinical trials, have shown the heart and vascular endothelium to be protected by limb RIPC (329,330). However, to date there are no published human studies on the benefits of limb RIPC in ameliorating liver IR injury.

The protective effects of limb RIPC against liver IR injury in the rabbit (227), and the rat (229) have previously been demonstrated. Recently a mouse model of limb RIPC followed by liver IR was described (226). The authors of this study used an elastic band to induce hindlimb ischaemia in female mice and they reported a reduction in liver IR injury. However, they did not objectively measure blood flow in the limb. In addition, elastic bands lose elasticity with repeated usage and will produce variable pressures when applied to the limb. Furthermore, the female hormone oestrogen and its derivatives are known to protect against IR injury of the liver (331). Therefore the variation in oestrogen levels during the oestrous cycle in females leads to variable susceptibility to IR injury congruent with the stage of the oestrous cycle (332). In light of this the majority of experimental IR injury models use male animals only.

Mice are the only species with commercially available transgenic strains. The use of transgenics in scientific research represents one of the most accurate methods of delineating the functions of specific gene products or proteins, and thereby of the underlying molecular pathways underpinning the benefits of RIPC. If the molecular mechanisms of RIPC are understood then it may be possible to develop targeted

pharmacological interventions to mitigate the harmful effects of IR injury. Mouse limb RIPC models have been described that offer protection against myocardial, pulmonary, and intestinal IR injury (234,333). Experimental hindlimb preconditioning may be performed either with the application of an external device to occlude femoral blood flow, such as with the use of a tourniquet or a rubber band; or maybe done through an open incision and direct clamping of the femoral artery, or femoral artery and vein. The open method has the advantage of not exerting any direct pressure on the neuro-musculature of the groin, which could lead to pressure necrosis of these structures and a consequent inflammatory reaction with disturbances in limb and systemic haemodynamics.

In the present study, we developed a mouse model of hindlimb RIPC that protects against liver IR injury and that could be utilized to shed light on the mechanisms underlying the protection of RIPC.

4.2 Materials and methods

The detailed methodology was described in chapter 3. A summary of the most pertinent points is given below.

4.2.1 *Mouse model of hindlimb remote ischaemic preconditioning of the liver*

Inbred male C57BL/6 wild type mice (Charles River laboratories, UK) were utilized in the present studies. The animals were anaesthetised using 2% isoflurane. Core

body temperature was maintained at 37.0 ± 0.5 ℃ using a heating pad and monitored by a rectal temperature probe.

Laparotomy was performed through a midline incision. The falciform ligament and the ligament connecting the caudate to the left lobe were divided. A microvascular clamp was then applied to the portal triad supplying the left and median lobes. Successful occlusion of the portal triad was confirmed by a change in colour and a reduction in microcirculatory blood flow (MBF) as measured by laser Doppler flowmetry (LDF). The animals were subjected to 40 minutes of hepatic ischaemia followed by two hours of reperfusion. At the end of the reperfusion period the animals were terminated by exsanguination through cardiac puncture and blood collection. The blood was immediately centrifuged and the plasma supernatant was stored at -70 ℃ until assayed for liver transaminases. The left and median liver lobes were harvested at the end of each procedure for histopathology and transition electron microscopy.

The preliminary experiments involved recovering the animals from anaesthesia during the two hour liver reperfusion period in order to assess general mobility and hindlimb function following RIPC. The RIPC protocol consisted of four minutes ischaemia followed by four minutes reperfusion for a total of six cycles. Cessation of blood flow to the hindlimb was confirmed by the change in foot colour and by the reduction in foot MBF as measured by LDF. From these preliminary experiments it became clear that the tourniquet technique resulted in limb paralysis probably secondary to hindlimb neuromuscular damage as evidenced by gross neuromuscular bruising in the preconditioned hindlimb soft tissues. Therefore the tourniquet

technique was abandoned and all remaining experiments were performed using the open method of preconditioning.

4.2.2 *Non-recovery experimental groups*

Four groups with a minimum of six animals in each were used (Figure 3.2). The total anaesthetic time was equal in all the groups. All animals underwent laparotomy, mobilization of the liver, and mobilization of the right femoral vascular bundle. In addition some of the groups were each subjected to a specific procedure as follows:

Sham: Only underwent the laparotomy, mobilization of the liver, and mobilization of the right femoral vascular bundle described above.
RIPC: The right hindlimb was preconditioned with 6 cycles of 4 minutes ischaemia followed by 4 minutes reperfusion, using a microvascular clamp to occlude the femoral vessels under an operating microscope.
IR: The median and left hepatic lobes were rendered ischaemic for 40 minutes followed by 2 hours reperfusion, using a microvascular clamp to occlude the portal triad branch to these lobes.
RIPC + IR: Animals were subjected to the RIPC followed by the IR procedures.

The plasma ALT and AST levels, and the histological and ultrastructural markers of liver damage were all assessed at the end of two hours of reperfusion following liver ischaemia (or equivalent time points in the sham and RIPC groups).

4.2.3 *Measurement of liver enzymes*

The concentrations of ALT and AST were measured in the plasma using an automated clinical analyzer (section 3.5). These enzymes are sensitive markers of liver injury which are released from injured hepatocytes into the circulation.

4.2.4 *Histopathology*

A liver biopsy was taken from the left ischaemic lobe of each animal at the end of the experiment and was immediately fixed in 10% formal saline. The fixed tissues were embedded in paraffin, and stained with H&E. Sections were assessed by a liver pathologist blinded to the animal groups. Each H&E sample was scored using two different methods as described in section 3.6.

4.2.5 *Transmission electron microscopy*

Liver biopsies were obtained from the left lobe at termination of the animals and were fixed in a glutaraldehyde / paraformaldehyde mixture overnight. An automated tissue processor (Leica EM TP) embedded the samples in Lemix epoxy resin. Stained semi-thin sections were examined under light microscopy to determine the areas exhibiting damage. Ultrathin sections of these were then cut, stained, and viewed with a transmission electron microscope. Representative areas were photographed and the images were interpreted by a transition electron microscopy (TEM) scientist who was blinded to the groups. Assessment of the images was performed according to the parameters outlined in section 3.7.

4.2.6 *Liver and hindlimb microcirculatory blood flow*

A dual channel laser Doppler flowmeter (DRT4, Moor Instruments Ltd., UK) was used to measure blood flow in the microvasculature of the liver and hindlimb (section 3.8). One probe was placed on the left liver lobe, whilst the second was placed on the sole of the right foot. In both cases the probe was positioned so that it was just in contact with the tissue surface. Hepatic LDF data was collected as the means of four readings recorded over a one minute period. Figure 3.6 shows the time points of the LDF recordings during the study protocol. The hindlimb LDF measurements were made but not recorded, as these were performed only to ensure adequate blood flow interruption to the hindlimb during ischaemia, with recovery of blood flow during hindlimb reperfusion.

4.2.7 *Animal survival and postoperative complications*

In order to evaluate the delayed benefits and side effects of hindlimb preconditioning, the clinical postoperative course of mice in the sham, IR, and RIPC + IR group (n = 6 per group) was followed for 28 days. Each group underwent its respective surgical procedure followed by a recovery period of up to 28 days. At the end of this period the animals were humanely terminated.

4.2.8 *Statistical analysis*

Values are expressed as mean ± SEM. One way analysis of variance (ANOVA) with Post Hoc Bonferroni correction for multiple comparisons was used. Paired-samples t-test was used to compare the means within a single group at different points in time. $P < 0.05$ was considered statistically significant in all analyses.

4.3 Results

4.3.1 *Preliminary recovery experiments: Hindlimb RIPC limits hepatic IR injury but the tourniquet technique causes hindlimb paralysis*

The initial experiments were designed to test: 1. the effectiveness of hindlimb RIPC in mitigating liver IR injury; and 2. the possible side effects of the tourniquet versus the open clamp techniques of hindlimb RIPC. To this end the mice were recovered from anaesthesia during the two hours of liver reperfusion.

The plasma ALT and AST levels were lower in the animals that had either the tourniquet (n = 2) or open clamp (n = 4) methods of hindlimb preconditioning prior to liver IR (RIPC + IR group) compared to the group that had liver IR alone. Whilst the difference in ALT levels between the IR and the two RIPC + IR (tourniquet and open clamp) groups did not reach statistical significance ($P > 0.05$), those of AST were significantly lower in the preconditioned groups ($P = 0.034$ vs RIPC + IR (tourniquet); $P = 0.004$ vs RIPC + IR (open clamp)). There were no significant differences in both the ALT or AST levels between the two techniques of preconditioning.

On recovery of the animals from general anaesthesia, the group that had the tourniquet technique of hindlimb RIPC was noted to be paralysed in the preconditioned limb upon ambulation. Moreover, physical bruising of skeletal muscles and femoral nerves were noted following animal termination and dissection of preconditioned hindlimbs. The group that was preconditioned using direct application of a microvascular clamp to the femoral vessels (open clamp technique) did not show paralysis, or neuromuscular bruising of the preconditioned hindlimb.

Similarly, the liver IR alone group with a sham exposure and mobilisation of vessels showed no limb neuromuscular damage.

Based on the results of the preliminary experiments showing equipotent benefit with both the invasive and non-invasive techniques of hindlimb preconditioning, but revealing neuromuscular paralysis only with the latter, all subsequent experiments ($n \geq 6$ in each group) were performed using the open clamp method of preconditioning. The biochemical, histological, and ultrastructural markers of liver damage were assessed at the end of the two hours of reperfusion following liver ischaemia in all these experiments, or the equivalent time points in the sham and RIPC groups (figure 3.2).

4.3.2 *Hindlimb RIPC reduces plasma transaminases levels*

The two groups (sham and RIPC) not subjected to liver IR had minimal increases in both plasma ALT and AST levels at the end of the experimental protocol. In comparison the IR group had significantly higher levels of both enzymes (figure 4.1), indicating significant liver damage. When hindlimb RIPC preceded liver IR (RIPC + IR group) there was a significant reduction in plasma levels of both enzymes in comparison to the IR group ($P < 0.05$).

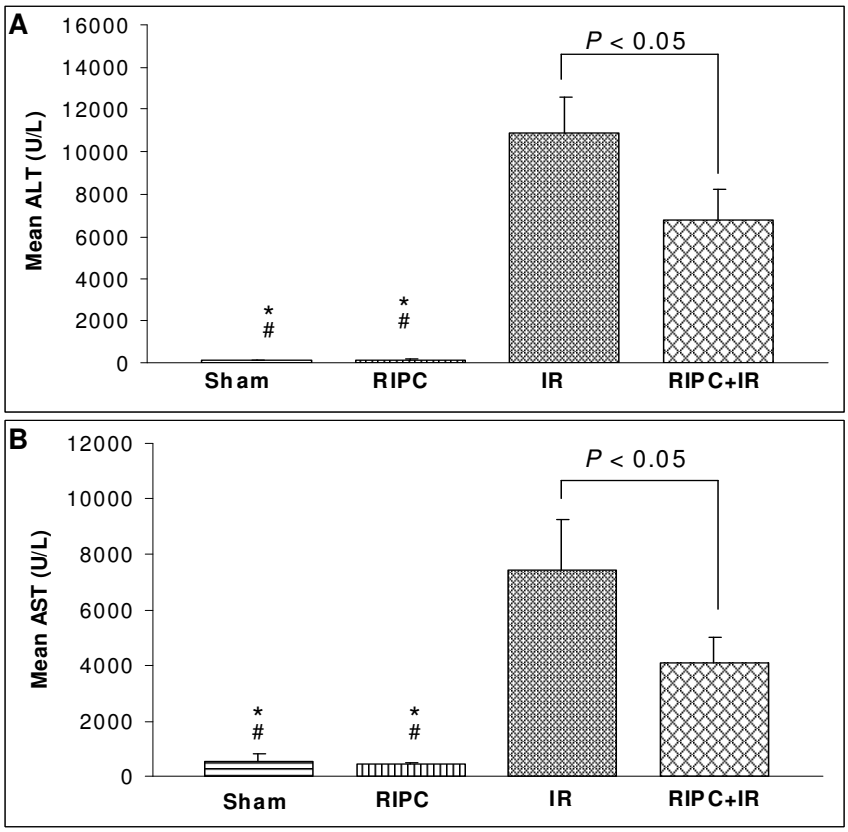

Figure 4.1. Plasma liver enzyme levels. (**A**) Alanine aminotransferase (ALT). **P* < 0.05 vs IR; #*P* < 0.05 vs RIPC+IR. (**B**) Aspartate aminotransferase (AST). **P* < 0.05 vs IR; #*P* < 0.05 vs RIPC+IR.

4.3.3 *Hindlimb RIPC attenuates IR-induced liver histopathological injury*

An overall histopathological grade was assigned to each sample (figure 4.2). The sham and RIPC groups showed minimal signs of liver IR injury with a mean overall grade of 0 in each. Liver IR resulted in a significant increase in the mean overall injury grade (IR group mean overall grade = 1.83) compared to the sham and RIPC groups ($P < 0.05$). Preconditioning prior to liver IR (RIPC + IR group) decreased the mean overall injury score to 1.33 ($P < 0.05$ vs sham or RIPC; $P > 0.5$ vs IR).

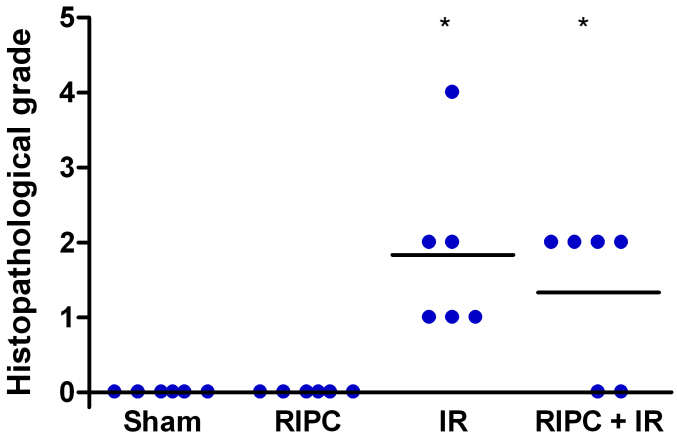

Figure 4.2. Vertical scatter plot of histopathological grades. Each dot represents the overall grade assigned to each individual liver biopsy sample (n = 6 per group). Horizontal bars represent the means. *$P < 0.05$ vs sham or RIPC.

To confirm the findings of the overall grade of injury and to further explore the histopathological features which are most improved by hindlimb preconditioning in liver IR injury, each sample was assessed and scored for each feature of injury as outlined in the methods. The sham and RIPC groups had equal mean scores in 6 out of the 10 individual features assessed. The remaining 4 features had a higher mean score in the RIPC compared to the sham, although in none of these was statistical significance achieved (figure 4.3).

Liver IR resulted in a higher mean score in all 10 individual features compared to both the sham and RIPC alone groups (figure 4.3). However, statistical significance ($P < 0.05$) was only achieved in 4 of these features (discohesive hepatocytes, liver cell ballooning, blurred intercellular borders, RBC extravasation).

In contrast the RIPC + IR group resulted in a higher mean score in 8 of the 10 individual features compared to both the sham and RIPC alone groups, with statistical significance achieved in only two of these features compared to sham (discohesive hepatocytes, liver cell ballooning) and in none compared to RIPC (figure 4.3). Compared to IR, the RIPC + IR group resulted in a lower mean score in 8 out of the 10 individual features. The remaining 2 features (neutrophil infiltration and nuclear pyknosis) had a higher mean score in the RIPC + IR compared to the IR group (figure 4.3). None of the differences between the RIPC + IR and the IR alone group reached statistical significance.

4.3.4 *Ultrastructural damage is ameliorated by hindlimb RIPC*

Table 4.1 details the ultrastructural damage seen in each of the animal groups. The sham group showed normal ultrastructural appearances. The RIPC group showed pleomorphic undamaged mitochondria, endoplasmic reticulum (ER) dilatation, phagolysosomal formation, lipid droplet formation, and cytosolic glycogen granules. The IR group exhibited extensive mitochondrial damage, ER dilatation, cytosolic vacuole formation, phagolysosomal formation, lipid droplet formation, glycogen depletion, bile canaliculi dilatation with damaged microvilli, and sinusoidal endothelial cell (SEC) disruption with extravasation of red blood cells (RBC) into the liver parenchyma. In contrast the main ultrastructural features exhibited by the RIPC + IR group consisted of pleomorphic undamaged mitochondria, ER dilatation, phagolysosomal formation, lipid droplet formation, glycogen depletion, and disruption of SEC but without RBC extravasation. Figure 4.4 shows representative transmission electron micrographs from each animal group.

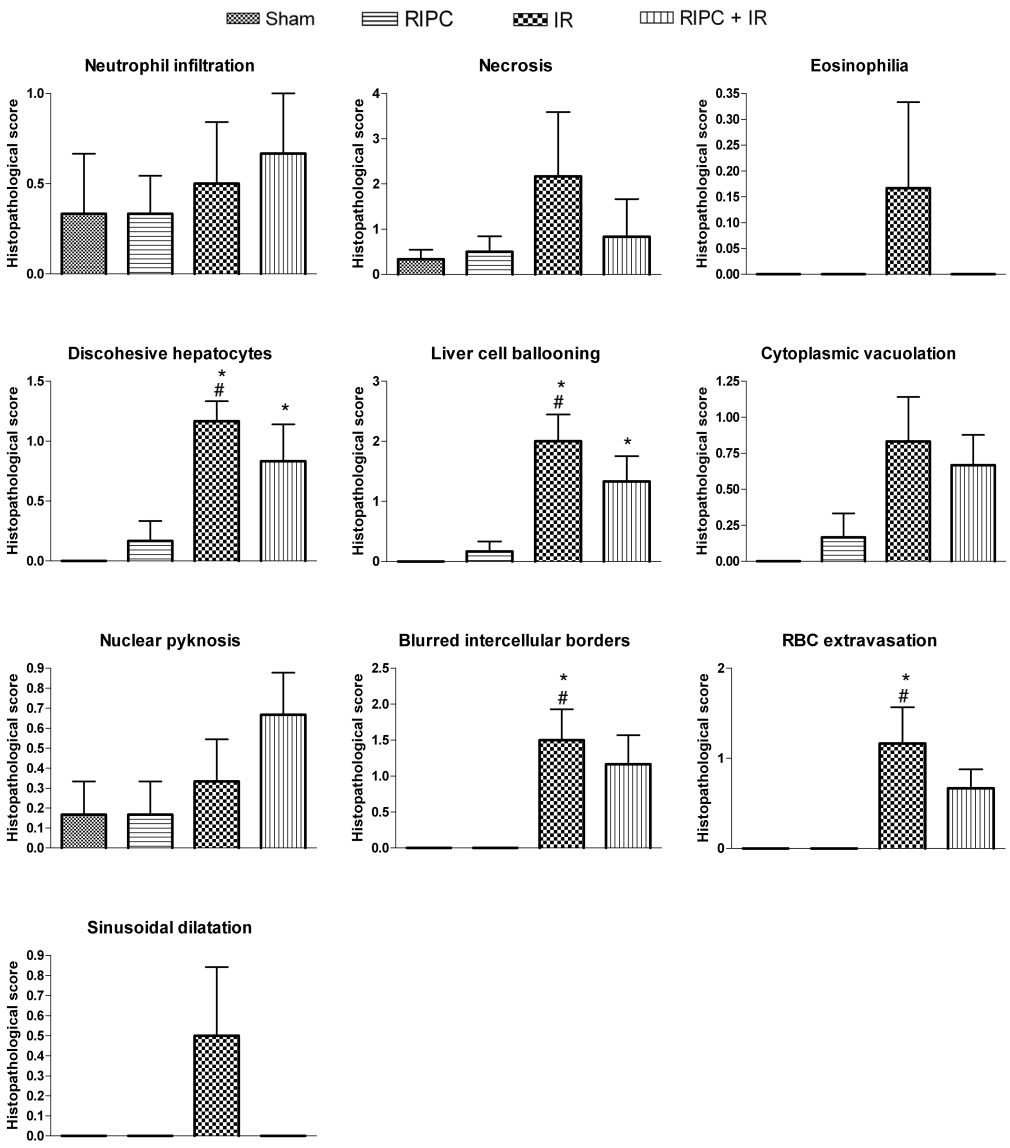

Figure 4.3. Histopathological scores of individual features of liver IR injury. Each bar chart is the mean histopathological score of six animals in that group. The error bars are the standard error of the means. **P* < 0.05 vs sham; #*P* < 0.05 vs RIPC.

Animal group	Mitochondrial damage	ER dilatation	Vacuolation	Phagolysos-omes	Lipid droplets	Glycogen granules	Bile canaliculi	Sinusoidal damage
Sham	Rare	Rare	Rare	Rare	Rare	Frequent	Rarely dilated, microvilli present	Normal SEC microvilli in SD
RIPC	Rarely damaged but pleomorphic	Frequent with vesiculation	Rare	Frequent	Frequent	Frequent	Rarely dilated, microvilli present	Rare SEC damage with sinusoidal debris. Micro-villi in SD
IR	Frequently damaged and pleomorphic	Homogenous dilatation and vesiculation	Abundant, variable size and contain amorphous material	Frequent	Frequent	Rare	Frequently dilated, microvilli disrupted	Severe disrup-tion to SEC, sinusoidal debris, frequent RBC extravasation, damaged SD microvilli
RIPC + IR	Rarely damaged but pleomorphic	Frequent with vesiculation	Rare	Frequent	Frequent	Rare	Rarely dilated, microvilli present	Frequent disruption to SEC, sinusoid-dal debris, rare RBC extravas-ation. Microvi-lli in SD

Table 4.1. Summary of TEM appearances in each animal group. *RBC*, red blood cell; *ER*, endoplasmic reticulum; *SD*, space of Disse; *SEC*, sinusoidal endothelial cell.

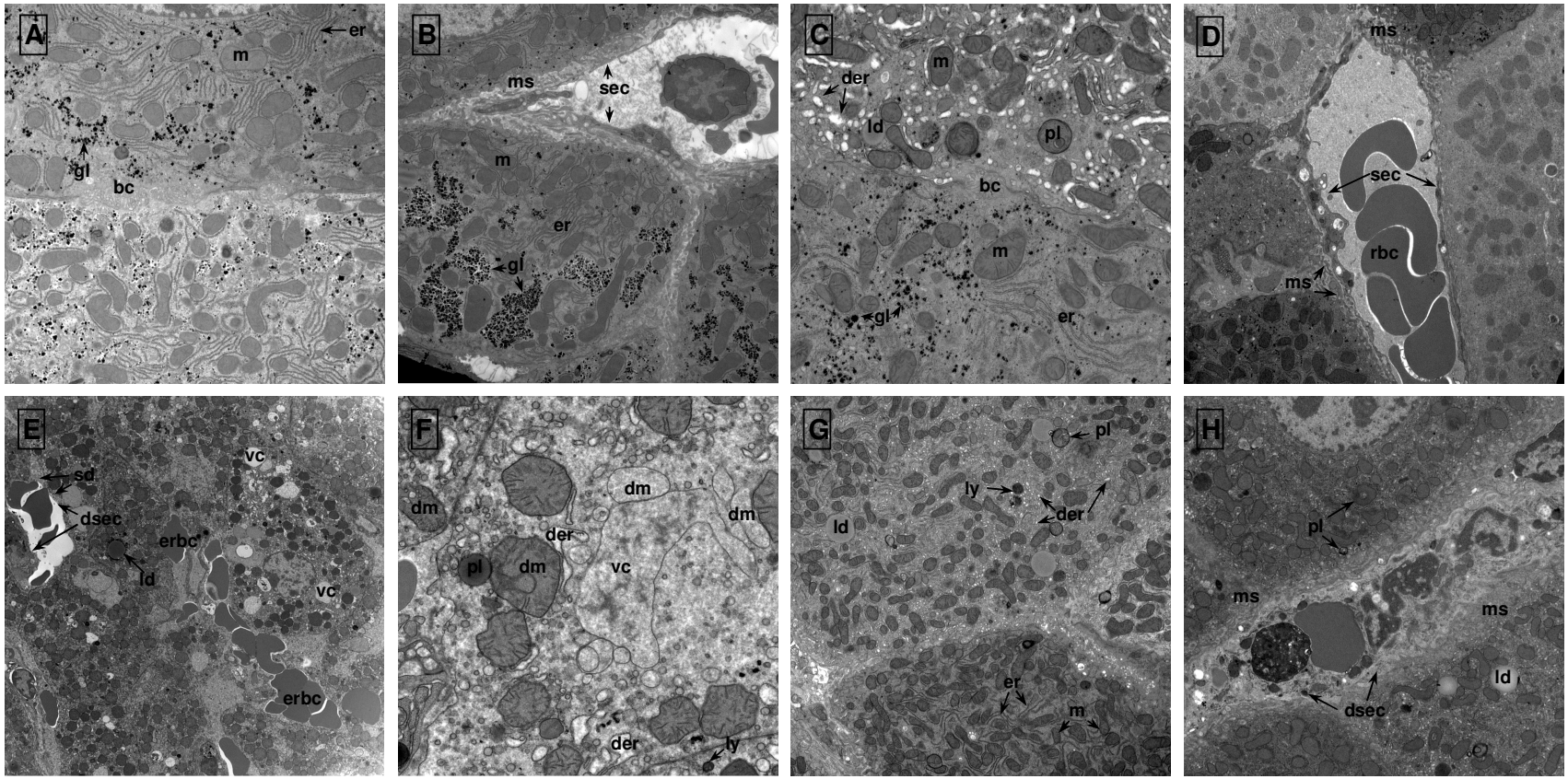

Figure 4.4. Hepatic transmission electron micrographs. The liver samples were taken at the end of the respective procedure in each group. **(A) & (B)** Sham group showing normal endoplasmic reticulum (er), bile canaliculi with microvilli (bc), mitochondria (m), glycogen (gl), sinusoidal endothelial cells (sec), and microvilli in space of Disse (ms). **(C) & (D)** RIPC group showing pleomorphic mitochondria (m), normal (er) and

dilated (der) endoplasmic reticulum, bile canaliculi with microvilli (bc), glycogen (gl), lipid droplets (ld), phagolysosomes (pl), sinusoidal endothelial cells (sec), microvilli in space of Disse (ms), and red blood cells in the sinusoidal lumen (rbc). **(E) & (F)** IR group demonstrating irreversibly damaged mitochondria (dm) with some merging into vacuoles (vc), dilatation and vesiculation of endoplasmic reticulum (der), lipid droplets (ld), lysosomes (ly) and phagolysosomes (pl), and severely damaged sinusoidal endothelial cells (dsec) associated with extravasation of red blood cells (erbc) and obliteration of the space of Disse (sd). **(G) & (H)** RIPC + IR group demonstrating pleomorphic mitochondria (m), normal (er) and dilated (der) endoplasmic reticulum, lipid droplets (ld), lysosomes (ly) and phagolysosomes (pl), damaged sinusoidal endothelial cells (dsec), and microvilli in space of Disse (ms).

4.3.5 *Hepatic microcirculatory blood flow is preserved by hindlimb RIPC*

The MBF expressed as a percentage of baseline (defined as 100%) is illustrated in figure 4.5.

The sham (group 1) and RIPC (group 2) groups did not show any significant changes in hepatic MBF, as compared to their respective baseline measurements or to each other. The IR (group 3) and RIPC + IR (group 4) groups exhibited constant MBF with no significant deviation either from their respective baselines, or mean values of other groups, up to the time point of hepatic ischaemia induction (*BLI* in figure 4.5).

With the onset of partial hepatic ischaemia, the blood flow in the affected lobe decreased to 39.1% and 41.0% of pre-ischaemic baseline levels in the IR and RIPC + IR groups respectively. At the end of 40 minutes of ischaemia, immediately preceding liver reperfusion, the flow remained low averaging 36.3% and 46.6% respectively in the two groups. The MBF levels during hepatic ischaemia were significantly lower in both the IR and RIPC + IR groups compared to their baselines and to the sham and RIPC groups (figure 4.5). There was no significant difference between the IR and RIPC + IR groups during hepatic ischaemia.

Upon reperfusion of the liver, recovery of the microcirculation was greater in the group with RIPC preceding liver IR as compared to the IR only group. At the beginning of liver reperfusion in the IR group the flow increased but was still low at 58.0% of baseline ($P = 0.006$ vs baseline, $P < 0.0001$ vs sham, $P = 0.001$ vs RIPC, P

= 0.046 vs RIPC + IR), whilst that of the RIPC + IR group showed much greater recovery of MBF to 84.3% ($P = 0.08$ vs baseline, $P > 0.05$ vs sham or RIPC). During the ensuing two hours of liver reperfusion, the MBF continued to improve in the RIPC + IR group, so that the mean flow at 30, 60, 90, and 120 minutes of reperfusion recovered towards 90% of baseline levels, and was not significantly different from either the baseline or from the sham or RIPC groups. In the RIPC + IR group the mean flow at 120 minutes was as high as 93.5% of baseline. In contrast over the same period the flow in the IR group remained significantly depressed, recording a mean of 53.4% of baseline at the end of two hours reperfusion. At all time points of reperfusion the flow was significantly lower in the IR group compared to the baseline and to the sham, RIPC, and RIPC + IR groups ($P < 0.01$ vs baseline, Sham, RIPC, or RIPC + IR, at 30, 60, 90, and 120 minutes reperfusion).

Considered together these findings show that antecedent hindlimb preconditioning preserves the blood flow through the hepatic microvasculature in livers subjected to IR injury.

4.3.6 *Animal survival and postoperative complications*

There were no postoperative complications or mortality during the 28 day recovery period. Furthermore, none of the mice suffered any problems with mobility during this interval.

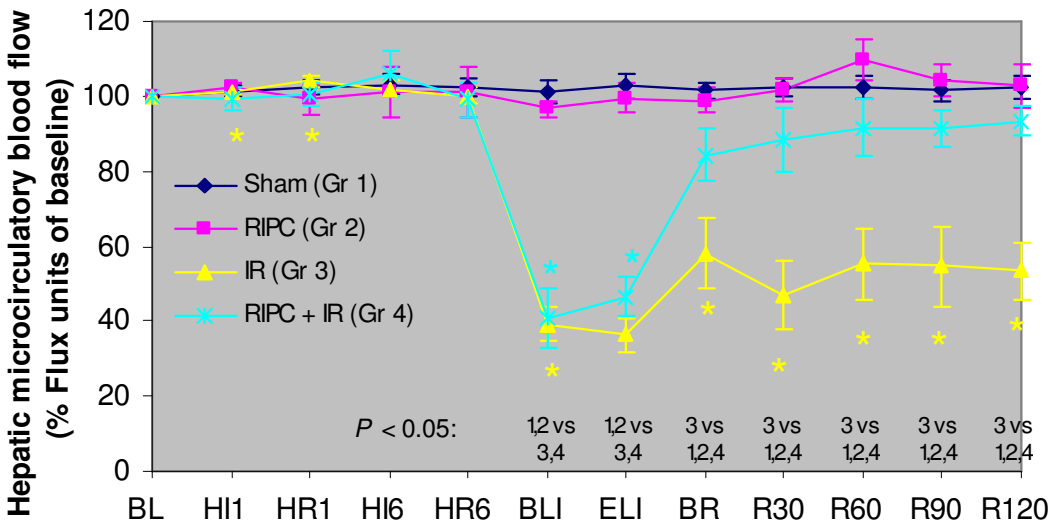

Figure 4.5. Hepatic microcirculatory blood flow, measured by LDF, is illustrated as mean percentage compared to pre-ischaemic baseline. The coloured * at each time point indicates P < 0.05 vs baseline value (100%) for each group. Significant (P < 0.05) inter-group differences are shown vertically above the time points on the x-axis. BL, baseline; HI, hindlimb ischaemia; HR, hindlimb reperfusion; BLI, beginning of liver ischaemia; ELI, end of liver ischaemia; BR, beginning of liver reperfusion; R30 to R120, liver reperfusion at 30, 60, 90, and 120 min post ischaemia.

4.4 Discussion

The clinical need for effective strategies to reduce IR injury emanating from liver surgery and transplantation is great. One of these strategies is hindlimb RIPC which has been shown to decrease hepatic IR injury in the rabbit (227) and rat (229). In this study we have described and validated a mouse model in which hindlimb RIPC significantly reduced liver IR injury. Mice are the only species that currently offer transgenic animals with targeted gene mutations, and therefore represent one of the most useful tools available to study the molecular pathways underpinning the protection exhibited by hindlimb RIPC upon liver IR injury.

The liver ischaemia protocol we used is well described in the literature (334), and encompasses clamping the left and median liver lobes thereby rendering 70% of the liver ischaemic. This produces a significant liver injury but also permits portal venous decompression through the right and caudate lobes, preventing intestinal venous congestion and ischaemia. In order to establish a hindlimb preconditioning protocol we initially used an inflatable tourniquet to occlude the blood flow to the hindlimb in a non-invasive manner. Whilst this technique did achieve hindlimb ischaemia, as measured by the MBF in the foot using LDF, it resulted in neuromuscular bruising and paralysis at tourniquet pressures needed to cause cessation of blood flow to the hindlimb. This was an important finding as the bruising indicated damage and ischaemia to the limb neuromuscular structures which in itself could cause remote IR injury of the liver (335,336). In our previous studies using an external tourniquet to induce hindlimb RIPC in the rabbit and rat (227,229), no hindlimb damage was sustained. The neuromuscular structures in the limbs of mice are more delicate and fragile compared to those of rabbits and rats; hence the mouse is much more susceptible to pressure necrosis brought about by external circumferential pressure devices applied to the limbs. Based on these findings we established an invasive model of hindlimb preconditioning that involved direct clamping of the femoral vascular bundle, whilst avoiding any soft tissue injury. All animals, including the sham and IR groups, underwent mobilisation of the femoral vessels thereby ensuring all the groups are exposed to comparable levels of surgical stress induced by the hindlimb incision and vascular bundle dissection. To verify limb ischaemia and ensure comparability between the groups we used LDF on the sole of the foot to measure MBF.

Recently Wang et al (226) described the use of an elastic band to produce hindlimb ischaemia in female mice. The authors did not determine whether hindlimb soft tissue injury was present. Furthermore the use of elastic bands can produce variable pressures (and therefore variable degrees of vessel occlusion) on application to the limb due to two factors. First repeated usage may result in loss of some of the elastic recoil of elastic bands (become slack); secondly the pressure exerted by the elastic band is dependent on the circumference of the thigh and hence the exact level of the band on the leg, with larger thighs being subjected to greater pressures. Objective confirmation of blood flow cessation to the limb is therefore essential in preconditioning models. In addition the female hormone oestrogen and its derivatives are known to protect against IR injury of the liver (331), therefore usage of female mice is to be avoided in IR research as the variation in oestrogen levels during the oestrous cycle may lead to variable susceptibility to IR injury (332). To ensure the reliability and validity of any animal model of limb RIPC it is important to address these confounding variables, otherwise systemic errors may be introduced into the results. In the invasive hindlimb preconditioning model we describe, the effects of confounding variables were minimised through the measurement and control of body temperature, utilisation of an inbred strain of mice, usage of only male animals of similar age and weight, random selection of mice into each experimental group, subjection of all animals to the same sham procedure in addition to any group-specific procedure, confirmation of liver and hindlimb ischaemia by LDF measurements, and assessment of histopathological and ultrastructural damage to the liver by experts blinded to group allocation. The model demonstrated a consistent reduction in plasma transaminases, histopathological and

ultrastructural liver injury, and an improvement in hepatic MBF as a result of remote preconditioning.

Other mouse models of limb RIPC have been used to ameliorate IR injury in other organs. In two of these studies bilateral limb rubber bands or tourniquets were used (234,333) for preconditioning, but assessment of the adequacy of limb blood flow interruption during ischaemia was not reported. In the third study external finger pressure was applied to the femoral vessels and limb ischaemia was verified by means of pulse oximetry (311). Although digital pressure is less likely to result in neuromuscular damage the degree of inflow occlusion is unlikely to be consistent.

The invasive hindlimb RIPC mouse model described herein is primarily to be utilized as a well-controlled, robust experimental model to study the mechanisms underlying RIPC. The preconditioning protocol is vital to the modulation of liver IR and is species specific (337). The optimal number of cycles and the length of each cycle have not been determined for different animal species. We found a protocol of six cycles of four minutes ischaemia followed by four minutes reperfusion results in significant reductions of liver IR injury in our model.

With this model of open clamping technique of limb preconditioning, both the ALT and AST plasma levels were significantly lower in the RIPC + IR compared to the IR alone group. In agreement with this, the overall histopathological grade (figure 4.2) and eight out of the ten individual features of histopathological injury (figure 4.3) showed less injury in the RIPC + IR compared to IR alone. Interestingly, in this model with a two hour reperfusion period all ten individual features had a higher

mean score in the IR compared to the sham group but statistical significance was only achieved in four of these features. In order to explain the lack of statistical significance for the RIPC + IR compared to IR alone, and in six of the ten individual features for the IR compared to sham, it is important to understand that the sequence of events in liver IR injury is conceptually divided into two phases (338). The early or acute phase covers the first two hours following reperfusion and is dominated by kupffer cell activation and release of various mediators such as reactive oxygen species and cytokines. The late phase commences at about six hours of reperfusion and is characterised by neutrophil accumulation in the liver and progression of hepatocyte and sinusoidal endothelial cell damage. These events form a continuum of injury progression, and importantly different cellular morphological changes may have different kinetics of expression and temporally lag behind the molecular events following microcirculation injury (339,340). In our mouse model liver biopsies were taken at the end of two hours of reperfusion, which represents the early phase of injury when histopathological features of IR injury are in their early stages before they have exhibited their full manifestations, hence explaining the lack of statistical significance in the eight histopathological features of liver IR injury (and the overall grade) that showed less damage with RIPC + IR compared to IR. In addition the fact that liver biopsies in our model were obtained at the end of two hours of reperfusion would also explain why statistical significance was only observed in four out of the ten features that had a higher mean score in the IR compared to sham. Previous studies support our results by showing that for a given period of liver ischaemia, the degree of histopathological manifestations of liver injury is dependent on the length of liver reperfusion. Hines *et al* (258) showed a 45 minute partial liver ischaemia results in a gradual increase in histopathological injury scores as length of the

reperfusion period increases with statistical significance only achieved between the sham and IR groups at six hours of reperfusion. Other studies support this concept of increasing severity of histopathological manifestations of liver IR injury with increasing liver reperfusion length, up to a 24 hour reperfusion period, for a given length of liver ischaemia (341,342). In contrast the histopathological benefits afforded by direct liver IPC do not seem to be dependent on the length of the reperfusion period, as there is significant attenuation of histopathological injury with IPC that is seen from 30 minutes post reperfusion in some studies, and that is extended to various time points of up to 48 hours of reperfusion in others (82,312,343-345).

Assessment of ultrastructural changes by TEM showed hindlimb RIPC acts on multiple subcellular structures to protect against liver IR. Specifically RIPC protected against mitochondrial damage, vacuole formation, bile canaliculi damage, and limited the extent of damage to the sinusoids. Mitochondrial damage is a central event in liver IR injury and has been shown, at least at an ultrastructural level, to be ameliorated by direct liver ischaemic preconditioning (312), and now we have demonstrated a reduction in mitochondrial ultrastructural damage by remote preconditioning. Hepatocyte vacuole formation has been shown to be induced by tissue anoxia in a time-dependent manner, with prominence of larger coalescing vacuoles as the anoxic period increases (315,346). Moreover, vacuoles are mainly thought to contain sinusoidal plasma and to a lesser extent cellular organelles debris. Vacuoles probably arise secondary to disruption of the plasma membrane in combination with the high intrahepatic venous blood pressure that forces the sinusoidal plasma into hepatocytes to form vacuoles (346). Our results in this study

show an abundance of vacuole formation in the IR group that are reduced by antecedent RIPC, indicating RIPC protects against the formation of vacuoles. Previous work has shown direct liver ischaemic preconditioning reduces IR-induced ultrastructural SEC injury (347). We have extended these results by showing RIPC of the hindlimb has similar beneficial effects in reducing the damaging effects of liver IR on the sinusoids and SEC. The RIPC alone group showed mild signs of hepatic ultrastructural injury which were probably caused by the systematic effects of the remote IR stimulus (335,336). Two main differences were noted between the RIPC alone and RIPC + IR group. The first of these pertained to an abundance of glycogen in the RIPC alone group and an almost complete lack of this in the RIPC + IR group. This is because during liver ischaemia, anaerobic metabolism of hepatic glycogen predominates, resulting in significantly less energy being produced per molecule of glycogen compared to the aerobic metabolism of the RIPC alone group, and therefore more of the hepatic glycogen stores are consumed by anaerobic metabolism during ischaemia in order to maintain the energy levels required for cellular function (25,26). The second difference concerned the more severe damage to the sinusoids and the SEC seen in the RIPC + IR compared to the RIPC alone group. Whilst the RIPC + IR group exhibited some signs of ultrastructural damage, the injury sustained by the IR alone group was noticeably much worse across all the parameters that were assessed, indicating RIPC prior to IR significantly attenuated ultrastructural evidence of damage.

In the present study MBF was assessed using LDF. Within the liver LDF measures blood flow in the sinusoids, arterioles, and portal and hepatic venules. Liver ischaemia caused significant reductions in MBF and upon reperfusion there was

minimal improvement in the IR group for the two hour reperfusion period. In contrast the RIPC + IR group showed significant improvement in LDF readings that started at reperfusion, and continued to recover towards baseline flow rates for the subsequent two hour reperfusion period. Our group has previously shown that direct liver IPC prior to liver IR results in improvements in MBF during reperfusion (279), and we are the first group now to show significant improvement in liver MBF with RIPC prior to liver IR. Multiple factors are thought to contribute to the reductions in MBF following hepatic IR injury (30). Additionally, our current TEM results indicate significant destruction of the sinusoids and the SEC with sinusoidal luminal debris. The end result is a significant reduction of MBF on reperfusion including some areas with complete absence of blood flow known as "no-reflow" (30). The observed benefits of RIPC upon the microcirculation indicate the factors responsible start working during liver ischaemia as there is significant improvement in RIPC + IR compared to the IR group commencing at the start of reperfusion. In agreement with the current results, we previously showed, using intravital microscopy in a rat model, hindlimb RIPC prior to liver IR significantly increases the ratio of perfused hepatic sinusoids (229).

The 28 day mouse recovery experiments were performed to evaluate the long term outcome of hepatic IR injury and hindlimb RIPC. The results showed no complications or mortality during this period indicating that the partial hepatic ischaemia model used is non-lethal, and that the hindlimb RIPC model we utilized does not have any complications associated with it.

The signal(s) mediating the effects of hindlimb RIPC may in theory be conveyed to the liver either through the blood or through a neural network (327). The evidence for a humoral signal is stronger and possible candidates include HMGB-1, adenosine, NO acting through nitrite, cytokines, and free radicals (226,327). Further research is needed to ascertain the exact identity of humoral mediators of hindlimb RIPC.

In conclusion we described and validated a new mouse model of hindlimb RIPC that significantly reduces liver IR injury. This experimental model is consistent, shows no side effects of preconditioning, minimises confounding variables, and should prove useful in investigating the mechanisms of RIPC in the mouse.

In this chapter it was shown hindlimb RIPC protects against liver IR injury in the mouse. In the next chapter we will investigate the role of nitric oxide, through the use of the nitric oxide scavenger C-PTIO, in mediating the protective effects of RIPC upon liver IR injury.

Chapter 5

The nitric oxide scavenger Carboxy-PTIO blocks the protective effects of remote ischaemic preconditioning

5.1 Introduction

NO is an important molecule in IR injury. Previous work has suggested a dichotomous role for NO in IR injury with some studies showing NO worsens IR injury (348,349); and others pointing to a protective role for NO, reviewed in Phillips *et al* (29). These opposing effects of the role of NO in IR injury maybe due to the enzymatic source and concentration of the synthesised NO, factors that are in turn influenced by the experimental conditions including, such variables as the length of the ischaemic insult, the organ being studied, the cellular redox status of the organ, time of reperfusion, and in vivo versus in vitro experimental set up. The concentration of released NO is important because it may determine the benefits, or otherwise, of NO in IR injury; with high concentrations of NO promoting the formation of reactive nitrogen species such as peroxynitrite ($ONOO^-$) that enhance IR injury; and lower concentrations of NO being protective (262,350,351).

Direct organ ischaemic preconditioning (IPC) protects against subsequent IR injury at least partially through an NO-dependent mechanism. This has been shown in several organ systems, including the liver (352). Supporting evidence for the role of NO in mediating the protection offered by direct IPC comes from experiments showing inhibition of nitric oxide synthase (NOS) isoforms by the non-selective NOS inhibitor N-Nitro-L-arginine methyl ester (L-NAME) results in abrogation of the protective effects of IPC (240,353). Additionally, IPC results in increased NOS expression (240,354) with a subsequent increase in the NO oxidation products, nitrite and nitrate, that connotes a rise in NO levels (240,355). In contrast to the known beneficial effects of NO in direct liver IPC, its role in RIPC of the liver is currently unknown.

NO is a highly reactive free radical molecule, with a short half life that is in the order of 5-10 seconds. Therefore direct measurement of in vivo NO production in IR research is impractical and quantification of the reaction products of NO such as nitrites, nitrates, and S-nitrosothiols is performed and the results are extrapolated to reflect the levels of NO. An alternative approach, in order to mitigate the inaccuracies associated with the assumption that all the NO reaction products bear a linear relationship to the concentration of NO in IR research, which it does not, is to directly eliminate the released NO through the use of the direct NO scavenger carboxy-PTIO (C-PTIO) (303).

There are no previous studies evaluating the effects of C-PTIO on the protection afforded by RIPC on liver IR injury. Therefore the aim of the present study was to determine the effects of scavenging the NO produced during hindlimb RIPC, through the use of C-PTIO, on liver IR injury. It was found that NO plays an important role in mediating the protective effects of RIPC on liver IR injury.

5.2 Materials and methods

The detailed methodology was described in chapter 3. A summary of the most pertinent points is given below.

5.2.1 *Animal surgical procedure*

Male inbred C57BL/6 wild type mice (Charles River laboratories, UK) were utilized in the present study. The animals were anaesthetised using 2% isoflurane. Core body temperature was maintained at 37.0 ± 0.5 ℃ using a heating pad and a rectal

temperature probe. Hepatic IR was performed as detailed in section 3.4.1. At the end of the reperfusion period the animals were terminated by exsanguination through needle cardiac puncture and blood collection. The blood was immediately centrifuged and the plasma supernatant was stored at -70 ℃ until assayed for liver transaminases. The left and median liver lobes were harvested at the end of each procedure for histopathology and transition electron microscopy. Hindlimb preconditioning consisted of microvascular clamping of the femoral vessels for four minutes followed by four minutes reperfusion for a total of six cycles as described in section 3.4.2.

5.2.2 *Experimental groups*

Four groups with a minimum of six animals in each were used (Figure 3.2). The total anaesthetic time was equal in all the groups. All animals underwent laparotomy, mobilization of the liver, and mobilization of the right femoral vascular bundle. In addition some of the groups were each subjected to a specific procedure as follows:

Sham: Only underwent the laparotomy, mobilization of the liver, and mobilization of the right femoral vascular bundle described above.

IR: The median and left hepatic lobes were rendered ischaemic for 40 minutes followed by 2 hours reperfusion, using a microvascular clamp to occlude the portal triad branch to these lobes.

RIPC + IR: The right hindlimb was preconditioned with 6 cycles of 4 minutes ischaemia followed by 4 minutes reperfusion, using a microvascular clamp to

occlude the femoral vessels under an operating microscope. This was followed by the IR group procedure described above.

C-PTIO + RIPC + IR: The NO scavenger C-PTIO was administered intravenously at a dose of 1 mg/kg in 50 µl of D-PBS, followed by the RIPC + IR procedure.

5.2.3 *Measurement of liver enzymes*

The concentrations of ALT and AST were measured in the plasma using an automated clinical analyzer as described in section 3.5.

5.2.4 *Histopathology*

A liver biopsy was taken from the left ischaemic lobe of each animal at the end of the experiment and was immediately fixed in 10% formal saline. The fixed tissues were embedded in paraffin, and stained with H&E. Sections were assessed by a liver pathologist blinded to the animal groups. Each H&E sample was scored using two different methods as described in section 3.6.

5.2.5 *Transmission electron microscopy*

Liver biopsies were obtained from the left lobe at termination of the animals and were fixed in a glutaraldehyde / paraformaldehyde mixture overnight, processed as described in section 3.7, and viewed with a transmission electron microscope. Representative areas were photographed and the images were interpreted by a transition electron microscopy (TEM) scientist who was blinded to the groups. Assessment of the images was performed according to the parameters outlined in section 3.7.

5.2.6 *Liver and hindlimb microcirculatory blood flow*

Laser Doppler flowmetry (LDF) was used to measure blood flow in the microvasculature of the liver as described in section 3.8. The probe was placed on the left liver lobe so that it was just in contact with the tissue surface. LDF data was collected as the mean of four readings recorded over a one minute period. In addition, a second LDF probe was positioned on the sole of the right foot to ensure blood flow interruption and reperfusion during femoral vessels clamping and unclamping respectively. Figure 3.6 shows the time points of the LDF recordings during the study protocol.

5.2.7 *Statistical analysis*

Values are expressed as mean ± SEM. One way analysis of variance (ANOVA) with Post Hoc Bonferroni correction for multiple comparisons was used. $P < 0.05$ was considered statistically significant in all analyses.

5.3 Results

The plasma transaminases levels, histopathological scores, ultrastructural changes, and MBF results of the C-PTIO + RIPC + IR group obtained in this chapter were compared to results of the sham, IR, and RIPC + IR groups described in chapter 4.

5.3.1 *C-PTIO increases plasma transaminases levels in hindlimb preconditioned mice undergoing liver IR*

Liver IR caused a significant rise in the plasma levels of ALT and AST compared to the sham group ($P < 0.05$). Antecedent hindlimb preconditioning (RIPC + IR group)

significantly reduced the plasma transaminases levels compared to IR alone ($P < 0.05$). Intravenous administration of C-PTIO prior to hindlimb RIPC and liver IR (C-PTIO + RIPC + IR group) resulted in a significant increase ($P < 0.05$) in the plasma levels of ALT and AST compared to the RIPC + IR group (figure 5.1).

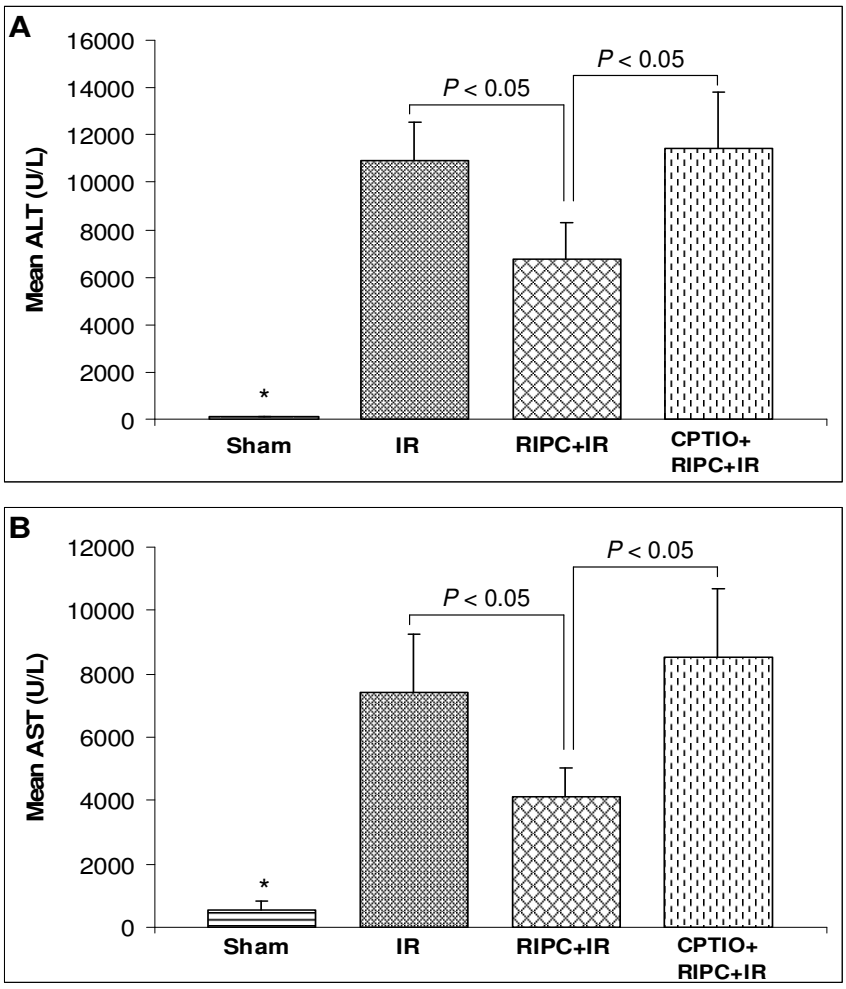

Figure 5.1. Plasma liver enzyme levels. (**A**) Alanine aminotransferase (ALT). *$P < 0.05$ vs IR, RIPC+IR, or C-PTIO (C-PTIO+RIPC+IR group). (**B**) Aspartate aminotransferase (AST). *$P < 0.05$ vs IR, RIPC+IR, or C-PTIO (C-PTIO+RIPC+IR group).

5.3.2 *C-PTIO non-significantly abrogates the beneficial effects of RIPC on liver histopathological injury*

The mean overall histopathological grade for each animal group is given in figure 5.2. The sham group showed minimal signs of liver IR injury with a mean overall grade of 0. Liver IR resulted in a significant increase in the mean overall injury grade (IR group mean overall grade = 1.83) compared to the sham group ($P < 0.05$). Preconditioning prior to liver IR (RIPC + IR group) decreased the mean overall injury score to 1.33, which is not significantly different from the sham or IR groups ($P > 0.05$). Administration of C-PTIO prior to RIPC + IR (C-PTIO + RIPC + IR group) resulted in an increase of the mean overall injury grade to 1.5 ($P < 0.05$ vs sham; $P > 0.05$ vs IR or RIPC + IR).

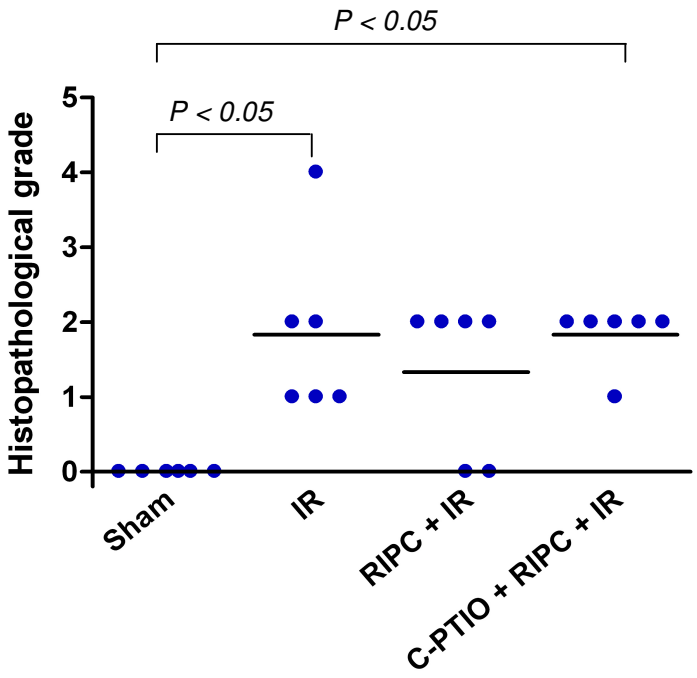

Figure 5.2. Vertical scatter plot of histopathological grades. Each dot represents the overall grade assigned to each individual liver biopsy sample (n = 6 per group). Horizontal bars represent the means.

Five individual histopathological features of liver IR injury (discohesive hepatocytes, liver cell ballooning, cytoplasmic vacuolation, blurred intercellular borders, RBC extravasation) showed a significant increase in the mean score in each of the IR and C-PTIO + RIPC + IR groups compared to sham ($P < 0.05$). Additionally, the mean score of the C-PTIO + RIPC + IR group in cytoplasmic vacuolation was significantly higher ($P < 0.05$) than the mean score in the RIPC + IR group (figure 5.3). Despite there being no statistically significant differences between the mean scores of the RIPC + IR compared to the C-PTIO + RIPC + IR group in the majority of the individual features assessed; there was a trend showing an increase of the mean scores in the C-PTIO + RIPC + IR compared to the RIPC + IR group in 7 of the individual features assessed (figure 5.3).

5.3.3 *C-PTIO nullifies the protective effects of hindlimb RIPC on specific features of ultrastructural damage in liver IR*

Figure 5.4 illustrates representative changes exhibited by each of the animal groups. The sham group showed normal ultrastructural appearances. The IR group exhibited extensive mitochondrial damage, ER dilatation, cytosolic vacuole formation, phagolysosomal formation, lipid droplet formation, glycogen depletion, bile canaliculi dilatation with microvilli damage, and sinusoidal endothelial cell (SEC) disruption with extravasation of red blood cells (RBC) into the liver parenchyma. In contrast the ultrastructural damage sustained by the RIPC + IR group consisted of ER dilatation, phagolysosomal formation, lipid droplet formation, glycogen depletion, and disruption of SEC but without RBC extravasation.

The administration of C-PTIO prior to RIPC + IR resulted in extensive mitochondrial damage, vacuole formation, lipid droplet formation, bile canaliculi dilatation with microvilli destruction, and homogenous SEC disruption with RBC extravasation. In addition this group exhibited frequent condensed crescent shaped lengths of ER indicative of ER membrane damage secondary to lipid peroxidation.

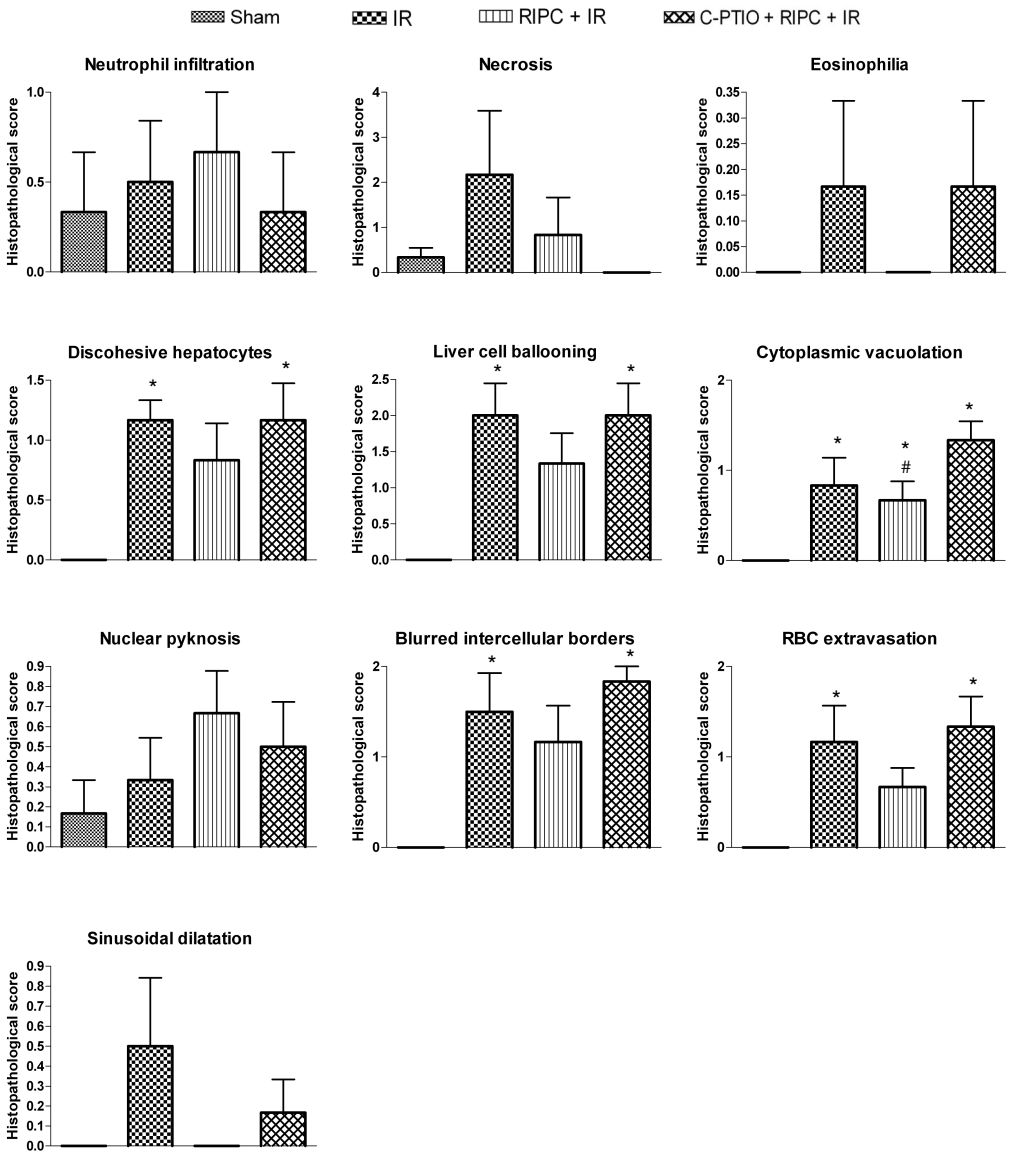

Figure 5.3. Histopathological scores of individual features of liver IR injury. Each bar chart is the mean histopathological score of six animals in that group. The error bars are the standard error of the means. **P* < 0.05 vs sham; #*P* < 0.05 vs C-PTIO + RIPC + IR.

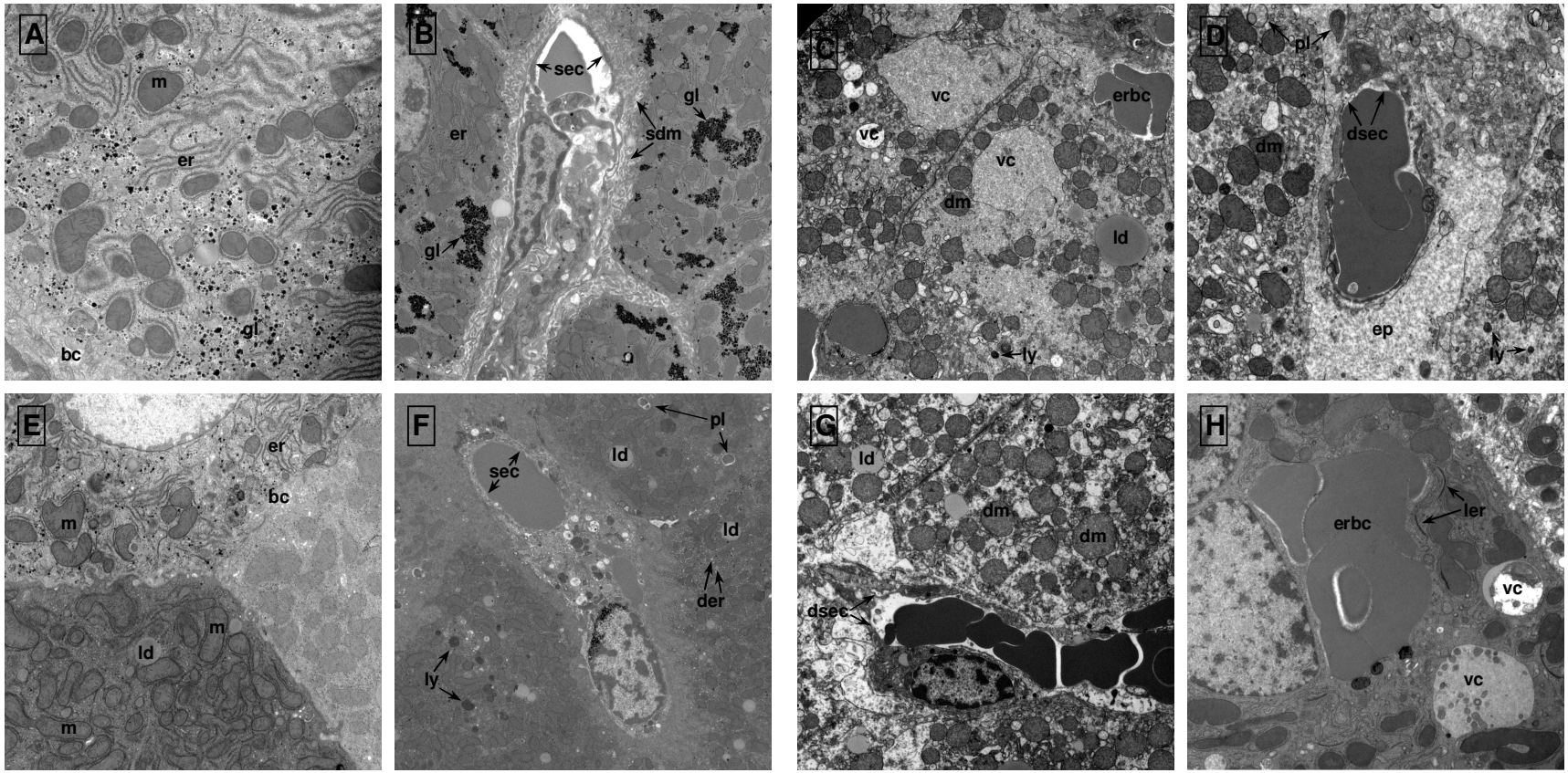

Figure 5.4. Hepatic transmission electron micrographs. The liver samples were taken at the end of the procedure in each group. **(A) & (B)** Sham group showing normal endoplasmic reticulum (er), bile canaliculi with microvilli (bc), mitochondria (m), glycogen (gl), and sinusoidal endothelial cells (sec) with microvilli in space of Disse (sdm). **(C) & (D)** IR group demonstrating irreversibly damaged mitochondria (dm) with

some merging into vacuoles (vc), dilatation and vesiculation of endoplasmic reticulum (der), lysosomes (ly) and phagolysosomes (pl), lipid droplets (ld), and severely damaged sinusoidal endothelial cells (dsec) associated with extravasated red blood cells (erbc) and plasma (ep). **(E) & (F)** RIPC + IR group demonstrating undamaged pleomorhic mitochondria (m), lipid droplets (ld), lysosomes (ly) and phagolysosomes (pl), normal (er) and dilated (der) endoplasmic reticulum, bile canaliculi with microvilli (bc), glycogen (gl), and damaged sinusoidal endothelial cells (sec) but without RBC extravasation. **(G) & (H)** C-PTIO + RIPC + IR group showing damaged mitochondria (dm), vacuolation (vc), lipid droplets (ld), severely damaged sinusoidal endothelial cells (dsec) associated with red blood cell extravasation (erbc), and condensed crescent shaped lengths of endoplasmic reticulum indicative of lipid peroxidation of the endoplasmic reticulum membrane (ler).

5.3.4 *The protective effects of hindlimb RIPC on hepatic microcirculatory blood flow in liver IR are abolished by C-PTIO*

Figure 5.5 illustrates hepatic MBF for the duration of the experiment. The sham group demonstrated constant hepatic MBF, whilst the IR and RIPC + IR exhibited a significant reduction of MBF during liver ischaemia. Upon reperfusion the IR group showed no significant improvement in MBF, whilst the RIPC + IR group demonstrated significant recovery of MBF towards baseline values compared to the IR group ($P < 0.05$).

C-PTIO administration prior to RIPC + IR (C-PTIO + RIPC + IR group) resulted in reductions of MBF throughout the duration of the experiment. During the first hindlimb ischaemia (HI1) the mean MBF was 93.8% of baseline ($P = 0.038$ vs sham; $P = 0.045$ vs IR; $P > 0.05$ vs RIPC + IR). Similarly, during the first hindlimb reperfusion (HR1) the mean MBF was 93.8% of baseline ($P = 0.025$ vs sham; $P = 0.007$ vs IR; $P > 0.05$ vs RIPC + IR). In comparison there were no significant differences in mean MBF values between the C-PTIO + RIPC + IR and the other groups during the sixth HI and HR. Commencement of liver ischaemia resulted in a significant reduction in MBF compared to the sham but not the IR or RIPC + IR groups. Following reperfusion, MBF in the C-PTIO + RIPC + IR group failed to recover, showing significant differences compared to the sham and RIPC + IR groups throughout reperfusion ($P < 0.05$). At the end of the 2 hour reperfusion period the mean MBF value was 48.2% of baseline in the C-PTIO + RIPC + IR group compared to 93.5% of baseline in the RIPC + IR group ($P < 0.0001$). There were no significant differences in the mean MBF values between the C-PTIO + RIPC + IR and the IR groups throughout the reperfusion period (figure 5.5).

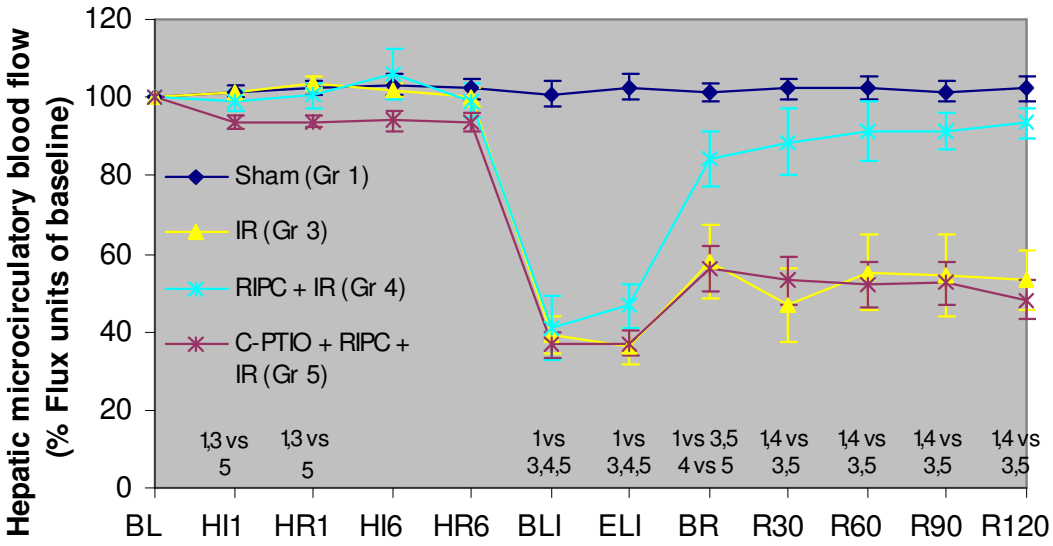

Figure 5.5. Hepatic microcirculatory blood flow, measured by LDF, is illustrated as mean percentage compared to pre-ischaemic baseline. Significant ($P < 0.05$) inter-group differences are shown vertically below each time point on the x-axis. BL, baseline; HI, hindlimb ischaemia; HR, hindlimb reperfusion; BLI, beginning of liver ischaemia; ELI, end of liver ischaemia; BR, beginning of liver reperfusion; R30 to R120, liver reperfusion at 30, 60, 90, and 120 min post ischaemia.

5.4 Discussion

C-PTIO is a nitronyl nitroxide that neutralises the actions of NO in biological systems in a reaction that results in the production of NO_2 and the amino nitroxide C-PTI (303,356). The substrate C-PTIO directly extinguishes the NO generated by NOS without affecting NOS activity (356). C-PTIO has been used extensively in vivo to investigate the biological effects of NO, including in liver IR research (302,357) where administration of C-PTIO has been shown to abolish the protective effects of nitrite-derived NO (302,357).

The role of NO in mediating the protective effects of RIPC on liver IR injury is currently unknown. The only study to allude to this measured the plasma nitrite and nitrate (NOx) levels in peripheral arterial and hepatic venous blood following hindlimb RIPC and hepatic IR in a rabbit model (227). The plasma NOx levels were non-significantly lowered following hepatic IR compared to the sham group in both peripheral arterial and hepatic venous blood. Hindlimb RIPC prior to hepatic IR resulted in an increase in NOx levels compared to the IR alone group which only reached statistical significance in hepatic venous blood samples but not in arterial samples (227). These results indicated RIPC prior to liver IR prevented a reduction in NOx plasma levels compared to IR alone. With regards to the role of NO in mediating the protective effects of RIPC in other organs, various experimental designs have been utilized to elicit this in different combinations of RIPC sites and organs subjected to index ischaemic insults. This approach mainly revolved around the use of NOS inhibitors to block NO synthesis, or the use of NOS knockout animals. Shahid et al (233) showed femoral artery preconditioning prior to myocardial ischaemia significantly reduces myocardial infarct size and improves cardiac function compared to non-preconditioned animals. Administration of the NOS inhibitor L-NAME abrogated the protection furnished by preconditioning (233). Similarly, infusion of L-NAME prior to hindlimb RIPC abolished its protective effects against subsequent abdominal adipocutaneous flap ischaemia (232). Other NOS inhibitors such as N omega-nitro-L-arginine (L-NNA) and S-methylthiosulfourea have also been shown to block the protective effects of femoral artery RIPC, but in these studies the index ischaemic insult was global brain ischaemia (358,359). The use of NOS knockout animals has been limited to a study

in which iNOS$^{-/-}$ mice lost the protection afforded by hindlimb RIPC in reducing myocardial IR injury compared to wild type animals (234).

The results of the current study showed that NO is a pre-requisite for full manifestations of the benefits of RIPC upon liver IR injury, as neutralisation of NO with C-PTIO abolished the protection of RIPC. The plasma liver enzymes showed a significant elevation in the C-PTIO + RIPC + IR compared to the RIPC + IR group. The overall histopathological grade and 7 individual histopathological features of liver IR injury, showed increased mean scores when NO was abolished using C-PTIO, although only in one individual feature, cytoplasmic vacuolation, was the difference statistically significant. The reason for this has been discussed in chapter 4 and mainly pertains to the short (2 hour) reperfusion period in this experimental model, which means histopathological manifestations of IR injury at levels detectable by light microscopy are in their early stages. However, when higher power studies using TEM were performed to assess liver ultrastructural IR injury, clearer negative effects of C-PTIO on RIPC protection were seen.

The ultrastructural changes in the C-PTIO + RIPC + IR group showed increased mitochondrial damage, ER membrane lipid peroxidation, and increased SEC damage compared to the RIPC + IR group. NO has many protective functions within cells. In liver IR injury NO has been shown to decrease hepatic injury by preserving the mitochondria and antioxidant enzyme activity (280,360,361), hence providing an explanation for the increase in mitochondrial damage and ER membrane lipid peroxidation observed in our study. Moreover, NO is one of the main endothelial cell homeostatic factors, fulfilling a range of functions to maintain the endothelium

physiological status quo, including anti-inflammatory actions (362). Therefore removal of NO in our study led to SEC damage to an extent not seen in the RIPC + IR group.

The explanation for the significant reductions in hepatic MBF during liver reperfusion, seen in the C-PTIO + RIPC + IR compared to the RIPC + IR group, is likely to be multifactorial. SEC damage was worse in the group receiving C-PTIO and this would have contributed to the reduction in blood flow within the sinusoids. In addition NO significantly increases hepatic MBF during direct liver IPC (279) and our results here indicate RIPC has a similar effect. Moreover, NO is a vasodilator (362) and is known to induce an increase in MBF in chronically ischaemic limbs which is significantly reduced by administration of C-PTIO (363). Therefore removal of NO through the use of C-PTIO in livers subjected to ischaemia in our experiments was likely to be a main contributor to the reductions in hepatic MBF seen during reperfusion. It is important to note that the use of C-PTIO has been shown either not to affect mean arterial blood pressure (364), or only to cause a slight transient increase in blood pressure (365); and therefore the failure of MBF recovery during liver reperfusion in the C-PTIO + RIPC + IR group in our experiments is likely to be independent of any changes in systemic blood pressure, although this was not directly measured in our study. C-PTIO was administered prior to the first cycle of hindlimb RIPC and interestingly resulted in a small but significant hepatic MBF reduction prior to any liver ischaemia induction, only during the first hindlimb RIPC cycle, compared to the sham and IR groups. This is likely a transient effect of C-PTIO administration as hepatic MBF values were not

significantly different from other groups during the second to the sixth hindlimb RIPC cycles.

An additional control animal group that could have been included in this study would have been C-PTIO + IR. However this group has been included in a previous study (302) and as expected showed a significant worsening of liver injury compared to the IR alone group. Hence this group was not repeated in the present study.

In conclusion, scavenging NO through the administration of C-PTIO prior to limb preconditioning and liver IR leads to abrogation of several of the protective effects of RIPC on liver IR injury. These results indicate that NO mediates the effects of RIPC by reducing ultrastructural damage to the mitochondria, ER membranes, and SEC. In addition NO is needed to preserve the protective effects of RIPC on hepatic MBF.

In this chapter it was shown NO is required for the protective effects of RIPC in liver IR injury. In the next chapter we will investigate the contribution of the nitric oxide synthase isoforms in the protection afforded by hindlimb RIPC.

Chapter 6

The role of nitric oxide synthase in remote ischaemic preconditioning of the liver

6.1 Introduction

Nitric oxide (NO) is synthesised by one of three nitric oxide synthase (NOS) isoforms. The expression of the neuronal NOS (nNOS) is mostly limited to neural tissue and will not be discussed further. Endothelial NOS (eNOS) is constitutively expressed in many cell types, including liver endothelial cells and hepatocytes (240-243). Inducible NOS (iNOS) is not expressed under normal circumstances, but is up-regulated in inflammatory conditions including ischaemia reperfusion (IR) injury of the liver, in hepatocytes, endothelial cells, biliary cells, kupffer cells, neutrophils, and T-lymphocytes (245-249).

There is a limited amount of literature on eNOS and iNOS in direct ischaemic preconditioning (IPC) of the liver. One study (240) assessed eNOS expression in IPC and showed increased expression in rats undergoing hepatic IPC + IR compared to those subjected to IR alone. Furthermore, the increase in eNOS expression was associated with significantly higher plasma nitrite and nitrate (NOx) levels in the preconditioned (IPC + IR) compared to the IR alone group. Three studies assessed iNOS expression in IPC. One of these, a human study that evaluated gene expression in living donor liver transplants, showed increased iNOS expression following IPC performed prior to liver procurement compared to non-preconditioned group (354). Similarly, iNOS expression was also increased in rats livers receiving IPC + IR compared to those subjected to IR alone (366). Additionally, this study demonstrated an increase in plasma NOx levels in association with the increased iNOS expression in the IPC group (366). In contrast the work by Koti *et al* (240) showed iNOS expression was absent in all experimental groups, including the IPC + IR and the IR alone groups.

The role of eNOS in remote ischaemic preconditioning (RIPC) of any organ has not been studied. However that of iNOS has, and three studies seem to indicate iNOS is required for the protection of RIPC. Li *et al* (234) demonstrated hindlimb RIPC protects against delayed myocardial ischaemia, at 24 hours post RIPC, that is associated with increased myocardial iNOS expression. However, $iNOS^{-/-}$ animals lose the protection provided by RIPC (234). Likewise, intestinal preconditioning protects against myocardial ischaemia 24 hours post preconditioning, which is accompanied by increased iNOS activity (367). Moreover, the relative iNOS inhibitors, aminoguanidine and S-methylisothiourea, inhibited the protective effects of intestinal RIPC (367). Spontaneous or induced brain ischaemia has also been shown to protect against subsequent myocardial ischaemia in wild type but not $iNOS^{-/-}$ animals 24 hours after brain ischaemia (368). However, iNOS expression was not increased in wild types at 24 hours post brain ischaemia, which was interpreted by the authors to indicate NO acts as a trigger rather than a mediator of RIPC (368).

The aim of the current study was to assess for the first time the contribution of eNOS in the protection furnished by RIPC on liver IR injury. Furthermore, we wished to examine the effects of RIPC on iNOS expression.

6.2 Materials and methods

The detailed methodology was described in chapter 3. A summary of the most pertinent points is given below.

6.2.1 *Animal surgical procedure*

Male inbred C57BL/6 wild type mice (Charles River laboratories, UK); and mice lacking the constitutively expressed enzyme, endothelial nitric oxide synthase ($eNOS^{-/-}$, bred in-house) were utilized in the present study. The animals were anaesthetised using 2% isoflurane. Core body temperature was maintained at 37.0 ± 0.5 ℃ using a heating pad and a rectal temperature probe. Hepatic IR was performed as detailed in section 3.4.1. At the end of the reperfusion period the animals were terminated by exsanguination through needle cardiac puncture and blood collection. The blood was immediately centrifuged and the plasma supernatant was stored at -70 ℃ until assayed for liver transaminases. The left and median liver lobes were harvested at the end of each procedure for histopathology and transition electron microscopy.

Hindlimb preconditioning consisted of microvascular clamping of the femoral vessels for four minutes followed by four minutes reperfusion for a total of six cycles as described in section 3.4.2.

6.2.2 *Experimental groups*

Four groups of $eNOS^{-/-}$ mice (figure 3.3) with a minimum of six animals in each were used to investigate the effects of RIPC on liver IR injury through the assessment of liver enzymes, histopathological scores, TEM damage, and MBF. In addition four groups of wild type mice (figure 3.2) were used to investigate the effects of RIPC on liver and hindlimb expression of eNOS and iNOS; as well as the cellular distribution of eNOS expression. The total anaesthetic time was equal in all the groups. All animals underwent laparotomy, mobilization of the liver, and

mobilization of the right femoral vascular bundle. In addition some of the groups were each subjected to a specific procedure as follows:

eNOS$^{-/-}$ groups:

Sham: Only underwent the laparotomy, mobilization of the liver, and mobilization of the right femoral vascular bundle described previously.

RIPC: The right hindlimb was preconditioned with 6 cycles of 4 minutes ischaemia followed by 4 minutes reperfusion, using a microvascular clamp to occlude the femoral vessels under an operating microscope.

IR: The median and left hepatic lobes were rendered ischaemic for 40 minutes followed by 2 hours reperfusion, using a microvascular clamp to occlude the portal triad branch to these lobes.

RIPC + IR: Animals were subjected to the RIPC followed by the IR procedures.

Wild type groups:

Sham: Only underwent the laparotomy, mobilization of the liver, and mobilization of the right femoral vascular bundle described above.

RIPC: The right hindlimb was preconditioned with 6 cycles of 4 minutes ischaemia followed by 4 minutes reperfusion, using a microvascular clamp to occlude the femoral vessels under an operating microscope.

IR: The median and left hepatic lobes were rendered ischaemic for 40 minutes followed by 2 hours reperfusion, using a microvascular clamp to occlude the portal triad branch to these lobes.

RIPC + IR: Animals were subjected to the RIPC followed by the IR procedures.

6.2.3 *Measurement of liver enzymes*

The concentrations of ALT and AST in the plasma of $eNOS^{-/-}$ animals were measured using an automated clinical analyzer as described in section 3.5.

6.2.4 *Histopathology*

The histopathological damage sustained by the $eNOS^{-/-}$ groups was assessed. A liver biopsy was taken from the left lobe of each animal at the end of the experiment and fixed in 10% formal saline. The fixed tissues were embedded in paraffin and stained with H&E. Sections were assessed by a liver pathologist blinded to the animal groups. Each H&E sample was scored using two different methods as described in section 3.6.

6.2.5 *Transmission electron microscopy*

Liver biopsies were obtained from the left lobes of $eNOS^{-/-}$ mice at termination, and were fixed in a glutaraldehyde / paraformaldehyde mixture overnight, processed as described in section 3.7, and viewed with a transmission electron microscope. Representative areas were photographed and the images were interpreted by a TEM scientist who was blinded to the groups. Assessment of the images was performed according to the parameters outlined in section 3.7.

6.2.6 *Liver and hindlimb microcirculatory blood flow*

$eNOS^{-/-}$ MBF measurements were performed in this chapter. Laser Doppler flowmetry (LDF) was used to measure blood flow in the microvasculature of the liver as described in section 3.8. One probe was placed on the left liver lobe so that

it was just in contact with the tissue surface. LDF data was collected as the mean of four readings recorded over a one minute period. In addition, a second LDF probe was positioned on the sole of the right foot to ensure blood flow interruption and reperfusion during femoral vessels clamping and unclamping respectively. Figure 3.6 shows the time points of the LDF recordings during the study protocol.

6.2.7 *eNOS and iNOS Western blot analysis*

Individual samples of liver and skeletal muscle tissues (100 mg) from wild type mice were homogenised in liquid nitrogen. Cell lysis was achieved by RIPA buffer and repeat vortexing. Following centrifusion, protein concentrations in the supernatants were measured by the modified Lowry protein assay kit. Protein denaturation was achieved by Laemmli sample buffer and heating to 95 ℃. Nu-polyacrylamide gel electrophoresis was used to separate the proteins, which were then electro-blotted onto polyvinylidene difluoride membrane. The membranes were incubated with either polyclonal rabbit anti-eNOS or anti-iNOS in a 1:200 dilution, followed by incubation with secondary goat anti-rabbit IgG antibody and illumination with Super Signal West Dura Extended Duration Substrate. The membranes were exposed to x-ray films for variable durations to visualise the proteins. The density of the eNOS protein bands were analysed with densitometry software.

6.2.8 *eNOS immunohistochemistry*

In order to ascertain the cellular distribution of eNOS in wild type animals, the left liver lobe and the thigh of the right hindlimb were biopsied at the end of the

experiment in each of the animals and were immediately fixed in 10% formal saline. The tissues were processed as described in section 3.10.

6.2.9 *Statistical analysis*

Values are expressed as mean ± SEM. One way analysis of variance (ANOVA) with Post Hoc Bonferroni correction for multiple comparisons was used. $P < 0.05$ was considered statistically significant in all analyses.

6.3 Results

6.3.1 *Antecedent hindlimb RIPC reduces plasma transaminases levels in wild type but not eNOS$^{-/-}$ mice*

In this study the sham and RIPC groups in eNOS$^{-/-}$ animals showed only small elevations of plasma ALT and AST. The IR group showed a significant rise of these enzymes compared to sham and RIPC ($P < 0.05$). Hindlimb preconditioning preceding liver IR (RIPC + IR group) in eNOS$^{-/-}$ animals did not reduce neither the plasma ALT nor the plasma AST compared to the IR alone group ($P > 0.05$) (figure 6.1).

These findings are in contrast to the previous findings in section 4.3.2 (figure 4.1) which demonstrated that in wild type animals hindlimb preconditioning preceding liver IR (RIPC + IR group) significantly reduced the plasma transaminases levels compared to IR alone ($P < 0.05$).

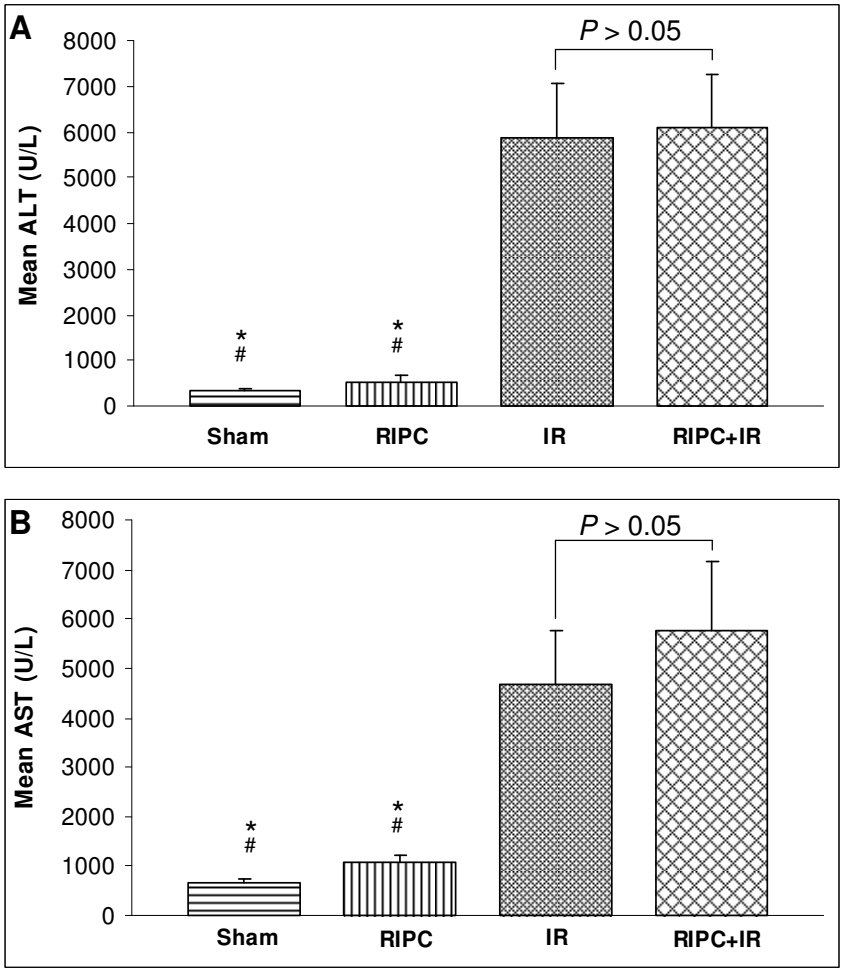

Figure 6.1. Plasma liver enzyme levels in eNOS$^{-/-}$ mice. (A) Alanine aminotransferase (ALT). *$P < 0.05$ vs IR; #$P < 0.05$ vs RIPC + IR. (B) Aspartate aminotransferase (AST). *$P < 0.05$ vs IR; #$P < 0.05$ vs RIPC + IR.

6.3.2 *Histopathological injury is attenuated by hindlimb RIPC preceding liver IR in wild type but not eNOS$^{-/-}$ animals*

The mean overall histopathological injury grades in wild type animal groups were given in section 4.3.3 (figure 4.2). For comparison these results of wild type groups are shown again next to the results of eNOS$^{-/-}$ animals in figure 6.2. The mean overall histopathological grades in eNOS$^{-/-}$ animals were: 0.33 in the sham, 0.5 in

the RIPC, 1.0 in the IR, and 1.0 in the RIPC + IR groups. None of the differences between these mean overall histopathological grades in the eNOS$^{-/-}$ mice reached statistical significance ($P > 0.05$) (figure 6.2). Wild type sham and RIPC groups demonstrated minimal signs of liver IR injury with a mean overall grade of 0 in each. However, the wild type IR group resulted in a significant increase in the mean overall injury grade (IR group mean = 1.83) compared to the sham and RIPC groups ($P < 0.05$). Preconditioning in wild types prior to liver IR (RIPC + IR group) decreased the mean overall injury grade to 1.33 ($P < 0.05$ vs sham or RIPC; $P > 0.05$ vs IR).

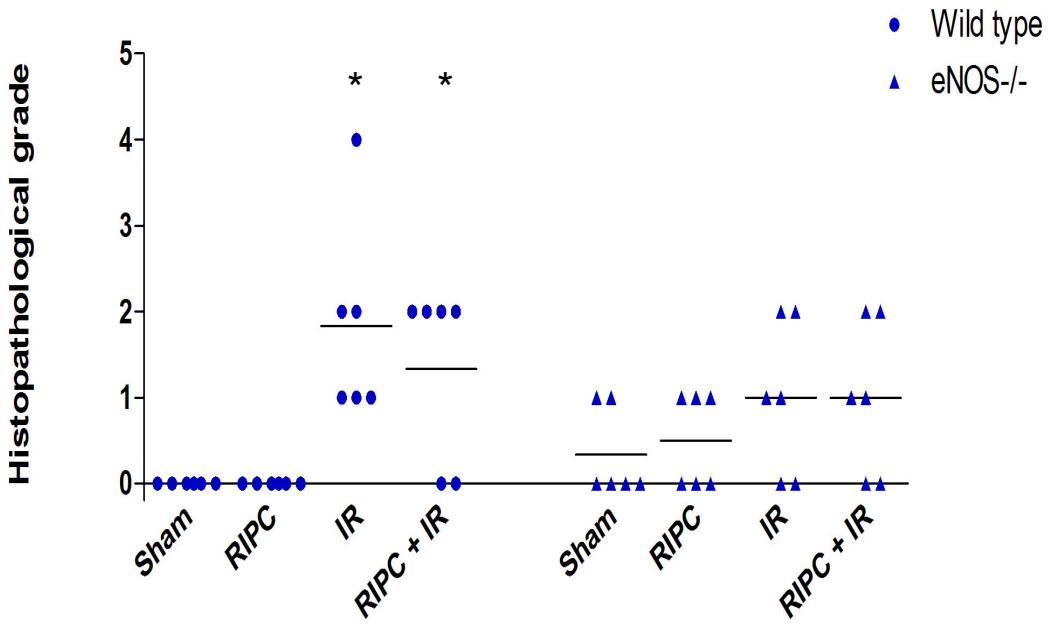

Figure 6.2. Vertical scatter plot of histopathological grades in wild type and eNOS$^{-/-}$ mice. Each point represents the overall grade assigned to each individual liver biopsy sample (n = 6 per group) in wild type and eNOS$^{-/-}$ mice. Horizontal bars represent the means. In the wild type group *$P < 0.05$ vs sham or RIPC.

The mean scores of individual histopathological features of liver IR injury in wild type mice were also given in section 4.3.3 (figure 4.3). For ease of comparison the results for each individual feature of liver IR injury in the wild type groups are shown next to the results of $eNOS^{-/-}$ animals in figure 6.3. There were no statistically significant differences, in any of the individual features of liver IR injury, between any of the $eNOS^{-/-}$ animal groups (figure 6.3). In comparison in wild type groups, 4 individual features (discohesive hepatocytes, liver cell ballooning, blurred intercellular borders, RBC extravasation) had a significantly higher mean score in the IR compared to the sham and RIPC groups ($P < 0.05$). In addition discohesive hepatocytes and liver cell ballooning were also significantly higher in the RIPC + IR compared to the RIPC group ($P < 0.05$). There were no other statistically significant differences amongst wild type groups.

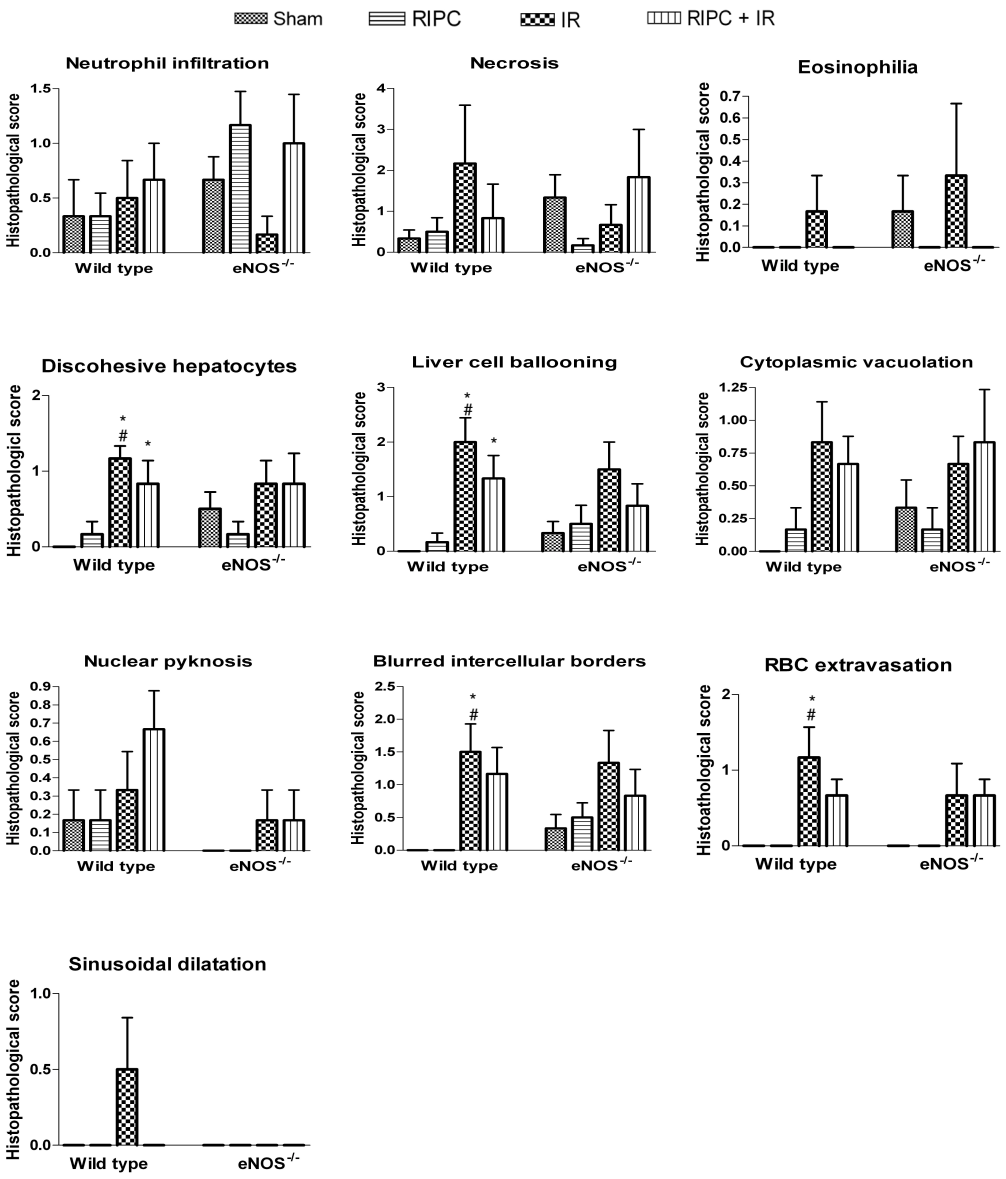

Figure 6.3. Histopathological scores of individual features of liver IR injury in wild type and eNOS$^{-/-}$ mice. Each bar chart is the mean histopathological score of six animals in that group. The error bars are the standard error of the means. In the wild type group *P < 0.05 vs sham; #P < 0.05 vs RIPC.

6.3.3 *Hepatic ultrastructural damage is ameliorated by hindlimb RIPC preceding liver IR in wild type but not eNOS$^{-/-}$ mice*

Representative ultrastructural appearances in each of the eNOS$^{-/-}$ groups are shown in figure 6.4. The sham group showed some ultrastructural disturbances consisting of sporadic endoplasmic reticulum (ER) dilatation, phagolysosomal and lipid droplet formation. The RIPC group showed frequent ER dilatation and phagolysosomal formation. The IR group exhibited extensive mitochondrial damage, ER dilatation, cytosolic vacuole formation, phagolysosomal formation, lipid droplet formation, glycogen depletion, bile canaliculi dilatation with microvilli disruption, and sinusoidal endothelial cell (SEC) disruption with extravasation of red blood cells (RBC) and plasma into the liver parenchyma. Importantly the RIPC + IR group sustained similar damage to the IR group, indicating the protective effects of hindlimb preconditioning on ultrastructural features of liver IR injury act through an eNOS-dependent mechanism.

In comparison the typical appearances seen in the wild type mouse groups were discussed in section 4.3.4 (figure 4.4). The sham group showed normal ultrastructural appearances. The RIPC group showed ER dilatation, phagolysosomal formation, and lipid droplet formation. The IR group exhibited extensive mitochondrial damage, ER dilatation, cytosolic vacuole formation, phagolysosomal formation, lipid droplet formation, glycogen depletion, bile canaliculi dilatation with microvilli damage, and SEC disruption with extravasation of RBC into the liver parenchyma. In contrast the ultrastructural damage sustained by the RIPC + IR group consisted of ER dilatation, phagolysosomal formation, lipid droplet formation, glycogen depletion, and disruption of SEC but without RBC extravasation.

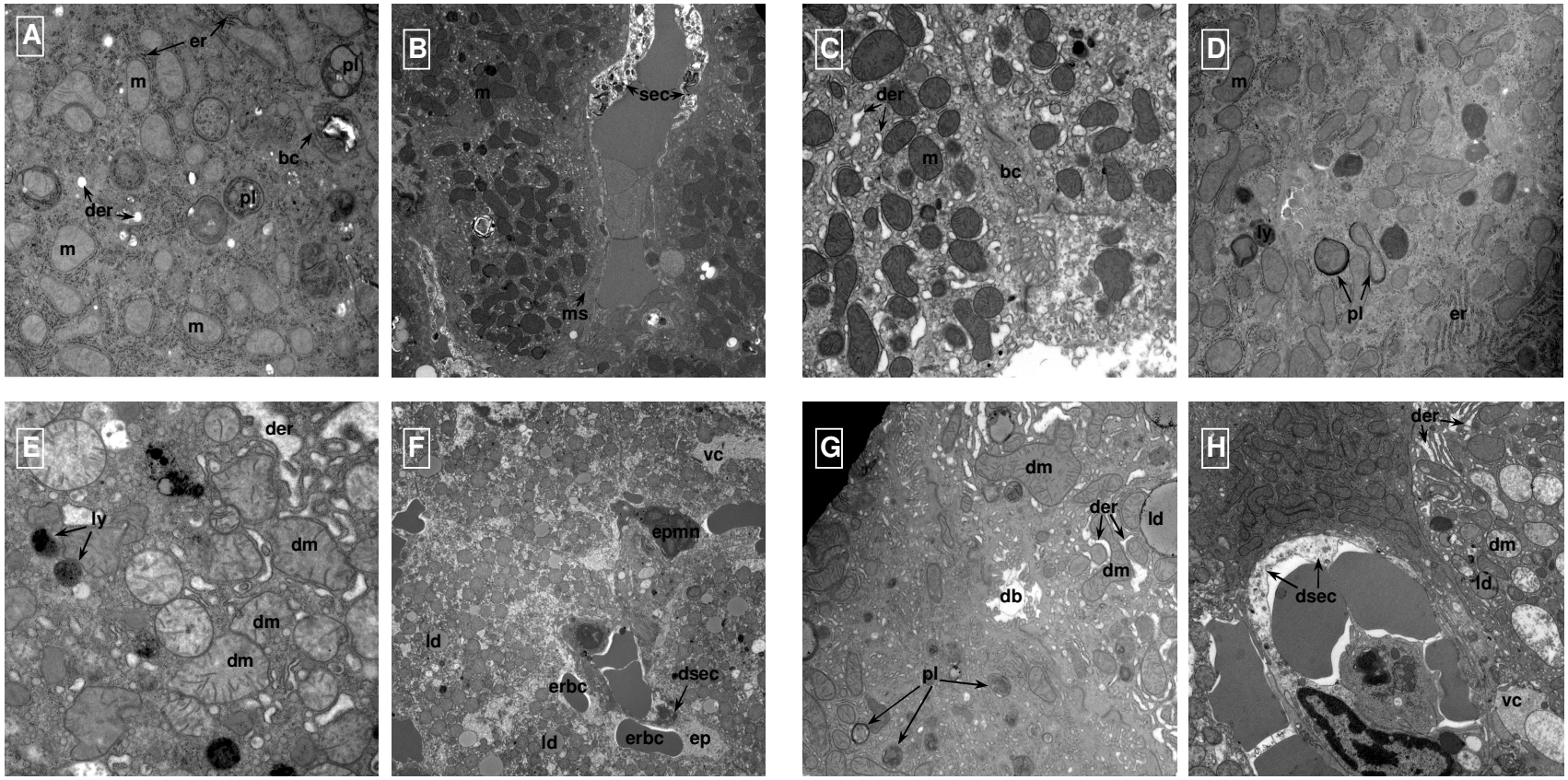

Figure 6.4. Hepatic transmission electron micrographs of eNOS$^{-/-}$ mice. The liver samples were taken at the end of the procedure in each group. **(A) & (B)** Sham group showing normal looking mitochondria (m), normal (er) and dilated (der) endoplasmic reticulum, phagolysosomes (pl),

bile canaliculi with microvilli (bc), sinusoidal endothelial cells (sec), and microvilli in the space of Disse (ms). **(C) & (D)** RIPC group demonstrating normal mitochondria (m), normal (er) and dilated (der) endoplasmic reticulum, and lysosomes (ly) with phagolysosomal (pl) formation. **(E) & (F)** IR group demonstrating damaged mitochondria (dm), dilated endoplasmic reticulum (der), vacuole formation (vc), lysosomes (ly), lipid droplet formation (ld), and damaged sinusoidal endothelial cells (dsec) with extravasated red blood cell (erbc), polymorphonucelocyte (epmn), and plasma (ep) into the hepatocytes. **(G) & (H)** RIPC + IR group showing damaged mitochondria (dm), dilated endoplasmic reticulum (der), vacuolation (vc), phagolysosome formation (pl), lipid droplet formation (ld), dilated bile canaliculi (dbc), and damaged sinusoidal endothelial cells (dsec) associated with extravasated red blood cell (erbc).

6.3.4 *Hepatic microcirculatory blood flow is preserved by hindlimb RIPC in wild type but not eNOS$^{-/-}$ animals*

In eNOS$^{-/-}$ mice, the sham and RIPC groups displayed constant hepatic MBF throughout the experimental protocol. MBF was significantly lower during liver ischaemia in the IR and RIPC + IR compared to the sham and RIPC groups ($P < 0.05$). Throughout liver reperfusion, the MBF remained significantly lower in the IR compared to the sham and RIPC groups, so that at the end of the 2 hour reperfusion period the mean MBF was 52.2% of baseline in the IR group (figure 6.5). The highest mean MBF during liver reperfusion in the IR group was recorded at 90 minutes and was 52.6% of baseline. The RIPC + IR group displayed transient improvement in MBF during the first 30 minutes of reperfusion with a mean value of 69.0% ($P = 0.034$ vs IR) and 76.5% ($P = 0.014$ vs IR) at the beginning and at 30 minutes of liver reperfusion respectively. During the remaining reperfusion period MBF in the RIPC + IR group dropped, with mean recorded values of 61.6%, 64.3%, and 62.6% at 60, 90, and 120 minutes reperfusion. The mean MBF values in the RIPC + IR group at 60, 90, and 120 minutes of reperfusion were significantly lower than those of the sham and RIPC groups ($P < 0.05$), but not significantly different from those of the IR group ($P > 0.05$) (figure 6.5).

These results are in stark contrast to those we discovered in wild type animals described in section 4.3.5 (figure 4.5). Following liver reperfusion wild type IR group did not significantly recover MBF values compared to the sham, IR, and RIPC + IR groups. At the end of the two hour reperfusion period the flow remained significantly low, recording a mean of 53.4% of baseline in the IR group. In contrast, MBF in the wild type RIPC + IR group continued to recover towards

baseline values during reperfusion, so that the mean flow at 120 minutes was 93.5% of baseline. At all time points of liver reperfusion the flow was significantly lower in the wild type IR group compared to the wild type sham, RIPC, and RIPC + IR groups ($P < 0.01$ vs sham, RIPC, or RIPC + IR, at 30, 60, 90, and 120 minutes reperfusion); and at the same time points there were no significant differences between mean MBF in the RIPC + IR compared to the sham and RIPC groups ($P > 0.05$).

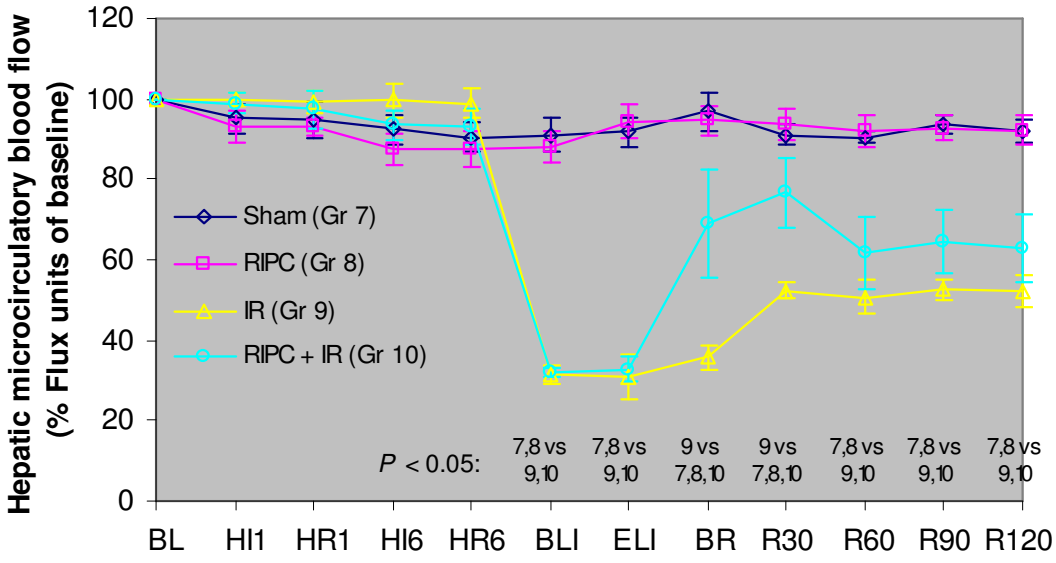

Figure 6.5. Hepatic microcirculatory blood flow in eNOS$^{-/-}$ mice, measured by LDF, is illustrated as mean percentage ± SEM of pre-ischaemic baseline (n = 6 for each group). Significant (P < 0.05) inter-group differences are shown vertically below each time point on the x-axis. BL, baseline; HI, hindlimb ischaemia; HR, hindlimb reperfusion; BLI, beginning of liver ischaemia; ELI, end of liver ischaemia; BR, beginning of liver reperfusion; R30 to R120, liver reperfusion at 30, 60, 90, and 120 min post ischaemia.

6.3.5 *Hindlimb RIPC alters iNOS but not eNOS expression in liver and hindlimb skeletal muscle of wild type mice*

At the end of the two hours of reperfusion eNOS expression, as assessed by Western blotting in liver and hindlimb skeletal muscle samples, was evident in all the animal groups (figure 6.6). As eNOS is constitutively expressed, semi-quantitative grading of the blots was performed using densitometric analysis of each protein band to ascertain differential expression between the groups. However none of the groups, either in liver or hindlimb skeletal muscle samples, revealed any significant difference in eNOS expression (data not shown). In contrast, at the end of two hours of reperfusion iNOS protein expression was only seen in the RIPC and RIPC+IR groups, in both the liver and hindlimb skeletal muscle samples (figure 6.7). The sham and IR groups did not show iNOS expression in either tissue type. Semi-quantitative densitometric analysis was not performed on the iNOS blots as iNOS is an inducible enzyme and the purpose of iNOS Western blots was to ascertain the effects of hindlimb RIPC on absolute iNOS expression.

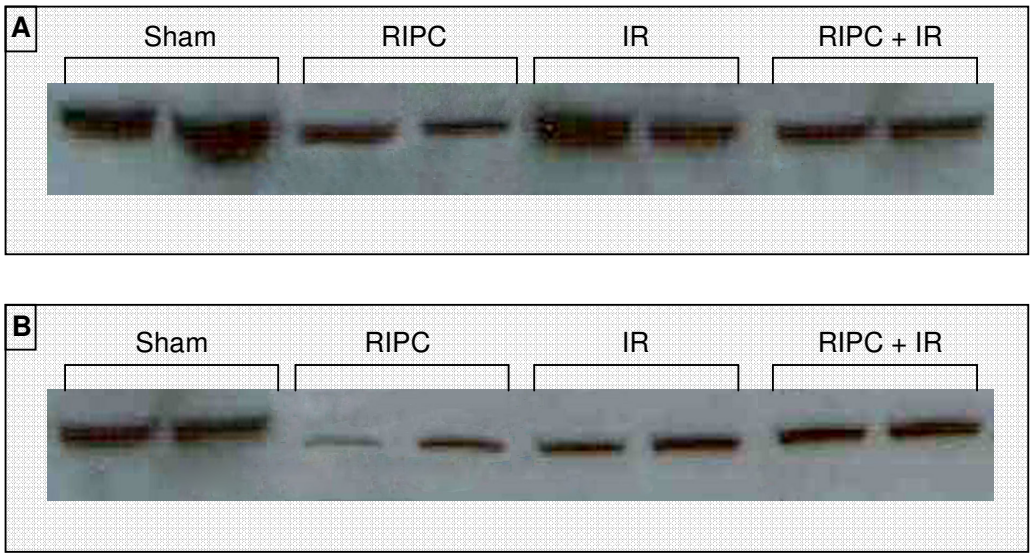

Figure 6.6. eNOS Western blots in wild type mice. Representative eNOS protein expression as measured by Western blotting. Each band represents an individual animal in the corresponding group. (**A**) Liver samples. (**B**) Hindlimb skeletal muscle samples.

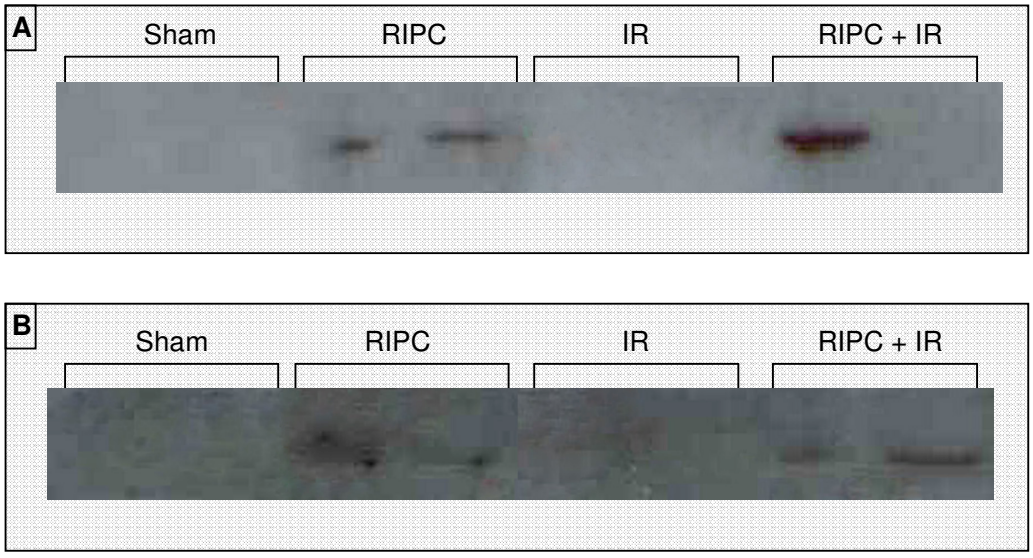

Figure 6.7. iNOS Western blots in wild type mice. Representative iNOS protein expression as measured by Western blotting. Each band represents an individual animal in the corresponding group. (**A**) Liver samples. (**B**) Hindlimb skeletal muscle samples.

6.3.6 *Cellular eNOS distribution in liver and hindlimb skeletal muscle of wild type mice*

Figure 6.8 and figure 6.9 illustrate representative photomicrographs of eNOS-stained immunohistochemical sections of the liver and hindlimb skeletal muscle respectively. The trophoblasts in the placental positive control sections stained universally, whilst the negative controls had no staining. Within the liver eNOS immunostaining was localized to hepatocytes and the vascular endothelium (figure 6.8). In the hindlimb skeletal muscle eNOS staining was seen in the myocytes and vascular endothelium (figure 6.9).

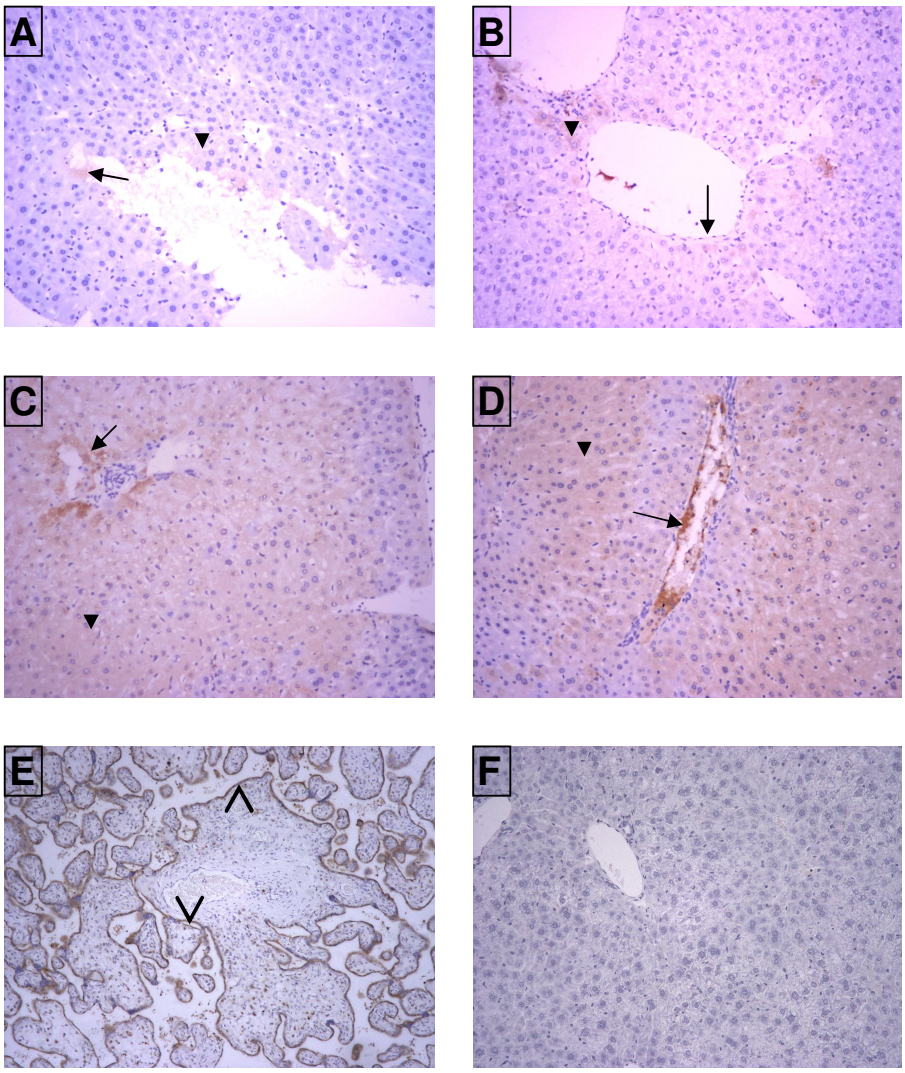

Figure 6.8. eNOS immunohistochemical staining of liver sections (X20 magnification) in wild type mice. The brown colour uptake is the eNOS stain. Both hepatocytes (closed arrow heads) and endothelial cells (arrows) demonstrated eNOS expression in all the experimental groups: **(A)** Sham; **(B)** RIPC; **(C)** IR; **(D)** RIPC + IR. **(E)** Placental positive control showing brown eNOS staining (open arrow heads) of the trophoblastic cell layer. **(F)** Liver negative controls showing lack of any brown staining.

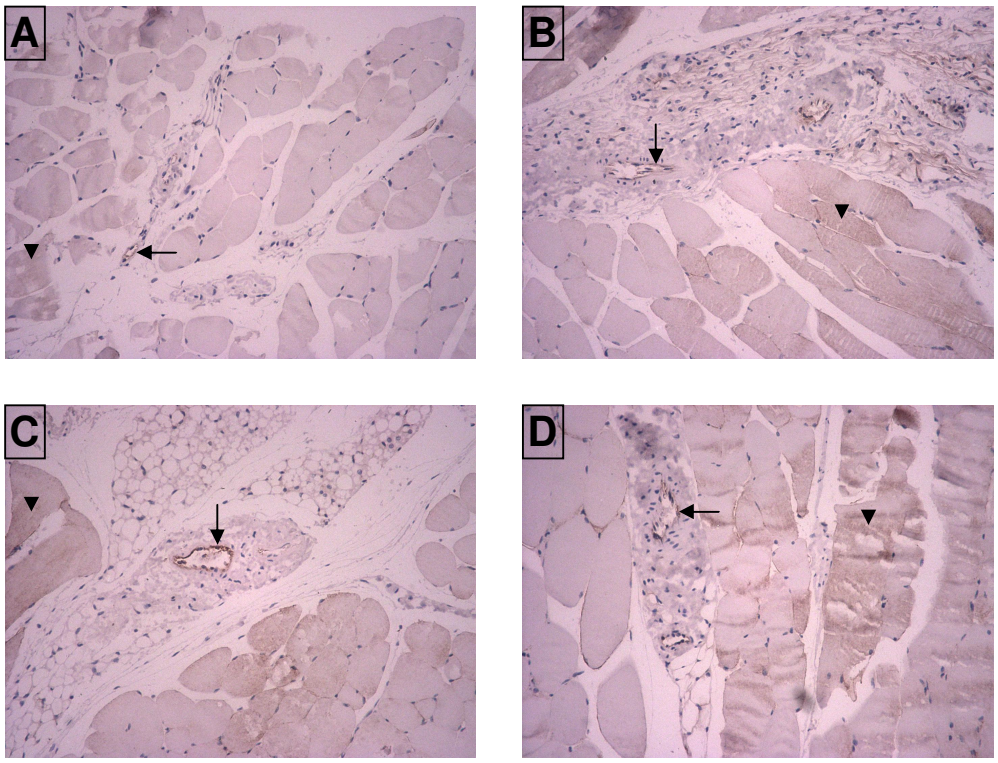

Figure 6.9. eNOS immunohistochemical staining of hindlimb skeletal muscle sections (X20 magnification) in wild type mice. The brown colour uptake is the eNOS stain. Both skeletal myocytes (arrow heads) and endothelial cells (arrows) demonstrated eNOS expression in all experimental groups: **(A)** Sham; **(B)** RIPC; **(C)** IR; **(D)** RIPC + IR.

6.4 Discussion

The findings of this study show that eNOS is a critical enzyme in mediating the protective effects of RIPC on liver IR injury. Moreover it was demonstrated that eNOS is responsible for the preservation of liver MBF in hindlimb preconditioned animals. Additionally hindlimb RIPC, but not liver IR, up-regulates the expression of iNOS in the liver and hindlimb skeletal muscle.

We previously established and validated a new mouse model in which hindlimb RIPC significantly ameliorated liver IR injury (chapter 4). In the current study the

same mouse model was used to begin exploring the molecular mechanisms underlying the protection offered by hindlimb RIPC against liver IR injury.

The eNOS and iNOS enzymes are responsible for manufacturing NO in vivo in extraneural tissues. Their role, if any, in the protection afforded by RIPC is unknown. $eNOS^{-/-}$ mice were used and the protection that had previously been exhibited by wild type mice (chapter 4) subjected to liver IR with antecedent hindlimb RIPC dissipated. The loss of protection of hindlimb preconditioning in $eNOS^{-/-}$ animals was evidenced by an increase in the plasma transaminases levels, histopathological injury scores, and ultrastructural markers of injury in the RIPC + IR compared to the IR alone group. This was in contrast to the decrease observed in these parameters of hepatic injury in the RIPC + IR compared to IR alone group in wild type mice. Amongst these parameters of liver IR injury the overall histopathological grades and the histopathological scores of individual features of liver IR injury showed a lack of statistical significance between the different $eNOS^{-/-}$ groups, and a lack of significance between the RIPC + IR compared to the IR alone group in wild type animals. This was due to the fact that liver biopsies for histopathological scoring were performed at 2 hours of reperfusion, which is too early for the full histopathological manifestations of liver IR injury.

Our group previously showed that eNOS-derived NO is an important mediator of the protective effects of direct liver ischaemic preconditioning (240). The current study adds to this by demonstrating, for the first time in any remote preconditioning model of any organ, that eNOS is an essential prerequisite for the protective effects of RIPC upon hepatic IR injury at 2 hours of liver reperfusion. Moreover hepatic and

hindlimb skeletal muscle eNOS protein expression, as semi-quantified by densitometric analysis of eNOS protein bands of Western blots, was similar amongst the various wild type animal groups. This would imply that at 2 hours of reperfusion it is likely that eNOS activation rather than increased expression causes the observed protection of RIPC, although eNOS activity was not specifically measured in this study. eNOS activation is controlled by several overlapping mechanisms that dynamically regulate eNOS function. These mechanisms include eNOS acylation, Ca^{2+} / calmodulin binding, phosphorylation, and denitrosylation (239,369); all process that can be completed in a much shorter time period than eNOS up-regulation. An increase in enzyme expression entails amino acid synthesis, DNA transcription, post-transcriptional modification and translation of mRNA, and post-translational modifications of the enzyme; processes that take hours to complete rather than the minutes required for the activation of the enzyme.

The expression of eNOS within the liver was observed in hepatocytes and the vascular endothelium; results that are congruent with those reported previously (240,241). In hindlimb skeletal muscle sections eNOS expression was apparent in the myocytes and vascular endothelium; cellular structures that have also been reported to express eNOS (370,371). It is likely that both hepatic and preconditioned hindlimb skeletal muscle eNOS contribute to the protection of RIPC. However, arguably it is also possible that only hindlimb eNOS is activated and increases its production of NO, that through one of its metabolic end products traverses the circulation to reach the liver where it exerts its protective effects. Alternatively, it maybe that a none NO-related, RIPC-induced factor, is released into the circulation to reach the liver and activate hepatic eNOS which then affords protection against

liver IR injury. Further research is needed to clarify this issue. An interesting result we uncovered was that iNOS expression, in the liver and hindlimb skeletal muscle, was only seen in the two groups subjected to hindlimb preconditioning, the RIPC alone group and the RIPC + IR groups. iNOS is induced in inflammatory conditions (372) and it would have been expected that iNOS might be up-regulated, at least within the liver, in the IR group. However, no iNOS expression was observed in any of the liver samples in the IR alone group subjected to Western blots. This may indicate a protective role for iNOS since its expression was only associated with hindlimb preconditioned mice. Only one previous study assessed iNOS expression following RIPC (234). In this study bilateral hindlimb preconditioning was followed by global myocardial ischaemia 24 hours post the RIPC stimulus resulting in significant reduction in the myocardial infarct size. The hindlimb RIPC was associated with increased myocardial iNOS mRNA expression starting at 3 hours post the RIPC stimulus and peaking at 24 hours (234). Furthermore, nuclear translocation of NF-κB was observed in heart and preconditioned skeletal muscle following hindlimb RIPC (234). NF-κB is a transcription factor that is well known for up-regulating iNOS expression, and therefore this study demonstrated that hindlimb RIPC results in iNOS expression in the myocardium, and possibly increases iNOS expression, through NF-κB activation in skeletal muscle; although direct iNOS expression was not measured in skeletal muscle (234). There are no previous studies that measure iNOS expression in RIPC of the liver.

In this study it was demonstrated that one of the mechanisms through which eNOS mediates the protective effects of RIPC on liver IR injury comprise preservation of hepatic MBF. We previously proved, in wild type animals, hindlimb RIPC prior to

liver IR preserves hepatic MBF during the early reperfusion period, compared to animals subjected to IR alone (chapter 4). In contrast, the current study failed to demonstrate preservation of hepatic MBF in the RIPC + IR group in $eNOS^{-/-}$ mice compared to liver IR alone group. This would indicate an essential role for eNOS in preservation of the hepatic microvasculature, which is in accord with the well known functions of eNOS-derived NO as a vascular homeostatic factor, acting to protect the endothelium against various insults (362). The non-significant improvement of hepatic MBF in the RIPC + IR compared to the IR alone group in $eNOS^{-/-}$ animals during the two reperfusion period is in contrast to the results in chapter 5 showing no improvement in the MBF of the C-PTIO + RIPC + IR group compared to the IR group. The explanation for this probably lies in the fact that C-PTIO 'mops-up' all of the synthesized NO, whilst $eNOS^{-/-}$ animals can maintain some NO production through up-regulation of iNOS.

In conclusion we demonstrated that eNOS is an essential prerequisite for the protective effects of hindlimb RIPC on liver IR injury. At 2 hours of reperfusion this is probably due to increased activation of eNOS rather than increased expression of this enzyme. We also demonstrated an increase in the expression of iNOS in preconditioned groups, which may be contributing to the protection of RIPC but this needs further research to prove.

In this chapter we demonstrated an essential function for eNOS in the protection afforded by RIPC. In the next chapter we will investigate the role of nitrite / nitrate as the signal released from the preconditioned hindlimb into the circulation to elicit protection against hepatic IR injury.

Chapter 7

Nitrite and nitrate as circulating carriers of nitric oxide induced by hindlimb RIPC

7.1 Introduction

Nitric oxide (NO) is a highly reactive free radical molecule and consequently has a short half life that is in the order of 5-10 seconds. NO, which is synthesised by one or more of the nitric oxide synthase (NOS) isoforms, is rapidly oxidised to nitrite (NO_2^-) and nitrate (NO_3^-). Oxidation to NO_2^- is accomplished either via auto-oxidation using molecular O_2, or through a more rapidly occurring reaction that utilizes the copper-containing protein ceruloplasmin (373). NO_3^- is generated by one of two reactions that utilize oxyhaemoglobin. In the first of these NO_2^- reacts with oxyhaemoglobin to generate NO_3^- and methaemoglobin (374). In the second reaction oxyhaemoglobin directly reacts with NO to yield NO_3^- (373).

Both NO_2^- and NO_3^- (NOx) are released into the circulation, and act as reservoirs of NO under specific circumstances (374,375). NO_2^- is reduced to NO by enzymatic and non-enzymatic pathways. Enzymatic nitrite reductases include xanthine oxidoreductase, cytochrome P450, and complexes III and IV of the mitochondrial electron transport chain (375). The non-enzymatic nitrite reductases include deoxyhaemoglobin and myoglobin (375). The reduction of NO_3^- to NO requires a nitrate reductase enzyme that was thought to be absent in mammalian cells. However, increasing evidence supports a role for xanthine oxidoreductase as a nitrate reductase (376,377). Additionally, dietary NO_3^- represents a significant contribution to the circulating pool of NO_2^-, through the conversion of NO_3^- to NO_2^- by the bacterial reductase enzyme found in the oral and gastrointestinal tract commensal population. The contribution of these pathways to the rate of NO generation from nitrite in a specific tissue type is dependent on the local pH and

oxygen tension, with acidosis and tissue hypoxia greatly enhancing NO production from the above pathways (375).

Organs subjected to ischaemia reperfusion are typically hypoxic and acidotic at the end of the ischaemic period, and consequently it is thought nitrite reduction to NO is greatly increased locally at these sites (373,375). Evidence supportive of NO_2^- protecting against IR injury, through its reduction to NO, is accumulating for most major organs. Exogenous administration of sodium nitrite protects against brain (378), heart (302), Kidney (379), and lung (380) IR injury. Moreover, inhalation of NO results in elevated plasma NOx levels, that have been shown to reduce heart (381), lung (380), and lower extremity (382) IR injury.

Experimental liver IR injury is also reduced by sodium nitrite administration (167,302). In further support of this, a human randomized controlled trial that assessed the benefits of inhaled NO in recipients of orthotopic liver transplants, found patients that were administered inhalational NO had significantly raised plasma NO_2^- levels that were associated with significant improvements in liver function tests in the postoperative period, significant decrease in hepatocyte apoptosis, and a significant decrease in hospital length of stay compared to placebo group (383). Evidence for the protective role of endogenously generated NO_2^- in liver IR injury comes from an experiment that utilized wild type and mice with cardiac-specific over-expression of eNOS (CS-eNOS-Tg). Plasma and hepatic NOx levels were elevated in the CS-eNOS-Tg mice compared to wild types, with a consequent significant protection against liver IR injury in CS-eNOS-Tg but not wild type mice (384).

The role of NOx generated as a consequence of hindlimb RIPC, in the protection against liver IR injury is currently unknown. The aim of the present study was to evaluate the role of endogenously generated NOx during hindlimb RIPC in wild type mice, in protecting against liver IR injury. Based on the initial results we elicited, we proceeded to determine the effects of exogenous nitrite administration on liver IR injury in $eNOS^{-/-}$ mice.

7.2 Materials and methods

The detailed methodology was described in chapter 3. A summary of the most pertinent points is given below.

7.2.1 *Animal surgical procedure*

Male inbred C57BL/6 wild type mice (Charles River laboratories, UK); and mice lacking the constitutively expressed enzyme, endothelial nitric oxide synthase ($eNOS^{-/-}$, bred in-house) were utilized in the present study. The animals were anaesthetised using 2% isoflurane. Core body temperature was maintained at 37.0 ± 0.5 ℃ using a heating pad and a rectal temperature probe. Hepatic IR was performed as detailed in section 3.4.1. At the end of the reperfusion period the animals were terminated by exsanguination through needle cardiac puncture and blood collection. The blood was immediately centrifuged and the plasma supernatant was stored at -70 ℃ until assayed for liver transaminases. The left and median liver lobes were harvested at the end of each procedure for histopathology and transition electron microscopy (TEM). Hindlimb preconditioning consisted of microvascular clamping of the femoral vessels for four minutes followed by four minutes reperfusion for a total of six cycles as described in section 3.4.2.

7.2.2 *Experimental groups*

Wild type animal groups (figure 3.2) were used to measure plasma NOx levels. The results of these experiments demonstrated a significant rise in plasma NOx levels in hindlimb preconditioned animals. Therefore further experiments were conducted to evaluate the effects of exogenous nitrite administration on liver IR injury in $eNOS^{-/-}$ animal groups (figure 3.3). Total anaesthetic time was equal in all the groups. All animals underwent laparotomy, mobilization of the liver, and mobilization of the right femoral vascular bundle. In addition some of the groups were each subjected to a specific procedure as follows:

Wild type groups:

Sham: Underwent the laparotomy, mobilization of the liver, and mobilization of the right femoral vascular bundle described above.

RIPC: The right hindlimb was preconditioned with 6 cycles of 4 minutes ischaemia followed by 4 minutes reperfusion, using a microvascular clamp to occlude the femoral vessels under an operating microscope.

IR: The median and left hepatic lobes were rendered ischaemic for 40 minutes followed by 2 hours reperfusion, using a microvascular clamp to occlude the portal triad branch to these lobes.

RIPC + IR: Animals were subjected to the RIPC followed by the IR procedures.

These wild type groups were used to measure the plasma NOx levels in the current chapter. The extent of liver injury in these groups was previously assessed in chapter 4 using plasma transaminases levels, evaluation of histopathological and ultrastructural features of IR injury, and hepatic MBF measurements.

eNOS$^{-/-}$ groups:

Sham: Underwent the laparotomy, mobilization of the liver, and mobilization of the right femoral vascular bundle described previously.

IR: The median and left hepatic lobes were rendered ischaemic for 40 minutes followed by 2 hours reperfusion, using a microvascular clamp to occlude the portal triad branch to these lobes.

Nitrite + IR: Underwent the IR procedure with administration of sodium nitrite, at a dose of 48 nmol in 50 μl of D-PBS (167,302), topically into the peritoneal cavity 20 minutes into liver ischaemia. To elicit the optimal time of sodium nitrite administration, plasma transaminases levels and liver MBF were measured in two additional eNOS$^{-/-}$ groups (n = 2 each) that received the sodium nitrite either immediately preceding liver ischaemia or just before liver reperfusion at the end of liver ischaemia.

These eNOS$^{-/-}$ groups were used in the present chapter to assess the plasma liver enzymes, histopathological and ultrastructural features of IR injury, and MBF measurements.

7.2.3 *Nitrite and nitrate measurements*

The plasma nitrite and nitrate (NOx) levels were measured in wild type mice using a commercially available colorimetric assay kit (Cayman Chemical, catalogue No. 780001) as detailed in section 3.11.

7.2.4 *Measurement of liver enzymes*

The plasma concentrations of ALT and AST were measured in the eNOS$^{-/-}$ groups using an automated clinical analyzer as described in section 3.5.

7.2.5 *Histopathology*

A liver biopsy was taken from the left lobe of each eNOS$^{-/-}$ animal at the end of the experiment and fixed in 10% formal saline. The fixed tissues were embedded in paraffin and stained with H&E. Sections were assessed by a liver pathologist blinded to the animal groups. Each H&E sample was scored for features of liver IR injury using two different methods as described in section 3.6.

7.2.6 *Transmission electron microscopy*

Liver biopsies were obtained from the left lobe of each eNOS$^{-/-}$ animal at termination, and were fixed in a glutaraldehyde / paraformaldehyde mixture overnight, processed as described in section 3.7, and viewed with a transmission electron microscope. Representative areas were photographed and the images were interpreted by a TEM scientist who was blinded to the groups. Assessment of the images was performed according to the parameters outlined in section 3.7.

7.2.7 *Liver and hindlimb microcirculatory blood flow*

Laser Doppler flowmetry (LDF) was used to measure blood flow in the liver microvasculature of eNOS$^{-/-}$ animals as described in section 3.8. The probe was placed on the left liver lobe so that it was just in contact with the tissue surface. LDF data was collected as the mean of four readings recorded over a one minute period.

In addition, a second LDF probe was positioned on the sole of the right foot to ensure blood flow interruption and reperfusion during femoral vessels clamping and unclamping respectively. Figure 3.6 shows the time points of the LDF recordings during the study protocol.

7.2.8 *Statistical analysis*

Values are expressed as mean ± SEM. One way analysis of variance (ANOVA) with Post Hoc Bonferroni correction for multiple comparisons was used. $P < 0.05$ was considered statistically significant in all analyses.

7.3 Results

The plasma transaminases levels, histopathological scores, ultrastructural changes, and MBF results of the Nitrite + IR group in $eNOS^{-/-}$ animals obtained in this chapter, were compared to the results of the sham and IR groups in $eNOS^{-/-}$ animals described in chapter 6.

7.3.1 *Hindlimb RIPC significantly increases plasma NOx levels*

Total plasma nitrite and nitrate (NOx) levels were measured in wild type animals. Both the RIPC and RIPC + IR groups showed a significant increase in plasma NOx levels compared to sham ($P < 0.05$) (figure 7.1). In addition the RIPC + IR group demonstrated a significant rise in the NOx levels compared to the IR group ($P < 0.05$).

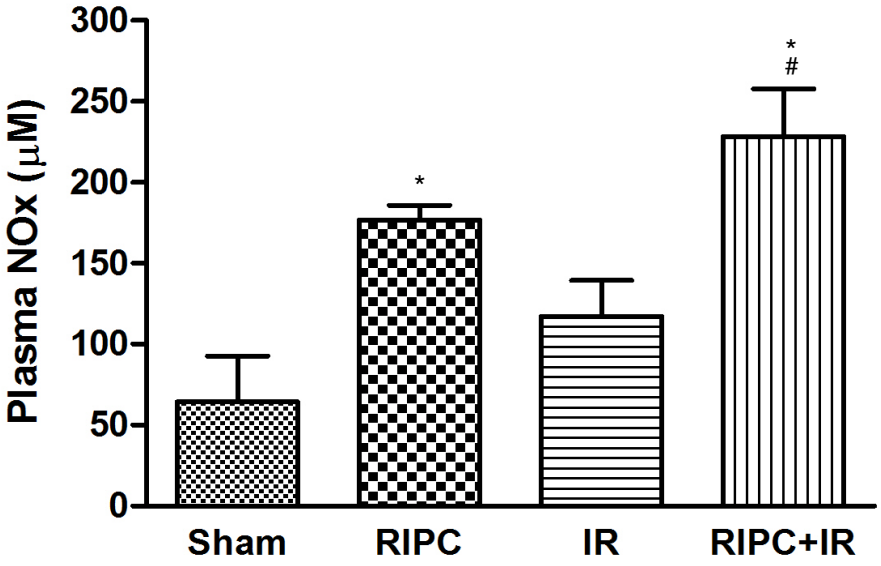

Figure 7.1. Plasma nitrite and nitrate (NOx) levels in wild type mice (n ≥ 6 per group). *$P < 0.05$ vs sham. #$P < 0.05$ vs IR.

7.3.2 *Sodium nitrite administration, to eNOS$^{-/-}$ mice subjected to hepatic IR, does not reduce plasma transaminases levels*

Liver IR resulted in a significant rise in the plasma ALT and AST compared to the sham group ($P < 0.05$). Sodium nitrite administration 20 minutes into IR did not reduce the plasma transaminases levels (figure 7.2). Two further experimental groups were performed (n = 2 each) to determine if the time of administration of sodium nitrite affects the transaminases levels. Neither the administration of sodium nitrite immediately preceding liver ischaemia nor just before liver reperfusion at the end of liver ischaemia, had any effect on plasma transaminases levels (data not shown).

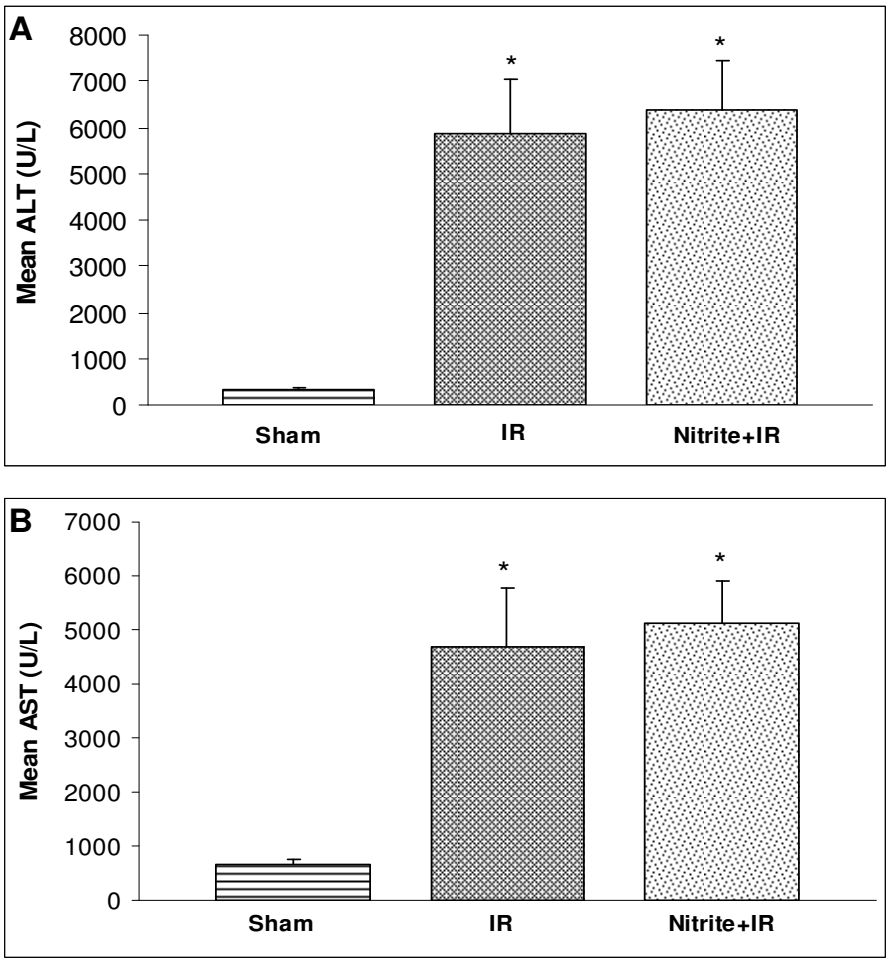

Figure 7.2. Plasma liver enzyme levels in eNOS$^{-/-}$ mice. (A) Alanine aminotransferase (ALT). *$P < 0.05$ vs sham. (B) Aspartate aminotransferase (AST). *$P < 0.05$ vs sham.

7.3.3 *Liver histopathological IR injury is not attenuated by sodium nitrite administration in eNOS$^{-/-}$ animals*

The sham group demonstrated some signs of liver IR injury with a mean overall grade of 0.33 (figure 7.3). The IR group resulted in a non-significant increase in the mean overall injury grade to 1.0. The administration of sodium nitrite during IR (nitrite + IR group) resulted in a significant worsening of the overall

histopathological manifestations of IR injury compared to the sham but not IR groups ($P < 0.05$ vs sham; $P > 0.05$ vs IR).

Four individual features of liver IR injury (liver cell ballooning, nuclear pyknosis, blurred intercellular borders, RBC extravasation) demonstrated significantly increased scores in the nitrite + IR compared to the sham group ($P < 0.5$) (figure 7.4). None of the other individual features of liver IR injury showed significant differences between any of the animal groups comparisons.

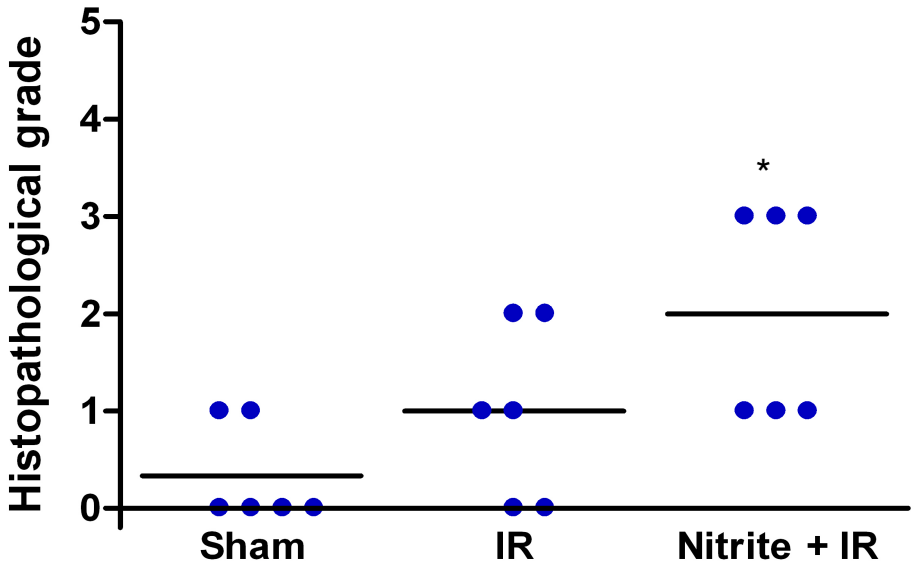

Figure 7.3. Vertical scatter plot of histopathological grades in eNOS$^{-/-}$. Each dot represents the overall grade assigned to each individual liver biopsy sample (n = 6 per group). Horizontal bars represent the means. *$P < 0.05$ vs sham.

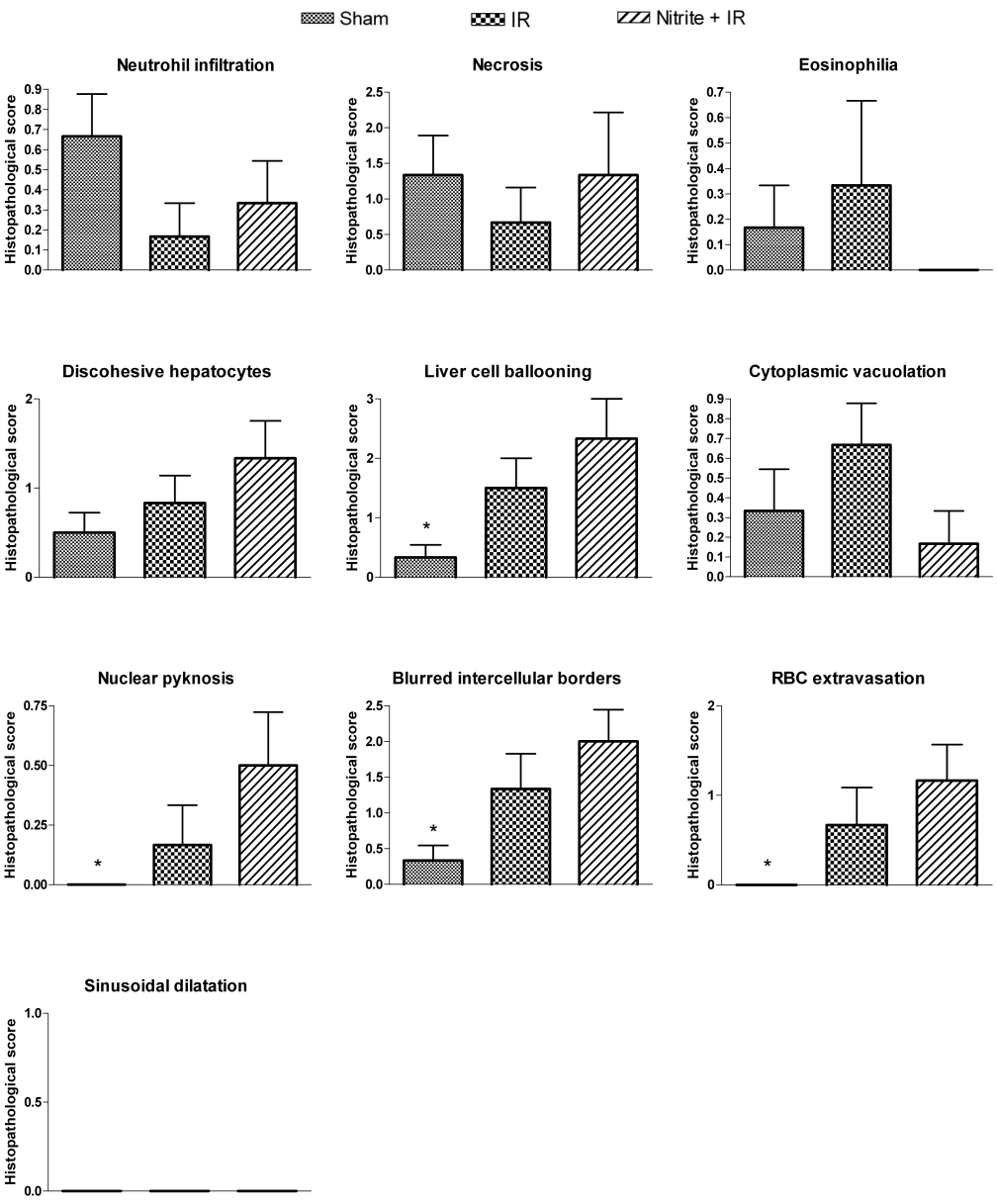

Figure 7.4. Histopathological scores of individual features of liver injury in eNOS$^{-/-}$ animals. Each bar chart is the mean histopathological score of six animals in that group. The error bars are the standard error of the means. **P* < 0.05 vs Nitrite + IR.

7.3.4 *IR-induced liver ultrastructural damage is not reduced by sodium nitrite administration in eNOS$^{-/-}$ mice*

Representative ultrastructural images from each of the groups are shown in figure 7.5. The sham group showed some ultrastructural disturbances consisting of sporadic ER dilatation, phagolysosomal and lipid droplet formation. The IR group exhibited extensive mitochondrial damage, ER dilatation, cytosolic vacuole formation, phagolysosomal formation, lipid droplet formation, glycogen depletion, bile canaliculi dilatation with microvilli disruption, and SEC disruption with extravasation of RBC and plasma into the liver parenchyma. Importantly the administration of nitrite during ischaemia (nitrite + IR) did not alter the IR-induced ultrastructural damage resulting in appearances that were comparable to those in the IR group (figure 7.5).

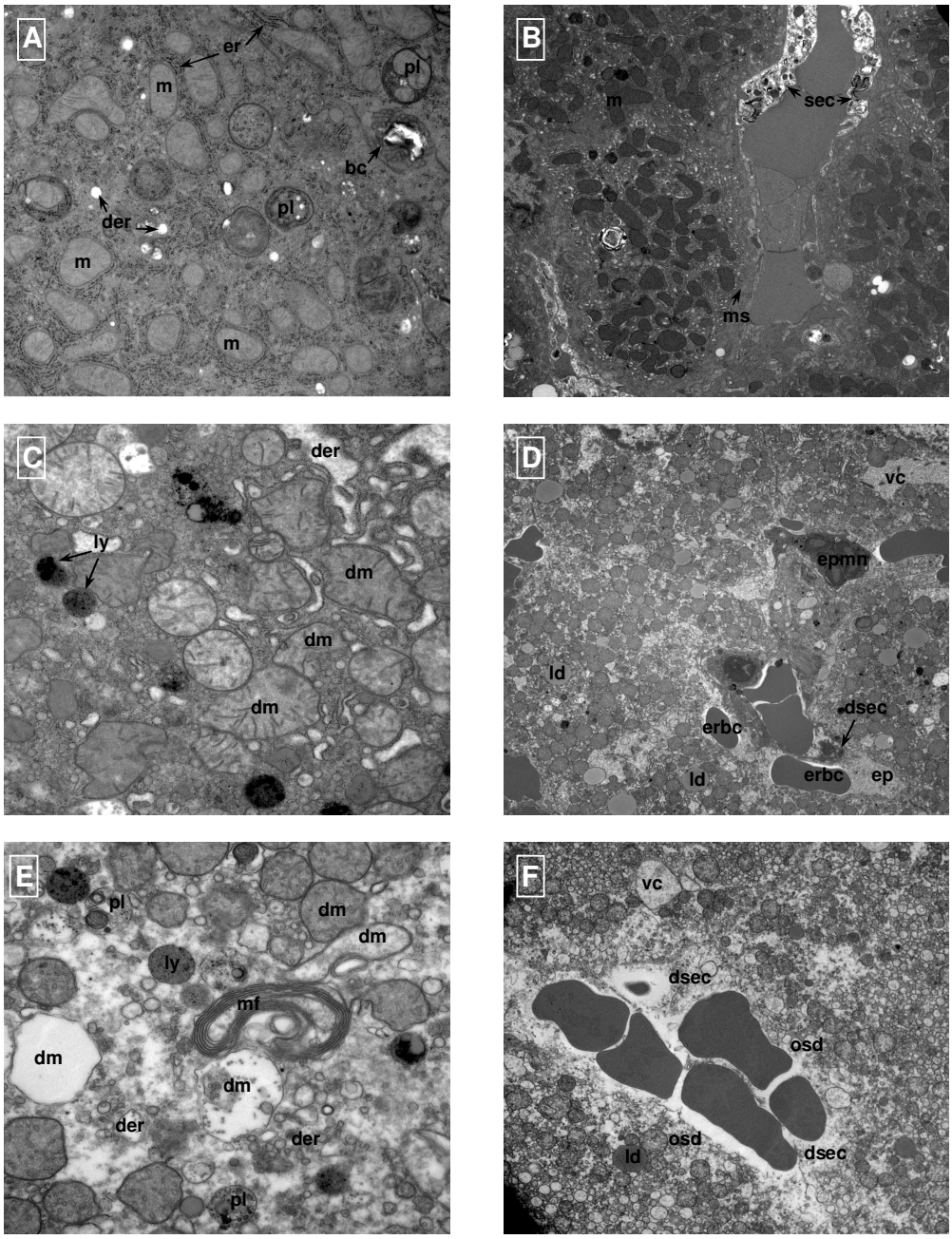

Figure 7.5. Hepatic transmission electron micrographs in eNOS$^{-/-}$ mice. The liver samples were taken at the end of the procedure in each group. **(A) & (B)** Sham group showing normal looking mitochondria (m), normal (er) and dilated endoplasmic reticulum (der), phagolysosomes (pl), bile canaliculi with microvilli (bc), sinusoidal endothelial cells (sec), and microvilli in the space of Disse (ms). **(C) & (D)** IR group demonstrating damaged mitochondria (dm), dilated endoplasmic reticulum (der), vacuole formation (vc), lysosomes (ly), lipid droplet formation (ld), and damaged sinusoidal endothelial cells (dsec) with extravasated red blood cell

(erbc), polymorphonucelocyte (epmn), and plasma (ep) into the hepatocytes. **(E) & (F)** Nitrite + IR group showing damaged mitochondria (dm), dilated endoplasmic reticulum (der), vacuolation (vc), lysosomes (ly) and phagolysosomal formation (pl), lipid droplet formation (ld), damaged sinusoidal endothelial cells (dsec) associated with obliteration of the space of Disse (osd), and myelin figure (mf) indicative of membranous damage.

7.3.5 *The reductions in hepatic microcirculatory blood flow seen with IR injury in eNOS$^{-/-}$ animals are unaffected by exogenous sodium nitrite*

Hepatic MBF remained relatively constant throughout the experiment in the sham group (figure 7.6).

In the IR group the MBF decreased from a mean of 99.3% of baseline during the pre-ischaemic period, to a mean of 31% of baseline during hepatic ischaemia (figure 7.6). Immediately following liver reperfusion, the mean MBF was 35.7%, and this improved to 52.3% of baseline at 30 minutes of reperfusion. The MBF remained relatively constant from then on, recording a reading of 52.2% at the end of the 2 hour reperfusion period.

Administration of nitrite during IR (nitrite + IR group) resulted in a mean MBF of 67.4% of baseline (figure 7.6) immediately following reperfusion, which is significantly higher than the MBF observed in the IR group at this time point ($P < 0.05$). Throughout the remainder of the reperfusion period the mean MBF ranged between 60.1% - 67.9% of baseline ($P > 0.05$ vs IR). Between 30 minutes to the end

of the reperfusion period at 2 hours, the difference between the sham and the other 2 groups (IR and nitrite + IR) was statistically significant ($P < 0.05$).

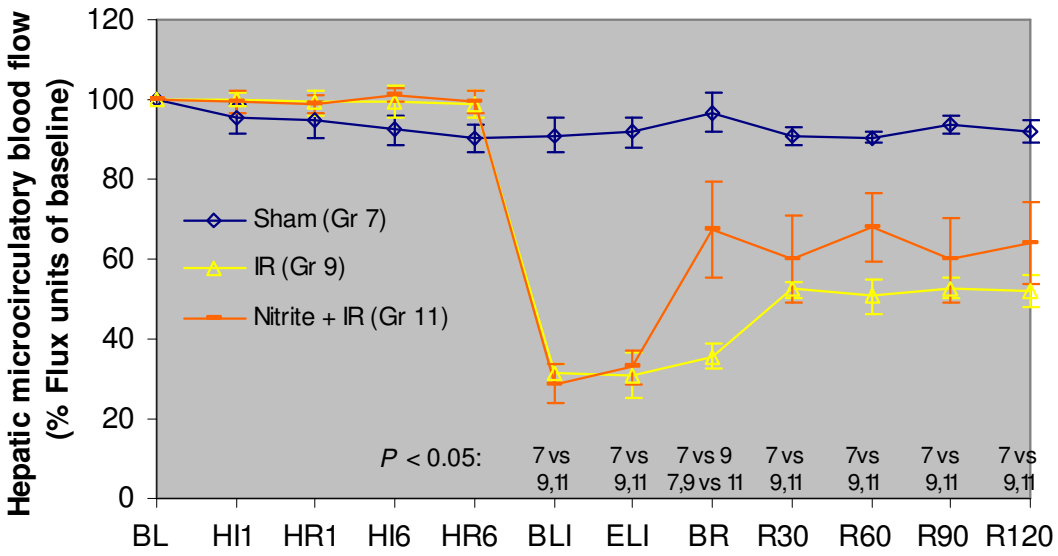

Figure 7.6. Hepatic microcirculatory blood flow in eNOS$^{-/-}$ animals, measured by LDF, is illustrated as mean percentage of pre-ischaemic baseline. Significant ($P < 0.05$) inter-group differences are shown vertically above the time points on the x-axis. BL, baseline; HI, hindlimb ischaemia; HR, hindlimb reperfusion; BLI, beginning of liver ischaemia; ELI, end of liver ischaemia; BR, beginning of liver reperfusion; R30 to R120, liver reperfusion at 30, 60, 90, and 120 min post ischaemia.

7.4 Discussion

The results of the experiments in this chapter showed that hindlimb RIPC (RIPC and RIPC + IR groups) in wild type mice results in a significant elevation of plasma NOx levels. In contrast exogenous nitrite administration to eNOS$^{-/-}$ mice did not attenuate liver IR injury.

The wild type animal experiments in this study demonstrated that RIPC alone significantly increases plasma NOx levels compared to sham animals. This indicates limb RIPC results in increased NO production that is rapidly oxidised to NO_2^- and NO_3^-. Further support for the theory that limb RIPC increases NO production comes from the demonstration in these experiments that RIPC + IR significantly increased plasma NOx levels compared to IR alone. In addition the RIPC + IR group had NOx levels that were significantly higher compared to those of sham. These results in combination with the results in chapter 4, showing that in wild type mice limb RIPC significantly reduces liver IR injury and increases hepatic MBF, would support the hypothesis that RIPC-induced NO synthesis is responsible for protection against liver IR injury. Only one previous publication described the measurement of plasma NOx levels following RIPC of the liver (227). In this study peripheral arterial and hepatic venous plasma NOx levels were quantified following hindlimb RIPC and hepatic IR in a rabbit model (227). The plasma NOx levels were non-significantly lowered following hepatic IR compared to the sham group in both peripheral arterial and hepatic venous blood. Hindlimb RIPC prior to hepatic IR resulted in an increase in NOx levels compared to the IR alone group which only reached statistical significance in hepatic venous blood samples but not in arterial samples (227), suggesting that liver IR leads to reduction in NO synthesis whilst antecedent limb RIPC acts to prevent this reduction in NO levels. In the present study we did not observe a reduction in plasma NOx levels in the IR compared to the sham group, but we did see a significant elevation of plasma NOx levels in the RIPC compared to the sham group and in the RIPC + IR compared to the IR group. Our results imply limb RIPC protects against liver IR injury through the elevation of NOx, and therefore NO levels.

Direct ischaemic preconditioning is known to increase NO synthesis (385) which in turn is rapidly oxidised to NO_2^- and NO_3^-. Oxidation to NO_2^- is accomplished via auto-oxidation using molecular O_2 and through a more rapidly occurring reaction that uses the protein ceruloplasmin (373). Oxidation of NO to NO_3^- uses oxyhaemoglobin as the oxidising agent (373). Circulating NO_2^- and NO_3^- enter the liver upon reperfusion to encounter an acidotic and a hypoxic environment that accelerate the reduction of these molecules to NO (375,386). Whilst NO, resulting from the reduction of NO_2^- and NO_3^- in the post-ischaemic liver environment, is the commonest pathway through which these molecules act to protect against IR injury (374,386); other NO-independent pathways may mediate the beneficial effects of NO_2^- and NO_3^-, however the role of these pathways in protection against liver IR injury is currently unclear (374,386).

Based on the findings of elevated plasma NOx levels in limb preconditioned wild type animals; exogenous sodium nitrite was administered to $eNOS^{-/-}$ animals to establish if exogenous nitrite possesses the beneficial effects we demonstrated with elevated endogenous NOx levels secondary to limb RIPC. However, we were unable to reproduce the protective effects of endogenous NOx through the administration of exogenous nitrite. Histopathologically the overall injury grade and 4 individual features of liver IR injury demonstrated a significant increase in the nitrite + IR group scores compared to the sham group scores. This is in contrast to the IR group scores which did not show significant differences from sham scores. These results could suggest that exogenous nitrite administration, at least on histopathological assessment, may increase liver damage in the context of IR. However, this would

need further research to establish, as neither the overall nor the individual features scores showed significant differences between the IR and IR + nitrite groups. More than a single explanation is possible for the lack of protection of exogenously administered nitrite to eNOS$^{-/-}$ mice. The dose of the administered nitrite was based on previous dosing studies (167,302) that showed 48 nmol of sodium nitrite elicits maximal protection in both, wild type and eNOS$^{-/-}$ animals. Moreover, the route and timing of nitrite administration was also as previously reported (167,302). Despite all of this we were unable to elicit protection against liver IR injury with exogenous nitrite administration. This may have been due to differing experimental variables such as the type of anaesthesia used or exact lengths of the ischaemia and reperfusion periods. Future dosing studies would be needed to clarify the role of exogenous nitrite in protection against liver IR injury. These experiments would evaluate the effects of altering the dose, timing and route of nitrite administration, on liver IR injury in the mouse model described in this thesis. An alternative explanation for the lack of efficacy of exogenous nitrite administration in eNOS$^{-/-}$ animals pertains to the fact that eNOS acts as a nitrite reductase under hypoxic conditions (387) leading to the reduction of nitrite to NO which in turn elicits protection. In an in vivo renal IR injury model, it has been shown that topical administration of nitrite to wild type but not eNOS$^{-/-}$ exhibit protection against kidney damage (388). Furthermore this has been corroborated by in vitro work in which wild type and eNOS$^{-/-}$ kidney homogenates, under hypoxic and acidotic conditions, had nitrite-derived NO quantified. The results showed that wild type homogenates produce significantly more NO compared to eNOS$^{-/-}$ homogenates (388). These results suggest that eNOS is an essential nitrite reductase under

hypoxic and acidotic conditions. The mechanisms underlying the nitrite reductase activity of eNOS are reviewed elsewhere (374).

In conclusion based on the results observed, endogenous circulating NOx levels are elevated following hindlimb RIPC and are associated with protection against liver IR injury. However, administration of exogenous nitrite to $eNOS^{-/-}$ mice at the dose, timing, and route described did not afford hepatic protection against liver IR injury.

In this chapter it was shown that hindlimb RIPC increases circulating levels of NO_2^- and NO_3^-. In the next chapter the role of the hepatic soluble guanylyl cyclase-cyclic GMP pathway in mediating the protective effects of hindlimb RIPC on liver IR injury will be evaluated.

Chapter 8

Importance of the hepatic sGC-cGMP pathway in the protective effects of RIPC against liver IR injury

8.1 Introduction

Nitric oxide (NO) may act through various pathways within the liver to exert its protective effects; including through the soluble guanylyl cyclase (sGC)-cyclic 3', 5' guanosine monophosphate (cGMP) pathway in the setting of liver IR injury (29).

The purification, quantification, and measurement of the activity of sGC is very difficult (389). Therefore, the inhibition or stimulation of sGC, using specific blockers or activators respectively, is used to elicit its functions in experimental models (389). sGC has been shown to mediate the protective effects of NO in liver IR injury, and administration of the sGC blocker ODQ abrogates these beneficial effects of NO, indicating NO acts through sGC in protecting the liver against IR injury (256,296,302,360). This has been shown in vivo (256,302) and in cultured hepatocytes models (296,360). Moreover, the specific sGC activator YC-1 reduces IR injury when administered to mice being subjected to liver IR (256).

Several experimental studies show NO protects against liver IR injury by elevating cGMP levels. Mice over-expressing the eNOS gene have significantly elevated hepatic cGMP levels compared to wild types which is associated with protection against liver IR injury (256). Other in vivo work showed rat pretreatment with the cGMP analogue 8-bromoguanosine 3',5' monophosphate (8-Br-cGMP) diminished subsequent hepatic IR injury (390). Furthermore, pretreatment with the non-selective NOS inhibitor N-omega-nitro-L-arginine (NA) worsens liver IR injury, however when the administration of NA is preceded by 8-Br-cGMP then the NA-induced adverse effects on IR are prevented (391) indicating that NOS-derived NO acts through cGMP to exert its protective effects. In vitro studies using cultured

hepatocytes further support the in vivo work, by demonstrating NO donors ameliorate hypoxia re-oxygenation injury through the elevation of cGMP levels (360). Moreover, re-oxygenation of hypoxic hepatocytes pretreated with 8-Br-cGMP ameliorated the IR-induced cell necrosis (296,360). The administration of the phosphodiesterase inhibitor sildenafil, which raises cGMP levels, to mice subjected to liver IR has also been shown to significantly ameliorate the IR injury (256).

The role of the sGC-cGMP pathway in mediating the protective effects of direct liver ischaemic preconditioning (IPC) has been evaluated. IPC reduces liver IR injury through increased production of hepatic cGMP (279). In contrast the role of the hepatic sGC-cGMP pathway in mediating the protective effects of RIPC on liver IR injury has not been studied. The aim of the current study was therefore to assess involvement of the hepatic sGC-cGMP pathway in mediating the protective functions of hindlimb RIPC on liver IR injury.

8.2 Materials and methods

The detailed methodology was described in chapter 3. A summary of the most pertinent points is given below.

8.2.1 *Animal surgical procedure*

Male inbred C57BL/6 wild type mice (Charles River laboratories, UK) were utilized in the present study. The animals were anaesthetised using 2% isoflurane. Core body temperature was maintained at 37.0 ± 0.5 ℃ using a heating pad and a rectal temperature probe. Hepatic IR was performed as detailed in section 3.4.1. At the end of the reperfusion period the animals were terminated by exsanguination through

needle cardiac puncture and blood collection. The blood was immediately centrifuged and the plasma supernatant was stored at -70 ℃ until assayed for liver transaminases. The left and median liver lobes were harvested at the end of each procedure for histopathology and transition electron microscopy. Hindlimb preconditioning consisted of microvascular clamping of the femoral vessels for four minutes followed by four minutes reperfusion for a total of six cycles as described in section 3.4.2.

8.2.2 *Experimental groups*

Four wild type groups with a minimum of six animals in each were used (Figure 3.2). The total anaesthetic time was equal in all the groups. All animals underwent laparotomy, mobilization of the liver, and mobilization of the right femoral vascular bundle. In addition some of the groups were each subjected to a specific procedure as follows:

Sham: Only underwent the laparotomy, mobilization of the liver, and mobilization of the right femoral vascular bundle described above.

IR: The median and left hepatic lobes were rendered ischaemic for 40 minutes followed by 2 hours reperfusion, using a microvascular clamp to occlude the portal triad branch to these lobes.

RIPC + IR: The right hindlimb was preconditioned with 6 cycles of 4 minutes ischaemia followed by 4 minutes reperfusion, using a microvascular clamp to occlude the femoral vessels under an operating microscope. This was followed by the IR group procedure described above.

ODQ + RIPC + IR: The sGC inhibitor ODQ was administered topically to the liver, in a volume of 100 µl of DMSO containing 600 µg of ODQ, followed by the RIPC + IR procedure.

8.2.3 *Measurement of liver enzymes*

The concentrations of ALT and AST were measured in the plasma using an automated clinical analyzer as described in section 3.5.

8.2.4 *Histopathology*

A liver biopsy was taken from the left lobe of each animal at the end of the experiment and fixed in 10% formal saline. The fixed tissues were embedded in paraffin and stained with H&E. Sections were assessed by a liver pathologist blinded to the animal groups. Each H&E sample was scored using two different methods as described in section 3.6.

8.2.5 *Transmission electron microscopy*

Liver biopsies were obtained from the left lobe at termination of the animals and were fixed in a glutaraldehyde / paraformaldehyde mixture overnight, processed as described in section 3.7, and viewed with a transmission electron microscope. Representative areas were photographed and the images were interpreted by a transition electron microscopy (TEM) scientist who was blinded to the groups. Assessment of the images was performed according to the parameters outlined in section 3.7.

8.2.6 *Liver and hindlimb microcirculatory blood flow*

Laser Doppler flowmetry (LDF) was used to measure blood flow in the microvasculature of the liver as described in section 3.8. The probe was placed on the left liver lobe so that it was just in contact with the tissue surface. LDF data was collected as the mean of four readings recorded over a one minute period. In addition, a second LDF probe was positioned on the sole of the right foot to ensure blood flow interruption and reperfusion during femoral vessels clamping and unclamping respectively. Figure 3.6 shows the time points of the LDF recordings during the study protocol.

8.2.7 *Measurement of hepatic cGMP*

Hepatic cGMP levels were measured using a commercially available enzyme immunoassay kit (Cayman Chemical, catalogue No. 581021) as detailed in section 3.12.

8.2.8 *Statistical analysis*

Values are expressed as mean ± SEM. One way analysis of variance (ANOVA) with Post Hoc Bonferroni correction for multiple comparisons was used. $P < 0.05$ was considered statistically significant in all analyses.

8.3 Results

The plasma transaminases levels, histopathological scores, ultrastructural changes, and MBF results of the ODQ + RIPC + IR group obtained in this chapter were compared to the results of the sham, IR, and RIPC + IR groups obtained in chapter 4.

8.3.1 *ODQ increases plasma transaminases levels in hindlimb preconditioned mice*

The results of the plasma transaminases are summarised in figure 8.1. Liver IR resulted in a significant increase in the plasma levels of ALT and AST compared to the sham group ($P < 0.05$). Hindlimb preconditioning preceding liver IR (RIPC + IR group) significantly reduced the plasma transaminases levels compared to IR alone ($P < 0.05$). Topical administration of ODQ to the liver, prior to hindlimb RIPC and liver IR (ODQ + RIPC + IR group), increases ALT and AST compared to the RIPC + IR group but this did not reach statistical significance.

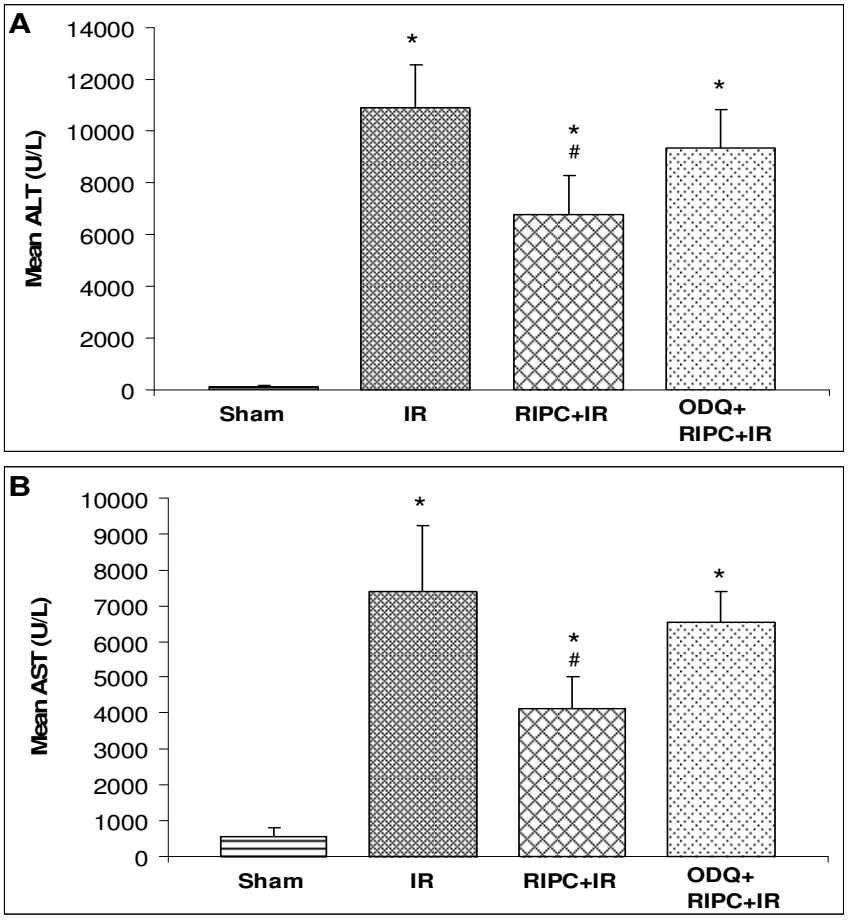

Figure 8.1. Plasma liver enzyme levels. (**A**) Alanine aminotransferase (ALT). *$P <$ 0.05 vs sham; #$P < 0.05$ vs IR. (**B**) Aspartate aminotransferase (AST). *$P < 0.05$ vs sham; #$P < 0.05$ vs IR.

8.3.2 *The protective effects of hindlimb RIPC on hepatic histopathological IR injury are diminished by ODQ*

The overall IR injury grade assigned to each sample and the mean overall grade for each animal group are both given in figure 8.2. The sham group showed minimal signs of liver IR injury with a mean overall grade of 0. Liver IR resulted in a significant increase in the mean overall injury grade (IR group mean overall grade = 1.83) compared to the sham group ($P < 0.05$). Preconditioning prior to liver IR (RIPC + IR group) decreased the mean overall injury score to 1.33, which is not significantly different from the sham or IR groups ($P > 0.05$). Administration of ODQ prior to RIPC + IR (ODQ + RIPC + IR group) resulted in an increase of the mean overall injury grade to 1.5 ($P < 0.05$ vs sham; $P > 0.05$ vs IR or RIPC + IR).

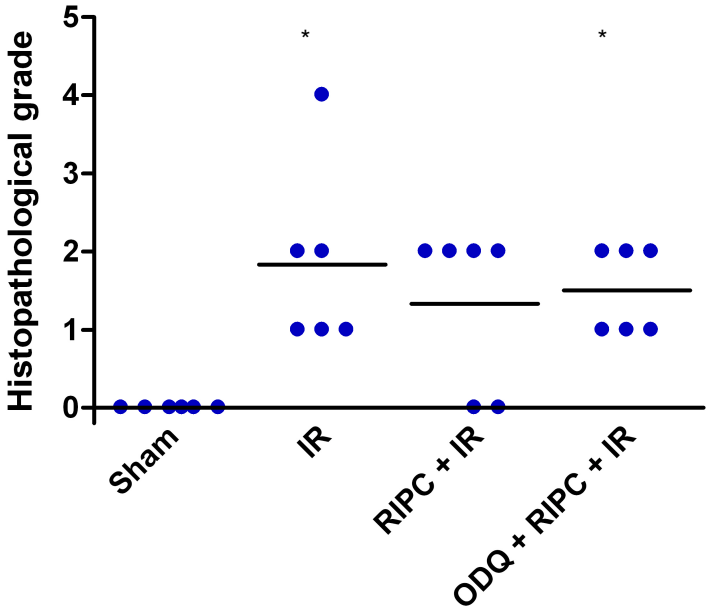

Figure 8.2. Vertical scatter plot of histopathological grades. Each dot represents the overall grade assigned to each individual liver biopsy sample (n = 6 per group). Horizontal bars represent the means. *$P < 0.05$ vs sham.

Assessment of the 10 individual histopathological features of liver IR injury revealed a higher mean score of all 10 features in the IR compared to the sham group, although statistical significance ($P < 0.05$) was only achieved in 5 of the 10 individual features. (figure 8.3).

Compared to IR, the RIPC + IR group resulted in a lower mean score in 8 out of the 10 individual features, although in none of these was statistical significance reached. The remaining 2 features (neutrophil infiltration and nuclear pyknosis) had a higher mean score in the RIPC + IR compared to the IR group (figure 8.3).

Administration of ODQ prior to RIPC + IR (ODQ + RIPC + IR group) resulted in a higher mean score in 7 out of the 10 individual features compared to the RIPC + IR group, although none of these reached statistical significance (figure 8.3). Two of the remaining features (sinusoidal dilatation and eosinophilia) had mean scores that were identical in the ODQ + RIPC + IR and the RIPC + IR group. One feature (nuclear pyknosis) showed a lower mean score in the ODQ + RIPC + IR compared to RIPC + IR.

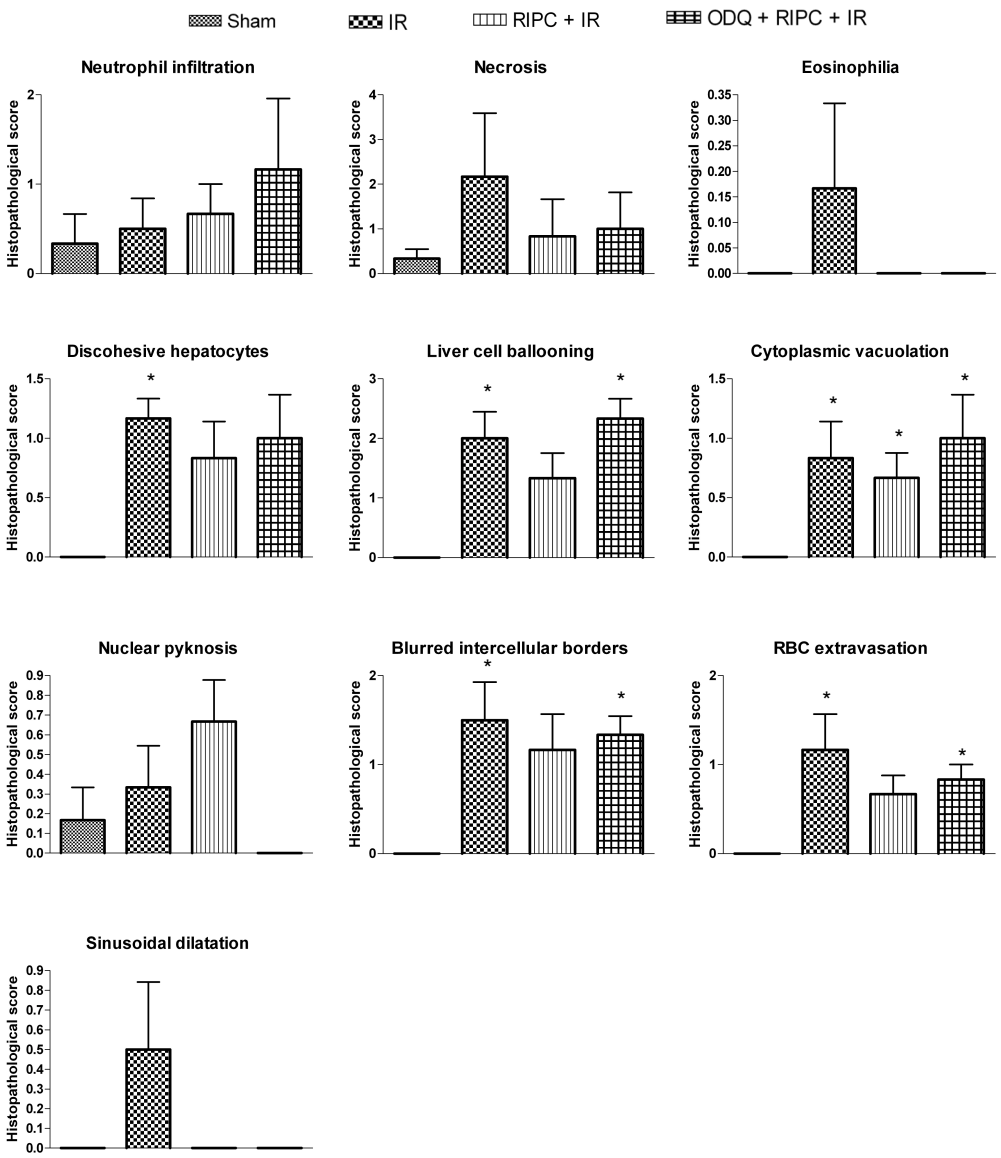

Figure 8.3. Histopathological scores of individual features of liver injury. Each bar chart is the mean histopathological score of six animals in that group. The error bars are the standard error of the means. **P* < 0.05 vs sham.

8.3.3 *ODQ inhibits the protective effects of hindlimb RIPC on ultrastructural damage in liver IR*

Figure 8.4 illustrates representative changes exhibited by each of the animal groups. The sham group showed normal ultrastructural appearances. The IR group exhibited extensive mitochondrial damage, ER dilatation, cytosolic vacuole formation, phagolysosomal formation, lipid droplet formation, glycogen depletion, bile canaliculi dilatation with microvilli damage, and sinusoidal endothelial cell (SEC) disruption with extravasation of red blood cells (RBC) into the liver parenchyma. In contrast the ultrastructural damage sustained by the RIPC + IR group consisted of ER dilatation, phagolysosomal formation, lipid droplet formation, glycogen depletion, and disruption of SEC but without RBC extravasation.

The administration of ODQ prior to RIPC + IR (ODQ + RIPC + IR group) resulted in appearances that are very similar to the IR group and that consisted of extensive mitochondrial damage, ER dilatation with vesiculation, vacuole formation, lipid droplet formation, glycogen depletion, and homogenous SEC disruption with RBC extravasation.

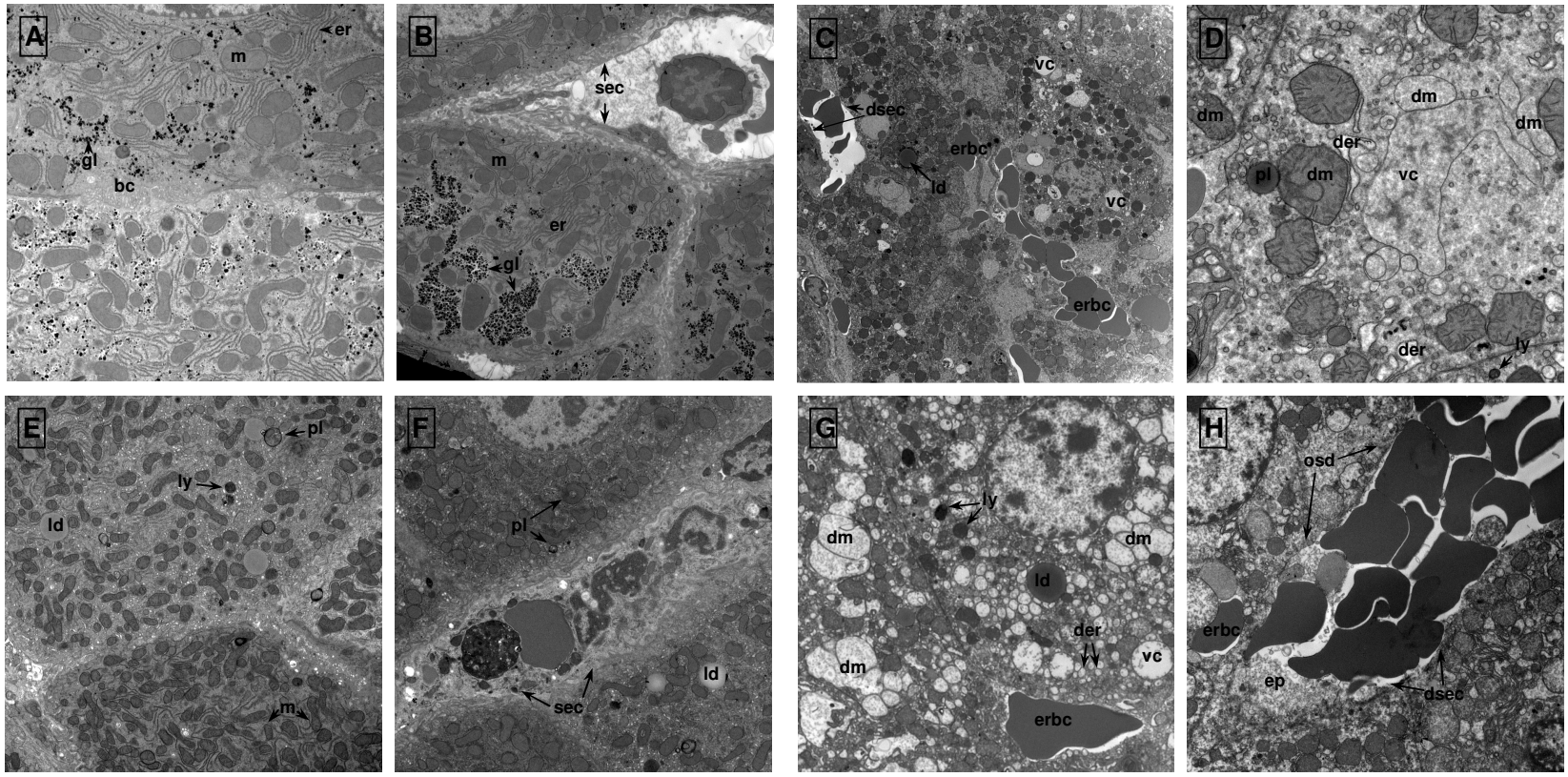

Figure 8.4. Hepatic transmission electron micrographs. The liver samples were taken at the end of the procedure in each group. **(A) & (B)** Sham group showing normal endoplasmic reticulum (er), bile canaliculi with microvilli (bc), mitochondria (m), glycogen (gl), and sinusoidal endothelial cells (sec). **(C) & (D)** IR group demonstrating irreversibly damaged mitochondria (dm) with some merging into vacuoles (vc),

dilatation and vesiculation of endoplasmic reticulum (der), lysosomes (ly) and phagolysosomes (pl), lipid droplets (ld), and severely damaged sinusoidal endothelial cells (dsec) associated with red blood cell extravasation (erbc). **(E) & (F)** RIPC + IR group demonstrating undamaged but pleomorhic mitochondria (m), lipid droplets (ld), lysosomes (ly) and phagolysosomes (pl), and damaged sinusoidal endothelial cells (sec) but without RBC extravasation. **(G) & (H)** ODQ + RIPC + IR group showing irreversibly damaged mitochondria (dm) some of which are coalescing into vacuoles (vc), dilatiation and vesiculation of endoplasmic reticulum (er), lipid droplets (ld), severely damaged sinusoidal endothelial cells (dsec) associated with obliteration of the space of Disse (osd) and extravasation of red blood cells (erbc) and plasma (ep).

8.3.4 *ODQ abolishes the protective effects of hindlimb RIPC on hepatic microcirculatory blood flow in liver IR*

Figure 8.5 illustrates hepatic MBF for the duration of the experiment. The sham group demonstrated constant hepatic MBF, whilst the IR and RIPC + IR exhibited a significant reduction of MBF during liver ischaemia compared to sham. Upon reperfusion the IR group showed no significant improvement in MBF, whilst the RIPC + IR group demonstrates significant recovery of MBF towards baseline values compared to the IR group ($P < 0.05$).

The ODQ + RIPC + IR group did not show significant deviations in MBF from the other groups during the pre-ischaemic period. However, during liver ischaemia MBF readings dropped significantly compared to the sham but not the IR or RIPC + IR groups. Upon reperfusion MBF in the ODQ + RIPC + IR group failed to recover, showing significant differences compared to the RIPC + IR group throughout reperfusion ($P < 0.05$). At the end of the 2 hour reperfusion period the mean MBF value was 41.5% of baseline in the ODQ + RIPC + IR group compared to 93.5% of baseline in the RIPC + IR group ($P < 0.0001$). There were no significant differences in the mean MBF values between the ODQ + RIPC + IR and the IR groups throughout the reperfusion period (figure 8.5).

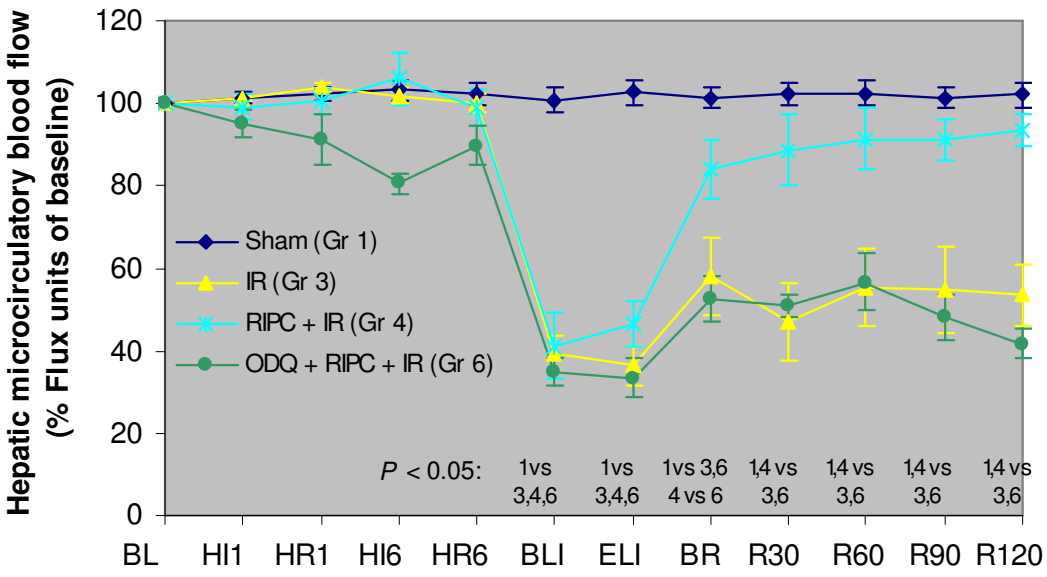

Figure 8.5. Hepatic microcirculatory blood flow, measured by LDF, is illustrated as mean percentage compared to pre-ischaemic baseline. Significant ($P < 0.05$) inter-group differences are shown vertically above the time points on the x-axis. BL, baseline; HI, hindlimb ischaemia; HR, hindlimb reperfusion; BLI, beginning of liver ischaemia; ELI, end of liver ischaemia; BR, beginning of liver reperfusion; R30 to R120, liver reperfusion at 30, 60, 90, and 120 min post ischaemia.

8.3.5 *RIPC alone but not RIPC + IR significantly elevates hepatic cGMP levels*

The RIPC alone group showed significantly higher levels of hepatic cGMP compared to the sham group. There were no significant differences between the remaining groups (figure 8.6).

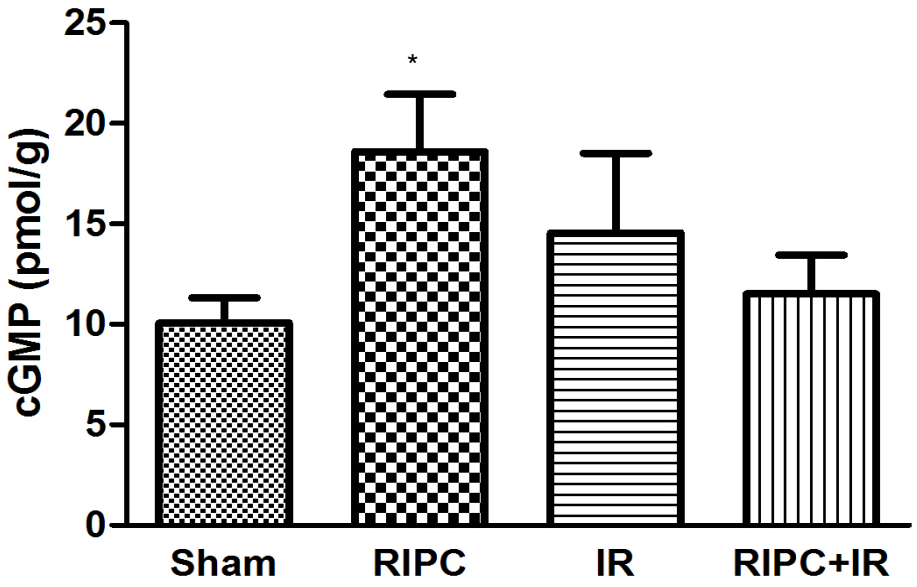

Figure 8.6. Hepatic cGMP levels in wild type mice (n = 6 per group). *$P < 0.05$ vs Sham.

8.4 Discussion

The results of the current study indicated that protective mechanisms of hindlimb RIPC include the hepatic sGC-cGMP pathway. This was attested to by a trend showing an elevation in the ALT and AST plasma levels, and an increase in the overall histopathological injury grade and in seven out of the ten individual features of liver IR injury, in the ODQ + RIPC + IR compared to the RIPC + IR group. Moreover, hepatic MBF measurements during liver reperfusion were significantly reduced in the ODQ + RIPC + IR compared to the RIPC + IR group. Finally, hepatic cGMP levels were significantly elevated in the RIPC alone group compared to the sham group.

Eukaryotic sGC possesses high affinity for NO as an activating ligand (392). More than a single explanation is possible as to why the enzyme and histopathological

markers of liver IR injury were not significantly higher in the ODQ + RIPC + IR compared to the RIPC + IR group. Firstly the selective sGC inhibitor ODQ acts through an interaction with the iron of haem prosthetic groups and therefore would bind not just sGC but also haemoglobin in the circulation and restrict its effectiveness when administered intravenously (389). To minimise the interaction with haemoglobin ODQ was administered topically to the liver in the present study. Topical administration however, would have still allowed interaction of ODQ with the haem iron centres of other proteins found in the liver such as cytochrome P450. Nonetheless, topical intraperitoneal ODQ has been used in multiple in vivo studies in the past to investigate the effects of inhibiting sGC on organ IR injury (256,302,393,394). The second explanation for the presence of a trend but not a significant difference in the increase in plasma enzymes and histopathological markers of liver IR injury may relate to the fact that NO can act through multiple different pathways (395-397) to exert its effects. Therefore it is feasible that NO acted through an alternate mechanism; such as formation of peroxynitrite, nitrosylation of thiol and amine groups, or nitration of amino acids such as tyrosine and tryptophan (395-397) that subsequently provided heptoprotection against liver IR injury; in addition to the sGC-cGMP pathway. However, this requires further research to ascertain.

The results of hepatic cGMP levels suggested this second messenger is at least partially responsible for mediating the effects of hindlimb RIPC. This is because the RIPC alone group had a significantly elevated levels of cGMP compared to sham; whilst at the same time the cGMP levels in the RIPC + IR group did not differ from those in the IR alone group. An alternate explanation is that IR completely abrogated

the effects of RIPC on hepatic cGMP levels. We are the first group to demonstrate a possible role for the hepatic sGC-cGMP pathway in mediating the protective effects of RIPC. Previous in vivo (256,390,391) and in vitro studies (296,360) have demonstrated a protective role for the NO-sGC-cGMP pathway in protecting against liver IR injury. Moreover, direct liver ischaemic preconditioning preceding liver IR (IPC + IR) significantly elevates cGMP levels compared to sham and IR alone (279).

In this study it was demonstrated that hepatic MBF during liver reperfusion is significantly reduced in the ODQ + RIPC + IR compared to the RIPC + IR group. Considering that sGC possesses high affinity for NO (392) and that the only known end product of sGC catalysis is cGMP, then these results suggest hindlimb RIPC acts through NO and the sGC-cGMP pathway to maintain hepatic MBF during the 2 hour reperfusion time period following liver ischaemia. In support of these results, a previous study showed that intraportal administration of the cGMP analogue 8-Br-cGMP for 30 minutes immediately prior to and following liver ischaemia in pigs results in a significant improvement in hepatic MBF, compared to control animals that received intraportal saline, as measured by LDF during 3 hours of liver reperfusion following 60 minutes of hepatic ischaemia (398).

In conclusion the sGC-cGMP pathway contributes to mediating the protective effects of hindlimb RIPC on liver IR injury. However, other pathways are probably involved as the protection exhibited by sGC-cGMP was incomplete. Additionally, the hindlimb RIPC-induced sGC-cGMP pathway preserves the hepatic MBF during the reperfusion period following liver ischaemia.

Chapter 9

Thesis discussion, conclusions, and future directions

9.1 Methodological considerations

9.1.1 *The experimental model*

Understanding the molecular mechanisms that underpin the protective effects of RIPC on liver IR injury will facilitate the design of pharmacological interventions that mimic the beneficial effects of RIPC. Animal models of liver IR injury offer standardised reproducible experimental strategies in which to dissect the molecular pathways mediating the beneficial effects of RIPC.

Experimental work using mice offers many advantages over the use of other animal species. The most important of these is the commercial availability of numerous transgenic strains that no other species offer. In addition mice reproduce quickly, are easy to maintain, and the mouse genome has many similarities to the human genome (399). For example, the mouse genome contains 2.5Gb whilst that of humans contain 2.9Gb; 40% of the human genome can be aligned to the mouse genome at the nucleotide level; both human and mouse genome contain 30000 genes each; and the proportion of mouse genes with a single identifiable orthologue in the human genome is approximately 80%, and the proportion of mouse genes without any homologue currently detectable in the human genome (and vice versa) seems to be less than 1% (399). The use of mice in research may also present disadvantages including the small size and therefore small circulating and solid tissue volumes; the cost which is strain-dependent; and breeding difficulty and high mortality seen in some strains.

In this thesis inbred C57BL/6 wild type and $eNOS^{-/-}$ mice were used. C57BL/6 mice are the commonest 'control' strain used in medical research. $eNOS^{-/-}$ mice have been

generated that had disruption to each of the four alleles found in the mouse eNOS gene (307,400-402). The $eNOS^{-/-}$ mice used in this research were originally produced as an F1 hybrid between SV129 and C57BL/6 (307), with all subsequent matings and generations conducted as SV129/BLK6 x SV129/BLK6 homozygotes in a closed colony.

The liver ischaemic model used in this thesis is well established and involves clamping the portal triad supplying the left and median lobes, rendering approximately 70% of the liver ischaemic. This partial hepatic ischaemia prevents mesenteric venous congestion and subsequent intestinal mucosal damage leading to bacterial translocation across the intestinal wall by permitting portal decompression through the caudate and right lobes of the liver (308-310). A disadvantage of partial hepatic ischaemia is that it does not accurately mimic clinical total hepatic ischaemia following performance of the Pringle manoeuvre during liver resections; or the total hepatic ischaemia livers are subjected to during transplantation. Animals poorly tolerate ischaemia to the whole liver. For example 30 minutes of total hepatic ischaemia in rabbits results in cardiac arrest due to metabolic acidosis (403). An alternative would have been a liver transplant model. However, such a model would have involved cold ischaemic injury to the liver, the molecular pathways of which differ from those mediating normothermic ischaemia. Moreover, liver transplantation in the mouse is technically very demanding, and all transplantation models involve denervation of the liver and may involve immunologically-mediated damage to donor livers once implanted in recipients; factors that could significantly influence the results of the endpoints assessed in this thesis.

An invasive hindlimb RIPC protocol involving open clamping of the femoral vessels was used based on the findings of the preliminary experiments that demonstrated non-invasive hindlimb RIPC resulted in hindlimb neuro-muscular bruising and paralysis. In contrast direct clamping of femoral vessels did not lead to any complications. Hence the decision was taken to adopt the open clamping technique. The other main advantage of the open method of femoral vessel occlusion is the ability to induce hindlimb ischaemia in every animal at exactly the same position on the thigh. In comparison it would be difficult to control the precise position of non-invasive techniques, such as the use of finger pressure or tourniquet to induce hindlimb ischaemia. Furthermore some non-invasive methods such as finger pressure or elastic bands may induce variable and unreliable pressures during vessel occlusion. The clinical applicability of the open clamping method to perform hindlimb RIPC in humans prior to liver resection or transplantation is limited as it is very unlikely femoral vessel dissection and direct clamping would be done for the sole purpose of preconditioning. In contrast, non-invasive techniques of femoral vessel occlusion may have better clinical applications in inducing hindlimb ischaemia. However, the gist of using an invasive technique in this thesis was to establish a well-controlled and validated animal model to be used for studying the mechanisms underlying the protective effects of RIPC on liver IR injury.

A total of 142 mice were used for this thesis. This number consisted of 113 animals that were used successfully in the experimental protocols. The remaining 29 animals used did not contribute to the experimental results as these either died during the experimental procedure, or sustained a complication such as perforation of the colon

from the rectal temperature probe or vessel damage from intravenous drug administration.

9.1.2 *Liver enzymes*

The liver is responsible for multiple metabolic and excretory pathways and consequently a single method of quantifying liver function is not possible. To fully assess the state of health of the liver would entail measurement of all the various functions performed by the liver, in addition to assessment of markers of liver injury. True liver function tests would entail measurement of the synthetic function of the liver such as serum levels of albumin and clotting factors; and measurement of the liver's excretory function such as indocyanine green clearance and rate of urea formation. Furthermore, the physiological reserve of the liver allows it to sustain severe damage with only minimal metabolic derangement.

Alanine aminotransferase (ALT) and aspartate aminotransferase (AST) are released into the circulation from damaged hepatocytes, where both enzymes are found in the cytoplasm. The degree of release of these enzymes into the circulation correlates with length of the ischaemic insult and subsequent liver injury (404-407). ALT is very specific for hepatocyte damage whilst AST is also released from many other tissue types such as cardiomyocytes, skeletal myocytes, and erythrocytes. Serum levels of both these enzymes reflect the integrity of the plasma membrane as well as the proportion of parenchymal cells affected. Therefore these enzymes are a measure of liver damage rather than liver function per se. Our results showed that WT animals had greater ALT and AST levels compared to $eNOS^{-/-}$ mice. This may reflect different sensitivity to IR injury between the two groups, but this would

require further research to clarify, especially as this thesis concentrated on the benefits or otherwise of RIPC in each species.

9.1.3 *Histopathology*

In this thesis two semi-quantitative injury grading scales were used; an overall score and scores of individual features of liver IR injury. The specific criteria in each of the scales has been described and used multiple times in various publications (81,294,302,312,313). A liver histopathologist performed the scoring whilst unaware of the animal grouping. This histological assessment of liver sections allows objective appraisal of ischaemically damaged tissue. However the main disadvantage of using such a technique at 2 hours of reperfusion is that lethally damaged cells may appear relatively intact at this early stage, and hence significant differences between the animal groups were frequently lacking despite demonstrating a trend. Ideally the histological assessment should have been performed at 8 to 48 hours of reperfusion.

9.1.4 *Transmission electron microscopy*

Transmission electron microscopy (TEM) facilitates assessment of structural damage to subcellular structures. Unlike histopathological damage to whole cells, which is not usually manifested during the early phase of reperfusion injury; damage to subcellular organelles of a cell is seen during the early phase of reperfusion, however the extent of such damage is organelle-dependent. For example nuclear damage manifests at a much later point in time compared to mitochondrial damage. Some ultrastructural appearances are indicative of biochemical processes within a cell. For example in chapter 5 the observation that some of the endoplasmic

reticulum (ER) within hepatocytes exhibited condensation was indicative of lipid peroxidation damage to the membranous structure of ER.

The assessment of the degree of ultrastructural damage on TEM was performed by a TEM scientist who was blinded to the animal groups. TEM may be best used for qualitative rather than quantitative damage appraisal. This is because it is very difficult to process and assess a whole section of a liver lobe for TEM. However sampling errors that could be introduced if a single liver biopsy was processed for TEM were minimized by performing multiple biopsies from different regions of the left liver lobe in each animal.

9.1.5 *Laser Doppler flowmetry*

Laser Doppler flowmetry (LDF) was used to: 1. quantify hepatic microcirculatory blood flow (MBF); 2. ensure adequate blood flow disruption during hindlimb ischaemia with adequate blood reperfusion during the preconditioning protocol. There is good evidence that hepatic IR injury results from altered MBF secondary to damage of the liver microvasculature (408-410). Moreover hepatic MBF alterations following reperfusion in liver transplant recipients directly correlate with the maximum postoperative AST levels (411). Changes in hepatic MBF following IR have also been shown to be useful in predicting the severity of liver IR injury (412).

Liver IR injury results in multiple consequences for the microcirculation that include Kupffer cell and sinusoidal endothelial cell swelling (25,26), an increase in the vasoconstrictors endothelin (27) and thromboxane A2 (28), and a decrease in the vasodilator nitric oxide (29). These effects combine to cause sinusoidal narrowing.

In addition, on reperfusion there is increased adhesion and aggregation of neutrophils and platelets in the sinusoids; with the end result being a significant reduction in MBF on reperfusion (30). LDF is a reliable optical technique for the assessment of hepatic microcirculation and provides continuous measurements of blood flow in the sinusoids, arterioles, and venules (317). The wavelength of the laser used was 785nm which measured MBF at a sampling rate of 1 Hz in tissue volumes of 0.6-2.3 mm^3. This penetration range of the LDF laser is considered sufficient to study MBF in a liver lobe with a maximum thickness of 4 mm. LDF does not measure MBF in the liver as a whole. This would be ideal; however, the positioning of the LDF probe on a fixed site of the liver surface permits the continuous measurement of MBF throughout the experimental procedure at that point which reflects the relative changes in MBF occurring elsewhere in the liver lobes subjected to IR. We previously studied intersite variability of LDF measurements and found a co-efficient of variation of ~ 4% (413). This suggested that a single point to assess hepatic MBF satisfactorily reflects the MBF in the rest of the affected lobe. The mean relative percentage alteration in liver MBF compared to baseline (which was taken as 100% in each experiment); and to the other animal groups as a percentage of baseline at each time point was quantified. Relative changes in MBF are more important than absolute values in these experiments as they reflect the consequences of each intervention on the liver microcirculation.

The use of LDF to assess the dynamic changes in the liver microcirculation of the mouse presents few challenges. One being motion artefact. Vibration and other movements of the LDF probe cause artefact signals on the laser Doppler monitor. In addition respiratory movements in the mouse may lead to liver movements.

However, these were considerably reduced by sufficient mobilisation of the liver to avoid diaphragmatic movements; and by positioning the probe loosely in a solid plastic tubing (held firmly in place by a clamp) with the laser emitting end protruding through the plastic tube and being loosely in contact with the surface of the liver, allowing the probe to move with any slight movement of the liver.

9.1.6 *Nitrite and nitrate studies*

Nitric oxide (NO) is a free radical molecule and therefore is highly unstable. The transient and volatile nature of NO means it is rapidly oxidised to nitrite and nitrate (NOx), the commonest stable end products of in vivo NO reactivity. The concentration of NOx is commonly used as a quantitative measure of NO production in vivo (414). Moreover both nitrite and nitrate are reduced to NO, a process that is accelerated in the hypoxic and acidotic liver environment (375,386) during IR. Therefore nitrite and nitrate act as circulating stable reservoirs of NO. A colorimetric assay kit was used to measure plasma NOx levels. This kit is well established, of proven efficacy, and has been used numerous times in the published literature (415,416).

Exogenous sodium nitrite was administered to $eNOS^{-/-}$ mice with the expectation that this would ameliorate liver IR injury. The dose and timing of the administered nitrite was based on those previously shown to significantly reduce liver IR injury in mice (167,302). However, no protection was elicited. This could be due to any one of multiple reasons discussed in chapter 7, and would entail the need for further dosing studies to determine the accurateness of the results described in previous studies.

9.1.7 *Assessment of the sGC-cGMP pathway*

The specific soluble guanylyl cyclase (sGC) blocker ODQ has been used numerous times in the published literature in vivo studies (256,302). ODQ interacts with the iron of haem prosthetic groups and therefore would bind to haemoglobin in the circulation and restrict its effectiveness when administered intravenously (389). However, topical administration to the liver as was done in chapter 8 circumvents the problem of the interaction between ODQ and haemoglobin. An enzyme immunoassay was used to measure cyclic GMP (cGMP) in liver samples. This technique is well established, of proven efficacy, and is well described in the published literature (256,279).

9.2. Summary of the thesis's findings

The aim of the thesis was to establish a mouse model of hindlimb RIPC that protects against liver IR injury, and subsequently to use this model to evaluate the role of the NO pathway in this protection.

In chapter 4 a model of hindlimb RIPC that protects against liver IR injury was established and validated in wild type mice. This model used open clamping of the femoral vessels to induce hindlimb RIPC rather than a tourniquet technique as the latter resulted in damage to the neuro-muscular structures in the limb. In contrast the open method had no side effects. This mouse model of limb RIPC significantly reduced liver IR injury and preserved hepatic MBF during the 2 hour liver reperfusion period.

In chapter 5 the NO scavenger C-PTIO was administered to wild type mice, and as a consequence the protective effects of hindlimb RIPC against liver IR injury disappeared. In addition, the C-PTIO + RIPC + IR group exhibited significantly lower hepatic MBF measurements, during the 2 hour liver reperfusion, compared to the RIPC + IR group. These findings indicated NO mediated the protective effects of limb RIPC against liver IR injury.

In chapter 6 $eNOS^{-/-}$ mice were used. The protection that had been exhibited by RIPC in wild type mice disappeared in $eNOS^{-/-}$ mice. Furthermore $eNOS^{-/-}$ mice did not demonstrate any benefit of limb RIPC on hepatic MBF, which is in contrast to the protective effects of limb RIPC on hepatic MBF observed in wild type mice. Liver and hindlimb skeletal muscle eNOS Western blots demonstrated equal protein expression amongst the various animal groups. eNOS immunohistochemistry showed eNOS was expressed in hepatocytes and the vascular endothelium within the liver; whilst within the hindlimb eNOS was expressed in skeletal myocytes and the vascular endothelium. Liver and hindlimb skeletal muscle iNOS Western blots showed protein expression only in the RIPC and RIPC + IR groups. Taken together these results indicated that eNOS is essential for the protective effects of limb RIPC on liver IR injury, and it is likely at 2 hours of liver reperfusion this protection is due to increased activation of eNOS rather than increased expression of this enzyme. Additionally there is increased expression of iNOS in preconditioned groups, which may be contributing to the protection of RIPC but this needs further research to prove.

In chapter 7 the initial experiments were performed on wild type mice to measure plasma nitrite and nitrate concentrations. The results showed hindlimb RIPC alone significantly increased plasma NOx levels compared to the sham group; and RIPC + IR significantly elevated plasma NOx compared to the IR and sham groups. Based on these results, the effects of exogenous nitrite on liver IR injury in $eNOS^{-/-}$ mice were assessed, and were found not to protect the liver against IR injury. The dose, route, and time of administration of the exogenous nitrite were based on previous published studies that administered nitrite to mice subjected to liver IR as discussed in chapter 7. Therefore, further nitrite dosing studies using the mouse model we describe in this thesis are needed to clarify what beneficial effects, if any, exogenous nitrite may have on liver IR injury.

In chapter 8 the sGC inhibitor ODQ was administered to wild type mice. The results showed the ODQ + RIPC + IR group sustained a non-significant increase in liver IR injury compared to the RIPC + IR group. However, hepatic MBF was significantly decreased during the 2 hour liver reperfusion period in the ODQ + RIPC + IR compared to the RIPC + IR group. Quantification of hepatic cGMP levels showed a significant increase of this second messenger in the RIPC compared to the sham group; but there was no significant difference between the IR and RIPC + IR groups. Taken together these results suggested that in the context of hindlimb RIPC, NO is likely to exert its protective effects against liver IR injury at least partially through the hepatic sGC-cGMP pathway. In addition NO may also be acting through a second different pathway to exert its protective effects and further research is warranted to identify other pathways that NO may be acting through.

9.3 Overall conclusions arising from thesis and future directions

The major conclusions drawn from this study were:

1. Hindlimb ischaemic preconditioning significantly attenuates liver IR injury in the mouse. In contrast to the tourniquet method, the invasive technique of inducing hindlimb ischaemia does not result in neuromuscular bruising and paralysis.
2. eNOS-derived NO mediates the protective effects of hindlimb RIPC on liver IR injury.
3. Circulating levels of nitrite and nitrate increase as a consequence of hindlimb RIPC. These circulating molecules are end products of NO oxidation and are associated with hepato-protection against liver IR injury.
4. The hepatic sGC-cGMP pathway is at least partially responsible for mediating the protective effects of hindlimb RIPC on liver IR injury.
5. Hindlimb RIPC, acting through NO, preserves hepatic MBF during liver reperfusion following liver ischaemia.

The above conclusions support the hypothesis of this thesis. The findings are applicable to the early reperfusion period as all the experiments, with the exception of the survival studies in chapter 4, were performed with a reperfusion period of 2 hours. The potential clinical applications of the findings arising from this thesis are two fold. Firstly, whilst it maybe clinically unethical to use an open technique of femoral vessel clamping for the sole purpose of hindlimb preconditioning preceding either liver surgery performed with the Pringle manoeuvre or liver transplantation; it would be acceptable clinically to use a non-invasive technique, such as a tourniquet, to induce hindlimb preconditioning. Secondly, and perhaps more pertinently, the new mouse model described in this thesis was designed with the main aim of having

a validated and robust animal model to study the mechanisms underlying the protective effects of RIPC. This would then facilitate the development of pharmacological agents that mimic the beneficial effects of hindlimb RIPC.

Although clinical non-invasive hindlimb RIPC would be simple to implement prior to liver surgery or transplantation; a number of legitimate concerns may arise from the use of this technique on humans such as safety of RIPC in diseased hindlimbs (e.g. peripheral arterial disease, diabetics), and the potential effect of RIPC on diseased livers (e.g. cirrhotic livers, fatty livers, post chemotherapy). The other major issues would be the optimal preconditioning protocol in humans and the time interval between RIPC and the beginning of surgery. An additional point of contention in liver transplantation would be whether maximal benefits are obtained by preconditioning the donor, the recipient, or both. All these issues would require well designed randomized clinical trials for worthwhile answers.

Based on the finding of this thesis potential therapeutic pharmacological strategies may aim to increase NO availability through the up-regulation of eNOS, an increase in endogenous nitrite and nitrate concentrations, up-regulation or decreased degradation of sGC-cGMP, or through the use of NO donors. An additional strategy may aim at mechanisms to preserve the hepatic microvasculature as MBF significantly decreases with liver IR and is preserved with hindlimb RIPC through an action involving eNOS and NO. These potential avenues for targeted drug development would entail significant scientific research.

Many questions have arisen as a result of the research findings in this thesis. The findings of this study are applicable to the early phase of IR injury as the experiments were performed with a reperfusion period of 2 hours. Future research needs to analyse the effects of RIPC during the late phase of IR injury as well as the role eNOS-derived NO plays during the late phase. Additionally the exact contribution of hindlimb versus liver eNOS to the protection elicited by RIPC needs further clarification. The most precise and scientifically-valid method of conquering this would be to use tissue-specific knockout mice that selectively lack the eNOS gene in the liver or hindlimb. In the present study iNOS expression in the liver and hindlimb skeletal muscle was faintly up-regulated at 2 hours of reperfusion. To further shed light on the role of iNOS in RIPC future research could utilize $iNOS^{-/-}$ animals in both early and late phase IR injury. The effects of RIPC probably represent a systemic phenomenon with cross-talk between different organs. For example is it possible that hindlimb RIPC up-regulates eNOS and / or iNOS in non-hepatic organs such as the heart or the kidney, which subsequently amplify the protection exhibited by the liver? Could preconditioning the hindlimb act as the triggering signal that initiates multi-organ protection with positive feedback loops between the organs? These questions remain unanswered.

It is now clear that disturbances to the microvasculature of the liver may represent a key mechanism through which IR injury acts to damage the liver. In this study it was demonstrated hindlimb RIPC significantly preserves the hepatic microvasculature and eNOS-derived NO plays a crucial role in this. Furthermore, preservation of liver MBF is associated with a significant reduction in liver IR injury. Previous work using intravital microscopy has shown hindlimb RIPC significantly increases liver

sinusoidal RBC velocity, sinusoidal blood flow, and the ratio of perfused hepatic sinusoids during the early phase (3 hours of reperfusion) of liver IR injury (229). The long term benefits or otherwise, of hindlimb RIPC on liver IR injury, may well depend on the long term effects of RIPC on hepatic microvascular perfusion. Therefore long term recovery studies (e.g. up to 28 days) using wild type and $eNOS^{-/-}$ mice supplemented with NO donors, and using techniques such as LDF and intravital microscopy, would be valuable in assessing the hepatic microvasculature.

Finally, RIPC offers a systematic means of protection against liver IR injury. Our understanding of the pathways mediating the protective effects of this phenomenon is increasing. It is hoped, with the culmination of enough knowledge about RIPC, mechanistic and / or pharmacological therapeutic strategies will eventually be developed and used in the clinical setting of liver resections and transplantation.

References

1. de GH, Rauen U. Ischemia-reperfusion injury: processes in pathogenetic networks: a review. Transplant Proc 2007; 39**:** 481-484.

2. Kim YI. Ischemia-reperfusion injury of the human liver during hepatic resection. J Hepatobiliary Pancreat Surg 2003; 10**:** 195-199.

3. Kupiec-Weglinski JW, Busuttil RW. Ischemia and reperfusion injury in liver transplantation. Transplant Proc 2005; 37**:** 1653-1656.

4. Schemmer P, Mehrabi A, Kraus T, Sauer P, Gutt C, Uhl W, et al. New aspects on reperfusion injury to liver--impact of organ harvest. Nephrol Dial Transplant 2004; 19 Suppl 4**:** iv26-iv35.

5. Rushing GD, Britt LD. Reperfusion injury after hemorrhage: a collective review. Ann Surg 2008; 247**:** 929-937.

6. Birrer R, Takuda Y, Takara T. Hypoxic hepatopathy: pathophysiology and prognosis. Intern Med 2007; 46**:** 1063-1070.

7. Belghiti J, Noun R, Malafosse R, Jagot P, Sauvanet A, Pierangeli F, et al. Continuous versus intermittent portal triad clamping for liver resection: a controlled study. Ann Surg 1999; 229**:** 369-375.

8. Hasegawa T, Ito Y, Wijeweera J, Liu J, Malle E, Farhood A, et al. Reduced inflammatory response and increased microcirculatory disturbances during hepatic ischemia-reperfusion injury in steatotic livers of ob/ob mice. Am J Physiol Gastrointest Liver Physiol 2007; 292**:** G1385-G1395.

9. Jang JH, Kang KJ, Kang Y, Lee IS, Graf R, Clavien PA. Ischemic preconditioning and intermittent clamping confer protection against ischemic injury in the cirrhotic mouse liver. Liver Transpl 2008; 14**:** 980-988.

10. Okaya T, Blanchard J, Schuster R, Kuboki S, Husted T, Caldwell CC, et al. Age-dependent responses to hepatic ischemia/reperfusion injury. Shock 2005; 24**:** 421-427.

11. Yokoyama Y, Nagino M, Nimura Y. Which gender is better positioned in the process of liver surgery? Male or female? Surg Today 2007; 37**:** 823-830.

12. Chen H, Peng CH, Deng XX, Qiu WH, Shen BY, Yang WP, et al. [The protective effect of heat shock protein 72 by Doxorubicin in cold ischemia-reperfusion injury of the rat liver]. Zhonghua Wai Ke Za Zhi 2006; 44**:** 310-313.

13. Manekeller S, Sioutis M, Hirner A, Minor T. [Influence of neoadjuvant chemotherapy on liver integrity and ischemic tolerance]. Z Gastroenterol 2008; 46**:** 17-21.

14. rias-Diaz J, Ildefonso JA, Munoz JJ, Zapata A, Jimenez E. Both tacrolimus and sirolimus decrease Th1/Th2 ratio, and increase regulatory T lymphocytes in the liver after ischemia/reperfusion. Lab Invest 2009; 89**:** 433-445.

15. Takeuchi D, Yoshidome H, Kurosawa H, Kimura F, Shimizu H, Ohtsuka M, et al. Interleukin-18 exacerbates pulmonary injury after hepatic ischemia/reperfusion in mice. J Surg Res 2010; 158**:** 87-93.

16. Weinbroum AA, Kidron A, Hochhauser E, Hochman A, Rudick V, Vidne BA. Liver glutathione level influences myocardial reperfusion injury following liver ischemia-reperfusion. Med Sci Monit 2001; 7**:** 1137-1144.

17. Behrends M, Hirose R, Park YH, Tan V, Dang K, Xu F, et al. Remote renal injury following partial hepatic ischemia/reperfusion injury in rats. J Gastrointest Surg 2008; 12**:** 490-495.

18. Weinbroum AA. N-acetyl-L-cysteine mitigates aortic tone injury following liver ischemia-reperfusion. J Cardiovasc Pharmacol 2005; 45**:** 509-515.

19. Weinbroum AA, Hochhauser E, Rudick V, Kluger Y, Karchevsky E, Graf E, et al. Multiple organ dysfunction after remote circulatory arrest: common pathway of radical oxygen species? J Trauma 1999; 47**:** 691-698.

20. Chan KC, Lin CJ, Lee PH, Chen CF, Lai YL, Sun WZ, et al. Propofol attenuates the decrease of dynamic compliance and water content in the lung by decreasing oxidative radicals released from the reperfused liver. Anesth Analg 2008; 107**:** 1284-1289.

21. Yoshidome H, Kato A, Edwards MJ, Lentsch AB. Interleukin-10 inhibits pulmonary NF-kappaB activation and lung injury induced by hepatic ischemia-reperfusion. Am J Physiol 1999; 277**:** L919-L923.

22. Wanner GA, Ertel W, Muller P, Hofer Y, Leiderer R, Menger MD, et al. Liver ischemia and reperfusion induces a systemic inflammatory response through Kupffer cell activation. Shock 1996; 5**:** 34-40.

23. Jaeschke H. Preservation injury: mechanisms, prevention and consequences. J Hepatol 1996; 25**:** 774-780.

24. Noble-Jamieson G, Barnes N. Diagnosis and management of late complications after liver transplantation. Arch Dis Child 1999; 81**:** 446-451.

25. He XS, Ma Y, Wu LW, Wu JL, Hu RD, Chen GH, et al. Dynamical changing patterns of glycogen and enzyme histochemical activities in rat liver graft undergoing warm ischemia injury. World J Gastroenterol 2005; 11**:** 2662-2665.

26. Selzner M, Selzner N, Jochum W, Graf R, Clavien PA. Increased ischemic injury in old mouse liver: an ATP-dependent mechanism. Liver Transpl 2007; 13**:** 382-390.

27. Peralta C, Closa D, Hotter G, Gelpi E, Prats N, Rosello-Catafau J. Liver ischemic preconditioning is mediated by the inhibitory action of nitric oxide on endothelin. Biochem Biophys Res Commun 1996; 229**:** 264-270.

28. Ishiguro S, Arii S, Monden K, Fujita S, Nakamura T, Niwano M, et al. Involvement of thromboxane A2-thromboxane A2 receptor system of the hepatic sinusoid in pathogenesis of cold preservation/reperfusion injury in the rat liver graft. Transplantation 1995; 59**:** 957-961.

29. Phillips L, Toledo AH, Lopez-Neblina F, naya-Prado R, Toledo-Pereyra LH. Nitric oxide mechanism of protection in ischemia and reperfusion injury. J Invest Surg 2009; 22**:** 46-55.

30. Montalvo-Jave EE, Escalante-Tattersfield T, Ortega-Salgado JA, Pina E, Geller DA. Factors in the pathophysiology of the liver ischemia-reperfusion injury. J Surg Res 2008; 147**:** 153-159.

31. Caban A, Oczkowicz G, bdel-Samad O, Cierpka L. Influence of Kupffer cells on the early phase of liver reperfusion. Transplant Proc 2002; 34**:** 694-697.

32. Shibuya H, Ohkohchi N, Seya K, Satomi S. Kupffer cells generate superoxide anions and modulate reperfusion injury in rat livers after cold preservation. Hepatology 1997; 25**:** 356-360.

33. Liu P, Xu B, Spokas E, Lai PS, Wong PY. Role of endogenous nitric oxide in TNF-alpha and IL-1beta generation in hepatic ischemia-repefusion. Shock 2000; 13**:** 217-223.

34. Ohkohchi N, Shibuya H, Tsukamoto S, Sakurada M, Oikawa K, Terashima T, et al. Kupffer's cells modulate neutrophile activity by superoxide anion and tumor necrosis factor-delta in reperfusion injury of liver transplantation-mechanisms of radical generation and reperfusion injury after cold ischemia. Transplant Proc 1999; 31**:** 1055-1058.

35. Hanschen M, Zahler S, Krombach F, Khandoga A. Reciprocal activation between CD4+ T cells and Kupffer cells during hepatic ischemia-reperfusion. Transplantation 2008; 86**:** 710-718.

36. Niwano M, Arii S, Monden K, Ishiguro S, Nakamura T, Mizumoto M, et al. Amelioration of sinusoidal endothelial cell damage by Kupffer cell blockade during cold preservation of rat liver. J Surg Res 1997; 72**:** 36-48.

37. Cutrin JC, Llesuy S, Boveris A. Primary role of Kupffer cell-hepatocyte communication in the expression of oxidative stress in the post-ischaemic liver. Cell Biochem Funct 1998; 16**:** 65-72.

38. Taniai H, Hines IN, Bharwani S, Maloney RE, Nimura Y, Gao B, et al. Susceptibility of murine periportal hepatocytes to hypoxia-reoxygenation: role for NO and Kupffer cell-derived oxidants. Hepatology 2004; 39**:** 1544-1552.

39. Nakano Y, Kondo T, Matsuo R, Hashimoto I, Kawasaki T, Kohno K, et al. Platelet dynamics in the early phase of postischemic liver in vivo. J Surg Res 2008; 149**:** 192-198.

40. Brock RW, Nie RG, Harris KA, Potter RF. Kupffer cell-initiated remote hepatic injury following bilateral hindlimb ischemia is complement dependent. Am J Physiol Gastrointest Liver Physiol 2001; 280**:** G279-G284.

41. Jaeschke H, Farhood A, Bautista AP, Spolarics Z, Spitzer JJ. Complement activates Kupffer cells and neutrophils during reperfusion after hepatic ischemia. Am J Physiol 1993; 264**:** G801-G809.

42. Jaeschke H. Mechanisms of Liver Injury. II. Mechanisms of neutrophil-induced liver cell injury during hepatic ischemia-reperfusion and other acute inflammatory conditions. Am J Physiol Gastrointest Liver Physiol 2006; 290**:** G1083-G1088.

43. Yadav SS, Howell DN, Gao W, Steeber DA, Harland RC, Clavien PA. L-selectin and ICAM-1 mediate reperfusion injury and neutrophil adhesion in the warm ischemic mouse liver. Am J Physiol 1998; 275**:** G1341-G1352.

44. Jaeschke H. Is anti-P-selectin therapy effective in hepatic ischemia-reperfusion injury because it inhibits neutrophil recruitment? Shock 1999; 12**:** 233-234.

45. Vardanian AJ, Busuttil RW, Kupiec-Weglinski JW. Molecular mediators of liver ischemia and reperfusion injury: a brief review. Mol Med 2008; 14**:** 337-345.

46. Caldwell CC, Okaya T, Martignoni A, Husted T, Schuster R, Lentsch AB. Divergent functions of CD4+ T lymphocytes in acute liver inflammation and injury after ischemia-reperfusion. Am J Physiol Gastrointest Liver Physiol 2005; 289**:** G969-G976.

47. Zwacka RM, Zhang Y, Halldorson J, Schlossberg H, Dudus L, Engelhardt JF. CD4(+) T-lymphocytes mediate ischemia/reperfusion-induced inflammatory responses in mouse liver. J Clin Invest 1997; 100**:** 279-289.

48. Khandoga A, Kessler JS, Hanschen M, Khandoga AG, Burggraf D, Reichel C, et al. Matrix metalloproteinase-9 promotes neutrophil and T cell recruitment and migration in the postischemic liver. J Leukoc Biol 2006; 79**:** 1295-1305.

49. Zhai Y, Shen XD, Hancock WW, Gao F, Qiao B, Lassman C, et al. CXCR3+CD4+ T cells mediate innate immune function in the pathophysiology of liver ischemia/reperfusion injury. J Immunol 2006; 176**:** 6313-6322.

50. Caldwell CC, Tschoep J, Lentsch AB. Lymphocyte function during hepatic ischemia/reperfusion injury. J Leukoc Biol 2007; 82**:** 457-464.

51. Khandoga A, Hanschen M, Kessler JS, Krombach F. CD4+ T cells contribute to postischemic liver injury in mice by interacting with sinusoidal endothelium and platelets. Hepatology 2006; 43**:** 306-315.

52. Kuboki S, Sakai N, Tschop J, Edwards MJ, Lentsch AB, Caldwell CC. Distinct contributions of CD4+ T cell subsets in hepatic ischemia/reperfusion injury. Am J Physiol Gastrointest Liver Physiol 2009; 296**:** G1054-G1059.

53. Lappas CM, Day YJ, Marshall MA, Engelhard VH, Linden J. Adenosine A2A receptor activation reduces hepatic ischemia reperfusion injury by inhibiting CD1d-dependent NKT cell activation. J Exp Med 2006; 203**:** 2639-2648.

54. Khandoga A, Biberthaler P, Messmer K, Krombach F. Platelet-endothelial cell interactions during hepatic ischemia-reperfusion in vivo: a systematic analysis. Microvasc Res 2003; 65**:** 71-77.

55. Sindram D, Porte RJ, Hoffman MR, Bentley RC, Clavien PA. Platelets induce sinusoidal endothelial cell apoptosis upon reperfusion of the cold ischemic rat liver. Gastroenterology 2000; 118**:** 183-191.

56. Pereboom IT, Lisman T, Porte RJ. Platelets in liver transplantation: friend or foe? Liver Transpl 2008; 14**:** 923-931.

57. Sindram D, Porte RJ, Hoffman MR, Bentley RC, Clavien PA. Synergism between platelets and leukocytes in inducing endothelial cell apoptosis in the cold ischemic rat liver: a Kupffer cell-mediated injury. FASEB J 2001; 15**:** 1230-1232.

58. Nocito A, Georgiev P, Dahm F, Jochum W, Bader M, Graf R, et al. Platelets and platelet-derived serotonin promote tissue repair after normothermic hepatic ischemia in mice. Hepatology 2007; 45**:** 369-376.

59. Qin X, Gao B. The complement system in liver diseases. Cell Mol Immunol 2006; 3**:** 333-340.

60. Arumugam TV, Shiels IA, Woodruff TM, Granger DN, Taylor SM. The role of the complement system in ischemia-reperfusion injury. Shock 2004; 21**:** 401-409.

61. Fondevila C, Shen XD, Tsuchihashi S, Uchida Y, Freitas MC, Ke B, et al. The membrane attack complex (C5b-9) in liver cold ischemia and reperfusion injury. Liver Transpl 2008; 14**:** 1133-1141.

62. Lehmann TG, Koeppel TA, Kirschfink M, Gebhard MM, Herfarth C, Otto G, et al. Complement inhibition by soluble complement receptor type 1 improves microcirculation after rat liver transplantation. Transplantation 1998; 66**:** 717-722.

63. Woodruff TM, Arumugam TV, Shiels IA, Reid RC, Fairlie DP, Taylor SM. Protective effects of a potent C5a receptor antagonist on experimental acute limb ischemia-reperfusion in rats. J Surg Res 2004; 116**:** 81-90.

64. Inderbitzin D, Beldi G, Avital I, Vinci G, Candinas D. Local and remote ischemia-reperfusion injury is mitigated in mice overexpressing human C1 inhibitor. Eur Surg Res 2004; 36**:** 142-147.

65. Kastelein RA, Hunter CA, Cua DJ. Discovery and biology of IL-23 and IL-27: related but functionally distinct regulators of inflammation. Annu Rev Immunol 2007; 25**:** 221-242.

66. Lentsch AB, Yoshidome H, Kato A, Warner RL, Cheadle WG, Ward PA, et al. Requirement for interleukin-12 in the pathogenesis of warm hepatic ischemia/reperfusion injury in mice. Hepatology 1999; 30**:** 1448-1453.

67. Husted TL, Blanchard J, Schuster R, Shen H, Lentsch AB. Potential role for IL-23 in hepatic ischemia/reperfusion injury. Inflamm Res 2006; 55**:** 177-178.

68. Husted TL, Lentsch AB. The role of cytokines in pharmacological modulation of hepatic ischemia/reperfusion injury. Curr Pharm Des 2006; 12**:** 2867-2873.

69. Myers KJ, Eppihimer MJ, Hall L, Wolitzky B. Interleukin-12-induced adhesion molecule expression in murine liver. Am J Pathol 1998; 152**:** 457-468.

70. Aggarwal S, Ghilardi N, Xie MH, de Sauvage FJ, Gurney AL. Interleukin-23 promotes a distinct CD4 T cell activation state characterized by the production of interleukin-17. J Biol Chem 2003; 278**:** 1910-1914.

71. Peralta C, Fernandez L, Panes J, Prats N, Sans M, Pique JM, et al. Preconditioning protects against systemic disorders associated with hepatic ischemia-reperfusion through blockade of tumor necrosis factor-induced P-selectin up-regulation in the rat. Hepatology 2001; 33**:** 100-113.

72. Colletti LM, Kunkel SL, Walz A, Burdick MD, Kunkel RG, Wilke CA, et al. The role of cytokine networks in the local liver injury following hepatic ischemia/reperfusion in the rat. Hepatology 1996; 23**:** 506-514.

73. Scales WE, Campbell DA, Jr., Green ME, Remick DG. Hepatic ischemia/reperfusion injury: importance of oxidant/tumor necrosis factor interactions. Am J Physiol 1994; 267**:** G1122-G1127.

74. Shibuya H, Ohkohchi N, Tsukamoto S, Satomi S. Tumor necrosis factor-induced, superoxide-mediated neutrophil accumulation in cold ischemic/reperfused rat liver. Hepatology 1997; 26**:** 113-120.

75. Schwabe RF, Brenner DA. Mechanisms of Liver Injury. I. TNF-alpha-induced liver injury: role of IKK, JNK, and ROS pathways. Am J Physiol Gastrointest Liver Physiol 2006; 290**:** G583-G589.

76. Colletti LM, Cortis A, Lukacs N, Kunkel SL, Green M, Strieter RM. Tumor necrosis factor up-regulates intercellular adhesion molecule 1, which is important in the neutrophil-dependent lung and liver injury associated with hepatic ischemia and reperfusion in the rat. Shock 1998; 10**:** 182-191.

77. Fu X, Sheng Z, Wang Y, Ye Y, Xu M, Sun T, et al. Basic fibroblast growth factor reduces the gut and liver morphologic and functional injuries after ischemia and reperfusion. J Trauma 1997; 42**:** 1080-1085.

78. Shito M, Wakabayashi G, Ueda M, Shimazu M, Shirasugi N, Endo M, et al. Interleukin 1 receptor blockade reduces tumor necrosis factor production, tissue injury, and mortality after hepatic ischemia-reperfusion in the rat. Transplantation 1997; 63**:** 143-148.

79. Kato A, Yoshidome H, Edwards MJ, Lentsch AB. Reduced hepatic ischemia/reperfusion injury by IL-4: potential anti-inflammatory role of STAT6. Inflamm Res 2000; 49**:** 275-279.

80. Bedirli A, Kerem M, Pasaoglu H, Erdem O, Ofluoglu E, Sakrak O. Effects of ischemic preconditioning on regenerative capacity of hepatocyte in the ischemically damaged rat livers. J Surg Res 2005; 125**:** 42-48.

81. Camargo CA, Jr., Madden JF, Gao W, Selvan RS, Clavien PA. Interleukin-6 protects liver against warm ischemia/reperfusion injury and promotes hepatocyte proliferation in the rodent. Hepatology 1997; 26**:** 1513-1520.

82. Matsumoto T, O'Malley K, Efron PA, Burger C, McAuliffe PF, Scumpia PO, et al. Interleukin-6 and STAT3 protect the liver from hepatic ischemia and reperfusion injury during ischemic preconditioning. Surgery 2006; 140**:** 793-802.

83. Teoh N, Field J, Farrell G. Interleukin-6 is a key mediator of the hepatoprotective and pro-proliferative effects of ischaemic preconditioning in mice. J Hepatol 2006; 45**:** 20-27.

84. Yoshidome H, Kato A, Edwards MJ, Lentsch AB. Interleukin-10 suppresses hepatic ischemia/reperfusion injury in mice: implications of a central role for nuclear factor kappaB. Hepatology 1999; 30**:** 203-208.

85. Le MO, Louis H, Demols A, Desalle F, Demoor F, Quertinmont E, et al. Cold liver ischemia-reperfusion injury critically depends on liver T cells and is improved by donor pretreatment with interleukin 10 in mice. Hepatology 2000; 31**:** 1266-1274.

86. Yagihashi A, Hirata K, Zou XM, Tsuruma T, Araya J, Yajima T, et al. Downregulation of cytokine-induced neutrophil chemoattractants and

reduction of reperfusion injury in liver allograft by interleukin-10. Transplant Proc 2000; 32**:** 2302.

87. Yoshidome H, Kato A, Miyazaki M, Edwards MJ, Lentsch AB. IL-13 activates STAT6 and inhibits liver injury induced by ischemia/reperfusion. Am J Pathol 1999; 155**:** 1059-1064.

88. Kato A, Yoshidome H, Edwards MJ, Lentsch AB. Regulation of liver inflammatory injury by signal transducer and activator of transcription-6. Am J Pathol 2000; 157**:** 297-302.

89. Ke B, Shen XD, Lassman CR, Gao F, Katori M, Busuttil RW, et al. Interleukin-13 gene transfer protects rat livers from antigen-independent injury induced by ischemia and reperfusion. Transplantation 2003; 75**:** 1118-1123.

90. Ke B, Shen XD, Gao F, Busuttil RW, Kupiec-Weglinski JW. Interleukin 13 gene transfer in liver ischemia and reperfusion injury: role of Stat6 and TLR4 pathways in cytoprotection. Hum Gene Ther 2004; 15**:** 691-698.

91. Kiemer AK, Vollmar AM, Bilzer M, Gerwig T, Gerbes AL. Atrial natriuretic peptide reduces expression of TNF-alpha mRNA during reperfusion of the rat liver upon decreased activation of NF-kappaB and AP-1. J Hepatol 2000; 33**:** 236-246.

92. Wanner GA, Muller P, Ertel W, Busch CJ, Menger MD, Messmer K. Differential effect of cyclooxygenase metabolites on proinflammatory cytokine release by Kupffer cells after liver ischemia and reperfusion. Am J Surg 1998; 175**:** 146-151.

93. Serizawa A, Nakamura S, Suzuki, Baba S, Nakano M. Involvement of platelet-activating factor in cytokine production and neutrophil activation after hepatic ischemia-reperfusion. Hepatology 1996; 23**:** 1656-1663.

94. Hines IN, Kawachi S, Harada H, Pavlick KP, Hoffman JM, Bharwani S, et al. Role of nitric oxide in liver ischemia and reperfusion injury. Mol Cell Biochem 2002; 234-235**:** 229-237.

95. Blotnick S, Peoples GE, Freeman MR, Eberlein TJ, Klagsbrun M. T lymphocytes synthesize and export heparin-binding epidermal growth factor-like growth factor and basic fibroblast growth factor, mitogens for vascular cells and fibroblasts: differential production and release by CD4+ and CD8+ T cells. Proc Natl Acad Sci U S A 1994; 91**:** 2890-2894.

96. Fu X, Cuevas P, Gimenez-Gallego G, Wang Y, Sheng Z. The effects of fibroblast growth factors on ischemic kidney, liver and gut injuries. Chin Med J (Engl) 1998; 111**:** 398-403.

97. Giatromanolaki A, Kotsiou S, Koukourakis MI, Sivridis E. Angiogenic factor expression in hepatic cirrhosis. Mediators Inflamm 2007; 2007**:** 67187.

98. Peng X, Wang B, Wang T, Zhao Q. Expression of basic fibroblast growth factor in rat liver fibrosis and hepatic stellate cells. J Huazhong Univ Sci Technolog Med Sci 2005; 25**:** 166-9, 222.

99. Hamanoue M, Kawaida K, Takao S, Shimazu H, Noji S, Matsumoto K, et al. Rapid and marked induction of hepatocyte growth factor during liver regeneration after ischemic or crush injury. Hepatology 1992; 16**:** 1485-1492.

100. Oe S, Hiros T, Fujii H, Yasuchika K, Nishio T, Iimuro Y, et al. Continuous intravenous infusion of deleted form of hepatocyte growth factor attenuates hepatic ischemia-reperfusion injury in rats. J Hepatol 2001; 34**:** 832-839.

101. Sakakura Y, Kaibori M, Oda M, Okumura T, Kwon AH, Kamiyama Y. Recombinant human hepatocyte growth factor protects the liver against hepatic ischemia and reperfusion injury in rats. J Surg Res 2000; 92**:** 261-266.

102. Colletti LM, Green ME, Burdick MD, Strieter RM. The ratio of ELR+ to ELR- CXC chemokines affects the lung and liver injury following hepatic ischemia/ reperfusion in the rat. Hepatology 2000; 31**:** 435-445.

103. Day YJ, Marshall MA, Huang L, McDuffie MJ, Okusa MD, Linden J. Protection from ischemic liver injury by activation of A2A adenosine receptors during reperfusion: inhibition of chemokine induction. Am J Physiol Gastrointest Liver Physiol 2004; 286**:** G285-G293.

104. Ke B, Shen XD, Tsuchihashi S, Gao F, Araujo JA, Busuttil RW, et al. Viral interleukin-10 gene transfer prevents liver ischemia-reperfusion injury: Toll-like receptor-4 and heme oxygenase-1 signaling in innate and adaptive immunity. Hum Gene Ther 2007; 18**:** 355-366.

105. Langdale LA, Wilson L, Jurkovich GJ, Liggitt HD. Effects of immunomodulation with interferon-gamma on hepatic ischemia-reperfusion injury. Shock 1999; 11**:** 356-361.

106. Ren X, Kennedy A, Colletti LM. CXC chemokine expression after stimulation with interferon-gamma in primary rat hepatocytes in culture. Shock 2002; 17**:** 513-520.

107. Shen XD, Ke B, Zhai Y, Gao F, Tsuchihashi S, Lassman CR, et al. Absence of toll-like receptor 4 (TLR4) signaling in the donor organ reduces ischemia and reperfusion injury in a murine liver transplantation model. Liver Transpl 2007; 13**:** 1435-1443.

108. Tsuchihashi S, Ke B, Kaldas F, Flynn E, Busuttil RW, Briscoe DM, et al. Vascular endothelial growth factor antagonist modulates leukocyte trafficking and protects mouse livers against ischemia/reperfusion injury. Am J Pathol 2006; 168**:** 695-705.

109. Kato A, Gabay C, Okaya T, Lentsch AB. Specific role of interleukin-1 in hepatic neutrophil recruitment after ischemia/reperfusion. Am J Pathol 2002; 161**:** 1797-1803.

110. Ma W, Wang ZR, Zhang YF, Shi L. [Effect of prostaglandin E1 on monocyte chemotactic protein-1 expression in Kupffer cells of rats with hepatic ischemia-reperfusion injury]. Nan Fang Yi Ke Da Xue Xue Bao 2006; 26**:** 1180-1183.

111. Shirasugi N, Wakabayashi G, Shimazu M, Oshima A, Shito M, Kawachi S, et al. Up-regulation of oxygen-derived free radicals by interleukin-1 in hepatic ischemia/reperfusion injury. Transplantation 1997; 64**:** 1398-1403.

112. Welborn MB, III, Moldawer LL, Seeger JM, Minter RM, Huber TS. Role of endogenous interleukin-10 in local and distant organ injury after visceral ischemia-reperfusion. Shock 2003; 20**:** 35-40.

113. Yanagida H, Kaibori M, Yoshida H, Habara K, Yamada M, Kamiyama Y, et al. Hepatic ischemia/reperfusion upregulates the susceptibility of hepatocytes to confer the induction of inducible nitric oxide synthase gene expression. Shock 2006; 26**:** 162-168.

114. Zhai Y, Shen XD, Gao F, Zhao A, Freitas MC, Lassman C, et al. CXCL10 regulates liver innate immune response against ischemia and reperfusion injury. Hepatology 2008; 47**:** 207-214.

115. Tacchini L, Cairo G, De PC, Massip M, Rosello-Catafau J, Peralta C. Up regulation of IL-6 by ischemic preconditioning in normal and fatty rat livers: association with reduction of oxidative stress. Free Radic Res 2006; 40**:** 1206-1217.

116. Dinant S, Vetelainen RL, Florquin S, van Vliet AK, van Gulik TM. IL-10 attenuates hepatic I/R injury and promotes hepatocyte proliferation. J Surg Res 2007; 141**:** 176-182.

117. Hamada T, Tsuchihashi S, Avanesyan A, Duarte S, Moore C, Busuttil RW, et al. Cyclooxygenase-2 deficiency enhances Th2 immune responses and impairs neutrophil recruitment in hepatic ischemia/reperfusion injury. J Immunol 2008; 180**:** 1843-1853.

118. Le MO, Louis H, Stordeur P, Collet JM, Goldman M, Deviere J. Role of reactive oxygen intermediates in interleukin 10 release after cold liver ischemia and reperfusion in mice. Gastroenterology 1997; 113**:** 1701-1706.

119. Zou XM, Yagihashi A, Hirata K, Tsuruma T, Matsuno T, Tarumi K, et al. Downregulation of cytokine-induced neutrophil chemoattractant and prolongation of rat liver allograft survival by interleukin-10. Surg Today 1998; 28**:** 184-191.

120. Ke B, Shen XD, Lassman CR, Gao F, Busuttil RW, Kupiec-Weglinski JW. Cytoprotective and antiapoptotic effects of IL-13 in hepatic cold

ischemia/reperfusion injury are heme oxygenase-1 dependent. Am J Transplant 2003; 3**:** 1076-1082.

121. Takeuchi D, Yoshidome H, Kato A, Ito H, Kimura F, Shimizu H, et al. Interleukin 18 causes hepatic ischemia/reperfusion injury by suppressing anti-inflammatory cytokine expression in mice. Hepatology 2004; 39**:** 699-710.

122. Cursio R, Miele C, Filippa N, Van OE, Gugenheim J. Alterations in protein tyrosine kinase pathways in rat liver following normothermic ischemia-reperfusion. Transplant Proc 2006; 38**:** 3362-3365.

123. Ke B, Shen XD, Gao F, Tsuchihashi S, Farmer DG, Briscoe D, et al. The CD154-CD40 T-cell co-stimulation pathway in liver ischemia and reperfusion inflammatory responses. Transplantation 2005; 79**:** 1078-1083.

124. Moriga T, Arii S, Takeda Y, Furuyama H, Mizumoto M, Mori A, et al. Protection by vascular endothelial growth factor against sinusoidal endothelial damage and apoptosis induced by cold preservation. Transplantation 2000; 69**:** 141-147.

125. Tsurui Y, Sho M, Kuzumoto Y, Hamada K, Akashi S, Kashizuka H, et al. Dual role of vascular endothelial growth factor in hepatic ischemia-reperfusion injury. Transplantation 2005; 79**:** 1110-1115.

126. Klune JR, Dhupar R, Cardinal J, Billiar TR, Tsung A. HMGB1: endogenous danger signaling. Mol Med 2008; 14**:** 476-484.

127. Mogensen TH. Pathogen recognition and inflammatory signaling in innate immune defenses. Clin Microbiol Rev 2009; 22**:** 240-73, Table.

128. Izuishi K, Tsung A, Jeyabalan G, Critchlow ND, Li J, Tracey KJ, et al. Cutting edge: high-mobility group box 1 preconditioning protects against liver ischemia-reperfusion injury. J Immunol 2006; 176**:** 7154-7158.

129. Tsung A, Sahai R, Tanaka H, Nakao A, Fink MP, Lotze MT, et al. The nuclear factor HMGB1 mediates hepatic injury after murine liver ischemia-reperfusion. J Exp Med 2005; 201**:** 1135-1143.

130. Pelinka LE, Harada N, Szalay L, Jafarmadar M, Redl H, Bahrami S. Release of S100B differs during ischemia and reperfusion of the liver, the gut, and the kidney in rats. Shock 2004; 21**:** 72-76.

131. Zhang J, Wang H, Xiao Q, Liang H, Li Z, Jiang C, et al. Hyaluronic acid fragments evoke Kupffer cells via TLR4 signaling pathway. Sci China C Life Sci 2009; 52**:** 147-154.

132. Pardo M, Budick-Harmelin N, Tirosh B, Tirosh O. Antioxidant defense in hepatic ischemia-reperfusion injury is regulated by damage-associated molecular pattern signal molecules. Free Radic Biol Med 2008; 45**:** 1073-1083.

133. Szabo G, Dolganiuc A, Mandrekar P. Pattern recognition receptors: a contemporary view on liver diseases. Hepatology 2006; 44**:** 287-298.

134. Katsargyris A, Klonaris C, Alexandrou A, Giakoustidis AE, Vasileiou I, Theocharis S. Toll-like receptors in liver ischemia reperfusion injury: a novel target for therapeutic modulation? Expert Opin Ther Targets 2009; 13**:** 427-442.

135. Arumugam TV, Okun E, Tang SC, Thundyil J, Taylor SM, Woodruff TM. Toll-like receptors in ischemia-reperfusion injury. Shock 2009; 32**:** 4-16.

136. Zhai Y, Qiao B, Shen XD, Gao F, Busuttil RW, Cheng G, et al. Evidence for the pivotal role of endogenous toll-like receptor 4 ligands in liver ischemia and reperfusion injury. Transplantation 2008; 85**:** 1016-1022.

137. Watanabe T, Kubota S, Nagaya M, Ozaki S, Nagafuchi H, Akashi K, et al. The role of HMGB-1 on the development of necrosis during hepatic ischemia and hepatic ischemia/reperfusion injury in mice. J Surg Res 2005; 124**:** 59-66.

138. Tsuchihashi S, Zhai Y, Fondevila C, Busuttil RW, Kupiec-Weglinski JW. HO-1 upregulation suppresses type 1 IFN pathway in hepatic ischemia/reperfusion injury. Transplant Proc 2005; 37**:** 1677-1678.

139. Ke B, Shen XD, Gao F, Busuttil RW, Kupiec-Weglinski JW. Interleukin 13 gene transfer in liver ischemia and reperfusion injury: role of Stat6 and TLR4 pathways in cytoprotection. Hum Gene Ther 2004; 15**:** 691-698.

140. Tsung A, Zheng N, Jeyabalan G, Izuishi K, Klune JR, Geller DA, et al. Increasing numbers of hepatic dendritic cells promote HMGB1-mediated ischemia-reperfusion injury. J Leukoc Biol 2007; 81**:** 119-128.

141. Tsung A, Klune JR, Zhang X, Jeyabalan G, Cao Z, Peng X, et al. HMGB1 release induced by liver ischemia involves Toll-like receptor 4 dependent reactive oxygen species production and calcium-mediated signaling. J Exp Med 2007; 204**:** 2913-2923.

142. Wang H, Li ZY, Wu HS, Wang Y, Jiang CF, Zheng QC, et al. Endogenous danger signals trigger hepatic ischemia/reperfusion injury through toll-like receptor 4/nuclear factor-kappa B pathway. Chin Med J (Engl) 2007; 120**:** 509-514.

143. Tsung A, Hoffman RA, Izuishi K, Critchlow ND, Nakao A, Chan MH, et al. Hepatic ischemia/reperfusion injury involves functional TLR4 signaling in nonparenchymal cells. J Immunol 2005; 175**:** 7661-7668.

144. Tsuchihashi S, Zhai Y, Bo Q, Busuttil RW, Kupiec-Weglinski JW. Heme oxygenase-1 mediated cytoprotection against liver ischemia and reperfusion injury: inhibition of type-1 interferon signaling. Transplantation 2007; 83**:** 1628-1634.

145. Zhai Y, Shen XD, O'Connell R, Gao F, Lassman C, Busuttil RW, et al. Cutting edge: TLR4 activation mediates liver ischemia/reperfusion inflammatory response via IFN regulatory factor 3-dependent MyD88-independent pathway. J Immunol 2004; 173**:** 7115-7119.

146. Zhai Y, Qiao B, Gao F, Shen X, Vardanian A, Busuttil RW, et al. Type I, but not type II, interferon is critical in liver injury induced after ischemia and reperfusion. Hepatology 2008; 47**:** 199-206.

147. Shen XD, Ke B, Zhai Y, Gao F, Busuttil RW, Cheng G, et al. Toll-like receptor and heme oxygenase-1 signaling in hepatic ischemia/reperfusion injury. Am J Transplant 2005; 5**:** 1793-1800.

148. Fan J, Li Y, Levy RM, Fan JJ, Hackam DJ, Vodovotz Y, et al. Hemorrhagic shock induces NAD(P)H oxidase activation in neutrophils: role of HMGB1-TLR4 signaling. J Immunol 2007; 178**:** 6573-6580.

149. Thobe BM, Frink M, Hildebrand F, Schwacha MG, Hubbard WJ, Choudhry MA, et al. The role of MAPK in Kupffer cell toll-like receptor (TLR) 2-, TLR4-, and TLR9-mediated signaling following trauma-hemorrhage. J Cell Physiol 2007; 210**:** 667-675.

150. Zeng S, Feirt N, Goldstein M, Guarrera J, Ippagunta N, Ekong U, et al. Blockade of receptor for advanced glycation end product (RAGE) attenuates ischemia and reperfusion injury to the liver in mice. Hepatology 2004; 39**:** 422-432.

151. Zeng S, Dun H, Ippagunta N, Rosario R, Zhang QY, Lefkowitch J, et al. Receptor for advanced glycation end product (RAGE)-dependent modulation of early growth response-1 in hepatic ischemia/reperfusion injury. J Hepatol 2009; 50**:** 929-936.

152. McBride HM, Neuspiel M, Wasiak S. Mitochondria: more than just a powerhouse. Curr Biol 2006; 16**:** R551-R560.

153. Glantzounis GK, Salacinski HJ, Yang W, Davidson BR, Seifalian AM. The contemporary role of antioxidant therapy in attenuating liver ischemia-reperfusion injury: a review. Liver Transpl 2005; 11**:** 1031-1047.

154. Shiva S, Moellering D, Ramachandran A, Levonen AL, Landar A, Venkatraman A, et al. Redox signalling: from nitric oxide to oxidized lipids. Biochem Soc Symp 2004; 107-120.

155. Jaeschke H. Role of reactive oxygen species in hepatic ischemia-reperfusion injury and preconditioning. J Invest Surg 2003; 16**:** 127-140.

156. Andrukhiv A, Costa AD, West IC, Garlid KD. Opening mitoKATP increases superoxide generation from complex I of the electron transport chain. Am J Physiol Heart Circ Physiol 2006; 291**:** H2067-H2074.

157. Zorov DB, Juhaszova M, Sollott SJ. Mitochondrial ROS-induced ROS release: an update and review. Biochim Biophys Acta 2006; 1757**:** 509-517.

158. Urakami H, Abe Y, Grisham MB. Role of reactive metabolites of oxygen and nitrogen in partial liver transplantation: lessons learned from reduced-size liver ischaemia and reperfusion injury. Clin Exp Pharmacol Physiol 2007; 34**:** 912-919.

159. Bryan NS, Grisham MB. Methods to detect nitric oxide and its metabolites in biological samples. Free Radic Biol Med 2007; 43**:** 645-657.

160. Kuo PC, Abe K, Schroeder RA. Superoxide enhances interleukin 1beta-mediated transcription of the hepatocyte-inducible nitric oxide synthase gene. Gastroenterology 2000; 118**:** 608-618.

161. Madesh M, Hajnoczky G. VDAC-dependent permeabilization of the outer mitochondrial membrane by superoxide induces rapid and massive cytochrome c release. J Cell Biol 2001; 155**:** 1003-1015.

162. Zhao K, Zhao GM, Wu D, Soong Y, Birk AV, Schiller PW, et al. Cell-permeable peptide antioxidants targeted to inner mitochondrial membrane inhibit mitochondrial swelling, oxidative cell death, and reperfusion injury. J Biol Chem 2004; 279**:** 34682-34690.

163. Hemnani T, Parihar MS. Reactive oxygen species and oxidative DNA damage. Indian J Physiol Pharmacol 1998; 42**:** 440-452.

164. Matsui N, Satsuki I, Morita Y, Inaizumi K, Kasajima K, Kanoh R, et al. Xanthine oxidase-derived reactive oxygen species activate nuclear factor kappa B during hepatic ischemia in rats. Jpn J Pharmacol 2000; 84**:** 363-366.

165. Sanlioglu S, Williams CM, Samavati L, Butler NS, Wang G, McCray PB, Jr., et al. Lipopolysaccharide induces Rac1-dependent reactive oxygen species formation and coordinates tumor necrosis factor-alpha secretion through IKK regulation of NF-kappa B. J Biol Chem 2001; 276**:** 30188-30198.

166. Szabo C, Ischiropoulos H, Radi R. Peroxynitrite: biochemistry, pathophysiology and development of therapeutics. Nat Rev Drug Discov 2007; 6**:** 662-680.

167. Shiva S, Sack MN, Greer JJ, Duranski M, Ringwood LA, Burwell L, et al. Nitrite augments tolerance to ischemia/reperfusion injury via the modulation of mitochondrial electron transfer. J Exp Med 2007; 204**:** 2089-2102.

168. Ischiropoulos H, Gow A. Pathophysiological functions of nitric oxide-mediated protein modifications. Toxicology 2005; 208**:** 299-303.

169. Gow AJ, Farkouh CR, Munson DA, Posencheg MA, Ischiropoulos H. Biological significance of nitric oxide-mediated protein modifications. Am J Physiol Lung Cell Mol Physiol 2004; 287**:** L262-L268.

170. Carafoli E, Santella L, Branca D, Brini M. Generation, control, and processing of cellular calcium signals. Crit Rev Biochem Mol Biol 2001; 36**:** 107-260.

171. Bianchi K, Rimessi A, Prandini A, Szabadkai G, Rizzuto R. Calcium and mitochondria: mechanisms and functions of a troubled relationship. Biochim Biophys Acta 2004; 1742**:** 119-131.

172. Barritt GJ, Chen J, Rychkov GY. Ca(2+) -permeable channels in the hepatocyte plasma membrane and their roles in hepatocyte physiology. Biochim Biophys Acta 2008; 1783**:** 651-672.

173. Berridge MJ, Bootman MD, Roderick HL. Calcium signalling: dynamics, homeostasis and remodelling. Nat Rev Mol Cell Biol 2003; 4**:** 517-529.

174. Delgado-Coello B, Trejo R, Mas-Oliva J. Is there a specific role for the plasma membrane Ca2+ -ATPase in the hepatocyte? Mol Cell Biochem 2006; 285**:** 1-15.

175. Studer RK, Borle AB. Na(+)-Ca2+ antiporter activity of rat hepatocytes. Effect of adrenalectomy on Ca2+ uptake and release from plasma membrane vesicles. Biochim Biophys Acta 1992; 1134**:** 7-16.

176. Zhang YH, Hancox JC. Regulation of cardiac Na+-Ca2+ exchanger activity by protein kinase phosphorylation--still a paradox? Cell Calcium 2009; 45**:** 1-10.

177. Pierobon N, Renard-Rooney DC, Gaspers LD, Thomas AP. Ryanodine receptors in liver. J Biol Chem 2006; 281**:** 34086-34095.

178. Castaldo P, Cataldi M, Magi S, Lariccia V, Arcangeli S, Amoroso S. Role of the mitochondrial sodium/calcium exchanger in neuronal physiology and in the pathogenesis of neurological diseases. Prog Neurobiol 2009; 87**:** 58-79.

179. Pfeiffer DR, Gunter TE, Eliseev R, Broekemeier KM, Gunter KK. Release of Ca2+ from mitochondria via the saturable mechanisms and the permeability transition. IUBMB Life 2001; 52**:** 205-212.

180. Belous AE, Jones CM, Wakata A, Knox CD, Nicoud IB, Pierce J, et al. Mitochondrial calcium transport is regulated by. J Cell Biochem 2006; 99**:** 1165-1174.

181. Belous A, Wakata A, Knox CD, Nicoud IB, Pierce J, Anderson CD, et al. Mitochondrial P2Y-Like receptors link cytosolic adenosine nucleotides to mitochondrial calcium uptake. J Cell Biochem 2004; 92**:** 1062-1073.

182. Kirichok Y, Krapivinsky G, Clapham DE. The mitochondrial calcium uniporter is a highly selective ion channel. Nature 2004; 427**:** 360-364.

183. Belous A, Knox C, Nicoud IB, Pierce J, Anderson C, Pinson CW, et al. Reversed activity of mitochondrial adenine nucleotide translocator in ischemia-reperfusion. Transplantation 2003; 75**:** 1717-1723.

184. Isozaki H, Fujii K, Nomura E, Hara H. Calcium concentration in hepatocytes during liver ischaemia-reperfusion injury and the effects of diltiazem and citrate on perfused rat liver. Eur J Gastroenterol Hepatol 2000; 12**:** 291-297.

185. Janicki PK, Wise PE, Belous AE, Pinson CW. Interspecies differences in hepatic Ca(2+)-ATPase activity and the effect of cold preservation on porcine liver Ca(2+)-ATPase function. Liver Transpl 2001; 7**:** 132-139.

186. Jiang N, Zhang ZM, Liu L, Zhang C, Zhang YL, Zhang ZC. Effects of Ca2+ channel blockers on store-operated Ca2+ channel currents of Kupffer cells after hepatic ischemia/reperfusion injury in rats. World J Gastroenterol 2006; 12**:** 4694-4698.

187. Lopez-Neblina F, Toledo-Pereyra LH, Toledo AH, Walsh J. Ryanodine receptor antagonism protects the ischemic liver and modulates TNF-alpha and IL-10. J Surg Res 2007; 140**:** 121-128.

188. Miller BA. The role of TRP channels in oxidative stress-induced cell death. J Membr Biol 2006; 209**:** 31-41.

189. Nieuwenhuijs VB, De Bruijn MT, Padbury RT, Barritt GJ. Hepatic ischemia-reperfusion injury: roles of Ca2+ and other intracellular mediators of impaired bile flow and hepatocyte damage. Dig Dis Sci 2006; 51**:** 1087-1102.

190. Anderson CD, Pierce J, Nicoud I, Belous A, Knox CD, Chari RS. Modulation of mitochondrial calcium management attenuates hepatic warm ischemia-reperfusion injury. Liver Transpl 2005; 11**:** 663-668.

191. Belous A, Knox C, Nicoud IB, Pierce J, Anderson C, Pinson CW, et al. Altered ATP-dependent mitochondrial Ca2+ uptake in cold ischemia is attenuated by ruthenium red. J Surg Res 2003; 111**:** 284-289.

192. Knox CD, Pierce JM, Nicoud IB, Belous AE, Jones CM, Anderson CD, et al. Inhibition of phospholipase C attenuates liver mitochondrial calcium overload following cold ischemia. Transplantation 2006; 81**:** 567-572.

193. Knox CD, Belous AE, Pierce JM, Wakata A, Nicoud IB, Anderson CD, et al. Novel role of phospholipase C-delta1: regulation of liver mitochondrial Ca2+ uptake. Am J Physiol Gastrointest Liver Physiol 2004; 287**:** G533-G540.

194. Anderson CD, Belous A, Pierce J, Nicoud IB, Knox C, Wakata A, et al. Mitochondrial calcium uptake regulates cold preservation-induced Bax translocation and early reperfusion apoptosis. Am J Transplant 2004; 4**:** 352-362.

195. Wang D, Dou K, Song Z, Liu Z. The Na+/H+ exchange inhibitor: a new therapeutic approach for hepatic ischemia injury in rats. Transplant Proc 2003; 35**:** 3134-3135.

196. Jaeschke H, Lemasters JJ. Apoptosis versus oncotic necrosis in hepatic ischemia/reperfusion injury. Gastroenterology 2003; 125**:** 1246-1257.

197. Carini R, Bellomo G, Benedetti A, Fulceri R, Gamberucci A, Parola M, et al. Alteration of Na+ homeostasis as a critical step in the development of irreversible hepatocyte injury after adenosine triphosphate depletion. Hepatology 1995; 21**:** 1089-1098.

198. Vairetti M, Richelmi P, Berte F, Currin RT, Lemasters JJ, Imberti R. Role of pH in protection by low sodium against hypoxic injury in isolated perfused rat livers. J Hepatol 2006; 44**:** 894-901.

199. Qian T, Nieminen AL, Herman B, Lemasters JJ. Mitochondrial permeability transition in pH-dependent reperfusion injury to rat hepatocytes. Am J Physiol 1997; 273**:** C1783-C1792.

200. Carini R, De Cesaris MG, Splendore R, Bagnati M, Bellomo G, Albano E. Alterations of Na(+) homeostasis in hepatocyte reoxygenation injury. Biochim Biophys Acta 2000; 1500**:** 297-305.

201. Carini R, De Cesaris MG, Splendore R, Bagnati M, Albano E. Ischemic preconditioning reduces Na(+) accumulation and cell killing in isolated rat hepatocytes exposed to hypoxia. Hepatology 2000; 31**:** 166-172.

202. Nishimura Y, Romer LH, Lemasters JJ. Mitochondrial dysfunction and cytoskeletal disruption during chemical hypoxia to cultured rat hepatic sinusoidal endothelial cells: the pH paradox and cytoprotection by glucose, acidotic pH, and glycine. Hepatology 1998; 27**:** 1039-1049.

203. Kokoszka JE, Waymire KG, Levy SE, Sligh JE, Cai J, Jones DP, et al. The ADP/ATP translocator is not essential for the mitochondrial permeability transition pore. Nature 2004; 427**:** 461-465.

204. Lemasters JJ. Modulation of mitochondrial membrane permeability in pathogenesis, autophagy and control of metabolism. J Gastroenterol Hepatol 2007; 22 Suppl 1**:** S31-S37.

205. Zorov DB, Juhaszova M, Yaniv Y, Nuss HB, Wang S, Sollott SJ. Regulation and pharmacology of the mitochondrial permeability transition pore. Cardiovasc Res 2009; 83**:** 213-225.

206. Lemasters JJ, Theruvath TP, Zhong Z, Nieminen AL. Mitochondrial calcium and the permeability transition in cell death. Biochim Biophys Acta 2009; 1787**:** 1395-1401.

207. He L, Lemasters JJ. Regulated and unregulated mitochondrial permeability transition pores: a new paradigm of pore structure and function? FEBS Lett 2002; 512**:** 1-7.

208. Baines CP, Kaiser RA, Purcell NH, Blair NS, Osinska H, Hambleton MA, et al. Loss of cyclophilin D reveals a critical role for mitochondrial permeability transition in cell death. Nature 2005; 434**:** 658-662.

209. Di LF, Bernardi P. A CaPful of mechanisms regulating the mitochondrial permeability transition. J Mol Cell Cardiol 2009; 46**:** 775-780.

210. Elmore SP, Qian T, Grissom SF, Lemasters JJ. The mitochondrial permeability transition initiates autophagy in rat hepatocytes. FASEB J 2001; 15**:** 2286-2287.

211. Lemasters JJ. Selective mitochondrial autophagy, or mitophagy, as a targeted defense against oxidative stress, mitochondrial dysfunction, and aging. Rejuvenation Res 2005; 8**:** 3-5.

212. Kim I, Rodriguez-Enriquez S, Lemasters JJ. Selective degradation of mitochondria by mitophagy. Arch Biochem Biophys 2007; 462**:** 245-253.

213. Qian T, Herman B, Lemasters JJ. The mitochondrial permeability transition mediates both necrotic and apoptotic death of hepatocytes exposed to Br-A23187. Toxicol Appl Pharmacol 1999; 154**:** 117-125.

214. Kim JS, He L, Lemasters JJ. Mitochondrial permeability transition: a common pathway to necrosis and apoptosis. Biochem Biophys Res Commun 2003; 304**:** 463-470.

215. Kim JS, Qian T, Lemasters JJ. Mitochondrial permeability transition in the switch from necrotic to apoptotic cell death in ischemic rat hepatocytes. Gastroenterology 2003; 124**:** 494-503.

216. Kim JS, Nitta T, Mohuczy D, O'Malley KA, Moldawer LL, Dunn WA, Jr., et al. Impaired autophagy: A mechanism of mitochondrial dysfunction in anoxic rat hepatocytes. Hepatology 2008; 47**:** 1725-1736.

217. Azoulay D, Eshkenazy R, Andreani P, Castaing D, Adam R, Ichai P, et al. In situ hypothermic perfusion of the liver versus standard total vascular exclusion for complex liver resection. Ann Surg 2005; 241**:** 277-285.

218. Dinant S, van Veen SQ, Roseboom HJ, van Vliet AK, van Gulik TM. Liver protection by hypothermic perfusion at different temperatures during total vascular exclusion. Liver Int 2006; 26**:** 486-493.

219. Dinant S, Roseboom HJ, Levi M, van Vliet AK, van Gulik TM. Hypothermic in situ perfusion of the porcine liver using Celsior or Ringer-lactate solution. Langenbecks Arch Surg 2009; 394**:** 143-150.

220. Dubay D, Gallinger S, Hawryluck L, Swallow C, McCluskey S, McGilvray I. In situ hypothermic liver preservation during radical liver resection with major vascular reconstruction. Br J Surg 2009; 96**:** 1429-1436.

221. Iniguez M, Dotor J, Feijoo E, Goni S, Prieto J, Berasain C, et al. Novel pharmacologic strategies to protect the liver from ischemia-reperfusion injury. Recent Pat Cardiovasc Drug Discov 2008; 3**:** 9-18.

222. Abu-Amara M, Gurusamy KS, Hori S, Glantzounis G, Fuller B, Davidson BR. Pharmacological interventions versus no pharmacological intervention for ischaemia reperfusion injury in liver resection surgery performed under vascular control. Cochrane Database Syst Rev 2009; CD007472.

223. Abu-Amara M, Gurusamy KS, Glantzounis G, Fuller B, Davidson BR. Pharmacological interventions for ischaemia reperfusion injury in liver resection surgery performed under vascular control. Cochrane Database Syst Rev 2009; CD008154.

224. Hausenloy DJ, Yellon DM. Preconditioning and postconditioning: underlying mechanisms and clinical application. Atherosclerosis 2009; 204**:** 334-341.

225. Pasupathy S, Homer-Vanniasinkam S. Ischaemic preconditioning protects against ischaemia/reperfusion injury: emerging concepts. Eur J Vasc Endovasc Surg 2005; 29**:** 106-115.

226. Wang F, Birch SE, He R, Tawadros P, Szaszi K, Kapus A, et al. Remote ischemic preconditioning by hindlimb occlusion prevents liver ischemic/reperfusion injury: the role of High Mobility Group-Box 1. Ann Surg 2010; 251**:** 292-299.

227. Kanoria S, Jalan R, Davies NA, Seifalian AM, Williams R, Davidson BR. Remote ischaemic preconditioning of the hind limb reduces experimental liver warm ischaemia-reperfusion injury. Br J Surg 2006; 93**:** 762-768.

228. Lai IR, Chang KJ, Chen CF, Tsai HW. Transient limb ischemia induces remote preconditioning in liver among rats: the protective role of heme oxygenase-1. Transplantation 2006; 81**:** 1311-1317.

229. Tapuria N, Junnarkar SP, Dutt N, Abu-Amara M, Fuller B, Seifalian AM, et al. Effect of remote ischemic preconditioning on hepatic microcirculation and function in a rat model of hepatic ischemia reperfusion injury. HPB (Oxford) 2009; 11**:** 108-117.

230. Gurcun U, Discigil B, Boga M, Ozkisacik E, Badak MI, Yenisey C, et al. Is remote preconditioning as effective as direct ischemic preconditioning in preventing spinal cord ischemic injury? J Surg Res 2006; 135**:** 385-393.

231. Chen XG, Wu BY, Wang JK, Bai T. [Mechanism of the protective effects of noninvasive limbs preconditioning on myocardial ischemia-reperfusion injury.]. Chin Med J (Engl) 2005; 118**:** 1723-1727.

232. Claytor RB, Aranson NJ, Ignotz RA, Lalikos JF, Dunn RM. Remote ischemic preconditioning modulates p38 MAP kinase in rat adipocutaneous flaps. J Reconstr Microsurg 2007; 23**:** 93-98.

233. Shahid M, Tauseef M, Sharma KK, Fahim M. Brief femoral artery ischaemia provides protection against myocardial ischaemia-reperfusion injury in rats: the possible mechanisms. Exp Physiol 2008; 93**:** 954-968.

234. Li G, Labruto F, Sirsjo A, Chen F, Vaage J, Valen G. Myocardial protection by remote preconditioning: the role of nuclear factor kappa-B p105 and inducible nitric oxide synthase. Eur J Cardiothorac Surg 2004; 26**:** 968-973.

235. Kuntscher MV, Schirmbeck EU, Menke H, Klar E, Gebhard MM, Germann G. Ischemic preconditioning by brief extremity ischemia before flap ischemia in a rat model. Plast Reconstr Surg 2002; 109**:** 2398-2404.

236. Kuntscher MV, Juran S, Altmann J, Menke H, Gebhard MM, Germann G. Role of nitric oxide in the mechanism of preclamping and remote ischemic preconditioning of adipocutaneous flaps in a rat model. J Reconstr Microsurg 2003; 19**:** 55-60.

237. Kuntscher MV, Kastell T, Sauerbier M, Nobiling R, Gebhard MM, Germann G. Acute remote ischemic preconditioning on a rat cremasteric muscle flap model. Microsurgery 2002; 22**:** 221-226.

238. Kuntscher MV, Kastell T, Altmann J, Menke H, Gebhard MM, Germann G. Acute remote ischemic preconditioning II: the role of nitric oxide. Microsurgery 2002; 22**:** 227-231.

239. Dudzinski DM, Igarashi J, Greif D, Michel T. The regulation and pharmacology of endothelial nitric oxide synthase. Annu Rev Pharmacol Toxicol 2006; 46**:** 235-276.

240. Koti RS, Tsui J, Lobos E, Yang W, Seifalian AM, Davidson BR. Nitric oxide synthase distribution and expression with ischemic preconditioning of the rat liver. FASEB J 2005; 19**:** 1155-1157.

241. McNaughton L, Puttagunta L, Martinez-Cuesta MA, Kneteman N, Mayers I, Moqbel R, et al. Distribution of nitric oxide synthase in normal and cirrhotic human liver. Proc Natl Acad Sci U S A 2002; 99**:** 17161-17166.

242. Osei SY, Ahima RS, Fabry ME, Nagel RL, Bank N. Immunohistochemical localization of hepatic nitric oxide synthase in normal and transgenic sickle cell mice: the effect of hypoxia. Blood 1996; 88**:** 3583-3588.

243. Zimmermann H, Kurzen P, Klossner W, Renner EL, Marti U. Decreased constitutive hepatic nitric oxide synthase expression in secondary biliary fibrosis and its changes after Roux-en-Y choledocho-jejunostomy in the rat. J Hepatol 1996; 25**:** 567-573.

244. Xia C, Misra I, Iyanagi T, Kim JJ. Regulation of interdomain interactions by calmodulin in inducible nitric-oxide synthase. J Biol Chem 2009; 284**:** 30708-30717.

245. Amersi F, Shen XD, Moore C, Melinek J, Busuttil RW, Kupiec-Weglinski JW, et al. Fibronectin-alpha 4 beta 1 integrin-mediated blockade protects genetically fat Zucker rat livers from ischemia/reperfusion injury. Am J Pathol 2003; 162**:** 1229-1239.

246. Cescon M, Grazi GL, Grassi A, Ravaioli M, Vetrone G, Ercolani G, et al. Effect of ischemic preconditioning in whole liver transplantation from deceased donors. A pilot study. Liver Transpl 2006; 12**:** 628-635.

247. Kimura H, Katsuramaki T, Isobe M, Nagayama M, Meguro M, Kukita K, et al. Role of inducible nitric oxide synthase in pig liver transplantation. J Surg Res 2003; 111**:** 28-37.

248. Koeppel TA, Mihaljevic N, Kraenzlin B, Loehr M, Jesenofsky R, Post S, et al. Enhanced iNOS gene expression in the steatotic rat liver after normothermic ischemia. Eur Surg Res 2007; 39**:** 303-311.

249. Meguro M, Katsuramaki T, Nagayama M, Kimura H, Isobe M, Kimura Y, et al. A novel inhibitor of inducible nitric oxide synthase (ONO-1714) prevents critical warm ischemia-reperfusion injury in the pig liver. Transplantation 2002; 73**:** 1439-1446.

250. Marletta MA, Hurshman AR, Rusche KM. Catalysis by nitric oxide synthase. Curr Opin Chem Biol 1998; 2**:** 656-663.

251. Stuehr DJ. Enzymes of the L-arginine to nitric oxide pathway. J Nutr 2004; 134**:** 2748S-2751S.

252. Hines IN, Harada H, Flores S, Gao B, McCord JM, Grisham MB. Endothelial nitric oxide synthase protects the post-ischemic liver: potential interactions with superoxide. Biomed Pharmacother 2005; 59**:** 183-189.

253. Kawachi S, Hines IN, Laroux FS, Hoffman J, Bharwani S, Gray L, et al. Nitric oxide synthase and postischemic liver injury. Biochem Biophys Res Commun 2000; 276**:** 851-854.

254. Lee VG, Johnson ML, Baust J, Laubach VE, Watkins SC, Billiar TR. The roles of iNOS in liver ischemia-reperfusion injury. Shock 2001; 16**:** 355-360.

255. Theruvath TP, Zhong Z, Currin RT, Ramshesh VK, Lemasters JJ. Endothelial nitric oxide synthase protects transplanted mouse livers against storage/reperfusion injury: Role of vasodilatory and innate immunity pathways. Transplant Proc 2006; 38**:** 3351-3357.

256. Duranski MR, Elrod JW, Calvert JW, Bryan NS, Feelisch M, Lefer DJ. Genetic overexpression of eNOS attenuates hepatic ischemia-reperfusion injury. Am J Physiol Heart Circ Physiol 2006; 291**:** H2980-H2986.

257. Serracino-Inglott F, Virlos IT, Habib NA, Williamson RC, Mathie RT. Differential nitric oxide synthase expression during hepatic ischemia-reperfusion. Am J Surg 2003; 185**:** 589-595.

258. Hines IN, Harada H, Bharwani S, Pavlick KP, Hoffman JM, Grisham MB. Enhanced post-ischemic liver injury in iNOS-deficient mice: a cautionary note. Biochem Biophys Res Commun 2001; 284**:** 972-976.

259. Jiang WW, Kong LB, Li GQ, Wang XH. Expression of iNOS in early injury in a rat model of small-for-size liver transplantation. Hepatobiliary Pancreat Dis Int 2009; 8**:** 146-151.

260. Tsuchihashi S, Kaldas F, Chida N, Sudo Y, Tamura K, Zhai Y, et al. FK330, a novel inducible nitric oxide synthase inhibitor, prevents ischemia and reperfusion injury in rat liver transplantation. Am J Transplant 2006; 6**:** 2013-2022.

261. Takamatsu Y, Shimada K, Yamaguchi K, Kuroki S, Chijiiwa K, Tanaka M. Inhibition of inducible nitric oxide synthase prevents hepatic, but not pulmonary, injury following ischemia-reperfusion of rat liver. Dig Dis Sci 2006; 51**:** 571-579.

262. Hon WM, Lee KH, Khoo HE. Nitric oxide in liver diseases: friend, foe, or just passerby? Ann N Y Acad Sci 2002; 962**:** 275-295.

263. Kaizu T, Ikeda A, Nakao A, Takahashi Y, Tsung A, Kohmoto J, et al. Donor graft adenoviral iNOS gene transfer ameliorates rat liver transplant preservation injury and improves survival. Hepatology 2006; 43**:** 464-473.

264. Jeyabalan G, Klune JR, Nakao A, Martik N, Wu G, Tsung A, et al. Arginase blockade protects against hepatic damage in warm ischemia-reperfusion. Nitric Oxide 2008; 19**:** 29-35.

265. Reid KM, Tsung A, Kaizu T, Jeyabalan G, Ikeda A, Shao L, et al. Liver I/R injury is improved by the arginase inhibitor, N(omega)-hydroxy-nor-L-arginine (nor-NOHA). Am J Physiol Gastrointest Liver Physiol 2007; 292**:** G512-G517.

266. Higa T, Shiraishi M, Mamadi T, Taira K, Oshiro T, Nozato E, et al. Limitations of exogenous L-arginine in exerting a cytoprotective effect on hepatic ischemia/reperfusion injury. Surg Today 2000; 30**:** 352-359.

267. Higa T, Shiraishi M, Hiroyasu S, Tomori H, Okuhama Y, Kusano T, et al. Effect of exogenous L-arginine for hepatic ischemia-reperfusion injury in an isolated rat liver in vitro. Transplant Proc 1998; 30**:** 3728-3729.

268. Langle F, Steininger R, Waldmann E, Grunberger T, Benditte H, Mittlbock M, et al. Improvement of cardiac output and liver blood flow and reduction of pulmonary vascular resistance by intravenous infusion of L-arginine during the early reperfusion period in pig liver transplantation. Transplantation 1997; 63**:** 1225-1233.

269. Geller DA, Chia SH, Takahashi Y, Yagnik GP, Tsoulfas G, Murase N. Protective role of the L-arginine-nitric oxide synthase pathway on

preservation injury after rat liver transplantation. JPEN J Parenter Enteral Nutr 2001; 25**:** 142-147.

270. Yagnik GP, Takahashi Y, Tsoulfas G, Reid K, Murase N, Geller DA. Blockade of the L-arginine/NO synthase pathway worsens hepatic apoptosis and liver transplant preservation injury. Hepatology 2002; 36**:** 573-581.

271. Pastor CM, Morris SM, Jr., Billiar TR. Sources of arginine for induced nitric oxide synthesis in the isolated perfused liver. Am J Physiol 1995; 269**:** G861-G866.

272. Langle F, Roth E, Steininger R, Winkler S, Muhlbacher F. Arginase release following liver reperfusion. Evidence of hemodynamic action of arginase infusions. Transplantation 1995; 59**:** 1542-1549.

273. Wu G, Morris SM, Jr. Arginine metabolism: nitric oxide and beyond. Biochem J 1998; 336 (Pt 1)**:** 1-17.

274. Shiraishi M, Hiroyasu S, Nagahama M, Miyaguni T, Higa T, Tomori H, et al. Role of exogenous L-arginine in hepatic ischemia-reperfusion injury. J Surg Res 1997; 69**:** 429-434.

275. Cottart CH, Do L, Blanc MC, Vaubourdolle M, Descamps G, Durand D, et al. Hepatoprotective effect of endogenous nitric oxide during ischemia-reperfusion in the rat. Hepatology 1999; 29**:** 809-813.

276. Burra P, Chirizzi L, Cardin R, Cadrobbi R, Baldan N, Calabrese F, et al. Warm hepatic ischemia in pigs: effects of L-arginine and oligotide treatment. J Invest Surg 2001; 14**:** 303-312.

277. Rhee JE, Jung SE, Shin SD, Suh GJ, Noh DY, Youn YK, et al. The effects of antioxidants and nitric oxide modulators on hepatic ischemic-reperfusion injury in rats. J Korean Med Sci 2002; 17**:** 502-506.

278. Koti RS, Seifalian AM, McBride AG, Yang W, Davidson BR. The relationship of hepatic tissue oxygenation with nitric oxide metabolism in ischemic preconditioning of the liver. FASEB J 2002; 16**:** 1654-1656.

279. Koti RS, Yang W, Dashwood MR, Davidson BR, Seifalian AM. Effect of ischemic preconditioning on hepatic microcirculation and function in a rat model of ischemia reperfusion injury. Liver Transpl 2002; 8**:** 1182-1191.

280. Chattopadhyay P, Shukla G, Verma A, Wahi AK. Attenuation of mitochondrial injury by L-arginine preconditioning of the liver. Biofactors 2007; 31**:** 99-106.

281. Chattopadhyay P, Verma N, Verma A, Kamboj T, Khan NA, Wahi AK. L-arginine protects from pringle manoeuvere of ischemia-reperfusion induced liver injury. Biol Pharm Bull 2008; 31**:** 890-892.

282. Li SQ, Liang LJ. Protective mechanism of L-arginine against liver ischemic-reperfusion injury in rats. Hepatobiliary Pancreat Dis Int 2003; 2**:** 549-552.

283. Uhlmann D, Scommotau S, Witzigmann H, Spiegel HU. Exogenous L-arginine protects liver microcirculation from ischemia reperfusion injury. Eur Surg Res 1998; 30**:** 175-184.

284. Scommotau S, Uhlmann D, Loffler BM, Breu V, Spiegel HU. Involvement of endothelin/nitric oxide balance in hepatic ischemia/reperfusion injury. Langenbecks Arch Surg 1999; 384**:** 65-70.

285. Valero R, Garcia-Valdecasas JC, Net M, Beltran J, Ordi J, Gonzalez FX, et al. L-arginine reduces liver and biliary tract damage after liver transplantation from non-heart-beating donor pigs. Transplantation 2000; 70**:** 730-737.

286. Uhlmann D, Uhlmann S, Spiegel HU. Endothelin/nitric oxide balance influences hepatic ischemia-reperfusion injury. J Cardiovasc Pharmacol 2000; 36**:** S212-S214.

287. Calabrese F, Valente M, Pettenazzo E, Ferraresso M, Burra P, Cadrobbi R, et al. The protective effects of L-arginine after liver ischaemia/reperfusion injury in a pig model. J Pathol 1997; 183**:** 477-485.

288. Nilsson B, Delbro D, Wallin M, Friman S. Protective effect of nitric oxide and prostaglandin E(2) in ischemia/reperfusion injury of the liver. Transplant Proc 2001; 33**:** 2518-2520.

289. Wang WT, Lin LN, Pan XR, Xu ZJ. [Effects of L-arginine on the function of platelet aggregation during hepatic ischemia/reperfusion injury]. Zhongguo Wei Zhong Bing Ji Jiu Yi Xue 2004; 16**:** 49-51.

290. Burra P, Ferraresso M, Cadrobbi R, Calabrese F, Cardin R, Parnigotto A, et al. Effect of L-arginine and oligotide on liver ischemia-reperfusion injury. Transplant Proc 1997; 29**:** 2992-2993.

291. Cheng XD, Jiang XC, Liu YB, Peng CH, Xu B, Peng SY. Effect of ischemic preconditioning on P-selectin expression in hepatocytes of rats with cirrhotic ischemia-reperfusion injury. World J Gastroenterol 2003; 9**:** 2289-2292.

292. Shimamura T, Zhu Y, Zhang S, Jin MB, Ishizaki N, Urakami A, et al. Protective role of nitric oxide in ischemia and reperfusion injury of the liver. J Am Coll Surg 1999; 188**:** 43-52.

293. Acquaviva R, Lanteri R, Li DG, Caltabiano R, Vanella L, Lanzafame S, et al. Beneficial effects of rutin and L-arginine coadministration in a rat model of liver ischemia-reperfusion injury. Am J Physiol Gastrointest Liver Physiol 2009; 296**:** G664-G670.

294. Giovanardi RO, Rhoden EL, Cerski CT, Salvador M, Kalil AN. Pharmacological preconditioning using intraportal infusion of L-arginine protects against hepatic ischemia reperfusion injury. J Surg Res 2009; 155**:** 244-253.

295. Rivera-Chavez FA, Toledo-Pereyra LH, Dean RE, Crouch L, Ward PA. Exogenous and endogenous nitric oxide but not iNOS inhibition improves function and survival of ischemically injured livers. J Invest Surg 2001; 14**:** 267-273.

296. Carini R, Grazia De CM, Splendore R, Domenicotti C, Nitti MP, Pronzato MA, et al. Signal pathway responsible for hepatocyte preconditioning by nitric oxide. Free Radic Biol Med 2003; 34**:** 1047-1055.

297. Carini R, Grazia De CM, Splendore R, Albano E. Stimulation of p38 MAP kinase reduces acidosis and Na(+) overload in preconditioned hepatocytes. FEBS Lett 2001; 491**:** 180-183.

298. Toei M, Saum R, Forgac M. Regulation and isoform function of the V-ATPases. Biochemistry 2010; 49**:** 4715-4723.

299. Abu-Amara M, Yang SY, Tapuria N, Fuller B, Davidson B, Seifalian A. Liver ischemia/reperfusion injury: processes in inflammatory networks--a review. Liver Transpl 2010; 16**:** 1016-1032.

300. Carini R, Trincheri NF, Alchera E, De Cesaris MG, Castino R, Splendore R, et al. PI3K-dependent lysosome exocytosis in nitric oxide-preconditioned hepatocytes. Free Radic Biol Med 2006; 40**:** 1738-1748.

301. Kim JS, Ohshima S, Pediaditakis P, Lemasters JJ. Nitric oxide: a signaling molecule against mitochondrial permeability transition- and pH-dependent cell death after reperfusion. Free Radic Biol Med 2004; 37**:** 1943-1950.

302. Duranski MR, Greer JJ, Dejam A, Jaganmohan S, Hogg N, Langston W, et al. Cytoprotective effects of nitrite during in vivo ischemia-reperfusion of the heart and liver. J Clin Invest 2005; 115**:** 1232-1240.

303. Akaike T, Yoshida M, Miyamoto Y, Sato K, Kohno M, Sasamoto K, et al. Antagonistic action of imidazolineoxyl N-oxides against endothelium-derived relaxing factor/.NO through a radical reaction. Biochemistry 1993; 32**:** 827-832.

304. Garthwaite J, Southam E, Boulton CL, Nielsen EB, Schmidt K, Mayer B. Potent and selective inhibition of nitric oxide-sensitive guanylyl cyclase by 1H-[1,2,4]oxadiazolo[4,3-a]quinoxalin-1-one. Mol Pharmacol 1995; 48**:** 184-188.

305. Schrammel A, Behrends S, Schmidt K, Koesling D, Mayer B. Characterization of 1H-[1,2,4]oxadiazolo[4,3-a]quinoxalin-1-one as a heme-site inhibitor of nitric oxide-sensitive guanylyl cyclase. Mol Pharmacol 1996; 50**:** 1-5.

306. Zweier JL, Samouilov A, Kuppusamy P. Non-enzymatic nitric oxide synthesis in biological systems. Biochim Biophys Acta 1999; 1411**:** 250-262.

307. Huang PL, Huang Z, Mashimo H, Bloch KD, Moskowitz MA, Bevan JA, et al. Hypertension in mice lacking the gene for endothelial nitric oxide synthase. Nature 1995; 377**:** 239-242.

308. Spiegel HU, Bahde R. Experimental models of temporary normothermic liver ischemia. J Invest Surg 2006; 19**:** 113-123.

309. Xing HC, Li LJ, Xu KJ, Shen T, Chen YB, Sheng JF, et al. Intestinal microflora in rats with ischemia/reperfusion liver injury. J Zhejiang Univ Sci B 2005; 6**:** 14-21.

310. Lemaire LC, van Wagensveld BA, van Gulik TM, Dankert J, van Lanschot JJ, Gouma DJ. Bacterial translocation to the thoracic duct in a setting of ischemia, partial resection and reperfusion of the porcine liver. Dig Surg 1999; 16**:** 222-228.

311. Konstantinov IE, Arab S, Li J, Coles JG, Boscarino C, Mori A, et al. The remote ischemic preconditioning stimulus modifies gene expression in mouse myocardium. J Thorac Cardiovasc Surg 2005; 130**:** 1326-1332.

312. Giovanardi RO, Rhoden EL, Cerski CT, Salvador M, Kalil AN. Ischemic preconditioning protects the pig liver by preserving the mitochondrial structure and downregulating caspase-3 activity. J Invest Surg 2009; 22**:** 88-97.

313. Neil DA, Hubscher SG. Are parenchymal changes in early post-transplant biopsies related to preservation-reperfusion injury or rejection? Transplantation 2001; 71**:** 1566-1572.

314. Falasca L, Tisone G, Palmieri G, Anselmo A, Di PD, Baiocchi L, et al. Protective role of tauroursodeoxycholate during harvesting and cold storage of human liver: a pilot study in transplant recipients. Transplantation 2001; 71**:** 1268-1276.

315. Monbaliu D, Libbrecht L, De VR, Vekemans K, Walter H, Liu Q, et al. The extent of vacuolation in non-heart-beating porcine donor liver grafts prior to transplantation predicts their viability. Liver Transpl 2008; 14**:** 1256-1265.

316. Lu Z, Dono K, Gotoh K, Shibata M, Koike M, Marubashi S, et al. Participation of autophagy in the degeneration process of rat hepatocytes after transplantation following prolonged cold preservation. Arch Histol Cytol 2005; 68**:** 71-80.

317. Hoff DA, Gregersen H, Hatlebakk JG. Mucosal blood flow measurements using laser Doppler perfusion monitoring. World J Gastroenterol 2009; 15**:** 198-203.

318. Rajan V, Varghese B, van Leeuwen TG, Steenbergen W. Review of methodological developments in laser Doppler flowmetry. Lasers Med Sci 2009; 24**:** 269-283.

319. Vongsavan N, Matthews B. Some aspects of the use of laser Doppler flow meters for recording tissue blood flow. Exp Physiol 1993; 78**:** 1-14.

320. Almond NE, Wheatley AM. Measurement of hepatic perfusion in rats by laser Doppler flowmetry. Am J Physiol 1992; 262**:** G203-G209.

321. Wheatley AM, Almond NE, Stuart ET, Zhao D. Interpretation of the laser Doppler flow signal from the liver of the rat. Microvasc Res 1993; 45**:** 290-301.

322. Wheatley AM. Does laser-Doppler flowmetry provide a quantitative measure of hepatic perfusion? Am J Physiol 1994; 266**:** G960-G962.

323. Ebrahimian TG, Tamarat R, Clergue M, Duriez M, Levy BI, Silvestre JS. Dual effect of angiotensin-converting enzyme inhibition on angiogenesis in type 1 diabetic mice. Arterioscler Thromb Vasc Biol 2005; 25**:** 65-70.

324. Ohta S, Nakamuta M, Fukushima M, Kohjima M, Kotoh K, Enjoji M, et al. Beraprost sodium, a prostacyclin (PGI) analogue, ameliorates concanavalin A-induced liver injury in mice. Liver Int 2005; 25**:** 1061-1068.

325. Heil M, Ziegelhoeffer T, Pipp F, Kostin S, Martin S, Clauss M, et al. Blood monocyte concentration is critical for enhancement of collateral artery growth. Am J Physiol Heart Circ Physiol 2002; 283**:** H2411-H2419.

326. Przyklenk K, Bauer B, Ovize M, Kloner RA, Whittaker P. Regional ischemic 'preconditioning' protects remote virgin myocardium from subsequent sustained coronary occlusion. Circulation 1993; 87**:** 893-899.

327. Tapuria N, Kumar Y, Habib MM, Abu-Amara M, Seifalian AM, Davidson BR. Remote ischemic preconditioning: a novel protective method from ischemia reperfusion injury--a review. J Surg Res 2008; 150**:** 304-330.

328. Carini R, Albano E. Recent insights on the mechanisms of liver preconditioning. Gastroenterology 2003; 125**:** 1480-1491.

329. Venugopal V, Hausenloy DJ, Ludman A, Di SC, Kolvekar S, Yap J, et al. Remote ischaemic preconditioning reduces myocardial injury in patients undergoing cardiac surgery with cold-blood cardioplegia: a randomised controlled trial. Heart 2009; 95**:** 1567-1571.

330. Loukogeorgakis SP, Panagiotidou AT, Broadhead MW, Donald A, Deanfield JE, MacAllister RJ. Remote ischemic preconditioning provides early and late protection against endothelial ischemia-reperfusion injury in humans: role of the autonomic nervous system. J Am Coll Cardiol 2005; 46**:** 450-456.

331. Eckhoff DE, Bilbao G, Frenette L, Thompson JA, Contreras JL. 17-Beta-estradiol protects the liver against warm ischemia/reperfusion injury and is associated with increased serum nitric oxide and decreased tumor necrosis factor-alpha. Surgery 2002; 132**:** 302-309.

332. Bessems M, 't Hart NA, Tolba R, Doorschodt BM, Leuvenink HG, Ploeg RJ, et al. The isolated perfused rat liver: standardization of a time-honoured model. Lab Anim 2006; 40**:** 236-246.

333. Eberlin KR, McCormack MC, Nguyen JT, Tatlidede HS, Randolph MA, Austen WG, Jr. Ischemic preconditioning of skeletal muscle mitigates remote injury and mortality. J Surg Res 2008; 148**:** 24-30.

334. Abe Y, Hines IN, Zibari G, Pavlick K, Gray L, Kitagawa Y, et al. Mouse model of liver ischemia and reperfusion injury: method for studying reactive oxygen and nitrogen metabolites in vivo. Free Radic Biol Med 2009; 46**:** 1-7.

335. Ott MC, Scott JR, Bihari A, Badhwar A, Otterbein LE, Gray DK, et al. Inhalation of carbon monoxide prevents liver injury and inflammation following hind limb ischemia/reperfusion. FASEB J 2005; 19**:** 106-108.

336. Yassin MM, Harkin DW, Barros D'Sa AA, Halliday MI, Rowlands BJ. Lower limb ischemia-reperfusion injury triggers a systemic inflammatory response and multiple organ dysfunction. World J Surg 2002; 26**:** 115-121.

337. Kanoria S, Jalan R, Seifalian AM, Williams R, Davidson BR. Protocols and mechanisms for remote ischemic preconditioning: a novel method for reducing ischemia reperfusion injury. Transplantation 2007; 84**:** 445-458.

338. Jaeschke H, Farhood A. Neutrophil and Kupffer cell-induced oxidant stress and ischemia-reperfusion injury in rat liver. Am J Physiol 1991; 260**:** G355-G362.

339. Ozaki M, Deshpande SS, Angkeow P, Bellan J, Lowenstein CJ, Dinauer MC, et al. Inhibition of the Rac1 GTPase protects against nonlethal ischemia/reperfusion-induced necrosis and apoptosis in vivo. FASEB J 2000; 14**:** 418-429.

340. Kehinde EO, Anim JT, Mojiminiyi OA, Al-Awadi F, Omu AE, Varghese R. Significance of determining the point of reperfusion failure in experimental torsion of testis. Int J Urol 2005; 12**:** 81-89.

341. Shen SQ, Zhang Y, Xiong CL. The protective effects of 17beta-estradiol on hepatic ischemia-reperfusion injury in rat model, associated with regulation of heat-shock protein expression. J Surg Res 2007; 140**:** 67-76.

342. Serafin A, Rosello-Catafau J, Prats N, Xaus C, Gelpi E, Peralta C. Ischemic preconditioning increases the tolerance of Fatty liver to hepatic ischemia-reperfusion injury in the rat. Am J Pathol 2002; 161**:** 587-601.

343. Cavalieri B, Perrelli MG, Aragno M, Mastrocola R, Corvetti G, Durazzo M, et al. Ischemic preconditioning attenuates the oxidant-dependent mechanisms of reperfusion cell damage and death in rat liver. Liver Transpl 2002; 8**:** 990-999.

344. Hart ML, Much C, Kohler D, Schittenhelm J, Gorzolla IC, Stahl GL, et al. Use of a hanging-weight system for liver ischemic preconditioning in mice. Am J Physiol Gastrointest Liver Physiol 2008; 294**:** G1431-G1440.

345. Tsuyama H, Shimizu K, Yoshimoto K, Nezuka H, Ito H, Yamamoto S, et al. Protective effect of ischemic preconditioning on hepatic ischemia-reperfusion injury in mice. Transplant Proc 2000; 32**:** 2310-2313.

346. Li X, Elwell MR, Ryan AM, Ochoa R. Morphogenesis of postmortem hepatocyte vacuolation and liver weight increases in Sprague-Dawley rats. Toxicol Pathol 2003; 31**:** 682-688.

347. Shimoda M, Iwasaki Y, Sawada T, Kubota K. Protective effect of ischemic preconditioning against liver injury after major hepatectomy using the intermittent pringle maneuver in swine. Pathobiology 2007; 74**:** 42-49.

348. Suzuki Y, Deitch EA, Mishima S, Lu Q, Xu D. Inducible nitric oxide synthase gene knockout mice have increased resistance to gut injury and bacterial translocation after an intestinal ischemia-reperfusion injury. Crit Care Med 2000; 28**:** 3692-3696.

349. Glantzounis GK, Rocks SA, Sheth H, Knight I, Salacinski HJ, Davidson BR, et al. Formation and role of plasma S-nitrosothiols in liver ischemia-reperfusion injury. Free Radic Biol Med 2007; 42**:** 882-892.

350. Chen T, Zamora R, Zuckerbraun B, Billiar TR. Role of nitric oxide in liver injury. Curr Mol Med 2003; 3**:** 519-526.

351. Ferdinandy P, Schulz R. Nitric oxide, superoxide, and peroxynitrite in myocardial ischaemia-reperfusion injury and preconditioning. Br J Pharmacol 2003; 138**:** 532-543.

352. Koti RS, Seifalian AM, Davidson BR. Protection of the liver by ischemic preconditioning: a review of mechanisms and clinical applications. Dig Surg 2003; 20**:** 383-396.

353. Caban A, Oczkowicz G, bdel-Samad O, Cierpka L. Influence of ischemic preconditioning and nitric oxide on microcirculation and the degree of rat liver injury in the model of ischemia and reperfusion. Transplant Proc 2006; 38**:** 196-198.

354. Barrier A, Olaya N, Chiappini F, Roser F, Scatton O, Artus C, et al. Ischemic preconditioning modulates the expression of several genes, leading to the overproduction of IL-1Ra, iNOS, and Bcl-2 in a human model of liver ischemia-reperfusion. FASEB J 2005; 19**:** 1617-1626.

355. Ofluoglu E, Kerem M, Pasaoglu H, Turkozkan N, Seven I, Bedirli A, et al. Delayed energy protection of ischemic preconditioning on hepatic ischemia/reperfusion injury in rats. Eur Surg Res 2006; 38**:** 114-121.

356. Maeda H, Akaike T, Yoshida M, Suga M. Multiple functions of nitric oxide in pathophysiology and microbiology: analysis by a new nitric oxide scavenger. J Leukoc Biol 1994; 56**:** 588-592.

357. Lu P, Liu F, Yao Z, Wang CY, Chen DD, Tian Y, et al. Nitrite-derived nitric oxide by xanthine oxidoreductase protects the liver against ischemia-reperfusion injury. Hepatobiliary Pancreat Dis Int 2005; 4**:** 350-355.

358. Vlasov TD, Korzhevskii DE, Polyakova EA. Ischemic preconditioning of the rat brain as a method of endothelial protection from ischemic/repercussion injury. Neurosci Behav Physiol 2005; 35**:** 567-572.

359. Vlasov TD, Korzhevskii DE, Poliakova EA. [Ischemic adaptation of the rat brain as a method for protection of endothelium from ischemic reperfusion injury]. Ross Fiziol Zh Im I M Sechenova 2004; 90**:** 40-48.

360. Kim JS, Ohshima S, Pediaditakis P, Lemasters JJ. Nitric oxide protects rat hepatocytes against reperfusion injury mediated by the mitochondrial permeability transition. Hepatology 2004; 39**:** 1533-1543.

361. Leite AC, Oliveira HC, Utino FL, Garcia R, Alberici LC, Fernandes MP, et al. Mitochondria generated nitric oxide protects against permeability transition via formation of membrane protein S-nitrosothiols. Biochim Biophys Acta 2010; 1797**:** 1210-1216.

362. Napoli C, Ignarro LJ. Nitric oxide and pathogenic mechanisms involved in the development of vascular diseases. Arch Pharm Res 2009; 32**:** 1103-1108.

363. Kumar D, Branch BG, Pattillo CB, Hood J, Thoma S, Simpson S, et al. Chronic sodium nitrite therapy augments ischemia-induced angiogenesis and arteriogenesis. Proc Natl Acad Sci U S A 2008; 105**:** 7540-7545.

364. Tozer GM, Prise VE, Chaplin DJ. Inhibition of nitric oxide synthase induces a selective reduction in tumor blood flow that is reversible with L-arginine. Cancer Res 1997; 57**:** 948-955.

365. Soler M, Camacho M, Molins-Pujol AM, Vila L. Effect of an imidazolineoxyl nitric oxide on prostaglandin synthesis in experimental shock: possible role of nitrogen dioxide in prostacyclin synthase inactivation. J Infect Dis 2001; 183**:** 105-112.

366. Lu XS, Zhan YQ, Yang XP. [Expression and transcription of inducible nitric oxide synthase in the liver ischemic preconditioning in rats]. Hunan Yi Ke Da Xue Xue Bao 2003; 28**:** 563-566.

367. Wang Y, Xu H, Mizoguchi K, Oe M, Maeta H. Intestinal ischemia induces late preconditioning against myocardial infarction: a role for inducible nitric oxide synthase. Cardiovasc Res 2001; 49**:** 391-398.

368. Tokuno S, Hinokiyama K, Tokuno K, Lowbeer C, Hansson LO, Valen G. Spontaneous ischemic events in the brain and heart adapt the hearts of

severely atherosclerotic mice to ischemia. Arterioscler Thromb Vasc Biol 2002; 22**:** 995-1001.

369. Dudzinski DM, Michel T. Life history of eNOS: partners and pathways. Cardiovasc Res 2007; 75**:** 247-260.

370. Shen GL, Lv H, Bi HY, Zhang W, Yao S, Yuan Y. Reduction expression of thrombomodulin and endothelial cell nitric oxide synthase in dermatomyositis. Neuropathology 2007; 27**:** 309-313.

371. Punkt K, Fritzsche M, Stockmar C, Hepp P, Josten C, Wellner M, et al. Nitric oxide synthase in human skeletal muscles related to defined fibre types. Histochem Cell Biol 2006; 125**:** 567-573.

372. Tinker AC, Wallace AV. Selective inhibitors of inducible nitric oxide synthase: potential agents for the treatment of inflammatory diseases? Curr Top Med Chem 2006; 6**:** 77-92.

373. Abe Y, Hines I, Zibari G, Grisham MB. Hepatocellular protection by nitric oxide or nitrite in ischemia and reperfusion injury. Arch Biochem Biophys 2009; 484**:** 232-237.

374. van Faassen EE, Bahrami S, Feelisch M, Hogg N, Kelm M, Kim-Shapiro DB, et al. Nitrite as regulator of hypoxic signaling in mammalian physiology. Med Res Rev 2009; 29**:** 683-741.

375. Lundberg JO, Weitzberg E, Gladwin MT. The nitrate-nitrite-nitric oxide pathway in physiology and therapeutics. Nat Rev Drug Discov 2008; 7**:** 156-167.

376. Li H, Samouilov A, Liu X, Zweier JL. Characterization of the magnitude and kinetics of xanthine oxidase-catalyzed nitrate reduction: evaluation of its role in nitrite and nitric oxide generation in anoxic tissues. Biochemistry 2003; 42**:** 1150-1159.

377. Jansson EA, Huang L, Malkey R, Govoni M, Nihlen C, Olsson A, et al. A mammalian functional nitrate reductase that regulates nitrite and nitric oxide homeostasis. Nat Chem Biol 2008; 4**:** 411-417.

378. Jung KH, Chu K, Ko SY, Lee ST, Sinn DI, Park DK, et al. Early intravenous infusion of sodium nitrite protects brain against in vivo ischemia-reperfusion injury. Stroke 2006; 37**:** 2744-2750.

379. Tripatara P, Patel NS, Webb A, Rathod K, Lecomte FM, Mazzon E, et al. Nitrite-derived nitric oxide protects the rat kidney against ischemia/reperfusion injury in vivo: role for xanthine oxidoreductase. J Am Soc Nephrol 2007; 18**:** 570-580.

380. Lundberg JO, Gladwin MT, Ahluwalia A, Benjamin N, Bryan NS, Butler A, et al. Nitrate and nitrite in biology, nutrition and therapeutics. Nat Chem Biol 2009; 5**:** 865-869.

381. Nagasaka Y, Fernandez BO, Garcia-Saura MF, Petersen B, Ichinose F, Bloch KD, et al. Brief periods of nitric oxide inhalation protect against myocardial ischemia-reperfusion injury. Anesthesiology 2008; 109**:** 675-682.

382. Mathru M, Huda R, Solanki DR, Hays S, Lang JD. Inhaled nitric oxide attenuates reperfusion inflammatory responses in humans. Anesthesiology 2007; 106**:** 275-282.

383. Lang JD, Jr., Teng X, Chumley P, Crawford JH, Isbell TS, Chacko BK, et al. Inhaled NO accelerates restoration of liver function in adults following orthotopic liver transplantation. J Clin Invest 2007; 117**:** 2583-2591.

384. Elrod JW, Calvert JW, Gundewar S, Bryan NS, Lefer DJ. Nitric oxide promotes distant organ protection: evidence for an endocrine role of nitric oxide. Proc Natl Acad Sci U S A 2008; 105**:** 11430-11435.

385. Montalvo-Jave EE, Pina E, Montalvo-Arenas C, Urrutia R, avente-Chenhalls L, Pena-Sanchez J, et al. Role of ischemic preconditioning in liver surgery and hepatic transplantation. J Gastrointest Surg 2009; 13**:** 2074-2083.

386. Lundberg JO, Weitzberg E. NO-synthase independent NO generation in mammals. Biochem Biophys Res Commun 2010; 396**:** 39-45.

387. Webb AJ, Milsom AB, Rathod KS, Chu WL, Qureshi S, Lovell MJ, et al. Mechanisms underlying erythrocyte and endothelial nitrite reduction to nitric oxide in hypoxia: role for xanthine oxidoreductase and endothelial nitric oxide synthase. Circ Res 2008; 103**:** 957-964.

388. Milsom AB, Patel NS, Mazzon E, Tripatara P, Storey A, Mota-Filipe H, et al. Role for endothelial nitric oxide synthase in nitrite-induced protection against renal ischemia-reperfusion injury in mice. Nitric Oxide 2010; 22**:** 141-148.

389. Hobbs AJ. Soluble guanylate cyclase: the forgotten sibling. Trends Pharmacol Sci 1997; 18**:** 484-491.

390. Galen FX, Cottart CH, Souil E, nh-Xuan AT, Vaubourdolle M, Nivet V, et al. [Role of nitric oxide synthase III and guanosine 3':5'- cyclic monophosphate in the protection exerted by nitric oxide on hepatic ischemia-reperfusion injury]. C R Acad Sci III 1999; 322**:** 871-877.

391. Cottart CH, Nivet-Antoine V, Do L, Al-Massarani G, Descamps G, Xavier-Galen F, et al. Hepatic cytoprotection by nitric oxide and the cGMP pathway after ischaemia-reperfusion in the rat. Nitric Oxide 2003; 9**:** 57-63.

392. Martin E, Berka V, Bogatenkova E, Murad F, Tsai AL. Ligand selectivity of soluble guanylyl cyclase: effect of the hydrogen-bonding tyrosine in the distal heme pocket on binding of oxygen, nitric oxide, and carbon monoxide. J Biol Chem 2006; 281**:** 27836-27845.

393. Kodani E, Xuan YT, Takano H, Shinmura K, Tang XL, Bolli R. Role of cyclic guanosine monophosphate in late preconditioning in conscious rabbits. Circulation 2002; 105**:** 3046-3052.

394. Shinmura K, Xuan YT, Tang XL, Kodani E, Han H, Zhu Y, et al. Inducible nitric oxide synthase modulates cyclooxygenase-2 activity in the heart of conscious rabbits during the late phase of ischemic preconditioning. Circ Res 2002; 90**:** 602-608.

395. Radi R. Nitric oxide, oxidants, and protein tyrosine nitration. Proc Natl Acad Sci U S A 2004; 101**:** 4003-4008.

396. Nathan C. The moving frontier in nitric oxide-dependent signaling. Sci STKE 2004; 2004**:** e52.

397. Gow AJ, Farkouh CR, Munson DA, Posencheg MA, Ischiropoulos H. Biological significance of nitric oxide-mediated protein modifications. Am J Physiol Lung Cell Mol Physiol 2004; 287**:** L262-L268.

398. Matsumoto H, Hirai R, Uemura T, Ota T, Urakami A, Shimizu N. Experimental evaluation of the effects of the intraportal administration of cyclic guanosine monophosphate on ischemia/reperfusion in the porcine liver. Surg Today 1999; 29**:** 1158-1163.

399. Waterston RH, Lindblad-Toh K, Birney E, Rogers J, Abril JF, Agarwal P, et al. Initial sequencing and comparative analysis of the mouse genome. Nature 2002; 420**:** 520-562.

400. Godecke A, Decking UK, Ding Z, Hirchenhain J, Bidmon HJ, Godecke S, et al. Coronary hemodynamics in endothelial NO synthase knockout mice. Circ Res 1998; 82**:** 186-194.

401. Gregg AR, Schauer A, Shi O, Liu Z, Lee CG, O'Brien WE. Limb reduction defects in endothelial nitric oxide synthase-deficient mice. Am J Physiol 1998; 275**:** H2319-H2324.

402. Shesely EG, Maeda N, Kim HS, Desai KM, Krege JH, Laubach VE, et al. Elevated blood pressures in mice lacking endothelial nitric oxide synthase. Proc Natl Acad Sci U S A 1996; 93**:** 13176-13181.

403. Kanoria S, Glantzounis G, Jalan R, Davies NA, Seifalian AM, Williams R, et al. A model to study total hepatic ischemia-reperfusion injury. Transplant Proc 2004; 36**:** 2586-2589.

404. Chavez-Cartaya R, Ramirez P, Fuente T, DeSola GP, Marin J, Pinero A, et al. Blood clearance of 99mTc-trimethyl-Br-IDA discriminates between different degrees of severe liver ischaemia--reperfusion injury in the rat. Eur Surg Res 1997; 29**:** 346-355.

405. Suzuki S, Nakamura S, Sakaguchi T, Ochiai H, Konno H, Baba S, et al. Alteration of reticuloendothelial phagocytic function and tumor necrosis

factor-alpha production after total hepatic ischemia. Transplantation 1997; 64**:** 821-827.

406. Sasaki H, Matsuno T, Nakagawa K, Tanaka N. Induction of apoptosis during the early phase of reperfusion after rat liver ischemia. Acta Med Okayama 1997; 51**:** 305-312.

407. Andreani P, Hoti E, de la SS, degli ED, Sebagh M, Lemoine A, et al. Ischaemic preconditioning of the graft in adult living related right lobe liver transplantation: impact on ischaemia-reperfusion injury and clinical relevance. HPB (Oxford) 2010; 12**:** 439-446.

408. Cutrn JC, Perrelli MG, Cavalieri B, Peralta C, Rosell CJ, Poli G. Microvascular dysfunction induced by reperfusion injury and protective effect of ischemic preconditioning. Free Radic Biol Med 2002; 33**:** 1200-1208.

409. Vollmar B, Menger MD. The hepatic microcirculation: mechanistic contributions and therapeutic targets in liver injury and repair. Physiol Rev 2009; 89**:** 1269-1339.

410. Vollmar B, Glasz J, Leiderer R, Post S, Menger MD. Hepatic microcirculatory perfusion failure is a determinant of liver dysfunction in warm ischemia-reperfusion. Am J Pathol 1994; 145**:** 1421-1431.

411. Klar E, Bredt M, Kraus T, Angelescu M, Mehrabi A, Senninger N, et al. Early assessment of reperfusion injury by intraoperative quantification of hepatic microcirculation in patients. Transplant Proc 1997; 29**:** 362-363.

412. Pannen BH. New insights into the regulation of hepatic blood flow after ischemia and reperfusion. Anesth Analg 2002; 94**:** 1448-1457.

413. Seifalian AM, Mallet SV, Rolles K, Davidson BR. Hepatic microcirculation during human orthotopic liver transplantation. Br J Surg 1997; 84**:** 1391-1395.

414. Zeballos GA, Bernstein RD, Thompson CI, Forfia PR, Seyedi N, Shen W, et al. Pharmacodynamics of plasma nitrate/nitrite as an indication of nitric oxide formation in conscious dogs. Circulation 1995; 91**:** 2982-2988.

415. Schiessl B, Strasburger C, Bidlingmaier M, Mylonas I, Jeschke U, Kainer F, et al. Plasma- and urine concentrations of nitrite/nitrate and cyclic Guanosinemonophosphate in intrauterine growth restricted and preeclamptic pregnancies. Arch Gynecol Obstet 2006; 274**:** 150-154.

416. Tang Y, Forsyth CB, Banan A, Fields JZ, Keshavarzian A. Oats supplementation prevents alcohol-induced gut leakiness in rats by preventing alcohol-induced oxidative tissue damage. J Pharmacol Exp Ther 2009; 329**:** 952-958.

Appendix
Publications directly arising out of work described in this thesis

Papers

1. **Abu-Amara M**, Yang S, Seifalian A, Fuller B, Davidson BR. Remote ischemic preconditioning by hindlimb occlusion prevents liver ischemic/reperfusion injury. *Annals of Surgery*. 2011;254:178-180.

2. **Abu-Amara M**, Yang S, Qualglia A, Rowley P, Seifalian A, Fuller B, Davidson B. Role of endothelial nitric oxide synthase in remote ischaemic preconditioning of the mouse liver. *Liver Transplantation*. 2011;17:610-619.

3. **Abu-Amara M**, Yang S, Quaglia A, Rowley P, de Mel A, Tapuria N, Seifalian A, Davidson B, Fuller B. Nitric oxide is an essential mediator of the protective effects of remote ischaemic preconditioning in a mouse model of liver ischaemia reperfusion injury. *Clinical Science*. 2011;121:257-266.

4. **Abu-Amara M**, Yang S, Tapuria N, Fuller B, Davidson BR, Seifalian A. Liver ischemia/reperfusion injury: Processes in inflammatory networks. A response letter. *Liver Transplantation*. 2010;17:96.

5. **Abu-Amara M**, Yang S, Quaglia A, Rowley P, Tapuria N, Seifalian A, Fuller B, Davidson BR. Effect of remote ischemic preconditioning on liver ischemia/reperfusion injury using a new mouse model. *Liver Transplantation*. 2010;17:70-82.

6. **Abu-Amara M**, Yang S, Tapuria N, Fuller B, Davidson BR, Seifalian A. Liver ischemia/reperfusion injury:Processes in inflammatory networks. A review. *Liver Transplantation*. 2010;16:1016-1032.

Abstracts

1. **Abu-Amara M**, Yang S, Seifalian A, Fuller B, Davidson BR. Nitric oxider in remote ischemic preconditioning of the liver: A novel role for an old molecule. *American Journal of Gastroenterology*. Accepted 2011.

2. **Abu-Amara M**, Yang S, Seifalian A, Fuller B, Davidson BR. Remote ischemic preconditioning protects the liver from ischemia reperfusion injury through the sGC-cGMP pathway. *American Journal of Gastroenterology*. Accepted 2011.

3. **Abu-Amara M**, Yang S, Seifalian A, Davidson B, Fuller B. Remote ischaemic preconditioning protects the hepatic microcirculation from liver ischaemia reperfusion injury through the nitric oxide / cyclic GMP pathway. *Transplant International*. Accepted 2011.

4. **Abu-Amara M**, Yang S, Seifalian A, Davidson B, Fuller B. Hindlimb remote ischaemic preconditioning induces hepatic iNOS expression leading to protection against liver IR injury. *British Journal of Surgery*. 2010;97(S2):80

5. **Abu-Amara M**, Yang S, Seifalian A, Davidson B, Fuller B. Mouse hindlimb remote ischaemic preconditioning reduces liver ischaemia reperfusion injury and

improves hepatic microcirculatory blood flow. *British Journal of Surgery*. 2010;97(S6):38.

6. **Abu-Amara M**, Yang S, Seifalian A, Davidson B, Fuller B. Nitric oxide and endothelial nitric oxide synthase activity are a prerequisite for the protective effects of hindlimb remote ischaemic preconditioning on liver ischaemia reperfusion injury. *British Journal of Surgery*. 2010;97(S6):30.

Presentations

1. **Abu-Amara M**, Yang S, Seifalian A, Fuller B, Davidson BR. Nitric oxider in remote ischemic preconditioning of the liver: A novel role for an old molecule. Poster presentation. *American College of Gastroenterology Annual Scientific Meeting*. Washington DC, USA. October 28 – November 2, 2011. Accepted.

2. **Abu-Amara M**, Yang S, Seifalian A, Fuller B, Davidson BR. Remote ischemic preconditioning protects the liver from ischemia reperfusion injury through the sGC-cGMP pathway. Poster presentation. *American College of Gastroenterology Annual Scientific Meeting*. Washington DC, USA. October 28 – November 2, 2011. Accepted.

3. **Abu-Amara M**, Yang S, Seifalian A, Davidson B, Fuller B. Remote ischaemic preconditioning protects the hepatic microcirculation from liver ischaemia reperfusion injury through the nitric oxide / cyclic GMP pathway. Oral presentation. *European Society for Organ Transplantation International Congress*. Glasgow, UK. 4-7 September 2011. Accepted.

4. **Abu-Amara M**, Shiyu Yang, Seifalian A, Davidson B, Fuller B. Hindlimb remote ischaemic preconditioning induces hepatic iNOS expression leading to protection against liver IR injury. Poster presentation. *ASGBI*. Liverpool, UK. 14-16 April 2010.

5. **Abu-Amara M**. Invited as a speaker to give an oral presentation on the 'Use of genetic knockout models to determine mechanisms of preconditioning' at the *Society of Academic & Research Surgery (SARS)* Parallel symposium entitled 'Organ Preconditioning'. *SARS*. London, UK. 6-7 January 2010.

6. **Abu-Amara M**, Shiyu Yang, Seifalian A, Davidson B, Fuller B. Nitric oxide and eNOS activity are a prerequisite for the protective effects of remote ischaemic preconditioning on liver ischaemia reperfusion injury. Oral presentation. *SARS*. London, UK. 6-7 January 2010.

7. **Abu-Amara M**, Shiyu Yang, Seifalian A, Davidson B, Fuller B. Mouse hindlimb ischaemic preconditioning reduces liver ischaemia reperfusion injury and improves hepatic microcirculatory blood flow. Oral presentation. *SARS*. London, UK. 6-7 January 2010.

8. **Abu-Amara M**, Yang S, Seifalian A, Davidson B, Fuller B. A novel model to study remote ischaemic preconditioning in the mouse liver. Poster presentation. *British Transplant Society*. Glasgow, UK. 16-18 April 2008.

Other publications on liver IR injury

1. **Abu-Amara M**, Gurusamy K, Glantzounis G, Hori S, Fuller B, Davidson B. Systematic review of randomized controlled trials of pharmacological interventions to reduce ischaemia reperfusion injury in elective liver resection with vascular occlusion. *HPB (Oxford).* 2010;12:4-14.

2. **Abu-Amara M**, Gurusamy K, Glantzounis G, Fuller B, Davidson BR. Pharmacological interventions for ischaemia reperfusion injury in liver resection surgery performed under vascular control. *Cochrane Database of Systematic Reviews. 2009 Oct 7;(4):CD008154.*

3. **Abu-Amara M**, Gurusamy K, Hori S, Glantzounis G, Fuller B, Davidson BR. Pharmacological interventions versus no pharmacological intervention for ischaemia reperfusion injury in liver resection surgery performed under vascular control. *Cochrane Database of Systematic Reviews.* 2009 Oct 7;(4):CD007472.

4. Tapuria N, Junnarkar SP, Dutt N, **Abu-Amara M**, Fuller B, Seifalian AM, Davidson BR. Effect of remote ischemic preconditioning on hepatic microcirculation and function in a rat model of hepatic ischemia reperfusion injury. *HPB (Oxford).* 2009;11:108-17.

5. Tapuria N, Kumar Y, Habib MM, **Abu-Amara M**, Seifalian AM, Davidson BR. Remote ischemic preconditioning: a novel protective method from ischemia reperfusion injury – a review. *Journal of Surgical Research*. 2008;150:304-30.